Rapeseed & Sunflower

FROM MEAL TO MEAT ANALOGUE

WANQING JIA

Propositions

1. Protein solubility is a prerequisite for chemical analysis but it is not a requirement for use in meat analogues.
   (this thesis)

2. The demand for complete removal of phenolic compounds from oilseeds limits the potential use of rapeseed and sunflower materials in foods.

   (this thesis)

3. A sound understanding of the concept and working principle of an experimental device is undervalued, but crucial for obtaining the correct results.

4. Simplification can only be done by scientists when they understand the full phenomenon.

5. Scientific progress is achieved through making small step each time.

6. To make a good proposition, it is essential to talk with other people to figure out the exact message.

7. It is helpful to compare yourself with others to recognize your progress, but comparing too much will not add to the research progress.

Propositions belonging to the thesis, entitled:

Rapeseed and sunflower: from meal to meat analogue

Wanqing Jia

Wageningen, 23 March 2022

Rapeseed and sunflower: from meal to meat analogue

Wanqing Jia

Thesis committee

Promotor

Prof. Dr A.J. van der Goot
Personal chair, Food Process Engineering
Wageningen University & Research

Co-promotor

Dr J.K. Keppler
Associate professor, Food Process Engineering
Wageningen University & Research

Other members

Prof. Dr ir MAJS. van Boekel, Wageningen University & Research
Prof. Dr K. Schwarz, University of Kiel, Germany
Dr LAM. Pouvreau, Wageningen University & Research
Dr D. Karefyllakis, Time-travelling Milkman, Wageningen, the Netherlands

Rapeseed and sunflower:
from meal to meat analogue

Wanqing Jia

Thesis
submitted in fulfillment of the requirements for the degree of doctor
at Wageningen University
by the authority of the Rector Magnificus,
Prof. Dr A.P.J. Mol,
in the presence of the
Thesis Committee appointed by the Academic Board
to be defended in public
on Wednesday 23 March 2022
at 1:30 p.m. in the Aula.

Contents

Chapter 1

General introduction

1.1 Novel food ingredients: rapeseed and sunflower cake

The worldwide demand for proteins to feed the increasing world population requires the introduction of novel protein sources. Plant-based proteins can be derived from oilseeds, cereals, legumes, and leaves. Among the oilseeds, proteins from rapeseed and sunflower meal obtained after oil extraction have not yet been used for food applications, but their potential explains recent interest, both economic and scientific (Von Der Haar, Müller, Bader-Mittermaier, & Eisner, 2014). Both rapeseed and sunflower are abundantly available, producing 71 mt and 57 mt of the oilseed in 2020/2021, the second and third largest worldwide after soybean (USDA, 2020). The primary purpose of oilseeds is to produce oil. According to the USDA data, this yields a large quantity of co-product, namely cake or meal (38 mt and 23 mt in 2020/2021). These co-products are rich in protein and are mainly used as feedstock for animals.

1.1.1 The rapeseed journey

Rapeseed is a bright-yellow flowering member of the genus *Brassica* with three basic species: *B. nigra, B. oleracea,* and *B. rapa*. Two main varieties are recognized nowadays: cabbage-type *(B. rapa)* and the hybrid mustard-type (e.g., *B. juncea* and *B. napus*). *B. rapa* grows in spring with a low oil yield, and *B. juncea* and *B. napus* grow in winter and are rich in oil (Gupta & Pratap, 2007). Reports on ancient history suggest that *B. rapa* was cultivated in Asian countries, such as India, China, and Japan, for more than 2000 years before it was introduced to western countries. Originally, it was used as a vegetable crop. *B. napus* was introduced to Asia in the early 18th century from southern Europe. In Europe, the cultivation of the oilseed types started in the northern Alps region as early as the 13th century (Daun, 2011). The oil was mainly used as lamp fuel because it is slow burning and has odorless characteristics (Appelqvist & Ohlson, 1972). Rapeseed oil was also used as a lubricant for steam engines since the 1800s (Buffet, 2017). Rapeseed was in high demand in Canada in the 1930s and during World War II because of the excellent lubricating properties of rapeseed oil for marine engines (Daun, 2011). More recently, its cultivation has increased significantly in Europe because of the potential to use the oil as biodiesel fuel after some modification, but primarily because it has a significantly lower gel point than most other

vegetable oils. Rapeseed produces more oil per land area unit than other oil sources, such as soybeans.

The use of rapeseed oil and other oil sources as edible oil was restricted in Europe until World War II. Since 1967, the International Rapeseed Congress has been held every 4 years, which has driven the development of rapeseed for human consumption as a cheap alternative edible oil to olive oil (Appelqvist & Ohlson, 1972). The main barrier for using rapeseed oil in foods is the high level of erucic acid, which causes heart disease in mammals and could lead to the hardening of the arteries (Kerja, 2004). Later developments led to lowering this erucic acid content, making the oil more nutritionally acceptable. However, the presence of glucosinolates limited the use of rapeseed meals for animal feed. Glucosinolates form chelates with minerals, leading to unavailability of essential minerals to animals during digestion (Kaczmarek, Korniewicz, Lipiński, & Mazur-Kuśnirek, 2016). Canada took the first pioneering step to breed a different rapeseed variety starting from *B. napus* and *B. rapa*. This variety is now called "canola". This variant contains less than 2% erucic acid in the oil and only 30 µmol/g glucosinolates in air-dried, oil-free meals. As a result, canola oil was added to the safe list of food products (GRAS) in the United States (Arntfield, 2011; Daun, 2011; Encyclopedia, 2021). The term "canola" came to be registered as a trademark in 1978 in Canada. This development enabled the use of rapeseed oil with relative freedom in human nutrition and the use of rapeseed meals in animal nutrition. Nowadays, canola is mostly grown in Canada and Australia. Rapeseed is now one of the most important oilseed crops grown in European countries and non-genetically modified rapeseed 00-cultivars with low content of erucic acid and glucosinolates are allowed by the European Food Safety Authority (Turck et al., 2020). The traditional varieties of rapeseed oil with a high level of erucic acid are still being produced in Asian countries and contain 22%−60% erucic acid in oils (Naczk & Shahidi, 1990).

The increasing demand for rapeseed oil to produce both edible oil and biodiesels leads to the generation of large amounts of the co-product, rapeseed meal. The meal was mainly used for the livestock feed. However, exploitation of this under-used meal in the food industry can generate even better economic competitiveness. In recent years, the nutritional value of rapeseed/canola meals (protein content of 36%−38%) has been recognized by the

food industry as an alternative plant protein source (Ivanova, Chalova, Uzunova, Koleva, & Manolov, 2016). Rapeseed protein has been recognized as a functional ingredient for its excellent physicochemical, functional, and nutritional properties similar to soy protein and has been added as a safe product for human consumption (GRAS) (Chmielewska et al., 2020; GRAS, 2016; Zahari et al., 2021). Commercially available canola protein isolates include Supertein, Puratein (Burcon, Nutrascience), CanolaPRO (DSM), and hydrolyzed isolates include Isolexx and Vitalexx (BioExx) (Chmielewska et al., 2020). The composition and nutritional value of rapeseed cake/meal are shown in Table 1-1.

1.1.2 The sunflower journey

Sunflower (*Helianthus annuus* L.) is a large hybrid crop and belongs to the largest family of flowering plants, the Compositae. It is grown mainly for three purposes: bird feed, human food, and oil production (Robertson, 1972). Two main types have been recognized, oilseed-type and confectionery-type, which account for 90% and 10% of the total sunflower production, respectively. Sunflower seeds consist of a hull and kernel with two cotyledons and an embryo. Non-oilseed sunflower generally has a striped seed and a relatively thick hull that remains loosely attached to the kernel, permitting easy dehulling (González-Pérez & Vereijken, 2007). The hull from sunflower seeds accounts for a higher proportion of the whole seeds compared with other commonly cultivated oilseeds (Salunkhe, Adsule, Chavan, & Kadam, 1992).

The cultivation of sunflower was first described in Arizona and New Mexico about 4500 years ago. It was then used to produce ground flour for cake, mush, or bread. The seeds were also eaten as a snack. After the discovery of America, the sunflower was transferred to Europe in the 16th century, where it was mainly used as an ornamental garden plant, and the seeds were consumed as a snack. The sunflower reached Russia in the late 18th century, and the extraction of edible oil was reported in the Proceedings of the Russian Academy in 1779. The use of oil from sunflower led to a rapid expansion of its cultivation after the discovery in Russia. In the 1910s, Russia developed sunflower varieties to produce a high yield of oil that is still the basis for several high-oil varieties currently grown in the world (Salunkhe et al., 1992). Worldwide interest in this crop started in the middle part of the 19th century. By

1960, most sunflower crop varieties had high oil and high crop yield, and breeding programs shifted to developing disease-resistant crops (Taha, Abbasy, El-Nockrashy, & Shoeb, 1981).

The production of sunflower oil yielded a large number of co-products, namely sunflower cake, and meal, which were mainly used for animal feed from the mid-1920s in the United States (Europe, 2020). Four types of the meal can be obtained: (1) mechanically extracted whole seed meal, (2) solvent-extracted whole seed meal, (3) dehulled mechanically extracted meal, (4) dehulled solvent-extracted meal. The chemical composition of the dehulled meal is significantly different from that of the whole seeds. Dehulled meal contains more protein and nitrogen-free extract and less ash and fiber than whole seed meal (Taha et al., 1981). Sunflower meal was found to have the potential to replace soybean meal in poultry diets due to its nutritional value, with a high protein content (36%–40%) (Haghighi Rad & Keshavarz, 1976). However, some challenges still exist for the use of sunflower meals in animal feed, such as the lack of lysine and the presence of anti-nutrients (Haghighi Rad & Keshavarz, 1976). Phytic acid (1.6% in the seeds and 4.3% in sunflower meals) was reported to be one of the anti-nutrients; this impairs the absorption of iron, zinc, and calcium (Miller, Pretorius, & du Toit, 1986; Pedroche, 2015). Another challenge with the use of sunflower meals is the presence of a high amount of chlorogenic acid, which leads to a dark green color during alkaline extraction of sunflower protein isolate. Thus, sunflower meal and protein products have been suggested as an alternative plant protein source where color and fiber content is not a serious problem (Salunkhe et al., 1992). However, the commercialization of sunflower protein is far behind that of rapeseed/canola protein, due to the low protein yield and functionality. Most of the research on sunflower protein has been limited to a lab scale. Nevertheless, developments in technology and additional nutrition research have enhanced the potential of using sunflower meals and their protein products in the human diet (Taha et al., 1981). The composition and the nutritional value of the sunflower cake/meal are shown in Table 1-1.

Table 1-1 The protein composition of rapeseed cake/meal and sunflower cake/meal, the dominant protein present, limiting amino acid and protein digestibility corrected amino acid score for pure protein in all the materials.

Components (g/100 g)	Rapeseed cake	Rapeseed meal	Sunflower cake	Sunflower meal	References
Crude protein	35.0–40.1	36	20–40	50	(Arrutia et al., 2020; Khattab & Arntfield, 2009)
- Globulin	Cruciferin: 60% of total protein，MW, 300–350 kDa, pI/T_d, 7.25/83 °C		Helianthinin: 70% of total protein, MW, 300–350 kDa, pI/T_d, 5.4/90 °C		(Perera et al., 2016; Von Der Haar et al., 2014; Wanasundara, 2011)
- Albumin	Napin: 20% of total protein, MW, 8–15 kDa, pI/ T_d, 11/120 °C		Sunflower albumin: 17%–34% of total protein, MW, 10–18 kDa, pI/ T_d, 4.1/118 °C		(Kortt & Caldwell, 1990; LÁSZTITY, et al.,1983; Perera et al., 2016)
Crude fat	11.8–16.7	2.75	20.7	1.6	(Arrutia et al., 2020; Khattab & Arntfield, 2009)
Ash	6.9	6.02	6.7	6.6	
Crude fiber	ND	11.63	20.1	20.8	
Limiting amino acid	First: lysine, Second: valine		First: lysine, Second: leucine		(Salunkhe et al., 1992; Ivanova et al., 2016)
Protein digestibility corrected amino acid score in protein isolate	0.86–0.93		0.59		(Alexandrino et al., 2017; Fleddermann et al., 2013)

1.2 Traditional protein fractionation toward less-refined fractions

As described in the previous section, rapeseed and sunflower cake/meal are not used directly as food ingredients yet because of the presence of some undesirable components, namely hulls, phytic acid, and phenolic compounds. (Tan, Mailer, Blanchard, & Agboola, 2011; Tranchino, Costantino, & Sodini, 1983). Therefore, fractionation processes are performed to remove the undesirable components and purify the protein. The most common way to acquire protein-enriched fractions from oilseed press cakes and meals is still based on the process described in one patent by Louis and Morton using aqueous extraction (1957) under alkaline conditions (Arrutia et al., 2020; Pedroche, 2015). This method, also called direct alkaline extraction, involves alkaline solubilization of protein from defatted oilseed material and removal of the insoluble material by centrifugation, followed by adjustment of the pH to precipitate the proteins at their isoelectric point (Arrutia et al., 2020; Tan et al., 2011).

However, one of the challenges in applying direction alkaline extraction for rapeseed and sunflower meal is the presence of phenolic compounds (Tan et al., 2011). These phenolic compounds are oxidized under alkaline conditions and form a protein-phenol complex (Laguna et al., 2019; McCue & Shetty, 2004) that leads to the darkening of the final product and affects the taste and smell negative. Therefore, it is common to have a washing process before the direct alkaline extraction process to remove the phenolic compounds using water and organic solvent mixtures. Water-ethanol mixtures with high ethanol content (> 90%) are preferred in the food industry and show good extractability for phenolic compounds, small sugars, or other undesired components, such as glucosinolates and phytates (Citeau, Regis, Carré, & Fine, 2018). Ethanol is considered a food-grade green solvent that is less toxic than other solvents according to the principles of green chemistry and green extraction (Chemat, Vian, & Cravotto, 2012; Prat et al., 2015). Typically, this washing process was essential for sunflower protein fractionation due to its high phenol content. Another challenge concerning rapeseed protein fractionation is the broad range of isoelectronic points for the different rapeseed proteins (Campbell, Rempel, & Wanasundara, 2016). The consequence is that multi-step precipitation at different pH values is required to improve the protein recovery yield (Blaicher, Elstner, Stein, & Mukherjee, 1983; Tan et al., 2011). Salt is often added to

increase the solubility of rapeseed protein. As a result, membrane filtration, such as ultrafiltration and dialysis, is needed after direct alkaline extraction to remove additional salt or any other small components (Tan, Mailer, Blanchard, & Agboola, 2011) (**Chapters 2 & 4**). This contributes to extra processing costs.

These highly refined protein fractions are often used to provide functionalities such as high solubility and light color and are added as functional ingredients in food products. However, the process required to obtain the pure protein fractions is intensive and requires a large amount of chemicals and organic solvents. A simpler fractionation process can be more sustainable and could still yield proteinaceous fractions with higher protein content than the meal (Van der Goot et al., 2016). A fractionation process with only aqueous ethanol washing of rapeseed and sunflower pressed cake was reported to yield less-refined protein concentrates, which still consisted of diverse components (carbohydrates, oil, phenolic compounds) rather than pure protein isolates (Berot & Briffaud, 1983; Von der Haar et al., 2014). If used correctly, phenolic compounds at certain ratios are reported to improve gelling and interfacial properties (Cao & Xiong, 2015; Karefyllakis, Altunkaya, Berton-Carabin, van der Goot, & Nikiforidis, 2017). Moreover, phenolic compounds have received increasing interest from nutritionists due to their antioxidative and anticarcinogenic properties, along with other effects beneficial to health (Ozdal, Capanoglu, & Altay, 2013; Singh, Singh, Kaur, & Singh, 2017). Therefore, complete removal of all the naturally present phenolic compounds is not necessary (**Chapters 4–6**). The extent of removal of phenolic compounds can be controlled by the parameters of the washing process by varying conditions such as the water-ethanol ratio, temperature, solid-liquid ratio, etc.

1.3 Phenolic compounds in rapeseed and sunflower meal

Phenolic compounds, so-called secondary plant metabolites, are present as free phenolic, soluble esters, or insoluble bound phenolics (Dvořáková et al., 2008; Kroll, Rawel, & Rohn, 2003). Although many different types of phenolic compounds exist, they all contain at least one aromatic ring with a hydroxyl group attached. The total phenol content in rapeseed meals is typically about 1%–2% of the dry matter, and the most abundant phenolic compound in rapeseed meals is sinapine (accounting for up to 80% of the total phenol content). The remaining 20% is composed of mono-, di-, and tri-sinapoyl esters of sugars

and/or kaempferol. Tannins are also present in rapeseed meals and are known to form complexes with proteins, minerals, and vitamins and reduce their bioavailability, and are thus considered as antinutritional factors. Condensed tannins are mostly present in rapeseed hulls. The amount of condensed tannins present in rapeseed meals ran from 426 to 772 mg/100 g expressed as catechin-equivalent (Salunkhe et al., 1992). Sunflower meal contains an even higher amount of phenolic compounds (2–4% of dry matter). The main phenolic compound in sunflower pressed cake is chlorogenic acid, accounting for 70% of the total phenol content (Lu, Tian, Cui, Liu, & Ma, 2020; Wildermuth, Young, & Were, 2016). Chlorogenic acid is an ester of quinic acid and caffeic acid, and quinic acid is a cyclohexane carboxylic acid that is responsible for an astringent taste (Deshpande et al., 2016). The remaining 30% are other phenolic acids, such as mono- and di-caffeoylquinic acids and coumaroyl- and feruloylquinic acids (Laguna et al., 2019).

Sunflower protein and chlorogenic acid can interact either covalently or non-covalently. These two interactions are not fully understood, but it is believed that they can take place simultaneously, although specific environmental conditions may favor either one under certain conditions (Keppler, Schwarz, & van der Goot, 2020). Chlorogenic acid can be oxidized by molecular oxygen at alkaline pH to o-quinone. These highly reactive o-quinones can react irreversibly with sulfhydryl and free amino groups of proteins, such as the ϵ-amino group of lysine, the indole nitrogen of tryptophan, and the sulfhydryl group of cysteine (Ozdal et al., 2013). A benzacridine derivative with a specific color can be formed when the ϵ-amino group of lysine interacts with o-quinone by absorbing oxygen. The thiol group can react with the o-quinones without absorbing oxygen, forming a colorless product, and this reaction can be used to prevent the formation of green color in sunflower products (Ozdal et al., 2013; Pierpoint, 1969). The o-quinones can also polymerize in the absence of proteins, giving rise to further secondary reactions. In contrast to the covalent interactions, the non-covalent interactions between protein and chlorogenic acid are reversible and can be created within seconds by hydrophobic association that can be stabilized subsequently by hydrogen bonding (Prigent et al., 2003). Hydrophobic associations mainly take place at pH 5, and ionic interactions are more prevalent at pH 7 (Wildermuth et al., 2016). The use of low pH results in stronger binding of chlorogenic acid because the ensuing dissociation of sunflower protein leads to more available binding sites (Sastry & Rao, 1990).

However, the presence of other components in sunflower meals hinders the study of the effect of interactions between protein and chlorogenic acid. Thus, the impact of the interactions on the techno-functional properties is often studied in a simplified model blend using dephenolized protein isolate with added chlorogenic acid (Karefyllakis et al., 2017; Prigent et al., 2003). In these model blends, it was found that the non-covalent interaction also improved the interfacial properties of sunflower proteins (Karefyllakis et al., 2017). The covalent interaction of some phenolic compounds was found to improve gelling and interfacial properties of proteins. However, this impact was reported to be concentration dependent. At high phenol-protein ratios, most of the thiol groups in the protein are blocked by the phenolic compounds, which leads to a loss of intrinsic protein cross-linking ability (Keppler et al., 2020) (**Chapter 5**).

1.4 Rapeseed and sunflower meal in foods: the meat analog application

Food products that simulate traditional meat products in terms of aesthetic, organoleptic, and nutritional characteristics are referred to as meat analogues. Specifically, the plant-based meat analogue industry is expanding rapidly in the global food marketplace for both the retail and foodservice sectors in recent years (2015–2020). Over the past few decades, several methods to create meat-like structures in plant-based materials have been developed, including 3D printing, high moisture extrusion cooking, and shear cell technology (Dekkers, Boom, & van der Goot, 2018; Kyriakopoulou, Dekkers, & van der Goot, 2019; Ramachandraiah, 2021). The shear cell relies on the thermo-mechanical shear flow to create fibrous, anisotropic structures (Cornet et al., 2020; Manski, van der Goot, & Boom, 2007). This technology is used in this thesis. In the past, highly purified rapeseed and sunflower protein isolates have been studied intensively as ingredients to be added in small amounts for specific functionalities, such as gelling, emulsifying, or foaming (Loveday, 2020). The intensive purification process to obtain highly purified rapeseed and sunflower protein isolates might not allow for their use as the main ingredient in a product, such as a meat analogue; rapeseed and sunflower protein concentrates are more suitable from an economic and sustainability point of view. Therefore, it is suggested that less-refined ingredients, including those from sunflower and rapeseed, could also be suitable for this purpose. At present, most meat analogues are based on the use of soy and pea protein as the main

ingredients due to their specific properties and low prices. Wheat gluten is added to create a second phase for the formation of a fibrous structure. Soy protein concentrate obtained by aqueous ethanol washing alone and by shear cell technology can form a fibrous structure because soy protein concentrate naturally consists of at least two phases: protein and carbohydrate (Grabowska et al., 2016). Rapeseed and sunflower concentrates also have comparable compositions and is considered potential ingredients for structuring properties (Berot & Briffaud, 1983; Yoshie-Stark, Wada, Schott, & Wäsche, 2006).

In addition to the composition, other properties are important to achieve a fibrous structure. Gel strength is important for a satisfactory product structure, preventing the formation of a soft and weakened texture (Samard & Ryu, 2019). Therefore, the rheologic properties of the elastic and viscous modulus of highly concentrated proteins have been studied with heating and cooling to understand the underlying structuring properties using a Closed Cavity Rheometer (Wittek, Zeiler, Karbstein, & Emin, 2020). Rapeseed protein isolate was reported to be able to initiate gel formation when used at high pressure or temperature, which is recommended as a characteristic for meat-like textures (Mupondwa, Li, & Wanasundara, 2018). Sunflower protein isolate with or without phenolic compounds showed potential to form a heat-induced gel (Mudasir Ahmad Malik & Saini, 2017). Further, sunflower protein concentrate was found to have a high water holding capacity (Zorzi, Garske, Flôres, & Thys, 2020). However, the potential of using rapeseed and sunflower meal or concentrate has not been described yet with shear cell technology. The presence of phenolic compounds is one of the main reasons for underutilization due to the complexation with protein. Traditionally, complete removal of phenolic compounds was seen as a prerequisite to use these materials, followed by the protein purification process. However, this treatment not only required intensive processing but also caused changes in the functional and structuring properties. The challenge is to understand what level of purification is necessary from a techno-functional point of view to improve the suitability of these ingredients for applications in meat analogues (**Chapters 3 & 6**).

1.5 Aim and outline of the thesis

Rapeseed and sunflower meals obtained after oil extraction are potential sources for human consumption due to their high protein content, unique amino acid composition, and

wide availability. However, the presence of phenolic compounds compromises the use of those resources for food applications. Thus, the overall aim of this work is to investigate how rapeseed and de-oiled sunflower kernel should be processed and to what extent removal of phenolic compounds is required to achieve functional properties relevant for meat analogue application. A key aspect is understanding the role of fractionation on the compositional change and the functional and structuring properties of the resulting ingredients.

In **Chapter 2**, two different fractionation routes are applied, yielding phenolic-containing rapeseed protein isolate by alkaline protein extraction combined with ultrafiltration/dialysis and the nearly dephenolized rapeseed protein concentrate obtained by aqueous ethanol washing from rapeseed meal. The resulting techno-functional properties are characterized and compared in terms of protein nativity, particle properties, and viscoelastic properties, which suggest their potential for diversity in food industry applications. Based on the findings from **Chapter 2**, the rapeseed protein concentrate was selected, and its structuring properties are discussed using shear cell technology in **Chapter 3**. Rapeseed protein concentrate and mixtures of rapeseed protein concentrate-wheat gluten are investigated. The results provided valuable insights into whether rapeseed protein concentrate alone can be structured into a fibrous structure for an alternative plant protein source for meat analogues. The rapeseed protein concentrate-wheat gluten ratios are studied to understand the effect of adding wheat gluten on the structuring properties. The outcomes are compared with results obtained with soy protein concentrate and soy protein concentrate-wheat gluten blends.

Chapter 4 describes the effect of aqueous ethanol washing on the effective removal of chlorogenic acid while retaining as much protein as possible. The effects of temperature, pH, and solvent quality are evaluated using the yield of phenolic compounds removal and protein loss. The experimental results are captured with the equilibrium constants, which are used to simulate a multi-step exhaustive washing process. The washed concentrates are assessed on their functional properties, such as protein nativity, microstructure, nitrogen solubility index, and water holding capacity. Characterization of the functional properties of the concentrate helps to evaluate the washing process applied and determine the optimal conditions for the food industry.

Chapter 5 describes a study using blends of dephenolized sunflower protein isolate and chlorogenic acid. The protein is modified through either covalent or non-covalent interaction for apparent chlorogenic acid-protein molar ratios of 1:10, 1:5, 1:1, 5:1 and 10:1 (which is mass ratio of 1:850, 1:450, 1:85, 1:15 and 1:10). The type and extent of protein modification, physicochemical properties, solubility, and gelling properties are evaluated in this model blend to find the critical ratio. The outcomes are used for a discussion on the translation of the results to design rules for less refined fractions with multiple components. In **Chapter 6**, the effect of the aqueous ethanol washing process for the de-oiled sunflower kernel and pressed sunflower kernel was assessed about their functional and structuring properties. Both materials are derived from the same starting material, sunflower kernel, but different de-oiling pre-treatments are applied: pre-pressing and de-oiling by 96% ethanol for de-oiled sunflower kernel, and full pressing for pressed sunflower kernel. The structuring properties of the two materials before and after washing are assessed using a closed cavity rheometer and shear cell technology. The ethanol content in the solvent is selected based on the outcomes of **Chapter 4**. This chapter provides a scientific insight for the food industry, linking the processing with the potential application of sunflower materials.

Chapter 7 summarizes the main findings of the previous chapters and concludes with a general discussion. The fractionation process is discussed towards their effect on the functional and structuring properties to investigate the existence of a generic behavior of rapeseed and sunflower material. In addition, the need to remove phenolic compounds from oilseeds for industrial processing is discussed.

1.6 References

Alexandrino, T. D., Ferrari, R. A., de Oliveira, L. M., de Cássia S.C. Ormenese, R., & Pacheco, M. T. B. (2017). Fractioning of the sunflower flour components: Physical, chemical, and nutritional evaluation of the fractions. *LWT*, *84*, 426–432.

Appelqvist, L.-A., & Ohlson, R. (1972). *Rapeseed. Cultivation, Composition, Processing and Utilization*. Elsevier.

Arntfield, S. D. (2011). Canola and other oilseed proteins. In: G. O. P. Williams, & P. A. Williams (Eds.), *Handbook of Food Proteins*. Woodhead Publishing.

Arrutia, F., Binner, E., Williams, P., & Waldron, K. W. (2020). Oilseeds beyond oil: press cakes and meals supplying global protein requirements. *Trends in Food Science and Technology*, *100*, 88–102.

Berot, S., & Briffaud, J. (1983). Parameters for obtaining concentrates from rapeseed and sunflower meal. *Qual Plant Plant Foods Hum Nutr, 33*, 237–242.

Blaicher, F. M., Elstner, F., Stein, W., & Mukherjee, K. D. (1983). Rapeseed protein isolates: Effect of processing on yield and composition of protein. *Journal of Agricultural and Food Chemistry*, *31*(2), 358–362.

Buffet, L. (2017). Reality check - 10 things you didn't know about EU biofuels policy. Campaigning for cleaner transport in Europe. Transport & Environment. Retrieved October 8, 2021.

Campbell, L., Rempel, C., & Wanasundara, J. (2016). Canola/rapeseed protein: Future opportunities and directions—workshop proceedings of IRC 2015. *Plants*, *5*(2), 17.

Canola Encyclopedia. (2021). History of canola seed development. Retrieved October 8, 2021.

Cao, Y., & Xiong, Y. L. (2015). Chlorogenic acid-mediated gel formation of oxidatively stressed myofibrillar protein. *Food Chemistry*, *180*, 235–243.

Chemat, F., Vian, M. A., & Cravotto, G. (2012). Green extraction of natural products: Concept and principles. *International Journal of Molecular Sciences*, *13*(7), 8615–8627.

Chmielewska, A., Kozłowska, M., Rachwał, D., Amarowicz, R., Nebesny, E., & Rosicka-, J. (2020). Canola/rapeseed protein – nutritional value, functionality, and food application: a review. *Critical Reviews in Food Science and Nutrition*.

Citeau, M., Regis, J., Carré, P., & Fine, F. (2018). Value of hydroalcoholic treatment of rapeseed for oil extraction and protein enrichment. *OCL*, *26*, 1.

Cornet, S. H. V., Snel, S. J. E., Schreuders, F. K. G., van der Sman, R. G. M., Beyrer, M., & van der Goot, A. (2020). Thermo-mechanical processing of plant proteins using shear cell and high-moisture extrusion cooking. *Critical Reviews in Food Science and Nutrition*.

Daun, J. K., Eskin, N. A. M., Hickling, D. (Eds.) (2011). *Canola Chemistry, Production, Processing and Utilization*. AOCS Press.

Dekkers, B. L., Boom, R. M., & van der Goot, A. J. (2018). Structuring processes for meat analogues. *Trends in Food Science and Technology*, *81*, 25–36.

Europe, N. (2020). History of the sunflower. Retrieved October 8, 2021

Fleddermann, M., Fechner, A., Rößler, A., Bähr, M., Pastor, A., Liebert, F., & Jahreis, G. (2013). Nutritional evaluation of rapeseed protein compared to soy protein for quality, plasma amino acids, and nitrogen balance - A randomized cross-over intervention study in humans. *Clinical Nutrition*, *32*(4), 519–526.

González-Pérez, S., & Vereijken, J. M. (2007). Sunflower proteins overview of their physicochemical structural and functional properties. *Journal of the Science of Food and Agriculture*, *87*, 2173–2191.

Grabowska, K. J., Zhu, S., Dekkers, B. L., De Ruijter, N. C. A., Gieteling, J., & Van Der Goot, A. J. (2016). Shear-induced structuring as a tool to make anisotropic materials using soy protein concentrate. *Journal of Food Engineering, 188*, 77–86.

GRAS. (2016). GRAS notice no. 683. The safety and the generally recognized as safe (GRAS) status of the proposed uses of canola/rapeseed protein isolate in human food.

Gupta, S. K., & Pratap, A. (2007). History, origin, and evolution. *Advances in Botanical Research, 45*, 1–20.

Haghighi Rad, F., & Keshavarz, K. (1976). Evaluation of the nutritional value of sunflower meal and the possibility of substitution of sunflower meal for soybean meal in poultry diets. *Poultry Science*, *55*(5), 1757–1765.

Ivanova, P., Chalova, V., Uzunova, G., Koleva, L., & Manolov, I. (2016a). Biochemical characterization of industrially produced rapeseed meal as a protein source in food industry. *Agriculture and Agricultural Science Procedia*, *10*, 55–62.

Kaczmarek, P., Korniewicz, D., Lipiński, K., & Mazur-Kuśnirek, M. (2016). Chemical composition of rapeseed products and their use in pig nutrition.

Karefyllakis, D., Altunkaya, S., Berton-Carabin, C. C., van der Goot, A. J., & Nikiforidis, C. V. (2017). Physical bonding between sunflower proteins and phenols: Impact on interfacial properties. *Food Hydrocolloids*, *73*, 326–334.

Keppler, J. K., Schwarz, K., & van der Goot, A. (2020). Covalent modification of food proteins by plant-based ingredients (polyphenols and organosulphur compounds): A commonplace reaction with novel utilization potential. *Trends in Food Science & Technology*, *101*, 38–49.

Kerja, E. P. T. (2004). In: C. Wrigley, H. Corke, & C. E. Walker (Eds.), *Encyclopedia of Grain Science*. Academic Press. (Canola)

Khattab, R. Y., & Arntfield, S. D. (2009). Functional properties of raw and processed canola meal. *LWT - Food Science and Technology*, *42*(6), 1119–1124.

Kortt, A. A., & Caldwell, J. B. (1990). Low molecular weight albumins from sunflower seed: identification of a methionine-rich albumin. *Phytochemistry*, *29*(9), 2805–2810.

Kyriakopoulou, K., Dekkers, B., & van der Goot, A. J. (2019). Plant-based meat analogues. In: C. M. Galanakis (Ed.), *Sustainable Meat Production and Processing*. Academic Press.

Laguna, O., Odinot, E., Bisotto, A., Baréa, B., Villeneuve, P., Sigoillot, J. C., … Lecomte, J. (2019). Release of phenolic acids from sunflower and rapeseed meals using different carboxylic esters hydrolases from *Aspergillus niger*. *Industrial Crops and Products*, *139*, 111579.

LÁsztity, R., Morsi, A.E.E., Mohamed, B., Samei, B.A., Ramadan, M.E.(1983) Solubility of sunflower proteins and gel filtration chromatography of their water-soluble fractions, *Periodica Polytechnica Chemical Engineering*, 28(1), pp. 55–62.

Loveday, S. M. (2020). Plant protein ingredients with food functionality potential. *Nutrition Bulletin*, *45*(3), 321–327.

Lu, H., Tian, Z., Cui, Y., Liu, Z., & Ma, X. (2020). Chlorogenic acid: A comprehensive review of the dietary sources, processing effects, bioavailability, beneficial properties, mechanisms of action, and future directions. *Comprehensive Reviews in Food Science and Food Safety, 19*, 3130–3158.

Malik, M. A., & Saini, C. S. (2017). Polyphenol removal from sunflower seed and kernel: Effect on functional and rheological properties of protein isolates. *Food Hydrocolloids*, *63*, 705–715.

Manski, J. M., van der Goot, A. J., & Boom, R. M. (2007). Formation of fibrous materials from dense calcium caseinate dispersions. *Biomacromolecules*, *8*(4), 1271–1279.

McCue, P., & Shetty, K. (2004). Health benefits of soy isoflavonoids and strategies for enhancement: A review. *Critical Reviews in Food Science and Nutrition*, *44*(5), 361–367.

Miller, N., Pretorius, H. E., & du Toit, L. J. (1986). Phytic acid in sunflower seeds, pressed cake and protein concentrate. *Food Chemistry*, *21*(3), 205–209.

Mupondwa, E., Li, X., & Wanasundara, J. P. D. (2018). Technoeconomic prospects for commercialization of *Brassica* (cruciferous) plant proteins. *Journal of the American Oil Chemists' Society*, *95*(8), 903–922.

Naczk, M., & Shahidi, F. (1990). Canola and rapeseed production, chemistry, nutrition and processing technology. In: F. Shahidi (Ed.), *Canola and Rapeseed*. 1st edition. CRC Press.

Ozdal, T., Capanoglu, E., & Altay, F. (2013). A review on protein-phenolic interactions and associated changes. *Food Research International*, *51*(2), 954–970.

Pedroche, J. (2015). *Utilization of Sunflower Proteins. Sunflower: Chemistry, Production, Processing, and Utilization*. AOCS Press.

Perera, S. P., Mcintosh, T. C., & Wanasundara, J. P. D. (2016). Structuring properties of cruciferin and napin of *Brassica napus* (canola) show distinct responses to changes in pH and temperature. *Plants*, *5*(36), 1–24.

Pierpoint, W. S. (1969). o-Quinones formed in plant extracts. Their reactions with amino acids and peptides. *Biochemical Journal*, *112*(5), 609–616.

Prat, D., Wells, A., Hayler, J., Sneddon, H., McElroy, C. R., Abou-Shehada, S., & Dunn, P. J. (2015). CHEM21 selection guide of classical- and less classical-solvents. *Green Chemistry*, *18*(1), 288–296.

Prigent, S. V. E., Gruppen, H., Visser, A. J. W. G., Van Koningsveld, G. A., De Jong, G. A. H., & Voragen, A. G. J. (2003). Effects of non-covalent interactions with 5-O-caffeoylquinic acid (chlorogenic acid) on the heat denaturation and solubility of globular proteins. *Journal of Agricultural and Food Chemistry*, *51*(17), 5088–5095.

Ramachandraiah, K. (2021). Potential development of sustainable 3d-printed meat analogues: A review. *Sustainability*, *13*(2), 1–20.

Robertson, J. A. (1972). Sunflowers: America's neglected crop. *Journal of the American Oil Chemists' Society*, *49*(4), 239–244.

Salunkhe, D. K., Adsule, R. N., Chavan, J. K., & Kadam, S. S. (1992). *World Oilseeds: Chemistry, Technology and Utilization*. New York: Van Nostrand Reinhold.

Samard, S., & Ryu, G. H. (2019). Physicochemical and functional characteristics of plant protein-based meat analogs. *Journal of Food Processing and Preservation*, *43*(10), 1–11.

Sastry, M. C. S., & Rao, M. S. N. (1990). Binding of chlorogenic acid by the isolated polyphenol-free 11 S protein of sunflower (*Helianthus annuus*) seed. *Journal of Agricultural and Food Chemistry*, *38*(12), 2103–2110.

Singh, B., Singh, J. P., Kaur, A., & Singh, N. (2017). Phenolic composition and antioxidant potential of grain legume

seeds: A review. *Food Research International*, *101*, 1–16.

Taha, F. S., Abbasy, M., El-Nockrashy, A. S., & Shoeb, Z. E. (1981). Countercurrent extraction-isoelectric precipitation of sunflower seed protein isolates. *Journal of the Science of Food and Agriculture*, *32*, 166–174.

Tan, S. H., Mailer, R. J., Blanchard, C. L., & Agboola, S. O. (2011a). Canola proteins for human consumption: extraction, profile, and functional properties. *Journal of Food Science, 76*, R16–R28.

Tan, S. H., Mailer, R. J., Blanchard, C. L., & Agboola, S. O. (2011b). Extraction and characterization of protein fractions from Australian canola meals. *Food Research International*, *44*(4), 1075–1082.

Tranchino, L., Costantino, R., & Sodini, G. (1983). Food grade oilseed protein processing: sunflower and rapeseed. *Qualitas Plantarum Plant Foods for Human Nutrition*, *32*(3–4), 305–334.

Turck, D., Castenmiller, J., De Henauw, S., Hirsch-Ernst, K. I., Kearney, J., Maciuk, A., … Knutsen, H. K. (2020). Safety of rapeseed powder from *Brassica rapa* L. and *Brassica napus* L. as a novel food pursuant to Regulation (EU) 2015/2283. *EFSA Journal*, *18*(7), 6197.

USDA. (2020). Oilseeds: world markets and trade.

Van Der Goot, A. J., Pelgrom, P. J. M., Berghout, J. A. M., Geerts, M. E. J., Jankowiak, L., Hardt, N. A., … Boom, R. M. (2016). Concepts for further sustainable production of foods. *Journal of Food Engineering, 168*, 42–51.

Von Der Haar, D., Müller, K., Bader-Mittermaier, S., & Eisner, P. (2014). Rapeseed proteins-production methods and possible application ranges. *OCL - Oilseeds and Fats*, *21*(1), 1–8.

Wanasundara, J. P. D. (2011). Proteins of Brassicaceae oilseeds and their potential as a plant protein source. *Critical Reviews in Food Science and Nutrition, 51*, 635–637.

Wildermuth, S. R., Young, E. E., & Were, L. M. (2016). Chlorogenic acid oxidation and its reaction with sunflower proteins to form green-colored complexes. *Comprehensive Reviews in Food Science and Food Safety*, *15*(5), 829–843.

Wittek, P., Zeiler, N., Karbstein, H. P., & Emin, M. A. (2020). Analysis of the complex rheological properties of highly concentrated proteins with a closed cavity rheometer. *Applied Rheology*, *30*(1), 64–76.

Yoshie-Stark, Y., Wada, Y., Schott, M., & Wäsche, A. (2006). Functional and bioactive properties of rapeseed protein concentrates and sensory analysis of food application with rapeseed protein concentrates. *LWT - Food Science and Technology*, *39*(5), 503–512.

Zahari, I., Ferawati, F., Purhagen, J. K., Rayner, M., Ahlström, C., Helstad, A., & Östbring, K. (2021). Development and characterization of extrudates based on rapeseed and pea protein blends using high-moisture extrusion cooking. *Foods*, *10*, 2397.

Zorzi, C. Z., Garske, R. P., Flôres, S. H., & Thys, R. C. S. (2020). Sunflower protein concentrate: A possible and beneficial ingredient for gluten-free bread. *Innovative Food Science and Emerging Technologies*, *66*, 102539.

Chapter 2

Assessing functional properties of rapeseed protein concentrate versus isolate for food applications

Abstract

Rapeseed protein concentrate (RPC) and isolate (RPI) were fractionated from rapeseed meal and their techno-functional properties were characterized. RPC prepared by aqueous ethanolic washing process yielded less refined and insoluble fractions with largely denatured protein. Hydrated insoluble RPC particles held 6.7 g water without swelling. RPI fractionated from aqueous extraction and ultrafiltration still contained certain phenolic compounds, but protein nativity was preserved including a high protein solubility of 78%. RPC dispersion with 40% w/w showed the highest apparent complex modulus G^* among all rapeseed materials. In contrast, the G^* for RPI dispersion increased upon heating, suggesting a thermal-induced denaturation and gelation capacity of the proteins. Thus, a largely denatured RPC free of phenolic compounds or a native but phenolic containing RPI were obtained by the applied processing conditions, which differ in their techno-functional properties and thus have different promising application potential in food applications.

Industrial relevance

The growing demand for the plant, as opposed to animal protein, has sparked the interest in exploring currently underutilized plant protein sources in the food industry. Rapeseed by-products obtained after oil extraction are promising but the presence of anti-nutritional components in rapeseed meals presents a barrier for its usage in food products. Aqueous ethanolic washing or aqueous extraction combined with membrane filtration were applied to remove the antinutritional factors from rapeseed meals to yield rapeseed protein concentrates and even more refined isolates. In this work, the functional properties of the fractionated rapeseed materials were characterized for their relevance in food applications. The similarities of the rheological properties between rapeseed protein concentrates and soy materials, as well as the presence of native proteins in RPI, might suggest their potential for diversity in food industry applications.

2.1 Introduction

Plant proteins from oilseeds and legumes can become an alternative to animal proteins. Rapeseed is one of the major crops cultivated for oil production next to soybean (USDA, 2020). Recently, the utilization of rapeseed oil for biodiesel generation has increased, leading to a higher production of rapeseed byproducts (meal) worldwide (Ivanova, Chalova, Uzunova, Koleva, & Manolov, 2016). The total production of rapeseed meals was 38 metric tons in 2018 worldwide (Laguna et al., 2018).

Rapeseed meal contains about 40% proteins, which are mainly composed of salt-soluble 12S globulins (cruciferin) and water-soluble 2S albumins (napin) (Bérot, Compoint, Larré, Malabat, & Guéguen, 2005). Both cruciferin and napin have high thermal stability, with a denaturation temperature (T_d) of 91 °C and 110 °C, respectively (Wu & Muir, 2008). Rapeseed proteins have a well-balanced amino acid profile with high quantities of indispensable amino acids (> 400 mg/ g protein), particularly sulfur-containing amino acids (such as methionine and cysteine) in 1:1 ratios (40-49 mg/ g protein) (Bos et al., 2007; Citeau, Regis, Carré, & Fine, 2016). However, the nutritional value is counterbalanced by the presence of glucosinolates, phenolic compounds (PC), and phytates (Tan, Mailer, Blanchard, & Agboola, 2011a). The main PC is sinapic acids of up to 1.8 g /g defatted meal and condensed tannins (500-800 mg catechin equivalents/ g defatted meal) (Tan et al., 2011b). The presence of these antinutritional factors limits the usage of rapeseed protein in food applications due to its association with bitter taste and formation of complexes with protein (Aider & Barbana, 2011; Khattab & Arntfield, 2009; Oscar Laguna et al., 2019; Naczk, Amarowicz, Sullivan, & Shahidi, 1998). Besides antinutritional factors, the hulls present in the meal also reduce its digestibility. Therefore, fractionation is often proposed to improve the applicability of rapeseed protein for human consumption (Das Purkayastha et al., 2014).

Rapeseed protein concentrates are often reported to be obtained by the aqueous ethanol washing process, which is an effective method to remove oil, soluble sugars, PC, and other anti-nutrients from oilseeds (Chemat et al., 2012; Kozlowska, Zadernowski, & Sosulski, 1983). Also aqueous ethanol solvent is a preferred green solvent due to low toxicity (Citeau et al., 2016; González-Pérez et al., 2002). However, rapeseed hulls are not effectively removed by the washing process. Thus, the large hulls can either be removed by sieving or

be milled into smaller fractions (Tranchino, Costantino, & Sodini, 1983; Wanasundara, 2011). In addition, the aqueous ethanol washing process in combination with high temperature was found to affect proteins. Aggregation and/or denaturation was reported and thus a reduced solubility, which hinders further protein purification (Kayser, Arnold, Steffen-Heins, Schwarz, & Keppler, 2020; Zuorro, Iannone, & Lavecchia, 2019). In contrast to protein concentrates, the fractionation process of rapeseed protein isolates usually starts with the defatting of rapeseed meals (Wu & Muir, 2008; Yoshie-Stark, Wada, & Wäsche, 2008). Proteins are thought to retain their native structure in hydrophobic organic solvents, such as hexane (Mattos & Ringe, 2001). Alkaline treatment followed by acid precipitation or ultrafiltration is a typical method to remove antinutrients and enrich the protein from the defatted meal (Yoshie-Stark et al., 2008). Insoluble fibers and hulls are removed by a centrifugation step after alkaline treatment. However, direct alkaline extraction with sodium chloride followed by acid precipitation was found to lead to low protein yield due to the wide range of isoelectric points of the constituent proteins (Tan et al., 2011a). Membrane filtration has proven to be suitable for the production of highly purified and functional rapeseed protein isolates (Yoshie-Stark et al., 2008). Membrane filtration can also be directly applied onto the supernatant after the alkaline treatment, which resulted in an isolate with potential gelling capacity (Yang, Wang, Vasanthan, & Chen, 2014).

Up to now, most research focused on the aqueous extraction of rapeseed protein isolate (RPI), while less attention has been paid to the functional properties of less refined rapeseed protein concentrate (RPC). In this work, we compared the functional properties of aqueous ethanol washed RPC with or without hull removal, as well as ultrafiltered RPI, and discussed their potential applications as a food ingredient. Physico-chemical properties (protein thermostability, nitrogen solubility index (NSI)), and techno-functional properties regarding structured gel formation (water binding capacity (WHC), particle hydration, and rheological properties during heating by oscillation in closed cavity rheometer (CCR)) are tested. The rheological properties of the rapeseed materials are further compared to soy protein concentrate (SPC), soy protein isolate (SPI), and wheat gluten (WG), since these ingredients are often used in meat analogue applications. In the end, the potential food applications will be discussed for the rapeseed materials, in terms of meat analogue or other food applications.

2.2 Materials and methods

2.2.1 Materials

Rapeseed cake (92% DM with 33.8% protein, 15.4% oil, 7.1% ash, 16.3% total fibers, 2.7% PC, and 2.6% tannins), rapeseed protein concentrate (RPC), and sieved rapeseed protein concentrate (sRPC) were provided by Avril Group, France. Petroleum ether was purchased from the Avantor company, and NaCl and NaOH were purchased from Sigma Aldrich (Missouri, USA). Soy protein isolate (SPI) (SUPRO 500E IP, 94% DM with 90% protein, 1% fat, and 5% ash) and soy protein concentrate (SPC, Alpha 8, 96% DM with 70 % protein in dry base, 2% fat, 7 ash, 18% dietary fiber, and total carbohydrates of 19.6%) were purchased from Solae (St Louis, MO). Vital wheat gluten (WG, 92% DM with 83% protein in dry base) was purchased from Barentz (Hoofddorp, Netherlands).

2.2.2 Methods

2.2.2.1 Preparation of rapeseed materials

Rapeseed meal (RSM)

The rapeseed cake (obtained through a de-hulling step and a cold-pressing step) was milled in an impact mill (ZPS50, Hosokawa-Alpine, Germany), which led to 80% de-hulled rapeseed meal (RPM). The conditions were ZPS speed of 6000 rpm, classifier wheel speed of 2500 rpm, a gas flow rate of 75 m^3/h, and feed rate of 6 rpm (circa 1.5 kg/h).

Defatted rapeseed meal (dRSM)

A defatted rapeseed meal was prepared by further defatting the RSM with petroleum ether in a custom-built Soxhlet extractor. The extraction was carried out at a sample/solvent ratio of 1:4 for 6 h, and the solvent in the sample was evaporated in the vacuum fume overnight.

Rapeseed protein concentrate (RPC)

RPC was obtained by defatting RSM with hexane and consecutive aqueous ethanol washing with 70% ethanol concentration and temperature of 75 °C, performed by Improved, Amiens, France. Milled rapeseed protein concentrate (mRPC) was prepared by milling RPC

with an impact mill (ZPS50, Hosokawa-Alpine, Germany). The conditions were ZPS speed of 6000 rpm, classifier wheel speed of 2500 rpm, a gas flow rate of 75 m^3/h, and feed rate of 6 rpm (circa 1.5 kg/h). Sieved rapeseed concentrate (sRPC) was obtained from RPC by using a 400 µm-sized sieve, performed by Improve, Amiens, France.

Rapeseed protein isolate (RPI)

RPI was produced in two steps: First, rapeseed protein was extracted by dispersing the dRSM in a 0.2M NaCl solution at a solid/solvent ratio of 1:8. The pH of the dispersion was adjusted to 8 using 1M NaOH. The dispersions were stirred for 1 h at 25 °C, followed by centrifugation at 8000 rpm for 10 min. The supernatant was collected after centrifugation. In the second step, ultrafiltration and dialysis were carried out to reduce the presence of small molecular weight components, such as glucosinolates, phytates, some PC, ash, and soluble sugars. Therefore, the supernatant of step 1 was subjected to ultrafiltration in an Amicon stirred cell of 400 mL (Millipore Co. Bedford, USA) through a disc membrane (Synder membrane filters, VT, PES, Sterlitech Corporation, USA). The membrane had a thickness of 76 mm and a molecular weight cut-off of 3 kDa. A final volume concentration factor of 4.4 was reached. The retentate was further dialyzed with a 3.5 kDa standard regenerated cellulose membrane tube (Spectra/Por 3, USA) in demineralized water for 72 h to further remove salts and other small molecular weight compounds. Afterward, the retentate was freeze-dried and saved in a 4°C fridge for further analysis. Protein recovery yield for RPI was calculated as follows:

$$Protein\ yield\ = \frac{M_{RPI} * X_{RPI}}{M_{RSM} * X_{RSM}} \cdot 100\% \quad [\%] \tag{1}$$

where M_{RPI} indicates the weight of freeze-dried RPI, and M_{RSM} indicates the weight of starting RSM, X_{RPI} and X_{RSM} indicate the protein fraction in the RPI and RSM. In total, two batches were made with the RPI.

2.2.2.2 Composition analysis

The composition of all rapeseed materials of RSM, dRSM, mRPC, sRPC and RPI was analyzed in terms of protein, ash, moisture, oil, total phenol content, and carbohydrate content. The nitrogen content was determined with the Dumas combustion method by using

a Nitrogen Analyzer (Flash EA 1112 Series, Thermo scientific, Netherlands). The protein content was calculated as the nitrogen content (N) multiplied by a conversion factor of 5.53 for rapeseed (Sari, Bruins, & Sanders, 2013). Ash content was determined with the AACC 08-01 method, moisture with the AACC 44-15.02 method, and oil content with the AACC 30-25.01 method. Oil content for RPI was not measured due to insufficient product obtained after the process and the oil was supposed to be removed by the defatting and fractionation process. Therefore, oil content in RPI was assumed to be zero. The total phenol content was measured with the Folin-Ciocalteu (FC) method (Drosou, Kyriakopoulou, Bimpilas, Tsimogiannis, & Krokida, 2015). The absorbance of the sample was measured at 750 nm using a spectrophotometer (DR3900, Laboratory VIS Spectrophotometer, Hach, USA). The total carbohydrates were calculated as the difference in DM and the known contents of constituents (protein, oil, total PC, ash). All measurements were performed in duplicates.

2.2.2.3 Soluble protein molecule profile with SDS-PAGE

The protein molecular size distribution of all rapeseed materials was characterized using SDS-PAGE. For this, mini-protein gels (low range PROTEAN TGXTM. 30μl, Bio-rad, Netherlands) were used. The samples were diluted in Milli-Q water to reach a concentration of 2 mg/mL in a falcon tube. Afterward, the samples were centrifuged to remove all the insoluble fractions, and the supernatant was used for the SDS-PAGE. In addition to this approach, the uncentrifuged sample (containing all material) was used for the SDS-PAGE analysis as a benchmark. The samples were prepared with Tris buffer containing 2% w/w SDS, 10% glycerol, 0.5% w/v bromophenol blue, and 5% b-mercaptoethanol. The sample was mixed with a vortexer and heated at 95 ℃ for 10 min, Afterward, the sample was centrifuged at 10000 rpm for 1 min. The electrophoresis was performed at 200 V for approximately 40 min in a Mini-Protean II electrophoresis cell (Bio-rad, Veenendaal, Netherlands). 5 µL of SDS-PAGE marker and 15 µL of the sample was loaded onto the gel wheels. The gels obtained after electrophoresis were stained using Bio-safe Coomassie Blue (Bio-rad, Netherlands). After 1 hour, the gels were washed with Millipore water and scanned using a Gel scanner (Biorad - GS900, Netherlands). Triplicates were performed for the SDS-PAGE, and only one single lane was selected to present the result in Fig. 2-1. The benchmark samples containing the whole sample material are presented in the Fig. S2-1.

2.2.2.4 Nitrogen solubility index (NSI)

NSI is defined as the amount of solubilized nitrogen from the original sample. Rapeseed material of 1 g and 49 g of Milli-Q water was mixed in a 50 mL falcon tube and rotated for 24 hour in a rotator (Bibby Scientific™ Stuart™ Rotator Disk SB3, Thermo Fisher Scientific, USA) for hydration at a speed of 20 rpm. Afterward, the dispersion was centrifuged at a speed of 15000×g, at 25 °C for 10 min. The supernatant was removed with a pipette and the wet pellet was transferred into an aluminum tray and dried in the oven at 105 °C for 24 h. The nitrogcontent in the dry pellet ($N_{dry\ pellet}$) and in the original sample ($N_{original}$) were measured with the Dumas combustion method by using a Nitrogen Analyzer (Flash EA 1112 Series, Thermo scientific, Netherlands). The mass of the original sample and dry pellet was weighed, showed as $M_{original}$ and $M_{dry\ pellet}$. The NSI was calculated as follows:

$$NSI = \frac{N_{original}*M_{original} - N_{dry\ pellet}*M_{dry\ pellet}}{N_{original}*M_{original}}\ [\%] \tag{2}$$

Duplicates were performed for each rapeseed material and dumas measurement was performed in duplicates for each dry pellet.

2.2.2.5 Thermal properties with DSC

The thermal properties of all the rapeseed materials were analyzed using DSC (TA instrument 250, USA). Approximately 8 mg of 20% (w/v) sample slurry was weighed in a pan volume of 60 µL. The pan was hermetically sealed and placed into the DSC cell. The pan was heated from 25 °C to 140 °C with a heating rate of 5 °C/min. Both the peak temperature and the integrated enthalpy values of the endothermic peaks were collected by the Trios data analysis software. The enthalpy was expressed based on total amount of protein in the dispersion to allow for the different protein contents in the samples. The measurements were performed in triplicates.

2.2.2.6 Particle properties

Scanning Electron Microscope (SEM) (JEOL JCM-7000, the Netherlands) was firstly used to observe the morphology of all the rapeseed materials. The dry samples were added on the double-side adhesive conductive carbon tabs and the samples were sputter-coated with gold. Compressed air was used to distribute the sample evenly on the surface of

carbon tabs. The accelerating voltage was 10 kV. SEM pictures were taken at a scale of 30-80 µm.

Particle hydration properties

Particle hydration of all the rapeseed materials was performed by making 2 w/v % dispersions in a 100 mL beaker with Milli-Q water and stirring at 300 rpm with a magnet. The dispersions were stirred for 24 h, and samples were taken at time intervals of 0, 1, and 24 h. Particle size distribution was measured using a Mastersizer-3000 device (Malvern Instrument Ltd., UK). The pH of the dispersion was measured with the pH meter at fresh with RSM, sRPC, and RPI as 6.24, 6.42, and 6.22 which was changed into 5.65, 6.58, and 6.23 after 24 h hydration.

Particle size distribution of the hydrated samples at different time intervals was measured using a Mastersizer-3000 device (Malvern Instrument Ltd., UK). For each sample, five replicate measurements were performed, and the average particle size was expressed in volume density and surface area density. Besides, a Microscope Axioscope (Carl Zeiss Microscopy, LLC, United States) with a camera was used to inspect the hydrated samples. The samples were prepared on a glass slide at 25 °C and covered with a coverslip. Snapshots of 100 µm were taken.

Water holding capacity (WHC)

In this work, the WHC is defined as the water that the insoluble part of the rapeseed material absorbed and retained after 24 h of hydration and subsequent centrifugation. WHC was determined by adding 1 g of material and 49 g of Milli-Q water in a 50 mL falcon tube, and a similar process was followed as the NSI measurement (section 2.5) to obtain the wet pellet and dry pellet. Duplicates were performed for each rapeseed material. The weight of the pellet ($M_{wet\ pellet}$) and after drying ($M_{dry\ pellet}$) was measured. The WHC was calculated as:

$$WHC = \frac{M_{wet\ pellet} - M_{dry\ pellet}}{M_{dry\ pellet}} \quad \text{[g water/g dry pellet]} \tag{3}$$

2.2.2.7 Viscoelastic properties

Viscoelastic properties were measured with a Closed Cavity Rheometer device (CCR) (RPA elite, TA instruments, USA). The complex modulus (G*) was calculated by the software based on the measured storage modulus (G') and loss modulus (G'').

Rapeseed materials, SPC, SPI, and WG were mixed with Milli-Q water, at 40% DM with a total mass of approximately 5 g, for a hydration time of 30 min. The samples were vacuum sealed in a plastic bag before, and the sample was taken out of the bag shortly before transferring into CCR. The samples were then placed in between two plastic foils in the closed cavity (disk geometry). A pressure of 4 bars was applied to prevent water evaporation. Pretests of frequency and strain sweep were performed to determine the linear viscoelastic region (LVR) at 120, 130, and 140 ℃, which revealed that measurements using a constant frequency of 1Hz and a strain of 1% were in the LVR up to a temperature of 120 ℃. Above 120 ℃, measurements were outside the LVR and therefore apparent complex modulus G* was reported instead of complex modulus. Temperature sweeps were performed by heating the samples from 40 ℃ to 150 ℃ using a heating rate of 10°/min, a constant strain of 1%, and a frequency of 1 Hz. After reaching 150 ℃, the sample was cooled until 40 ℃ by blowing dry air over the disk. Time sweep experiments were performed at temperatures of 120 ℃ and 140 ℃ for 15 min with a constant strain of 1% and a frequency of 1Hz. Then, samples were cooled to 40 ℃. Duplicates were performed under each condition.

2.2.2.8 Statistics analysis

The data of DSC was analyzed using SPSS software (IBM statistical analysis Version 25.0). Univariate general linear model with LSD test was performed to investigate significant differences between the rapeseed samples of RSM, dRSM, mRPC, sRPC, and RPI. Differences were considered significant if $P < 0.05$.

2.3 Results and discussion

2.3.1 Characterization

Composition

The composition of all rapeseed materials is shown in Table 2-1. The protein content in the RPI reached 94%, and the yield was 36%. This is in the same range as previously reported by Yoshie-Stark et al (2008) for ultrafiltrated rapeseed protein isolate (98% protein content and 36% protein recovery yield). sRPC showed higher protein content compared to the mRPC: Protein enrichment is because sieving removes macroscopic hulls (larger than 400 µm), which contain a low amount of protein.

The concentrates possessed the lowest content of PC (less than 0.2%), which indicates that PC was effectively removed by the aqueous ethanol washing treatment. The high total content of PC (i.e., 3.6%) was measured in the RPI sample. Nevertheless, 78% of the PC present in the original sample was removed during the ultrafiltration process. The remaining PC either have a high molecular weight (large condensed tannins that could not pass the filter membrane) or interacted with the proteins and were thus retained. The ash content within RPI was much lower compared to the other rapeseed materials, indicating an effective ash removal by ultrafiltration and dialysis. The carbohydrate content of concentrates was lower than that of RSM and dRSM due to the removal of soluble components, such as sugars. sRPC presents a slightly lower carbohydrate content than mRPC, which is caused by the removal of the macroscopic hulls by sieving.

Gel Electrophoresis

SDS-PAGE analysis was performed to investigate the effect of processing on the soluble protein composition of all rapeseed materials. Fig. 2-1 shows the bands of proteins separated by the mass (kDa) of soluble rapeseed materials under reducing conditions by adding 2-mercaptoethanol. RSM, dRSM, and RPI showed similar profiles. In total, 5 major bands (between 10, 18-25, and 26-37 kDa) were found. The results were in agreement with the findings of Akbari et al (2015) that cruciferin dissociates into α-polypeptides (26.7-37.1 kDa) and β-polypeptides (18.3-22.9 kDa) chains in the presence of 2-mercaptoethanol. In addition, also the napin dissociated into two bands of 5 and 10 kDa.

Table 2-1 Composition analysis of RSM, dRSM, mRPC, sRPC and RPI on a dry basis. Protein recovery yield of dRSM and RPI were 98% and 36% respectively.

Composition (%)	RSM	dRSM	mRPC	sRPC	RPI
Protein	32.8 ± 0.3	38.7 ± 0.7	58.4 ± 0.3	61.9 ± 0.3	94.4 ± 1.7
Oil	19.4 ± 0.6	1.5 ± 0.04	0.8 ± 0.01	0.8 ± 0.02	ND
TPC	2.2 ± 0.03	2.6 ± 0.03	0.2 ± 0.002	0.2 ± 0.002	3.60 ± 0.01
Ash	7.0 ± 0.01	8.1 ± 0.3	8.5 ± 0.02	8.8 ± 0.004	1.4 ± 0.06
Total carbohydrates[*]	38.7	50.7	32.1	28.3	0.7

[*]*Total carbohydrates were calculated by the difference*

The high molecular weight bands between 37-100 kDa present in the meal and RPI are not described in the literature yet. One hypothesis is that these bands correspond to covalently cross-linked complexes of proteins and PC. Since these complexes were present in RSM, dRSM and RPI, one can speculate that they were already formed before the isolate preparation in the defatting process.

In the case of concentrates (mRPC and sRPC), less bands were visible. The major band of 10 kDa indicates the presence of napin, whereas the other major band of 20 kDa for mRPC and four major bands for sRPC (molecular weights of 20-21, 29-33 kDa) are probably related to the dissociated cruciferin in the presence of the 2-mercaptoethanol. In contrast to RPI, RSM and dRSM, there were no high molecular weight bands above 37 kDa. It is speculated that the aggregates are probably removed by aqueous ethanol washing as discussed in the previous section, or the concentrates were hardly soluble, therefore these high molecular weight proteins were removed with the pellet of insoluble proteins. In Fig. S1, more bands in the molecular weight range between 18-37 kDa are shown for both concentrates when both soluble and insoluble fractions were used. This indicates that the cruciferin in the concentrates is mainly insoluble.

Protein thermostability and solubility

Protein thermostability was measured with the DSC to understand the effect of process conditions on the nativity of protein. The protein denaturation temperature (T_d), the
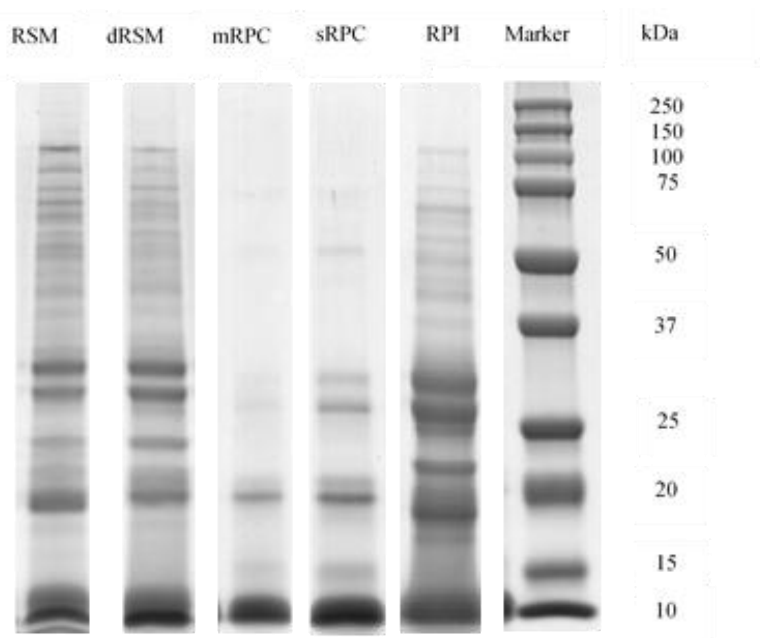
Fig. 2-1 SDS PAGE for the soluble protein fractions of RSM, dRSM, mRPC, sRPC and RPI by adding the 2-mercaptoethanol.

onset T_d and the protein denaturation enthalpy (ΔH) of the samples are shown in Table 2-2. Two denaturation peaks were detected for rapeseed materials at 86-89 ℃ and 107-109 ℃. This result is consistent with the results previously reported of 91 ℃ and 110 ℃ for purified cruciferin and napin fraction (Wu & Muir, 2008). The onset temperature for the first and second denaturation peaks is around 79-82 ℃ and 96-102 ℃.

The increase of $T_{d,1}$ for dRSM compared to that of RSM indicates enhanced thermal stability, and the decrease of denaturation enthalpy for the second peak as ΔH_2 for dRSM suggests partial denaturation of napin by defatting with petroleum ether (Griebenow & Klibanov, 1996). Hardly any denaturation peak of cruciferin was detected for both mRPC and sRPC. The relatively high temperature of 75 ℃ used during the aqueous ethanolic treatment might result in nearly complete denaturation of cruciferin, as this temperature is very close to the onset T_d of cruciferin. Another explanation for the complete denaturation of cruciferin could be that the contact of ethanol with the protein leads to protein denaturation (Peng, Xu, Li, & Tang, 2020). The decrease in ΔH_2 was observed for both concentrates. Likewise, the exposure of napin to the aqueous ethanolic solvent is responsible for partial

denaturation of napin. For RPI, the denaturation enthalpy of cruciferin increased, whereas the denaturation enthalpy of napin decreased. A possible explanation is that fractionation leads to a higher loss of napin than cruciferin, which increased the cruciferin concentration in the RPI, and thus its response in the DSC measurement. This is confirmed by the observation that the SDS-PAGE band of napin (10 kDa) was less intense in the case of RPI compared to other rapeseed materials (Fig. 2-1).

The NSI of rapeseed samples is shown in Fig. 2-2. Slightly higher solubility of dRSM was found compared to that of RSM. Both mRPC and sRPC displayed values below 20%, indicating a low protein solubility. This lower solubility was in line with the high protein denaturation in RPC observed in DSC results (Table 2-2). In contrast to RPC, RPI exhibited a high NSI (76%) and a high protein nativity. The native rapeseed proteins cruciferin and napin are expected to be soluble at pH 6, also because their pI values are higher (7.2 and 11, respectively). The remaining 24% insoluble protein in RPI might be due to the low salt content, as any salt added during extraction was removed by the dialysis process. Salt is known to facilitate protein solubility. Wanasundara et al (2012) reported that the removal of salt by dialysis changes the soluble protein composition.
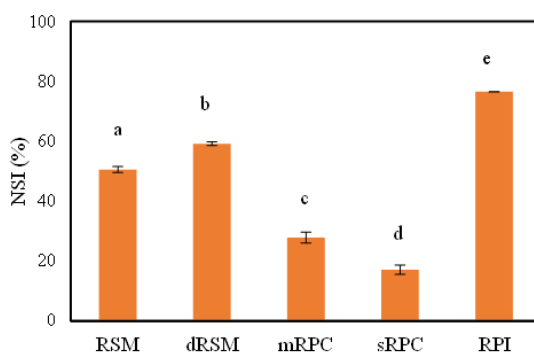
Fig.2-2 Nitrogen solubility index (NSI) for the rapeseed materials of RSM, dRSM, mRPC, sRPC and RPI.

Table 2-2 The onset of denaturation temperature, denaturation peak temperature, and denaturation enthalpy of rapeseed materials

Significant differences (P < 0.05) within one column are indicated by superscript letters
ND: not determ

Rapeseed fractions	Onset $T_{d,\,1}$ (°C)	$T_{d,\,1}$ (°C)	ΔH_1 (J/g protein)	Onset $T_{d,\,2}$ (°C)	$T_{d,\,2}$ (°C)	ΔH_2 (J/g protein)
RSM	79.70 ± 0.64^a	86.49 ± 0.95^a	2.31 ± 0.28^a	98.50 ± 0.50^a	107.70 ± 1.12^a	3.17 ± 0.28^a
dRSM	81.88 ± 1.19^b	90.54 ± 1.05^b	2.89 ± 0.75^c	100.71 ± 0.57^b	108.01 ± 0.20^a	1.35 ± 0.13^b
mRPC	82.20 ± 0.09^b	89.43 ± 1.21^b	0.05 ± 0.01^b	$97.22 \pm 1.41^{a,c}$	108.23 ± 1.56^a	1.18 ± 0.26^b
sRPC	ND	ND	ND	$96.26 \pm 0.26^{a,c}$	108.20 ± 0.79^a	1.25 ± 0.36^b
RPI	79.22 ± 0.59^a	88.92 ± 0.56^b	3.45 ± 0.43^c	102.31 ± 1.85^b	108.67 ± 0.40^a	0.30 ± 0.03^c

2.3.2 Particle properties

Morphology

The particles of the rapeseed fractions were visualized by representative SEM images (Fig.2-3), to understand the morphology change of the cellular matrix induced by the different process conditions. Laguna et al (2018) reported globular protein bodies to be stored inside the cellular matrix in RSM. There is no evidence of globular protein bodies in meal and concentrates in Fig. 2-3, since the surface of the RSM particles was more compact and less opened compared to the reported milled rapeseed kernels from a dry fractionation. In Laguna's work, the cell wall structure was opened by an intensive milling process leading to an average particle size of less than 100 µm. Here, milling was less intensive, as evidenced by a larger average particle size of 100-400 µm. The less intensive milling could be a reason for observing a more complete cell wall structure of rapeseed particles for the meal and concentrates in the present study. This could explain that the protein bodies and other components were entrapped inside the matrix. The SEM pictures of RPI showed disordered flake fragments and it is likely that the protein bodies in the cellular matrix were dissolved into the water during isolate fractionation and formed flakes during freeze-drying. A similar structure of flakes was also found in the literature concerning the freeze-dried soluble plant protein (Berghout, 2015; Jiang et al., 2014).

Particle hydration properties

The rapeseed materials were hydrated with water and the change of particle size during hydration was measured to understand the melting and swelling of the particles as a function of time. It is hypothesized that the insoluble part of the flakes and cellular matrix observed in SEM with a size larger than 100 µm will either decrease in size with increasing hydration time due to dissolvement or increase in size caused by swelling.

RSM and dRSM dispersions showed similar particle sizes in Fig. 2-3. For RSM, the particle distribution of the large particles above 100 µm changed towards a larger size during hydration, while particles sizes of dRSM were hardly changed. The difference might be associated with the oil removal from RSM: defatting could result in a more hydrophobic nature of the dRSM, reducing its water uptake and thus its swelling capacity, or it could have

affected the cellular matrix leading to a more closed and compact structure. The volume of small particles with the size of approximately 7-10 µm increased over time for RSM. One explanation might be associated with structural changes of the fibers during hydration towards smaller structures. On the other hand, a similar increase of small particles (between 7 to 10 µm) was found with RPI as well. Therefore, the increase of small particles might also be explained by the liberating of remaining insoluble protein particles from RSM and RPI, which disentangled into smaller particles further upon prolonged hydration. This is confirmed by the presence of around 24% insoluble protein fraction in RPI, according to different calculations based on the 76% soluble protein determined in NSI (section 3.2.3). Unlike these rapeseed materials, hardly any small particles were produced during hydration for mRPC and sRPC and the particles seem to retain in their original state. The large particles of concentrates remained even more stable in size distribution compared to RSM and dRSM. This result indicates that both RPCs were hardly hydrated. It is possible that the aqueous ethanol treatment led to dense and even glassy particles, which do not allow water to penetrate the particles. Similar observations have been found for soy okara (Jankowiak, Trifunovic, Boom, & Van Der Goot, 2014).

Water holding capacity (WHC)

WHC is an important property since it can provide information about the juiciness and tenderness of food products such as meat or meat analogues (Cornet et al., 2021; Dijkstra, Linnemann, & Van Boekel, 2003). The WHC of the insoluble fractions from rapeseed materials is shown in Fig. 2-4. WHC of RSM was found to be 6.2 g water/g dry pellet and that of dRSM showed the highest value of 9.3 g water/g dry pellet. The concentrates of mRPC showed slightly higher WHC values of 6.7 g water/g dry pellet compared to 5.6 g water/g dry pellet in the case of sRPC. The lowest WHC was found with RPI.

The differences in the WHC among rapeseed materials could be the result of the following two reasons. Firstly, different components within the rapeseed fractions might hold different amounts of water, such as protein and carbohydrates, and the composition between the fractions was different. The WHC of rapeseed protein is likely to be similar low as the WHC of RPI since RPI was mainly composed of the native protein. In contrast to protein, for carbohydrates, it has been reported that the water-insoluble dietary fiber can lead to high
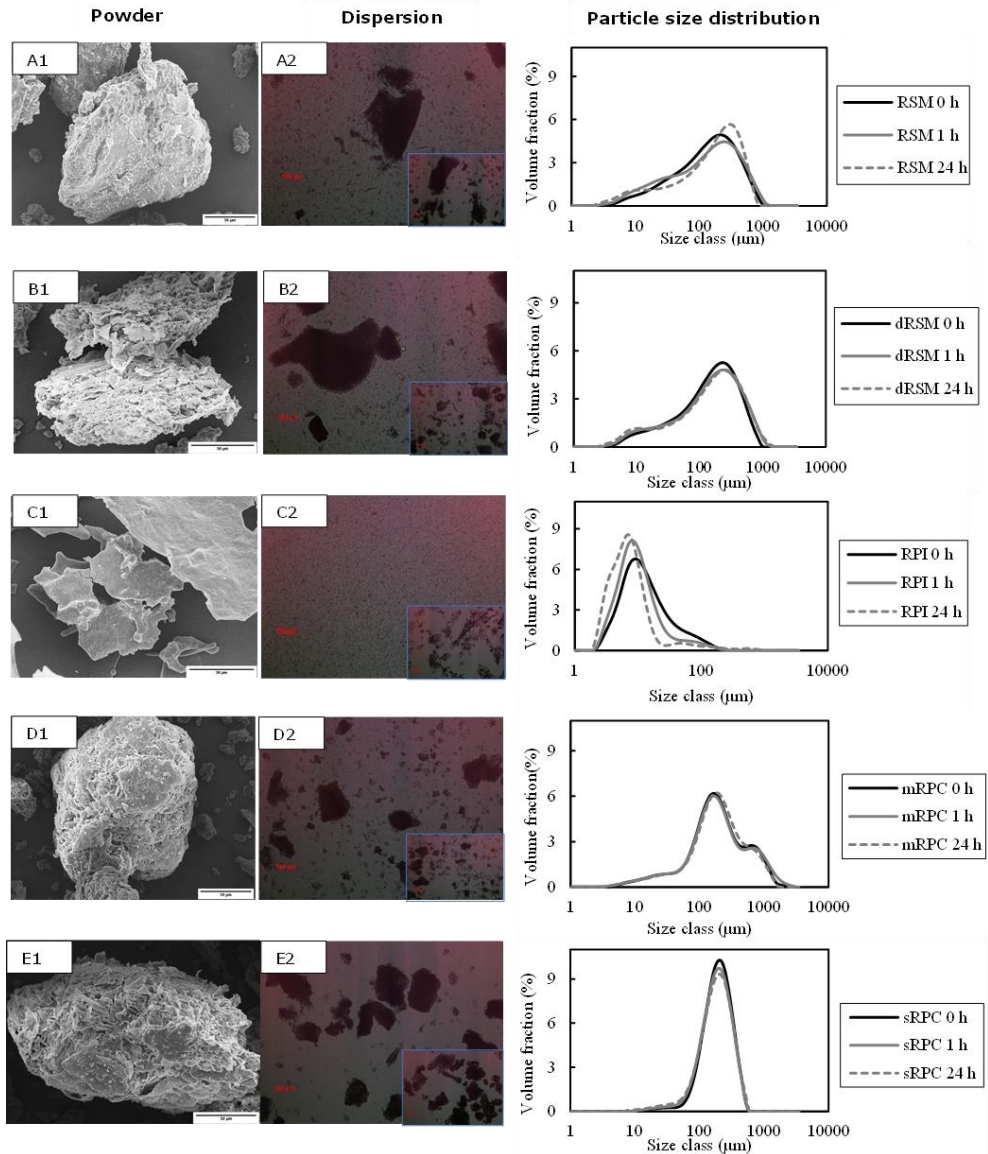
Fig.2-3 SEM images of RSM, dRSM, mRPC, sRPC and RPI (A1-E1), and light microscopy of particle hydration in a 2% dispersion, snapshots were taken fresh (small picture on the right bottom corner) and after 24 h (A2-E2). Particle size distribution of RSM, dRSM, mRPC, sRPC and RPI (A3-E3) during hydration in water at the time interval of 0 min, 30 min, 1 h and 24 h. The scale of the light microscopy is 100 µm and the scale of SEM is 50 µm.

WHC (Yamazaki, Murakami, & Kurita, 2005), which explains the slightly higher WHC in the concentrates. Slightly lower WHC with the sRPC compared to mRPC also indicate that macroscopic hulls removed by sieving contribute to the WHC. However, the impact of PC on the WHC is still unclear yet. Muhammad et al (2014) reported higher WHC after PC removal from soybean and flaxseed protein isolate, while other authors reported that PC did not modify the WHC of sunflower protein concentrates (Alu'datt, Rababah, & Alli, 2014; Salgado, Ortiz, Petruccelli, & Mauri, 2012).

Secondly, the WHC was also reported to be influenced by the structure of the pellet and the hydration of the particles. Since the proteins within rapeseed meal and concentrates were likely trapped inside the cellular matrix, the water held by the cellular matrix and in between the particles might have a big impact on the WHC. This was further visualized with the wet pellets shown in Table 3. The pellets of the different rapeseed fractions were found to be composed of sand-like particles, except for the consistent gel-like pellet of RPI. The high WHC of rapeseed concentrates is unexpected, considering that these sand-like particles do not seem to swell (Fig 2-3) and have a low protein solubility (Fig 2-2). This confirms the assumption that aqueous ethanolic treatment leads to a glassy matrix in RPC which probably hindered hydration and water uptake. The hypothesis is that after hydration, the wet pellet formed a viscous gel which was held together by interstitial water between the hardly swollen particles.
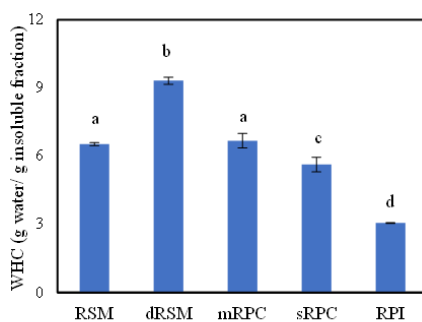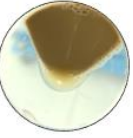
Fig.2-4 Water holding capacity (WHC) for RSM, dRSM, mRPC, sRPC and RPI.

Table 2-3 Pictures of dry powder, particle hydration samples with 2% w/w dispersion after centrifugation, wet pellet after removal of supernatant for the RSM, dRSM, mRPC, sRPC, and RPI. CCR samples of temperature sweep from 40-150 °C for 40% rapeseed materials, WG, SPC, and SPI of 40% DM.

Rapeseed fractions	RSM	dRSM	mRPC	sRPC	RPI
Powder					
Particle hydration (2% w/w concentration)					
Wet insoluble pellet					
CCR rapeseed samples (40% DM) Tempearture sweep (40-150 ℃)					
CCR samples (40% DM) WG/SPC/SPI Temperature sweep (40-150 ℃) From left to right)					

2

Hydration effect on color change

The color of the RPI solution and insoluble pellet was much darker compared to the rest of the materials in Table 2-3. The color formation could be due to covalent interaction between proteins and PC as indicated in the discussion about the composition of the fractions (Table 2-1) and the SDS-PAGE (Fig 2-1). Further, oxidized PC condensation products are also of a dark color (Keppler, Schwarz, & Jan van der Goot, 2020). The light color of the concentrated solution also indicates that most of the PC was removed by the aqueous ethanol washing.

2.3.3 Rheological properties

Rheological properties with temperature sweep and time sweep can be used to assess the potential structuring properties of the rapeseed materials. The comparison was made with soy protein concentrate (SPC), soy protein isolate (SPI), and wheat gluten (WG), which are commonly used for the structuring purpose in meat analogue applications.

The apparent complex modulus G^* was measured by oscillation while heating at 1% strain and 1 Hz frequency with the rapeseed materials of 40 % DM. In Fig.2-5 A1, three regions can be identified for RSM, a region with a constant apparent G^* value (50 kPa from 40 to 80 °C), a region where the apparent G^* slightly increased (70 kPa at 118 °C), and a region where the apparent G^* decreased (17 kPa at 150 °C). A similar pattern was found with dRSM with approximately three times higher apparent G^* values. This result indicates that the fat removal of RSM has a positive impact on viscoelastic properties. Both concentrates mRPC and sRPC show a decrease in apparent G^* starting from 580 kPa for mRPC and 643 kPa for sRPC at 40 °C, which decreased to around 110 kPa at 150 °C for both concentrates. The apparent G^* of both concentrates was found to be higher than the rest of the rapeseed materials during heating, which might be linked to their glassy and hardly hydrated particle properties as shown in Fig 2-3. For RPI two peaks were observed. The first peak was found to be around 8 kPa at 95 °C. After a slight decrease, the apparent G^* was further increased to the second peak of 15 kPa at 125 °C and finally decreased to 3 kPa at 150 °C. The two peaks were corresponded to the two denaturation peaks of cruciferin and napin obtained with DSC in Table 2-2.

The apparent G^* was also measured with WG, SPI and SPC under the same conditions as rapeseed materials as a comparison (Fig. 2-5A2). WG showed stable apparent G* from 40 to 98 °C and an increase was found from 4 kPa at 98 °C to 30 kPa at 130 °C, followed by a decrease to 22 kPa at 150 °C. Heat-induced polymerization of WG was reported to be caused by the formation of disulfide bonds (Domenek, Morel, Bonicel, & Guilbert, 2002; Emin & Schuchmann, 2017). Similar to WG, RPI is also rich in sulphur-containing amino acid, which can contribute to crosslinking during heating. Besides, the decrease of apparent G^* for WG above 130 °C was explained by the degradation of the crosslinked structure (Emin, Quevedo, Wilhelm, & Karbstein, 2017), and this effect is likely to occur in

RPI as well. A decreasing trend was found with the apparent $G*$ of SPC and SPI when heated from 25 °C to 150 °C, and this is an expected behavior as increased temperature normally leads to lower viscosity. Above 120 °C, the decrease was more pronounced and suggested structure breakdown. Remarkably, the $G*$ of sRPC and mRPC hardly decreased when heated above 120 °C and the value was stable for both RPC materials in the whole temperature range. The results showed a stronger material of rapeseed concentrates during heating even compared to the soy protein materials and WG. One might speculate the result to be linked with the aqueous ethanolic treatment which make the RPCs glassy and more compacted. Also, the presence of high fiber content in the RPCs is likely to cause the strong rheological properties.
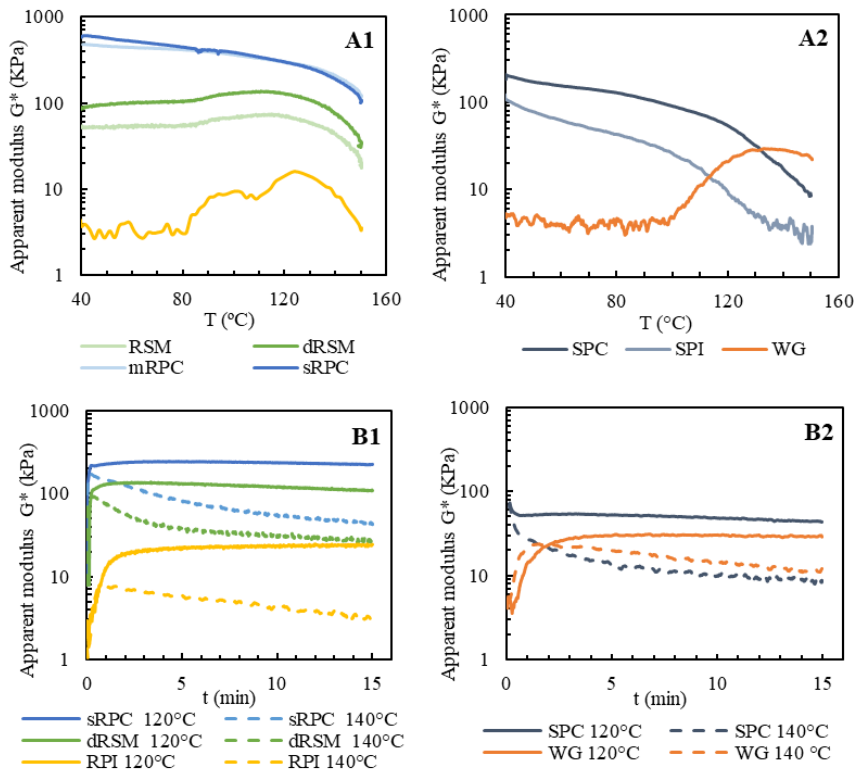
2

Fig.2-5 Apparent complex modulus $G*$ for anisothermal experiments from 40-150 °C for RSM, dRSM, mRPC, sRPC, RPI (A1) and SPC, SPI, WG (A2); Apparent complex modulus for isothermal experiments at 120 °C and 140 °C for dRSM, sRPC and RPI (B1) and SPC and WG (B2). An instability of the curve below 5 kPa was observed that corresponds to the detection limit of the machine.

Fig.2-5 B1-B2 displays the effect of processing time on the apparent $G*$ of sRPC, dRSM, RPI, SPC and WG through isothermal time sweep at 120 ℃ and 140 ℃. The samples of sRPC and dRSM showed a prompt initial increase which was a result of the sample heating up to the set temperature. After the initial increase, the $G*$ for sRPC and dRSM was stable at 240 kPa and 140 kPa when heated at 120 ℃, respectively. The initial increase of apparent $G*$ for RPI and WG was a bit slower, but then the apparent $G*$-value remained more or less constant. Unlike rapeseed materials and WG, no initial increase was found for SPC. The $G*$-value was constant during the full 15 min when heated at 120 ℃. This might indicate the structure formation prior to experiment by the vacuum of the material and the structure was stable upon heating at 120 ℃.

For all the materials studied, the rheological properties of apparent $G*$ seems to be hardly affected by the time sweep at 120 ℃ for 15 min. It is also reported stable complex viscosity of WG with 16 kPa during time sweep with the same conditions at 120 ℃ (Emin & Schuchmann, 2017), and this value was found to be similar as the apparent $G*$ of WG (between 20-30 kPa) at 120 ℃. Therefore, the structure degradation hardly occurred at this temperature. It is interesting to observe that the degradation started when heating at 140 ℃ for all the materials studied. sRPC and SPC showed a fast decrease of the $G*$ at the first 5 min and the decrease became slower Afterward at 140 ℃. However, a plateau was reached after a fast decreasing of the apparent of $G*$ in case of dRSM around 5 min heating. The trend of decreasing with $G*$ for RPI and WG was similar, shown in a slow pattern and continuously upon heating at 140 ℃. This is in accordance with the temperature sweep results shown above, where lowering of the apparent G* took place at elevated temperatures. Also, the complex viscosity of the WG was reported to be decreased from approximately 12 kPa to 8 kPa after 15 min of time sweep at 140 ℃, and this value is similar to the WG (22-11 kPa) presents in Fig. 2-5. The apparent $G*$ of the rapeseed materials at different temperatures agreed with the temperature sweep results comparing the same temperatures.

2.3.4 Rapeseed materials for food application

An outlook for the potential application of the rapeseed materials is discussed in this section, concerning the different process conditions of defatting, aqueous ethanol washing, and aqueous extraction combined with ultrafiltration. As can be seen in Fig. 2-4 and Table

2-2, dRSM combines high WHC and interesting rheological behavior which is promising from a functional point of view. Both RPCs contained hardly any PC and similar functional and structuring properties were found with both RPCs. The presence of hulls with small particle size in the mRPC might require further investigation on digestibility and sensory properties. Sieving turned out to be effective for the removal of the hull fractions of sRPC, which is a potential ingredient for food application. High apparent G^* were found with RPCs compared to the rest of the rapeseed fractions, SPI, SPC and WG, indicating the formation of the structures with strong mechanical strength (Fig. 2-5), as needed for example for meat analogue production (Dekkers, Emin, Boom, & van der Goot, 2018; Emin & Schuchmann, 2017).

RPI is the most refined protein fractions of all tested samples, but still contained certain amount of PC (Table 2-1). Its high protein solubility (Fig. 2-2) can make the material suitable for food applications that require native protein with high solubility, i.e., emulsifying and foaming properties (Lawal, 2005). The rheological properties of RPI during heating showed certain similarities to those of WG. The sulphur-containing amino acids and PC present in the RPI have the potential to contribute to the polymerization, which can also be of interest in structure formation processes (for example for meat and dairy analogues) (Keppler et al., 2020). However, the sensory properties need to be tested since a considerable amount of PC are still in the material. If low PC is desired, then further treatment is still required for the RPI.

From a processing and economic point of view, less treatment is generally preferred. Therefore, the less refined RPC is a potential plant protein source to be used in sustainable food products. RPC could be considered as an alternative for SPC and given its under usage as a waste stream or as feedstock after oil extraction, it is even more economically valuable. Further purified RPI that still contains some PC could polymerize, which is a key property of WG. Therefore, it is interesting to further investigate possible similarities in behavior between RPI and WG for structuring purposes. RPI might be suitable for other applications, such as emulsifying and foaming, in which high solubility and low gelling capacity is required. The low protein recovery yield of RPI led to a loss of protein during fractionation,

also by-products were generated during fractionation which is not as economically favorable as RPC.

2.4 Conclusion

In this study, the effect of fractionation on the techno-functional properties of rapeseed materials was studied. The results clearly showed that the fractionation process strongly affects the obtained material: Nearly dephenolized RPC was obtained from the aqueous ethanolic washing process, but the proteins were mostly denatured with reduced solubility under the process condition applied. In contrast, RPI obtained through aqueous extraction and ultrafiltration process still contained a high amount of PC, but the proteins were native. The changes in material composition and protein nativity are reflected in the techno-functional properties. The insoluble RPC particles hardly swelled during hydration, but held more water compared to the insoluble RPI particles. The RPC dispersion with 40% DM showed highest complex modulus G^* with rheological measurement, compared to the other rapeseed/soy materials and WG. Therefore, the insoluble RPC produced through aqueous ethanol washing process has a good potential for structuring purposes that require high WHC and certain mechanically strength, such as meat analogues structures. In addition, the less refined material also produces less waste-streams and caters to the need for obtaining sustainable produced raw materials.

In contrast to RPC, the measured G^* of RPI dispersions showed an increase upon heating at 80 ℃ and 110 ℃ suggesting a thermal induced structure formation. The highly soluble RPI with preserved protein nativity has a different structuring potential than RPC and seems mostly suitable for food application that require high solubility (for example plant-drinks) and certain gelation capacities at different high temperatures (such as texturized products). However, this material is more strongly refined than RPC. In the future, the effect of different fractionation processes on functionality and composition needs to be further explored in order to obtain tailored functional fractions for food applications.
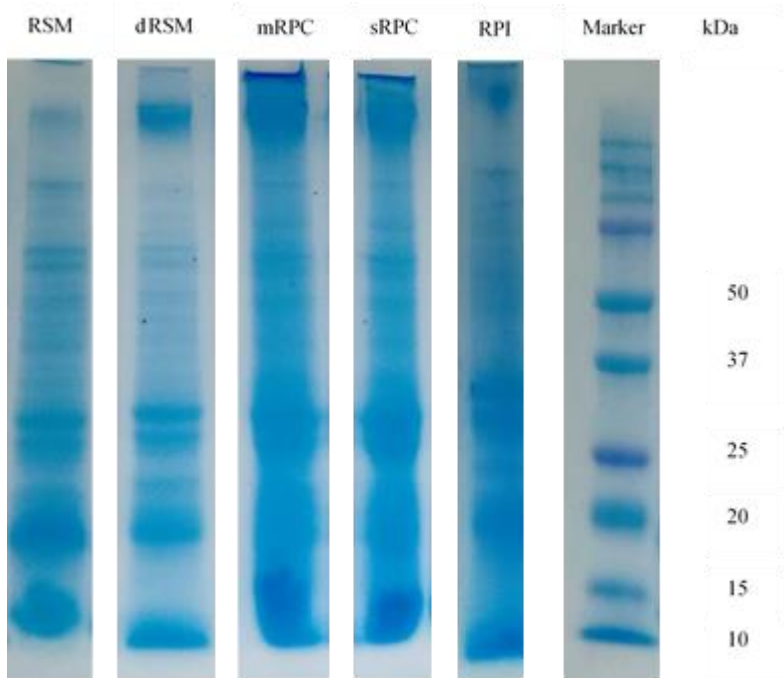
2.5 Supporting information

Fig.S2-1 SDS-PAGE of rapeseed materials: RSM, dRSM, mRPC, sRPC and RPI with complete protein fractions including soluble and insoluble proteins.

2.6 References

Aider, M., & Barbana, C. (2011). Canola proteins: Composition, extraction, functional properties, bioactivity, applications as a food ingredient and allergenicity - A practical and critical review. *Trends in Food Science and Technology*, 22(1), 21–39.

Akbari, A., & Wu, J. (2015). An integrated method of isolating napin and cruciferin from defatted canola meal. *LWT - Food Science and Technology*, 64(1), 308–315.

Alu'datt, M. H., Rababah, T., & Alli, I. (2014). Effect of phenolic compound removal on rheological, thermal and physico-chemical properties of soybean and flaxseed proteins. *Food Chemistry,* 146, 608–613.

Berghout, J. A. M. (2015). Functionality-driven fractionation of lupin seeds. PhD thesis

Bérot, S., Compoint, J. P., Larré, C., Malabat, C., & Guéguen, J. (2005). Large scale purification of rapeseed proteins (Brassica napus L.). *Journal of Chromatography* B, 818(1), 35–42.

Bos, C., Airinei, G., Mariotti, F., Benamouzig, R., Bérot, S., Evrard, J., … Gaudichon, C. (2007). The poor digestibility of rapeseed protein is balanced by its very high metabolic utilization in humans. The Journal of Nutrition, 137(3), 594–600.

Chemat, F., Vian, M. A., & Cravotto, G. (2012). Green extraction of natural products: Concept and principles. *International Journal of Molecular Sciences*, 13(7), 8615–8627.

Citeau, M., Regis, J., Carré, P., & Fine, F. (2016). Value of hydroalcoholic treatment of rapeseed for oil extraction and protein enrichment. *OCL,* 26(1).

Cornet, S. H. V, Snel, S. J. E., Lesschen, J., Van der Goot, A.J., & Van Der Sman, R. G. M.. (2021). Enhancing the water holding capacity of model meat analogues through marinade composition. *Journal of Food Engineering*, 290, 110283.

Das Purkayastha, M., Gogoi, J., Kalita, D., Chattopadhyay, P., Nakhuru, K. S., Goyary, D., & Mahanta, C. L. (2014). Physicochemical and Functional Properties of Rapeseed Protein Isolate: Influence of Antinutrient Removal with Acidified Organic Solvents from Rapeseed Meal. *Journal of Agricultural and Food Chemistry*, 62(31), 7903–7914.

Dekkers, B. L., Emin, M. A., Boom, R. M., & van der Goot, A. J. (2018). The phase properties of soy protein and wheat gluten in a blend for fibrous structure formation. Food *Hydrocolloids*, 79, 273–281.

Dijkstra, D. S., Linnemann, A. R., & Van Boekel, T. A. J. S. (2003). Towards Sustainable Production of Protein-Rich Foods: Appraisal of Eight Crops for Western Europe. PART II: Analysis of the Technological Aspects of the Production Chain. *Critical Reviews in Food Science and Nutrition*, 43(5), 481–506.

Domenek, S., Morel, M.-H., Bonicel, J., & Guilbert, S. (2002). Polymerization Kinetics of Wheat Gluten upon Thermosetting. A Mechanistic Model. *Journal of Agricultural and Food Chemistry,* 50, 5947–5954.

Drosou, C., Kyriakopoulou, K., Bimpilas, A., Tsimogiannis, D., & Krokida, M. (2015). A comparative study on different extraction techniques to recover red grape pomace polyphenols from vinification byproducts. *Industrial Crops and Products*, 75, 141–149.

Emin, M. A., Quevedo, M., Wilhelm, M., & Karbstein, H. P. (2017). Analysis of the reaction behavior of highly concentrated plant proteins in extrusion-like conditions. *Innovative Food Science and Emerging Technologies.* 44, 15-20.

Emin, M.A., & Schuchmann, H. P. (2017). A mechanistic approach to analyze extrusion processing of biopolymers by numerical, rheological, and optical methods. *Trends in Food Science & Technology*, 60, 88–95.

González-Pérez, S., Merck, K. B., Vereijken, J. M., Van Koningsveld, G. A., Gruppen, H., & Voragen, A. G. J. (2002). Isolation and characterization of undenatured chlorogenic acid free sunflower (*Helianthus annuus*) proteins. *Journal of Agricultural and Food Chemistry*, 50(6), 1713–1719.

Griebenow, K., & Klibanov, A. M. (1996). On Protein Denaturation in Aqueous-Organic Mixtures but Not in Pure Organic Solvents. *Journal of the american chemical society.* 118 (47).

Ivanova, P., Chalova, V., Uzunova, G., Koleva, L., & Manolov, I. (2016). Biochemical Characterization of Industrially Produced Rapeseed Meal as a Protein Source in Food Industry. *Agriculture and Agricultural Science Procedia*, 10, 55–62.

Jankowiak, L., Trifunovic, O., Boom, R. M., & Van Der Goot, A. J. (2014). The potential of crude okara for isoflavone production. *Journal of Food Engineering*, 124, 166–172.

Jiang, L., Wang, J., Li, Y., Wang, Z., Liang, J., Wang, R., … Zhang, M. (2014). Effects of ultrasound on the structure and physical properties of black bean protein isolates. *Food Research International*, 62, 595–601.

Kayser, J. J., Arnold, P., Steffen-Heins, A., Schwarz, K., & Keppler, J. K. (2020). Functional ethanol-induced fibrils: Influence of solvents and temperature on amyloid-like aggregation of beta-lactoglobulin. *Journal of Food Engineering*, 270(Oct), 109764.

Keppler, J. K., Schwarz, K., & Van der Goot, A.J.. (2020). Covalent modification of food proteins by plant-based ingredients (polyphenols and organosulphur compounds): A commonplace reaction with novel utilization potential. *Trends in Food Science & Technology*, 101(Oct), 38–49.

Khattab, R. Y., & Arntfield, S. D. (2009). Functional properties of raw and processed canola meal. LWT - *Food Science and Technology*, 42(6), 1119–1124.

Kozlowska, H., Zadernowski, R., & Sosulski, F. W. (1983). Phenolic acids in oilseed flours. *Food / Nahrung,* 27(5), 449–453.

Laguna, O., Barakat, A., Alhamada, H., Durand, E., Baréa, B., Fine, F., … Lecomte, J. (2018). Production of proteins and phenolic compounds enriched fractions from rapeseed and sunflower meals by dry fractionation processes. *Industrial Crops and Products*, 118(Dec), 160–172.

Laguna, O., Odinot, E., Bisotto, A., Baréa, B., Villeneuve, P., Sigoillot, J.-C., … Lecomte, J. (2019). Release of phenolic acids from sunflower and rapeseed meals using different carboxylic esters hydrolases from Aspergillus niger. *Industrial Crops and Products*, 139, 111579.

Lawal, O. S. (2005). Functionality of native and succinylated Lablab bean (Lablab purpureus) protein concentrate. *Food Hydrocolloids*, 19(1), 63–72.

Mattos, C., & Ringe, D. (2001). Proteins in organic solvents. *Current Opinion in Structural Biology*, 11(6), 761–764.

Naczk, M., Amarowicz, R., Sullivan, A., & Shahidi, F. (1998). Current research developments on polyphenolics of rapeseed/canola: A review. *Food Chemistry*, 62(4), 489–502.

Peng, L. P., Xu, Y. T., Li, X. T., & Tang, C. H. (2020). Improving the emulsification of soy β-conglycinin by alcohol-induced aggregation. *Food Hydrocolloids*, 98(May), 105307.

Salgado, P. R., Ortiz, S. E. M., Petruccelli, S., & Mauri, A. N. (2012). Functional food ingredients based on sunflower protein concentrates naturally enriched with antioxidant phenolic compounds. JAOCS, *Journal of the American Oil Chemists' Society,* 89(5), 825–836.

Sari, Y. W., Bruins, M. E., & Sanders, J. P. M. (2013). Enzyme assisted protein extraction from rapeseed, soybean, and microalgae meals. *Industrial Crops and Products*, 43(1), 78–83.

Tan, S. H., Mailer, R. J., Blanchard, C. L., & Agboola, S. O. (2011a). Canola Proteins for Human Consumption: Extraction, Profile, and Functional Properties. *Journal of Food Science.* 76(1).

Tan, S. H., Mailer, R. J., Blanchard, C. L., & Agboola, S. O. (2011b). Extraction and characterization of protein fractions from Australian canola meals. *Food Research International*, 44(4), 1075–1082.

Tranchino, L., Costantino, R., & Sodini, G. (1983). Food grade oilseed protein processing: sunflower and rapeseed. *Qualitas Plantarum Plant Foods for Human Nutrition*, 32(3–4), 305–334.

USDA. (2020). Oilseeds: world markets and Trade. Circular Series FOP 06-17. *Global Oilseed Consumption Continues to Grow Despite Slowing Trade and Production*, 1–50.

Wanasundara, J. P. D. (2011). Proteins of Brassicaceae Oilseeds and their Potential as a Plant Protein Source. *Critical Reviews in Food Science and Nutrition.* 51(7) 638-677.

Wanasundara, J. P. D., Abeysekara, S. J., McIntosh, T. C., & Falk, K. C. (2012). Solubility differences of major storage proteins of brassicaceae oilseeds. *JAOCS, Journal of the American Oil Chemists' Society*, 89(5), 869–881.

Wu, J., & Muir, A. D. (2008). Comparative Structural, Emulsifying, and Biological Properties of 2 Major Canola Proteins, Cruciferin and Napin. *Journal of Food Science*, 73(3), C210–C216.

Yamazaki, E., Murakami, K., & Kurita, O. (2005). Easy Preparation of Dietary Fiber with the High Water-Holding Capacity from Food Sources. *Plant Foods for Human Nutrition*, 60, 17–23.

Yang, C., Wang, Y., Vasanthan, T., & Chen, L. (2014). Impacts of pH and heating temperature on formation mechanisms and properties of thermally induced canola protein gels. *Food Hydrocolloids*, 40, 225–236.

Yoshie-Stark, Y., Wada, Y., & Wäsche, A. (2008). Chemical composition, functional properties, and bioactivities of rapeseed protein isolates. *Food Chemistry*, 107(1), 32–39.

Zuorro, A., Iannone, A., & Lavecchia, R. (2019). Water-organic solvent extraction of phenolic antioxidants from brewers' spent grain. *Processes,* 7(3).

2

Chapter 3

Rapeseed protein concentrate as a potential ingredient for meat analogues

Abstract

The potential for using rapeseed protein concentrate (RPC) as a novel protein source for meat analogues was investigated using shear cell technology with RPC-only and RPC-wheat gluten (WG) mixtures. The resulting products were characterized by texture analyzer, confocal laser scanning microscopy (CLSM) and X-ray micro-tomography. Soy protein concentrate (SPC) was chosen as the benchmark because of its known capacity to create fibrous structures. Both RPC-only and RPC-WG mixtures could be transformed into fibrous products when processed at 140 ℃ and 150 ℃ with 40 wt% dry matter. The fibrous structure was improved by adding of WG into RPC at 140 ℃ and the color of the RPC-WG product became lighter with more WG added. CLSM images revealed that the protein formed a continuous phase, and the RPC inherent polysaccharides acted as a dispersed phase. Overall, RPC is concluded as a promising alternative protein source after SPC for meat analogue applications.

Industrial relevance

Rapeseed meal, which is a by-product from extraction of rapeseed oil, is currently mainly used as animal feed and seldom applied as a food ingredient. This study provides valuable insights into the potential of rapeseed protein concentrate produced by washing rapeseed meal with aqueous ethanol as an alternative plant protein for meat analogues. The outcomes of this study demonstrated the potential of rapeseed protein concentrates for structuring purposes, which is a step towards its commercial use as an environmentally sustainable meat analogue ingredient.

3

3.1 Introduction

Plant-based meat analogues have received great interest from consumers who want to reduce their meat consumption. It is recognized that over-consumption of meat products is not only unhealthy but can also lead to environmental issues and ethical concerns about animal welfare. Shear cell technology has been reported to produce anisotropic fibrous meat analogues using (mixtures of) protein isolates or concentrates from soy, peas, wheat, and fababean (Dekkers, Nikiforidis, & Van der Goot, 2016; Grabowska et al., 2016; Grabowska, Tekidou, Boom, & van der Goot, 2014; Schreuders et al., 2019). Plant-based meat analogues from sources such as legumes, oilseeds and cereals are gaining importance to address consumer demands and sustainability in future food supply. An important breakthrough would be the increased use of underutilized protein-rich by-products in meat analogue applications.

Rapeseed meal is a by-product obtained after oil extraction, but it is seldom used for food applications. It has been suggested as an interesting alternative plant protein source due to its high protein content (35%–40%) and well-balanced amino acid profile (Tan et al., 2011). In addition, favorable functionality has been reported with respect to emulsifying, gelling and oil/water binding properties (Asgar, Fazilah, Huda, Bhat, & Karim, 2010; Von Der Haar et al., 2014; Wanasundara, 2011). The commercial value of this by-product would also increase significantly by making it suitable for application in meat analogues. Highly refined rapeseed protein isolates have been proposed as binders for meat products (Wanasundara, McIntosh, Perera, Withana-Gamage, & Mitra, 2016). A recent consumer study showed that the use of rapeseed protein as a main ingredient for meat analogues has gained consumer interest and attention (Banovic & Sveinsdóttir, 2021).

The formation of fibrous materials in shear cells is favored when plant materials consist of two immiscible phases that deform and align upon shearing (Grabowska et al., 2014). Two immiscible phases can be achieved through mixing purified ingredients with different water holding capacities (WHCs) (i.e., soy protein isolate [SPI] and wheat gluten [WG]), or they can be present naturally in a single but less purified ingredient, such as soy protein concentrate (SPC) (i.e., proteins and polysaccharides). Rapeseed protein concentrate (RPC) is obtained from rapeseed meal after aqueous alcohol washing. As a result, the

composition of RPC is similar to that of SPC in that it contains both proteins and polysaccharides (Wanasundara, 2011; Wanasundara et al., 2016). The polysaccharides mainly originate from the hulls and the cotyledon in rapeseed meal and are present as cellulose, hemicellulose and pectins. RPC has been studied in a shear cell before for fish feed to partially replace other plant protein sources, but at lower temperature than normally used to make fibrous materials. A solid, homogeneous material was obtained (Draganovic, Boom, Jonkers, & Van Der Goot, 2014). It showed potential to solidify, which is one of the requirements to become a suitable meat analogue ingredient.

Thus, the aim of this study was to investigate the structuring potential of RPC-only and RPC-WG mixtures for meat analogue production in a shear cell using different temperatures and ratios of RPC and WG. WG is often used in plant protein mixtures to enhance fiber formation in meat analogues (Cornet et al., 2021). The structuring properties of the product was compared with that from SPC and an SPC-WG mixture by texture analyzer using the uniaxial tensile test. The morphology of the structure was visualized by confocal laser scanning microscopy (CLSM). The air porosity of the sheared product was analyzed by X-ray microtomography (XRT).

3.2 Materials and methods

3.2.1 Materials

RPC was provided by the Avril Group (France). Vital WG (Viten) was purchased from Roquette (Zaventem, Belgium). SPC (Alpha 8 IP; Solae Europe SA, Le Grand-Saconnex, Switzerland) was purchased from Dupont (Wilmington, DE, USA). NaCl was obtained from Sigma-Aldrich (Zwijndrecht, the Netherlands). Rhodamine B (Sigma R 6626; Sigma-Aldrich) and Calcofluor-white (Fluka, 18909; Sigma-Aldrich) were used as staining agents for CLSM. The dry matter composition of RPC, SPC and WG is shown in Table 3-1; the composition of RPC was obtained from the Avril Group and the composition for SPC and WG is listed according to the manufacturer's specifications.

The WHC and nitrogen solubility index (NSI) were also measured, and the results are given in Table 3-1. The ability of the insoluble fraction to holding water was determined by adding 1 g of material and 49 g of Milli-Q water to a 50-mL Falcon tube and rotated for

24 h in a rotator (Bibby Scientific Stuart Rotator Disk SB3, Thermo Fisher Scientific, Waltham, MA, USA) for hydration at a speed of 20 rpm. The dispersion was then centrifuged at a speed of $15,000 \times g$ at 25 °C for 10 min. The wet pellet was transferred into an aluminium tray and dried in the oven at 105 °C for 24 h. The nitrogen content in the dry pellet ($N_{dry\ pellet}$) and in the original sample ($N_{original}$) were measured with the Dumas combustion method using a nitrogen analyzer (Flash EA 1112 Series; Thermo Scientific, Breda, the Netherlands). The mass of the original sample, wet pellet and dry pellet were obtained, denoted as $M_{original}$, $M_{wet\ pellet}$ and $M_{dry\ pellet}$. The WHC and NSI were calculated using equations (1) and (2).

$$\text{WHC} = \frac{M_{wet\ pellet} - M_{dry\ pellet}}{M_{dry\ pellet}} \text{ [g water/g dry pellet]} \tag{1}$$

$$\text{NSI} = \frac{N_{original} \times M_{original} - N_{dry\ pellet} \times M_{dry\ pellet}}{N_{original} \times M_{original}} \text{ [\%]} \tag{2}$$

Table 3-1 Composition of RPC, SPC and WG, as well as the water holding capacity (WHC) and nitrogen solubility index (NSI).

Composition (% in dry base)	RPC	SPC	WG
Protein	55.9	73.9	79.4
Oil	2.2	2.1	NA
Ash	8.9	7.7	NA
Carbohydrate	33.6	21.9	12.61
- Insoluble fiber	30.1	16.4	NA
- Soluble fiber (pectin)	3.4	3.3	NA
- Soluble sugars	0.1	2.2	NA
WHC (g water/g dry pellet)	4.9 ± 0.4	6.3 ± 1.0	1.6 ± 0.03
NSI (%)	19.5 ± 0.7	42.9 ± 3.6	10.3 ± 3.9

NA, not applicable.

3.2.2 Methods

3.2.2.1 Structure formation

Sample preparation

Aqueous dispersions of RPC, SPC, WG, RPC-WG mixtures, and SPC-WG mixtures were prepared, and the compositions are listed in Table 3-2. Preliminary tests showed that a fibrous structure could be formed with RPC-only at 40 wt% dry matter. Therefore, 40 wt% was selected for all the tests in the paper, as well as 1 wt% sodium chloride, and 59 wt% demineralized water. For each experiment, samples with a total weight of 90 g were prepared as explained in the next section. Results with lower RPC concentrations are shown in Fig. S1. Samples were prepared by mixing sodium chloride with demineralized water in a plastic beaker. RPC and SPC were added to the beaker and mixed using a flat spoon, which was covered with a parafilm to prevent water evaporation. WG, if used in mixtures, was added after 30 min hydration, mixed thoroughly with a flat spoon and immediately transferred to a shear cell for further processing.

Table 2. Overview of the shear cell experiments with respect to the composition of RPC-only, SPC-only, RPC-WG mixtures and SPC-WG mixtures and the temperature applied in the shear cell.

Sheared/heated product	Composition (wt%)	T (°C)
RPC-only	40	25, 120, 130, 140, 150
RPC-WG mixtures	20-20	95, 120, 130, 140
RPC-WG mixtures	32-8, 26-14, 20-20, 14-26,8-32	140
WG-only	40	140
SPC-only	40	95, 120, 140
SPC-WG mixtures	20-20	

Structure formation

A high-temperature conical shear cell (HTSC) (Wageningen University, Wageningen, the Netherlands) was used for the structuring experiments. The HTSC was

designed in house and has been described previously. It is a cone-cone device with a rotating bottom cone to produce a defined simple shear flow (Grabowska et al., 2016). Heating and cooling were done using an external oil bath. The protein mixtures, which were hydrated for 30 min before shearing, were transferred to the preheated HTSC and then sheared for 15 min at 30 rpm at a set temperature. Different temperatures were tested in this study form 85 °C to 150 °C. The shearing was stopped, and the shear cell was cooled down to 25 °C in 15 min to allow removal of the pancake-shaped sample. The sample was stored in a plastic bag. All tests were done in duplicate.

3.2.2.2 Analysis

Macrostructure

The morphologies of sheared and heated products of RPC, SPC-only, and the mixtures of RPC-WG, SPC-WG were analyzed by manually deforming the samples in a direction parallel to the shear flow and then the structure formed was inspected visually.

Color measurement

The color of the sheared samples from RPC-only and RPC-WG mixtures were determined using a colorimeter (Chroma Meter CR-400, Konica Minolta, Country). The color intensity was indicated as L* (perceptual lightness), a* (-a* = green and +a* = red) and b* (-b* = blue and +b* = yellow).

Tensile strength analysis

The mechanical properties of the sheared samples were measured using a texture analyzer (Stable Micro System, Godalming, UK). Tensile stress, tensile strain and Young's modulus (YM) were measured by uniaxial tensile tests, which were performed at room temperature with a constant deformation speed of 1 mm/s. Three tensile bars were cut from the samples using a dog-bone-shaped cutter in the parallel and perpendicular directions along the shearing direction. The width and thickness of the tensile bars were then measured using a digital calliper (Mitutoyo, Kawasaki, Japan) to calculate the initial cross-sectional area. The edges of the tensile bars were fixed into tensile grips, resulting in an initial length of 15.5 mm (L_0) for the sample. The force needed to break the sample $F(t)$ was recorded by the Exponent

software (Stable Micro System). The true stress (σ) and true strain (ε) were calculated based on the assumption that the volume of the tensile bar did not change during elongation (Choung & Cho, 2008; Raheem, 2014).

$$\sigma = \frac{F(t)}{A_0} \times \frac{L(t)}{L_0} \ [Pa] \tag{3}$$

$$\varepsilon = \ln \frac{L(t)}{L_0} \ [mm/mm] \tag{4}$$

where L_0 is the initial length of the sample and $L(t)$ is the length of the sample at fracture time t. A_0 is the initial cross-sectional area. YM was calculated from the slope of the tensile stress-strain curve with the tensile strain between 0.5 and 1.5. The anisotropic index (AI) was calculated as the quotient of the parallel value and the perpendicular value:

$$AI_{\sigma} = \frac{\sigma_{par}}{\sigma_{per}} \ [-] \tag{5}$$

$$AI_{\varepsilon} = \frac{\varepsilon_{par}}{\varepsilon_{per}} \ [-] \tag{6}$$

$$AI_{YM} = \frac{YM_{par}}{YM_{per}} \ [-] \tag{7}$$

Microstructure

A confocal laser scanning microscope (type 510; Zeiss, Oberkochen, Germany) was used to visualize the structured samples on a microscopic scale. RPC-WG and SPC-WG mixtures were frozen before cutting the samples along the shear flow direction into rectangular shapes with dimension of approximately $3 \times 5 \times 10$ mm. The samples were frozen quickly using liquid nitrogen. A cryomicrotome (Micron CR50-H, Adamas Instruments, Rhenen, the Netherlands) was used at $-20\ °C$ to slice the sample into 40-µm-thick specimens. The specimens were then stained with a mixed solution of Rhodamine B 0.002 wt% and Calcoflour White 0.01 wt% at a 1:1 ratio, after which they were covered with a glass and stored in dark for 1 h before analysis. Excitation light in CLSM was provided by two lasers: a HeNe laser at 543 nm for Rhodamine B, and a blue/violet diode laser at 405 nm for Calcoflour White. A 10× EC Plan-Neofluar/0.5 objective lens was used to take the images. The blue edition of the ZEN software (Carl Zeiss Microscopy, Jena, Germany) was used to analyze the images.

Morphology

Scanning Electron Microscope (SEM) (JEOL JCM-7000, the Netherlands) was used to observe the morphology of the RPC, SPC and WG dry powders. The dry samples were added on the double-side adhesive conductive carbon tabs and the samples were sputter-coated with gold. Compressed air was used to distribute the sample evenly on the surface of carbon tabs. The accelerating voltage was 10 kV. The SEM pictures were taken at a scale of 50 μm.

X-ray microtomography

Inclusion of air in the fibrous products was analyzed non-invasively and non-destructively using XRT (GE Phoenix v|tome|x m; General Electric, Wunstorf, Germany). A 240 kV micro focus tube with tungsten target was used with a voltage of 80 kV and a current of 90 μA. The images were recorded by a detector (GE DXR detector array with 2024×2024 pixels and pixel size 200 μm) located 815 mm from the X-ray source. Fragments $4 \times 5 \times 20$ mm were cut from the sheared samples. The fragments were placed into an Eppendorf tube to avoid moisture loss and positioned 28.55 mm from the X-ray source, resulting in a spatial resolution of 7 μm. Full scans of 1500 projections were taken by placing the sample on a rotary stage over 360° with steps of 0.24°. The projections obtained were reconstructed into a single 3D structure using the GE reconstruction software (GE, Wunstorf, Germany), with the first projection skipped. Reconstructed images of the samples were analyzed using Avizo imaging software version 9.2.2. Two reconstructed images were used to calculate the porosity of the samples.

3.2.2.3 Statistical analysis

The statistics in this paper were analyzed using SPSS software, version 25.0 (IBM, Armonk, NY, USA). A univariate general linear model with the least significant difference (LSD) test was carried out to investigate the significant differences with respect to Fig. 3-1, 3-2, 3-3. Differences were considered significant when $P < 0.05$, which are shown in the appendix Table S3-1. The same test was applied to the color measurement and the differences are shown as the small letters in Fig. 3-9.

3.3 Results

3.3.1 Effect of temperature effect on the structuring properties

RPC-only and SPC-only

RPC-only dispersions with 40 wt% were sheared at 120, 130, 140 and 150 °C in the shear cell. The resulting structures are shown in Table 3-3. A fibrous structure was obtained after processing at 140 °C or 150 °C; the latter resulted in a more pronounced fibrous material. A crumbled gel-like structure was obtained when RPC was sheared at lower temperatures of 120 °C or 130 °C. The mechanical properties of the sheared and heated products were measured using a texture analyzer and the results are shown in Fig. 3-1. For RPC-only, tensile stress and strain values in the parallel direction increased with higher temperature, whereas the value in the perpendicular direction was similar for all temperatures. The AI value was >1 after processing at 140 °C, which corresponds to the mechanical anisotropy. The sample produced at 120 °C was too brittle to allow good measurements. Shearing at 150 °C led to more anisotropy, up to an AI value of 3. Results showed that YM was independent of temperature in both directions, and thus the stiffness of the product was similar after processing at different temperatures.

To place the results with RPC in a broader context, we compared its structuring capacity with SPC. The macrostructure of SPC-only product is shown in Table 3-4. For the SPC-only sheared product, a crumble structure was observed below 120 °C. Thin fibers and layers were found when SPC-only was sheared at 140°C. The mechanical properties of the SPC-only products are shown in Fig. 3-2 (A–C). The value for the tensile stress in the parallel direction increased with higher process temperature, with an exception for the product processed at 130 °C. The tensile stress in the perpendicular direction appeared to be independent of temperature, again except at 130 °C. As a result, the AI value increased when processing at a higher temperature. With respect to the tensile strain, the lowest value was observed at 130 °C. Although the values in the parallel and perpendicular direction fluctuated at different temperatures, the AI value increased from 1 to 2 in the temperature range studied. The YM decreased in both directions when a higher temperature was applied, resulting in similar AI values.

Table 3-3 Macrostructure of the sheared samples from RPC (40 wt%) and RPC-WG (20-20 wt%) at 95, 120, 130, 140 and 150 °C.

Temperature	95 °C	120 °C	130 °C	140 °C	150 °C
RPC-only	NA				
RPC-WG					
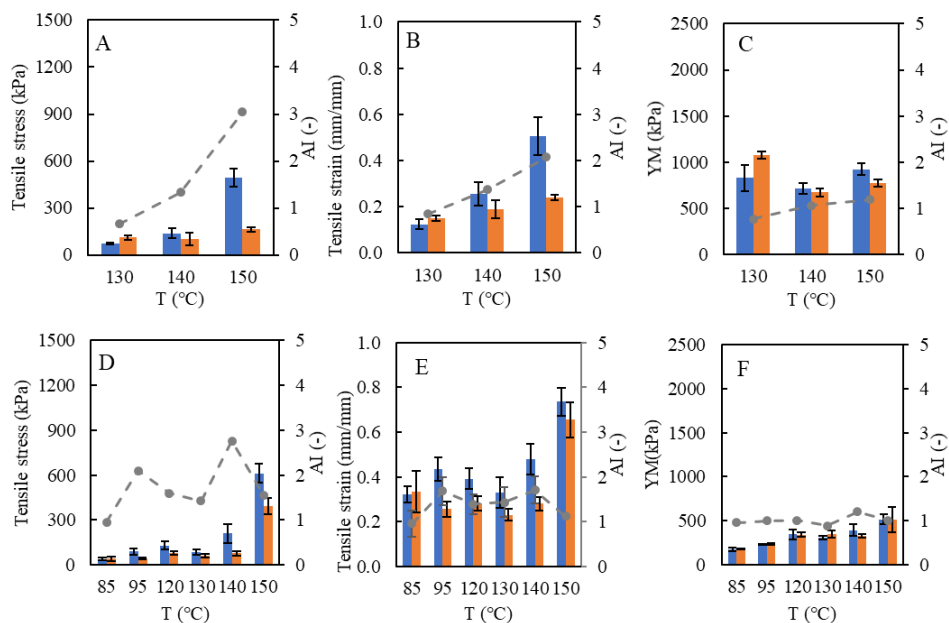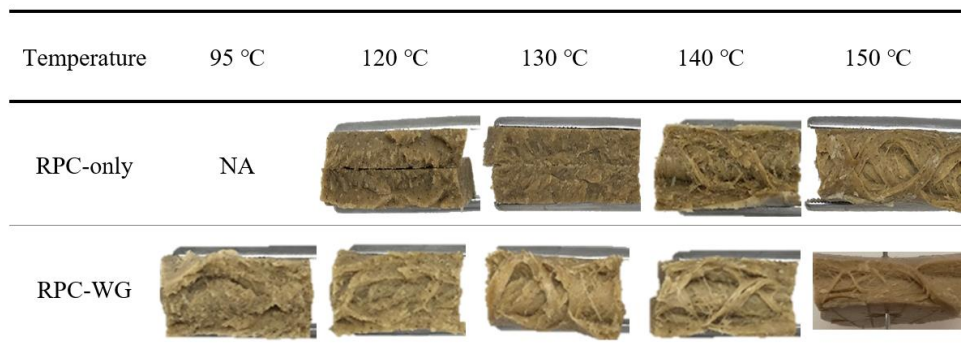
Fig. 3-1 Tensile stress (A), tensile strain (B) and YM (C) of the sheared 40 wt% RPC sample at 130, 140 and 150 °C. Tensile stress, tensile strain and YM of the 40 wt% RPC-WG at 85, 95, 120, 130, 140 and 150 °C are shown in (D), (E) and (F). Blue bars indicate the parallel direction, orange bars indicate the perpendicular direction, and the dotted grey line indicates the anisotropic index. The statistical analysis is showed in the appendix Table S3-1.

Table 3-4 Macrostructure of SPC (40 wt%) and SPC-WG (20-20 wt%) at 95, 120, 130, 140 and 150 °C.

Temperature	95 °C	120 °C	130 °C	140 °C	150 °C
SPC-only					
SPC-WG					
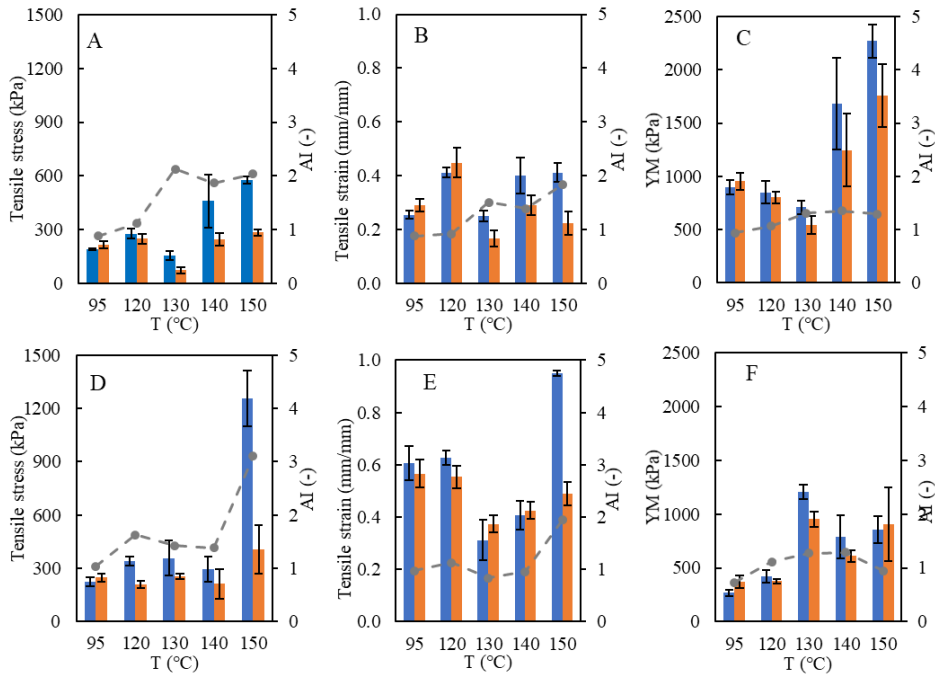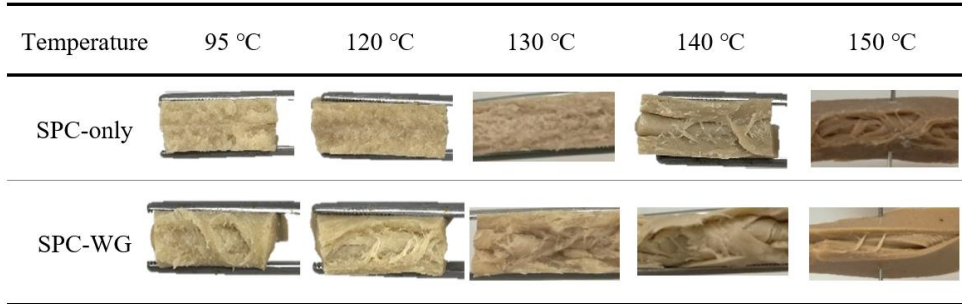
Fig. 3-2 Tensile stress (A), tensile strain (B) and YM (C) of the 40 wt% SPC. Tensile stress, tensile strain and YM of 40 wt% SPC-WG of 20:20 are shown in (D), (E) and (F). Temperatures of 95, 120, 130, 140 and 150 °C were tested. Blue bars indicate the parallel direction, orange bars indicate the perpendicular direction, and the dotted grey line indicates the anisotropic index. The statistical analysis is showed in the appendix Table S3-1.

RPC-WG and SPC-WG mixtures

The 20-20 wt% RPC-WG mixture led to lighter-colored fibrous products when processed at 130 °C and 140 °C (Table 3-3). A gel-like structure with tiny fibers was formed at 150 °C for RPC-WG, whereas a gel-like and crumble structure was generated at 95 °C and 120 °C. Mostly, the tensile stress in the parallel direction increased with temperature, except for a slight decrease when processed at 130 °C (Fig. 3-1 D-F). Although the trend for the perpendicular direction was less obvious, the highest value was obtained at 150 °C. The AI value remained between 1 and 2 at most temperatures, which suggests limited mechanical anisotropy. The highest AI value of 2.8 was obtained for tensile stress in the parallel direction at 140 °C. The YM of RPC-WG products showed a slight increase with increasing temperature for both directions, but the values were much lower compared with the RPC-only product. The AI value of the RPC-WG product sheared at 150 °C was nearly 1, which is in line with the gel structure observed in Table 3-3. The structures of sheared products with respect to the 20-20 wt% SPC-WG mixture processed at 95, 120, 130, 140 and 150 °C are shown in Table 3-4. The 20-20 wt% SPC-WG product showed a crumble gel structure below 130 °C similar to the RPC-WG product. A gel structure with layers was obtained after processing at 140 °C and 150 °C.

The mechanical properties of the SPC-WG products are shown in Fig. 3-2 (D–F). The highest tensile stress was found at 150 °C. This led to the highest AI value of 3, which was similar to the AI value for the RPC-only product at 150 °C. However, no fibrous structure was observed at 150 °C despite the high AI value. This might be because the fibrous structure was too small to be visible by eye, and the current methods in fibrous structure quantification is still limited (Schreuders, Schlangen, Kyriakopoulou, Boom, & van der Goot, 2021). From the observation, the product structure could be characterized best as a gel with layers (Table 3-4). At lower processing temperatures, lower tensile stress values were found for both directions; they were similar to the value in the perpendicular direction leading to an AI value of ~1. The lowest tensile strain value was obtained when processing at 130 °C. Due to a decrease in tensile strain for both directions at 130°C and 140°C, a similar AI value of 1 was found for both products. An increase in YM was found at 130°C, and the AI value of YM was slightly increased from 95 °C to 140 °C.

Despite the differences in the mechanical properties, the structures observed for the SPC-only and SPC-WG products were hardly dependent on the temperature at 40 wt%. In the case of RPC-only and RPC-WG products, a processing temperature of 140 °C was sufficient to obtain fibrous products. Therefore, 140 ℃ was applied in further investigations of the fibrous structure at different RPC and WG ratios.

3.3.2 Effect of composition on the structuring properties

This section describes the effect of adding different amounts of WG to the RPC and SPC on the structure of the products (Table 3-5). All RPC-WG products showed a fibrous structure. The RPC-WG mixtures were a light grey color, which became brown when the product contained more RPC. The tensile stress values of the RPC-WG mixtures (Fig. 3-3) were between 100 and 300 kPa for the parallel direction and ranged from 50 to 100 kPa for the perpendicular direction. On average, AI values of ~3 were obtained, which were higher than the average AI value of 1.3 for the RPC-only sample. The large standard deviation of the tensile stress in the parallel direction was probably caused by the heterogeneity of the fibrous material at the length scale of the sample. Fibers were clearly visible in that size range. When overviewing all the mechanical data of RPC-WG, AI value was approximately 3 for all the ratios. The fibrous structure formed was different at low WG ratios for 32-8 and 26-14 wt% compared to higher WG ratios between 20-20 and 8-32 wt%. An increase in WG led to more pronounced fibrous products with tiny fibers and even more than the WG-only product.

In the case of SPC-WG products, gel-like structures were observed with 32-8 wt% (Table 3-5), which is similar to SPC-only. Gel-like structures with layers were formed with the product containing SPI-WG ratios of 26-14 and 20-20 wt%. The fibrous structure became more pronounced when the product contained more WG. The tensile stress for the parallel direction increased from products containing SPC-WG with ratios of 40-0 to 26-14 wt%, whereas the value decreased in the perpendicular direction leading to a highest AI value of 5 for the product with the ratio 26-14 wt%. This result indicated that the addition of WG to SPC enhanced the anisotropy of tensile stress and strain; the 20-20 wt% product was the exception.

Table 3-5 Macrostructure of RPC-WG and SPC-WG with ratios of 40-0, 32-8, 26-14, 20-20, 14-26, 8-32, 0-40 wt% at 140 ℃.
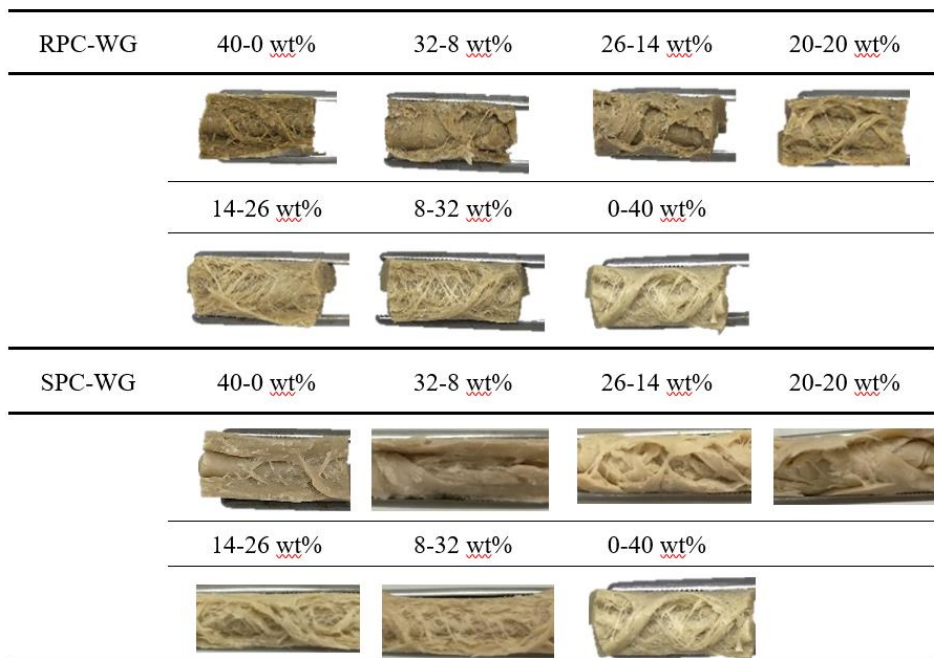
The YM decreased when the WG content increased in the RPC-WG and SPC-WG products and this effect was also found to be higher with the SPC-WG product. The AI value for the YM was close to 1 for almost all products. Thus, the addition of WG above a certain ratio can improve the fibrous structure formation for the SPC-WG and RPC-WG products.

3.3.3 Microstructure

CLSM was used to examine the microstructure and the distribution of protein and polysaccharides in the sheared RPC and RPC-WG products. The results obtained with the fluorescence channel are shown in Fig. 3-4 and 3-5.

For the sheared RPC-only products, intact RPC particles were observed at room temperature and after processing at 120℃ (Fig. 3-4). These particles were found to be similar as observed by SEM pictures in the appendix (Fig. S3-2), with the particle size of approximately 200 μm (Jia, Rodriguez-Alonso, Bianeis, Keppler, & van der Goot, 2021).
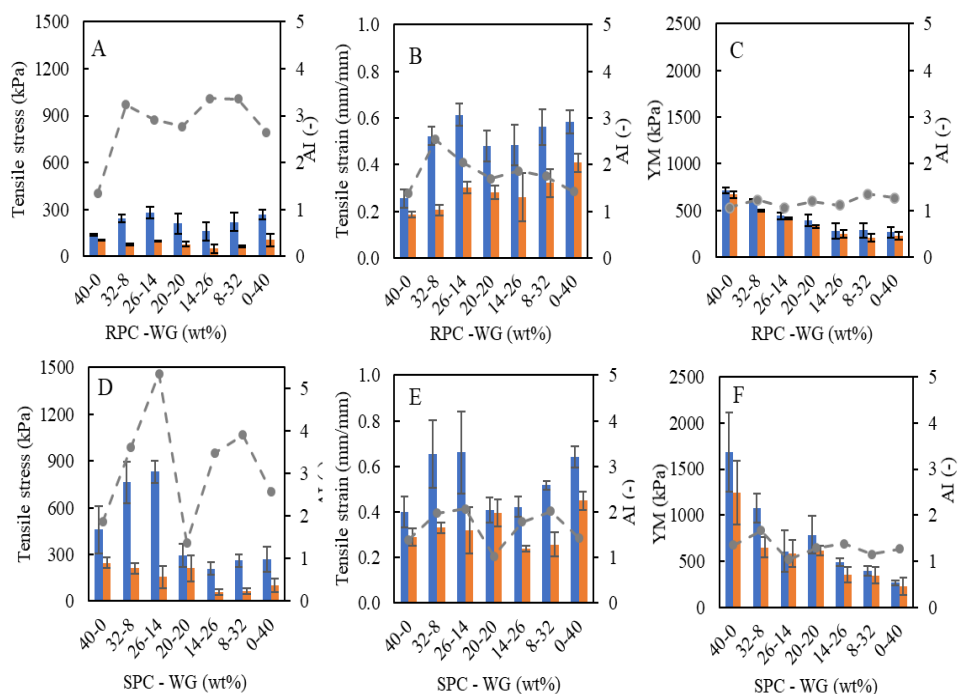
Fig. 3-3 Tensile stress, tensile strain and YM for RPC-WG and SPC-WG at ratios of 40-0, 32-8, 26-14, 20-20, 14-26, 8-32 and 0-40 wt% are shown. Shearing conditions of 140 °C, 30 rpm and 15 min were tested. Blue bars indicate the parallel direction, orange bars indicate the perpendicular direction, and the dotted grey line indicates the anisotropic index. The statistical analysis is showed in the appendix Table S3-1.

The RPC particles are consisted of proteins (stained red) surrounded by polysaccharides (represented by the blue color). The polysaccharide phase became better visible at 120 °C onwards. This might be due to the finely dispersed unheated RPC particles became aggregated by heating and hearing at higher temperatures. The intact RPC particles disappeared at 140 °C, forming a more continuous protein phase and dispersed polysaccharide phase. The structure was broken apart during sample preparation and the breaking part were found within the polysaccharide phase in Fig. 3-4 (C and D). In the case of RPC-WG 20-20 wt%, individual RPC particles were still observed at 95 °C and 120 °C in Fig. 3-4 (E and F); the WG already formed a connected phase between the individual RPC particles, thus forming another phase.
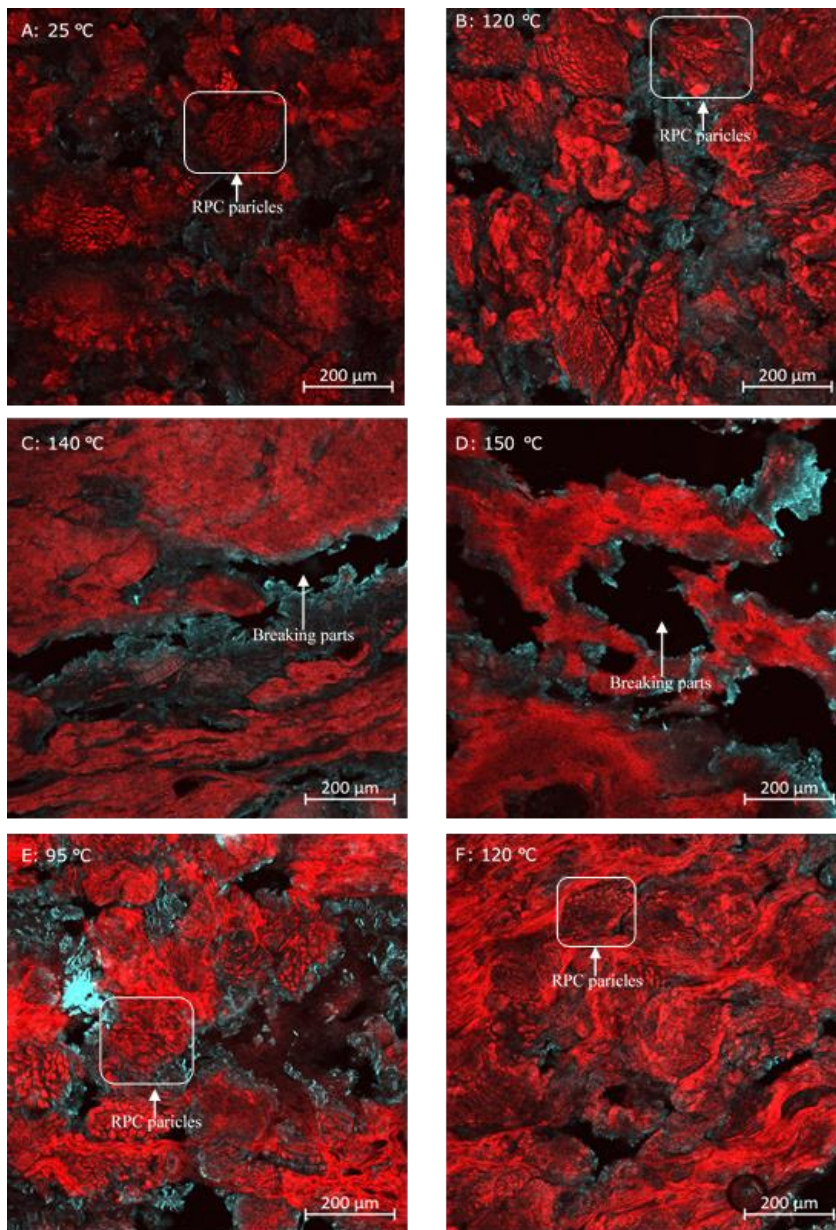
Fig. 3-4 Microstructure of the sheared products from RPC-only was obtained at shear temperatures of (A) 25 °C, (B) 120 °C, (C) 140 °C and (D) 150°C by CLSM under the fluorescence channel. The sheared product from RPC-WG (20-20 wt %) at 95 °C and 120 °C is shown in (E) and (F). The products were sheared at 30 rpm by 15 min. Scale bars, 200 µm; each image was selected from three images.
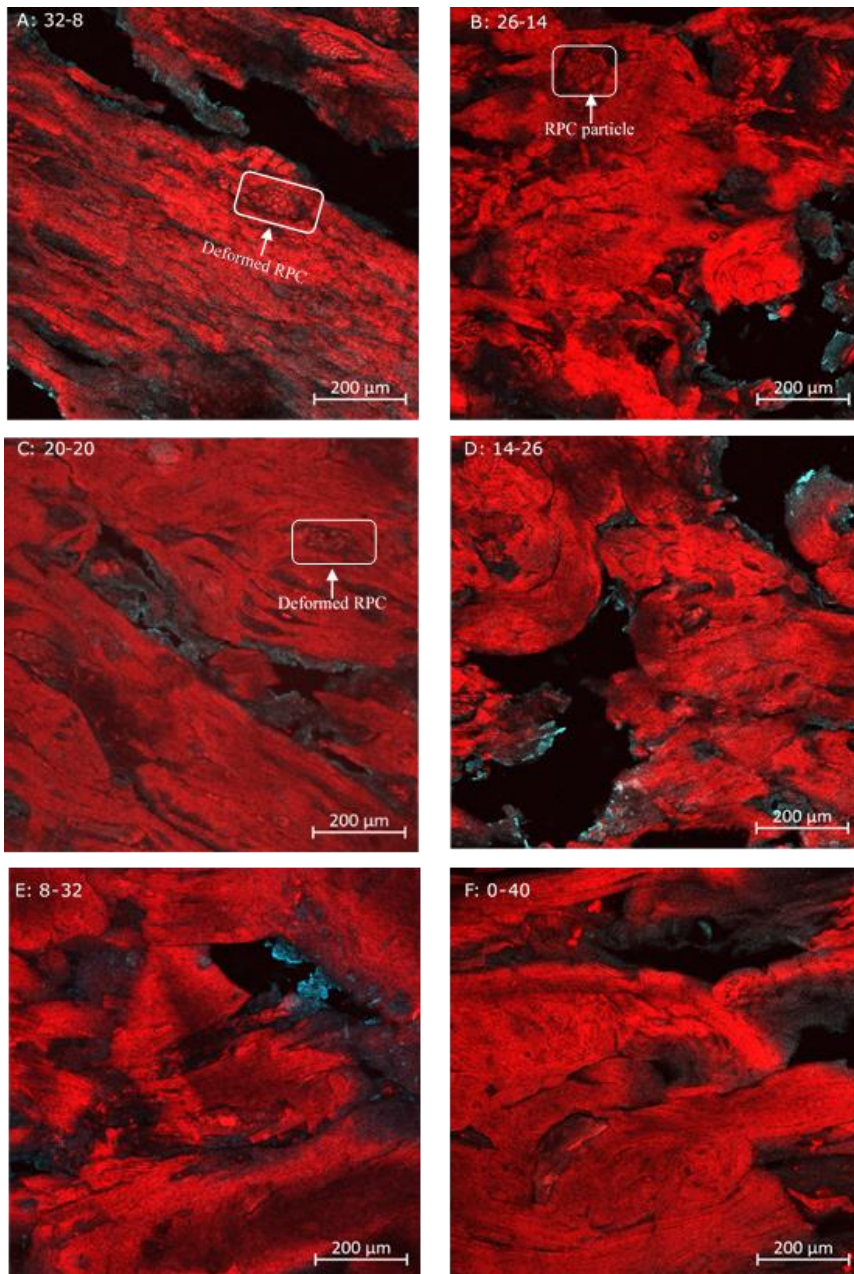
Fig. 3-5 Microstructure of the sheared products from RPC-WG at ratios of 32-8, 26-14, 20-20, 14-26, 8-32 and 0-40 wt% under process conditions of 140 ℃, 30 rpm and 15 min by CLSM under the fluorescence channel. Scale bars, 200 µm; each image was selected from three images.

The RPC particles disappeared for the 20-20 wt% product when the material was processed at higher temperatures of 140 °C, although a few deformed RPC particles were still visible (Fig. 3-5C). The microstructures of RPC-WG with other ratios processed at 140 °C are also shown in Fig. 3-5. Similar to the 20-20 wt% RPC-WG product, deformed RPC particles were visible in the 32-8 wt% RPC-WG product. These deformed RPC particles consisted of protein and fiber and were dispersed in a continuous phase. However, the proteins from RPC and WG were hardly distinguishable for all the mixing ratios tested at 140 °C, which indicates that the protein from RPC and WG was mixed at a much smaller length scale than visible with CLSM (i.e. 200 µm).

3.3.4 Incorporation of air

The reconstructed 3D X-ray tomography image of air in Fig. 3-6 showed air inclusion (void fraction) in RPC product when sheared at 25 °C. The void fraction became smaller when the products were sheared at a higher temperature. Hardly any air remained after shearing the products at 140 °C and 150 °C. The overall void fractions are shown in Fig. 3-7A. The void fraction decreased from 24 vol% for the product sheared at 25 °C to 5 vol% when the products were sheared at 120 °C. Almost all air had escaped when the product was processed at 140 °C, and an even lower void fraction of 0.01 vol% was measured after processing at 150 °C. These results could be explained by considering that the hydrated RPC particles were not fully melted at lower temperature, thus spaces remained available for air between the particles. The void fractions obtained with the sheared RPC-WG product were all <0.3 vol% at 140 °C, whereas slightly more air was found with the RPC-WG mixture of 8-32 wt% and 0-40 wt% in Fig. 3-7B. Therefore, it is suggested that the air void fraction of the sheared product is more dependent on the processing temperature than the RPC-WG ratios at 140 °C.
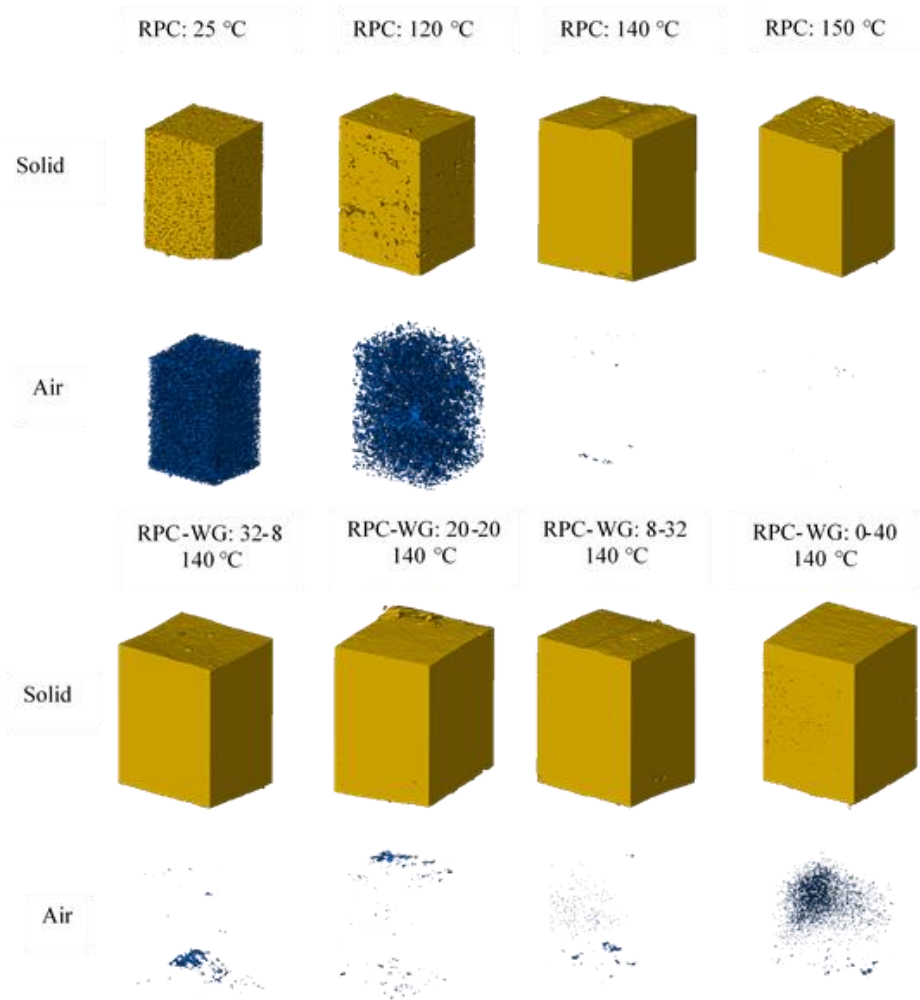
Fig. 3-6 X-ray microtomography images of a reconstructed trimetric image of the solid (yellow) sheared 40 wt% RPC products at 25, 120, 140 and 150 °C and RPC-WG product with ratios of 40-0, 32-8, 20-20, 8-32 and 0-40 wt% at 140 °C and the corresponding reconstructed trimeric image of the air in blue.
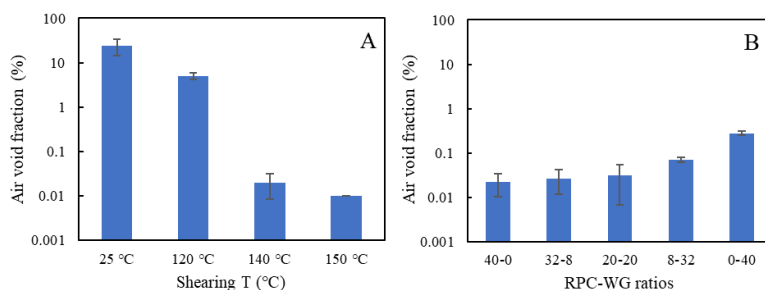
Fig. 3-7 Air void fraction of sheared RPC product at 25 °C, 120 °C, 140 °C and 150 °C (A) and sheared RPC-WG products with RPC ratios of 40-0, 32-8, 20-20, 8-32 and 0-40 wt% (B).

3.4 Discussion

Previous research revealed the importance of naturally existing immiscible phases of protein and polysaccharides for fibrous structure formation by SPC-only or SPI/pea protein isolate-WG mixtures in the shear cell (Grabowska et al., 2016; Schreuders et al., 2019). Here, we aimed to demonstrate that fibrous materials can also be obtained with RPC-only, similar to SPC-only, by using the remaining polysaccharides in the material as a second phase. We also aimed to test the effect of adding WG as an additional phase to the RPC on the structuring capacity.

Fibrous material in 40 wt% RPC-only was achieved at 140 °C and 150 °C. In contrast, the SPC-only sheared product of 40 wt% at these temperatures was characterized as a layered gel with some tiny fibers. This result was similar to previous results for a 40 wt% SPC-only sheared product; a fibrous structure was reported when the dry mass content was increased to 45 wt% with SPC-only (Grabowska et al., 2016). However, we found the tensile stress at 140 °C to be higher than reported earlier, which we attributed to different batches of SPC. Grabowska et al. (2016) used the break-up and alignment of the polysaccharide phase as an explanation for the fibrous structure formation for the sheared SPC-only product at 140 °C. Here, it is hypothesized that melting of RPC particles (consisting of protein and polysaccharides) happened at 140 °C, which explains the need for a high temperature (Fig. 3-4). Without this melting, RPC still behaves as a sand-like material that hardly takes up water during hydration, as we observed when mixing RPC and water at room temperature.

Melting of RPC at 140 °C makes it possible for the polysaccharides to be more easily aligned along the shearing direction and thus act as a dispersed phase to the proteins.

Similarly, RPC particles melting at 140 °C released proteins from the particles, and the proteins were mixed with WG in subsequent shearing in the RPC-WG mixtures. This can explain the continuous protein phase with no clear phase separation between the protein from WG and RPC after shearing and heating at 140 °C (Section 3.3.3). Furthermore, with respect to the 20-20 wt% RPC-WG and SPC-WG mixtures, a temperature of 130 °C was sufficient to create fibrous structures in both cases (Tables 3-3 and 3-4), but the mechanical properties were found to be relatively low at that temperature (Fig. 3-1 and 3-2). In the above discussion, it is hypothesized that the melting of RPC particles at 140 °C and subsequent availability of proteins is a prerequisite for fiber formation in RPC-only. Similar to that observation, the RPC particles in the RPC-WG mixture are not melted sufficiently at 130 °C, whereas WG already acts as a continuous phase and thus induces fiber formation at lower temperatures than observed for RPC-only, but the dispersed phase will be weak because of lack of melting. Therefore, the effect of adding WG to RPC might play an important role to reduce the temperature required for fiber formation. Schreuders et al. (2019) reported fibrous structure formation for PPI-WG (20-20% wt) at 120 °C and SPI-WG (20-20 wt%) at 140 °C, and the lowest mechanical properties were found at 130 °C. In that paper, WG was introduced as a second phase. A similar air inclusion effect as reported for PPI and SPI-WG mixtures was also observed for the RPC-WG sheared products at different shearing temperatures (Section 3.3.4). The low air porosity found at 140°C for RPC-only and RPC-WG mixtures also suggests the melting of RPC particles and the formation of a compact structure. However, further investigations would be needed to understand the two-phase system when WG is added to the RPC-WG mixtures at different temperatures.

A dry mass of 40 wt% was needed for the fibrous structure formation for RPC-only, results showed in the appendix Fig. S3-1, which is lower compared with 45 wt% for SPC-only (Grabowska et al., 2016). A comparison between RPC and SPC reveals that RPC has a lower protein content (22.4 vs 29.6 wt%) and higher polysaccharide content (13.2 vs 8.6 wt%) than SPC. In the case of the RPC-WG and SPC-WG mixtures, less WG was required for fibrous structure formation with RPC than for SPC. This yielded a wider range of ratios

required for fibrous structure formation with respect to the RPC-WG product (32-8 to 8-32 wt%) compared with the SPC-WG product (26-14 and 8-32 wt%) (Fig. 3-8A and Table 3-5). The composition of the mixtures with respect to protein and polysaccharides might affect the fibrous structure formation. The addition of WG to the concentrates increased the overall protein content and decreased the polysaccharide content. Thus, we plotted the tensile properties of all the tested materials at 140 °C against protein/polysaccharides ratios in Fig. 3-8 (B and C). The tensile properties were enhanced with increasing protein ratio (below 6 for SPC-WG 20-20 wt%) and the minimum AI value was found at 20-20wt%, but no fibrous structure was found in this region. This result suggested a change of the system from soy protein continuous phase into the WG continuous phase, and the change is hypothesized to be with the ratio of 20-20 wt%. Cornet et al., (2021) also reported that structuring the protein mixtures with respect to the SPI-WG and fababean isolate-WG in Shear Cell resulted in fibrous structures at gluten contents $\geq$ 0.5 wt/wt and the effect of gluten on swelling and fiber formation is universal for the tested proteins. A fibrous structure formed with ratios ranging between 2-7 for RPC-WG and 7-9 for SPC-WG, which suggests that a higher protein/polysaccharides ratio is necessary for fibrous structure formation with SPC-WG than for RPC-WG. The ratio of protein/polysaccharide might be one of the factors to explain the effect of the composition on fibrous structure formation. Besides protein/polysaccharides ratio, the other factors might also play a role in the structuring properties, such as amino acid profile and rheological characterization upon melting. Cysteine and methionine are the sulphur containing amino acid, which is important for the cross-linking properties by forming disulfide bonding upon heating (Berghout, Boom, & van der Goot, 2015). Furthermore, not only the amount of disulfide bonds in the protein plays a role, but also the accessibility of disulfide and free thiol groups is important for network formation (Cornet et al., 2020). Further investigation on these factors is still required to explain why a certain ratio is necessary.

The composition and the ratio of the concentrate are not only influencing the mechanical properties of the fibrous structure formed but also the color of the final product. The product became lighter when more WG was added in the RPC-WG mixtures (Table 3-5). The color of the sheared sample was measured by the colorimeter, indicating as L* (perceptual lightness), a* (-a* = green and +a* = red) and b* (-b* = blue and +b* = yellow).

Results in Fig. 3-9 showed that L* and b* was significantly increased by adding of the WG into RPC till the RPC-WG ratio of 26-14, while the intensity of a* was similar between the ratio of 40-0 and 26-14, and significantly decreased by further adding of WG. The change in the color is not necessarily related to change in the dominant continuous protein phase because both proteins from RPC and WG were mixed thoroughly which is hard to distinguish on the product scale (Section 3.3.1). It is most likely that the addition of lighter colored WG diluted the already darker colored RPC content. In addition, oxidized tannins in RPC form darkly colored polymers during processing at high temperatures. In the presence of WG, however, such oxidized tannins could react with available thiol groups from WG instead of polymerizing, which would reportedly form uncolored complexes (Keppler et al., 2020; Ozdal et al., 2013).

3
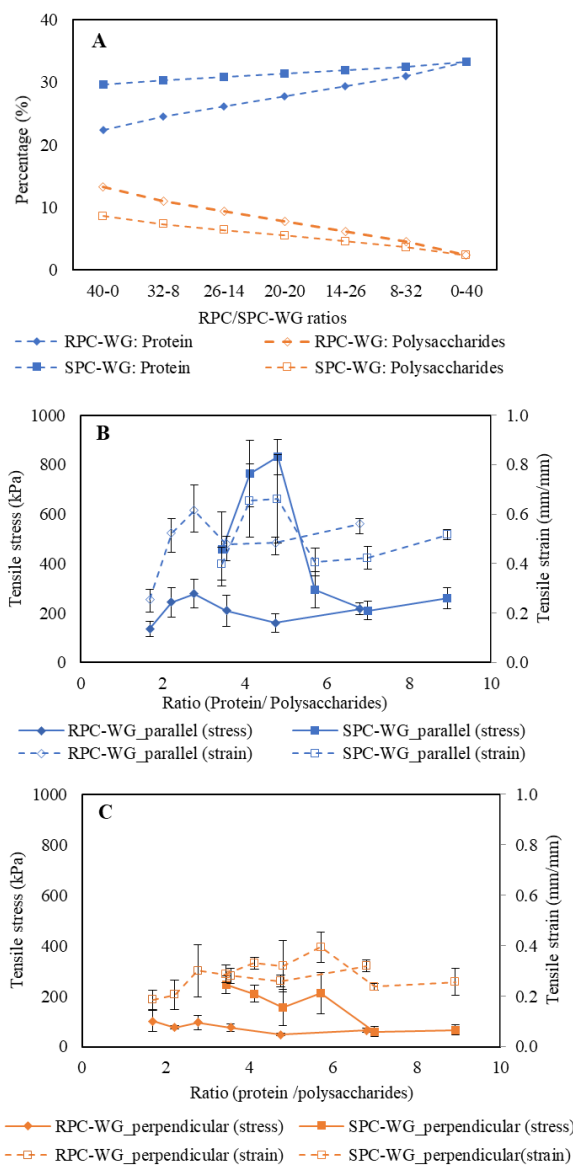
Fig. 3-8 The composition (A) of protein and polysaccharides of the RPC-WG mixtures and SPC-WG mixtures. The tensile stress (kPa) and tensile strain (mm/mm) of RPC-WG and SPC-WG mixtures at parallel direction (B) and perpendicular direction (C) as a function of the protein and polysaccharides ratio.
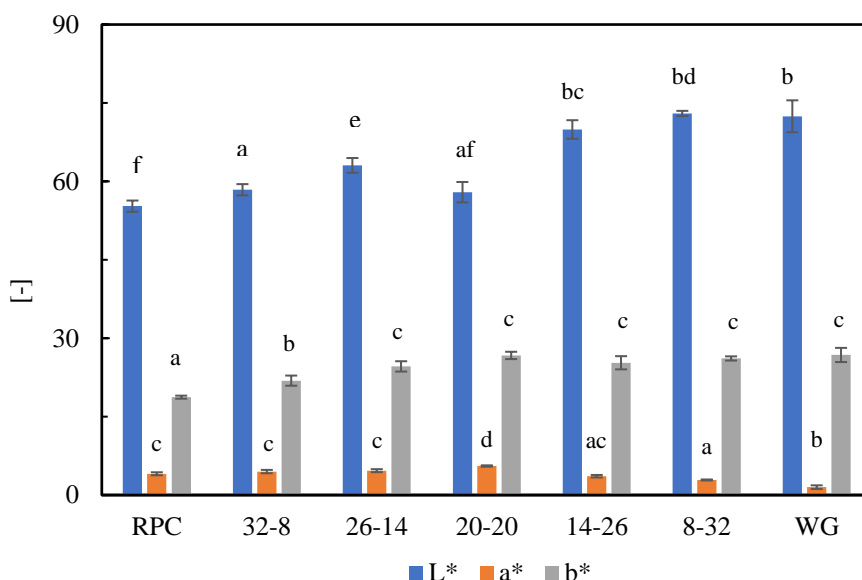
Fig. 3-9 Color intensity of the sheared RPC-only, RPC-WG mixtures at different ratios and WG-only products, indicated as L* (perceptual lightness), a* (-a* = green and + a* =red) and b* (-b* = blue and + b* =yellow). The statistics were analyzed with respect to L*, a* and b* individually and showed as the small letters.

3.5 Conclusion

This study reveals the potential of RPC as a novel ingredient for application in meat analogues. RPC could be used to make fibrous products even without the presence of WG. In addition, RPC formed more pronounced fibers compared with SPC under the same conditions. Also, in combination with WG, we noticed that RPC offers more possibilities to create a wide range of fibrous products compared with SPC at 140°C. This is because complete melting of RPC particles only occurred at a processing temperature of 140°C or above. The addition of WG into RPC at 140°C showed two effects: improved anisotropic structure with increased AI value on tensile stress for all ratios; lighter color of the sheared RPC-WG product than the RPC-only product. The structure formation observed in the RPC-/SPC-only product was explained by the presence of polysaccharides in those ingredients, although the mechanism of the exact structure formation process is not yet fully understood.

3.6 Supporting information

| 30 | 32.5 | 35 wt% | 37.5 | 40 wt% |
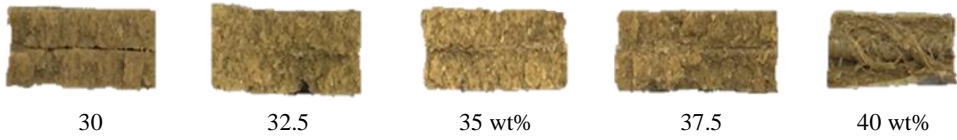
Fig. S3-1 Macrostructure of RPC product at different dry matter content of 30, 32.5, 35, 37.5 and 40 wt% sheared at 140 °C, 30 rpm and 15 min in the shear cell.

A: RPC (rapeseed protein concentrate)
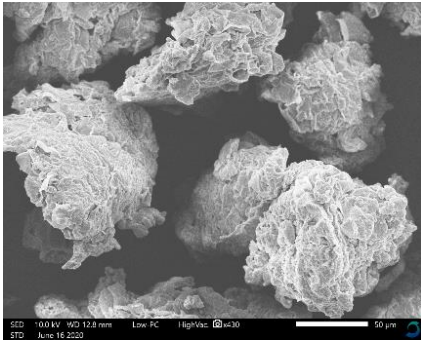
B: SPC (soy protein concentrate)
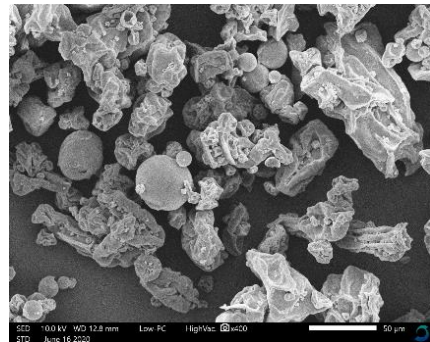
C: WG (wheat gluten)
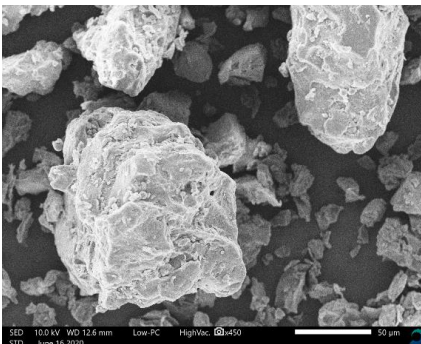
Table S3-1 Statistical analysis of the tensile strength properties with respect to Fig. 3-1, 3-2, and 3-3. Differences are compared within each column and are shown as small letters.

RPC (40%)	Fig 3-1a	Fig 3-1b	Fig 3-1c
Par-130 °C	a	a	ac
Par-140°C	ac	c	c
Par-150°C	b	b	ab
Per-130°C	ac	ac	b
Per-140°C	ac	ac	c
Per-150°C	c	c	ac
RPC-WG (20-20)	Fig 3-1d	Fig 3-1e	Fig 3-1f
Par-85°C	a	a	a
Par-95°C	a	aed	a
Par-120°C	a	aced	ab
Par-130°C	a	a	b
Par-140°C	b	ac	c
Par-150°C	c	b	c
Per-85°C	a	a	a
Per-95°C	a	ade	a
Per-150°C	a	adec	ac
Per-130°C	a	ad	b
Per-140°C	a	ad	c
Per-150°C	d	b	c

SPC (40%)	Fig. 3-2a	Fig. 3-2b	Fig. 3-2c	SPC-WG (20-20)	Fig. 3-2d	Fig. 3-2e	Fig. 3-2f
Par-120	a	c	a	Par-120	a	a	a
Par-130	b	a	a	Par-130	a	c	b
Par-140	c	c	b	Par-140	a	c	b
Par-150	d	c	bd	Par-150	b	b	b
Par-95	a	a	a	Par-95	a	a	a
Per-120	a	c	a	Per-120	a	a	a
Per-130	e	b	a	Per-130	a	c	b
Per-140	a	a	ba	Per-140	a	c	ab
Per-150	a	ab	b	Per-150	a	ac	b
Per-95	a	a	a	Per-95	a	a	a

SPC (40%)	Fig. 3-3a	Fig. 3-3b	Fig3 3-3c	SPC-WG (20-20)	Fig. 3-3d	Fig. 3-3e	Fig. 3-3f
Par-120	a	c	a	Par-120	a	a	a
Par-130	b	a	a	Par-130	a	c	b
Par-140	c	c	b	Par-140	a	c	b
Par-150	d	c	bd	Par-150	b	b	b
Par-95	a	a	a	Par-95	a	a	a
Per-120	a	c	a	Per-120	a	a	a
Per-130	e	b	a	Per-130	a	c	b
Per-140	a	a	ba	Per-140	a	c	ab
Per-150	a	ab	b	Per-150	a	ac	b
Per-95	a	a	a	Per-95	a	a	a

3.7 References

Asgar, M.A., Fazilah, A., Huda, N., Bhat, R., & Karim, A.A. (2010). Nonmeat Protein Alternatives as Meat Extenders and Meat Analogs. *Comprehensive Reviews in Food Science and Food Safety*, *9*(5), 513–529.

Banovic, M., & Sveinsdóttir, K. (2021). Importance of being analogue: Female attitudes towards meat analogue containing rapeseed protein. *Food Control*, *123* (Oct).

Berghout, J.A.M., Boom, R.M., & van der Goot, A.J. (2015). Understanding the differences in gelling properties between lupin protein isolate and soy protein isolate. *Food Hydrocolloids*. 43, (465-472)

Choung, J.M., & Cho, S.R. (2008). Study on true stress correction from tensile tests. *Journal of Mechanical Science and Technology*, *22* (6), 1039–1051.

Cornet, S.H.V., Bühler, J.M., Goncalves, R., Bruins, M.E., van der Sman, R.G.M., & van der Goot, A.J. (2021). Apparent universality of leguminous proteins in swelling and fiber formation when mixed with gluten. *Food Hydrocolloids*, 106788.

Cornet, S.H.V., Snel, S.J.E., Schreuders, F.K.G., van der Sman, R.G.M., Beyrer, M., & van der Goot, A. J. (2020). Thermo-mechanical processing of plant proteins using shear cell and high-moisture extrusion cooking. *Critical Reviews in Food Science and Nutrition*, 1–18.

Dekkers, B.L., Nikiforidis, C.V., & van der Goot, A.J. (2016). Shear-induced fibrous structure formation from a pectin / SPI blend. *Innovative Food Science and Emerging Technologies*, *36*, 193–200.

Draganovic, V., Boom, R.M., Jonkers, J., & Van Der Goot, A.J. (2014). Lupine and rapeseed protein concentrate in fish feed: A comparative assessment of the techno-functional properties using a shear cell device and an extruder. *Journal of Food Engineering*. 126 (178-189)

Grabowska, K.J, Zhu, S., Dekkers, B.L., De Ruijter, N.C.A., Gieteling, J., & Van der Goot, A.J. (2016). Shear-induced structuring as a tool to make anisotropic materials using soy protein concentrate. *Journal of Food Engineering*, *188*, 77–86.

Grabowska, K.J., Tekidou, S., Boom, R.M., & van der Goot, A.J. (2014). Shear structuring as a new method to make anisotropic structures from soy–gluten blends. *Food Research International*, *64* (0), 743–751.

Jia, W., Rodriguez-Alonso, E., Bianeis, M., Keppler, J.K., & van der Goot, A.J. (2021). Assessing functional properties of rapeseed protein concentrate versus isolate for food applications. *Innovative Food Science & Emerging Technologies*, *68* (Feb), 102636.

Keppler, J.K., Schwarz, K., & van der Goot, A.J. (2020). Covalent modification of food proteins by plant-based ingredients (polyphenols and organosulphur compounds): A commonplace reaction with novel utilization potential. *Trends in Food Science & Technology*, *101*(Oct), 38–49.

Ozdal, T., Capanoglu, E., & Altay, F. (2013). A review on protein-phenolic interactions and associated changes. *Food Research International*, *51*(2), 954–970. https://doi.org/10.1016/j.foodres.2013.02.009

Raheem, Z. (2014). Standard test Method for Tensile Properties of Plastics. *ASTM International*, *82*(January), 1–15. https://doi.org/10.1520/D0638-14

Schreuders, F.K.G., Dekkers, B.L., Bodnár, I., Erni, P., Boom, R.M., & van der Goot, A.J. (2019). Comparing structuring potential of pea and soy protein with gluten for meat analogue preparation. *Journal of Food Engineering*, *261*(May), 32–39.

Schreuders, Floor K.G., Schlangen, M., Kyriakopoulou, K., Boom, R.M., & van der Goot, A.J. (2021). Texture methods for evaluating meat and meat analogue structures: A review. *Food Control*, *127* (April), 108103.

Tan, S.H., Mailer, R.J., Blanchard, C.L., & Agboola, S.O. (2011). Canola proteins for human consumption: extraction, profile, and functional properties. *Journal of Food Science*. 76 (1), R16-28.

Von Der Haar, D., Müller, K., Bader-Mittermaier, S., & Eisner, P. (2014). Rapeseed proteins-Production methods and possible application ranges. *OCL - Oilseeds and Fats*, *21*(1), 1–8.

Wanasundara, J.P.D. (2011). Proteins of *Brassicaceae* oilseeds and their potential as a plant protein source. *Critical Reviews in Food Science and Nutrition*. 51 (7), 635-677.

Wanasundara, J.P.D., McIntosh, T.C., Perera, S.P., Withana-Gamage, T.S., & Mitra, P. (2016). Canola/rapeseed protein-functionality and nutrition. *Ocl*. 23(4), D407.

3

Chapter 4

Removal of phenolic compounds from de-oiled sunflower kernels by aqueous ethanol washing

Abstract

Selective removal of phenolic compounds (PCs) from de-oiled sunflower kernel is generally considered a key step for food applications, but this often leads to protein loss. PC removal yield and protein loss were assessed during an aqueous or aqueous ethanol washing process with different temperatures, pH-values and ethanol contents. PC yield and protein loss increased when the ethanol content was < 60% or when a higher temperature was applied. Our main finding is that preventing protein loss should be the key objective when selecting process conditions. This can be achieved using solvents with high ethanol content. Simulation of the multi-step exhaustive process showed that process optimization is possible with additional washing steps. PC yield of 95% can be achieved with only 1% protein loss using 9 steps and 80% ethanol content at 25 ℃. The functional properties of the resulting concentrates were hardly altered with the use of high ethanol solvents.

4.1 Introduction

Sunflower (*Helianthus annuus* L.) is the third most cultivated oilseed crop in the world after soy bean and rapeseed (USDA, 2020). Sunflower meal is the main by-product obtained after oil extraction. Because of its high protein content (25%–55% w/w), sunflower meal is often suggested for food applications, but it is still mainly used for animal feed (Laguna et al., 2019; Pickardt, Eisner, Kammerer, & Carle, 2015). The high content of phenolic compounds (PCs) (1%–4% on a dry basis) restricts its use in the food industry, because the presence of chlorogenic acid (CGA) in sunflower meal. This can lead to dark green and brown coloring under alkaline conditions or during aqueous processing through the formation of protein and PC complexes (Ozdal, Capanoglu, & Altay, 2013a; Pedrosa et al., 2000). In addition, the formation of these complexes can lower the nutritional value of the protein by altering its digestibility and bioavailability (Karefyllakis, Salakou, Bitter, Van der Goot, & Nikiforidis, 2018), and the functionality of the protein is changed (Keppler et al., 2020; Rawel, Meidtner, & Kroll, 2005). Therefore, removal of PCs is generally considered a prerequisite for enhanced use of the sunflower proteinaceous fraction in food applications.

Previous studies have mainly focused on obtaining a purified protein isolate by complete removal of PCs (Albe Slabi et al., 2020; Pickardt et al., 2015a). However, a low protein yield in these studies and the use of large amounts of water and chemicals make the process less suitable for producing refined ingredients for modern food applications (González-Pérez et al., 2002; Karefyllakis et al., 2017). Furthermore, many food applications do not require the use of completely purified proteins. Other components, such as carbohydrates, can have a positive function as well, and retaining them can result in improved resource use efficiency. Washing processes using a mixture of water and ethanol are often suggested as food-grade solvents to remove PCs, yielding less refined protein concentrate (Chemat et al., 2012; Prat et al., 2015). The ratio of water and ethanol in the solvent mixtures is used to finetune the polarity of the solvent, and thereby control the selectivity of the extraction of both PCs and proteins (Jankowiak, Trifunovic, et al., 2014). Protein in a polar nature can be better extracted with water compared to low-polarity solvent of ethanol (Chemat et al., 2012). In addition to solvent (mixture) selection, temperature and pH are known to influence the removal of PCs. It is reported that a higher temperature and alkaline

4

pH can increase the amount of PCs removed in the extract by increasing their solubility (González-Pérez, Vereijken, Koningseld, Gruppen, & Voragen, 2005; Sripad, Prakash, & Rao, 1982). However, protein solubility also increases with increased temperature and alkaline pH (Sathe, Zaffran, Gupta, & Li, 2018), which leads to protein loss. Further, protein nativity might also be affected by the use of a high temperature (Molina, Petruccelli, & Añón, 2004). Certain process conditions favor the formation of protein-PC complexes through covalent interaction, especially at alkaline pH. For this reason, process conditions at a lower pH can be beneficial to reduce protein loss and avoid covalent protein and PC interactions. The challenge therefore is to select the process conditions such that they lead to effective PC removal while minimizing protein loss.

In this study, the selective removal of PCs from de-oiled sunflower kernel (DSK) through washing is investigated. The aim was to investigate the effect of different water–ethanol content and process temperature on the effective removal of PCs from DSK while retaining as much protein as possible. The outcomes of the experiments were used to determine the equilibrium constants, which were used to simulate multi-step processes. The washed concentrates were assessed on their functional properties, such as protein nativity, microstructure, nitrogen solubility index (NSI) and water holding capacity (WHC). Both NSI and WHC are important when considering material as a protein source for modern food applications, such as meat analogues (Jia et al., 2021). It is hypothesized that the yield of PC removal and protein loss will be largely influenced by the ethanol content and temperature, and the functional properties of the resulting washed concentrates will be affected by high temperature and high ethanol content (Taha et al., 2011; Sripad & Rao, 1987)

4.2 Materials & methods

4.2.1 Materials

DSK, provided by Avril (Bruz, France), was obtained after mechanical pressing of sunflowers. The proximate composition of DSK is 51.0% protein, 8.0% moisture, 3.9% PCs, 6.4% fat, 7.5% ash and the rest will be carbohydrates mainly. Ethanol (96%) was purchased from EMD Millipore Corporation (Darmstadt, Germany). Folin-Ciocalteu (F-C) reagent was obtained from MP Biomedicals (Illkirch, France). Analytical grade trifluoroacetic acid (purity of 99%), gallic acid, CGA, HCl and NaOH were obtained from Sigma-Aldrich (St

Louis, MO, USA). Acetonitrile ULC-MS (purity of 99.97%) was obtained from Actu-All chemicals (Oss, the Netherlands), anhydrous sodium carbonate (purity $\geq$ 99.5%) was obtained from VWR International (Darmstadt, Germany). Ultrapure water was purified with a Milli-Q Lab Water System (Milli-Q IQ 7000 Ultrapure Lab Water System, Merck KGaA, Darmstadt, Germany) and was used in this study.

4.2.2 Methods

4.2.2.1 Sample preparation

Aqueous washing

Aqueous washing was performed under varied process conditions with different pH and temperature as follows: pH 4 at 25 °C, pH 4 at 75 °C; pH 7 at 25 °C; pH 7 at 75 °C. Milli-Q Water was preheated to 75 °C in a water bath (TW8 Water Bath, Julabo, the Netherlands) before the washing process.

Five grams of DSK was mixed with 50 mL of Milli-Q water in a 100-mL glass Schott bottle with lid, leading to a dispersion with a solid-to-liquid ratio of approximately 1:10. Then, the pH was adjusted to the desired value with 0.1 M HCl or 0.1 M NaOH. In the next step, the dispersion was mixed using a Stirring Drybath 15-250 (2mag AG, Munich, Germany) with a magnet at 400 rpm and controlled temperature for 10 min. A preliminary test showed that the washing time from 5 min to 60 min had hardly any impact on the amount of PCs being removed. The dispersion was vacuum filtrated using a vacuum pump system (SC 950; Germany) with filter paper (grade 4; Whatman, Sigma-Aldrich). The pellet remaining on the filter paper was transferred into the Schott bottle and used as the starting material for the next washing step. We tried to transfer as much material as possible into the bottle, but slight material losses were unavoidable at this stage. The extracts were collected in a Büchner flask and transferred into a 50-mL Falcon tube for further analysis. Up to 5 sequential steps were performed with the same protocol, making a total of 6 steps. After 6 washing steps, the final pellet obtained after filtration was freeze dried and stored at 4 °C. Fresh extracts of 1 mL from each step were kept in a fridge at 4 °C, and the rest of the extracts

were freeze dried and stored at 4 °C. The scheme for the aqueous washing is shown in Fig. 4-1.
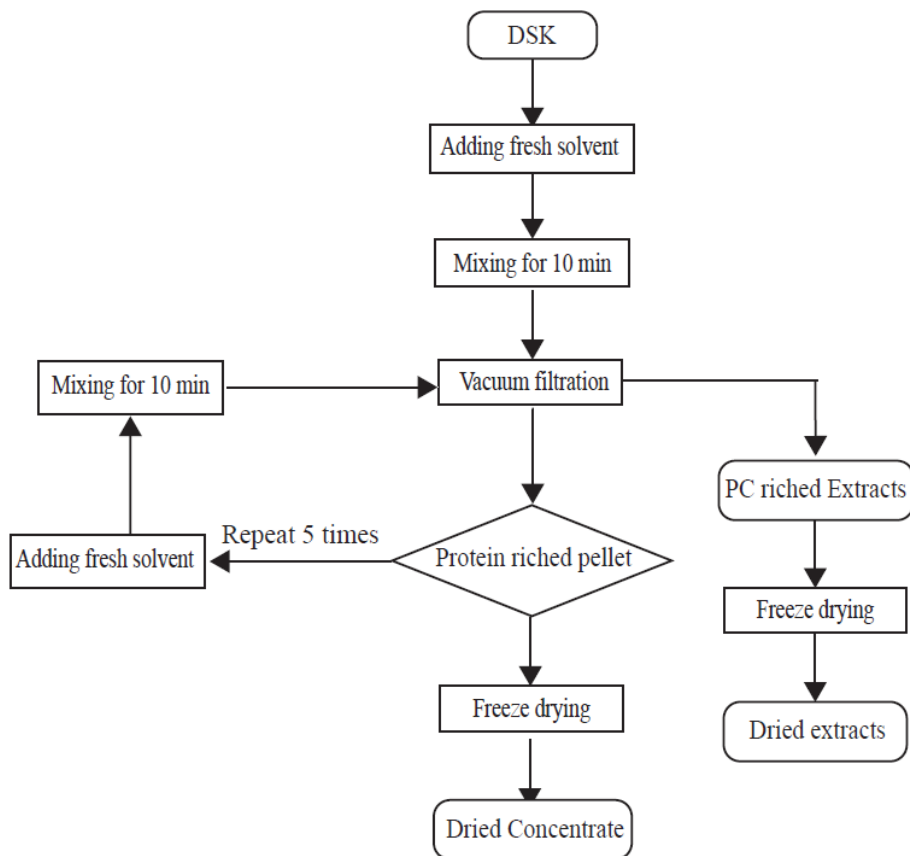
Fig. 4-1 Schematic overview of the aqueous washing for de-oiled sunflower kernels (DSK).

Aqueous ethanol washing

Aqueous ethanol solvents were prepared by mixing water with ethanol. The ratio of the volume of ethanol to the total solvent volume is referred to in this study as the ethanol content: 0%, 20%, 40%, 60%, 80% and 100% (the purity of the ethanol used in this study was 96%). The mass of the mixtures was converted to the density of the aqueous ethanol solvents: 0.998, 0.970, 0.939, 0.896, 0.851, 0.801, respectively. Water–ethanol mixtures were prepared separately with the correct volume in a cylinder, mixed in a Schott bottle and placed

in the water bath at the correct temperature before adding DSK. The washing process was performed at two different temperatures (25 °C and 50 °C) for all solvents with different ethanol content.

Five grams of DSK was mixed with 50 mL of solvent in a 100-mL glass Schott bottle with lid, creating a dispersion with a solid-to-liquid ratio of 1:10 (g/mL). Next, the dispersion was mixed using a Stirring Drybath 15-250 with a magnet at 400 rpm and controlled temperature (25 °C or 50 °C). After mixing for 10 min, the dispersion was filtrated using a vacuum pump system (SC 950) with grade 4 Whatman filter paper. The extracts were collected in a Büchner flask and transferred into a 50-mL Falcon tube. The wet pellet remaining on the filter paper was transferred into the Schott bottle and used as the starting material for the next washing step. Up to 2 sequential steps were performed with the same protocol, making a total of 3 steps. After 3 washing steps, the final pellet obtained after filtration was freeze dried and stored at 4 °C. Fresh extracts of 1 mL from each step were kept in a fridge at 4 °C, and the rest of the extracts were pre-concentrated in a rotary evaporator (RC900, KNF, Freiburg, Germany) to remove most of the ethanol before freeze drying. The extract of each step was transferred to a 250-mL flask and placed in the rotary evaporator at 40 °C and 100 rpm under an operating pressure of 150 mbar. The evaporation was carried out until the volume of the liquid remained constant. The scheme for the aqueous ethanol washing is shown in Fig. 4-2.

Both aqueous washing and aqueous ethanol washing process were reproduced with 2 batches. The pellet is referred to as the concentrate in the following discussion, except in Section 4.3.

4.2.2.2 Analysis of the extract

The TPC in the extracts was measured using the Folin-Ciocalteau (F-C) method (Drosou et al., 2015; Ghosh & Seijas, 2014). The CGA content was measured using HPLC (Karefyllakis et al., 2018). The protein content in the extracts was measured using the Dumas method (Pickardt et al., 2009).
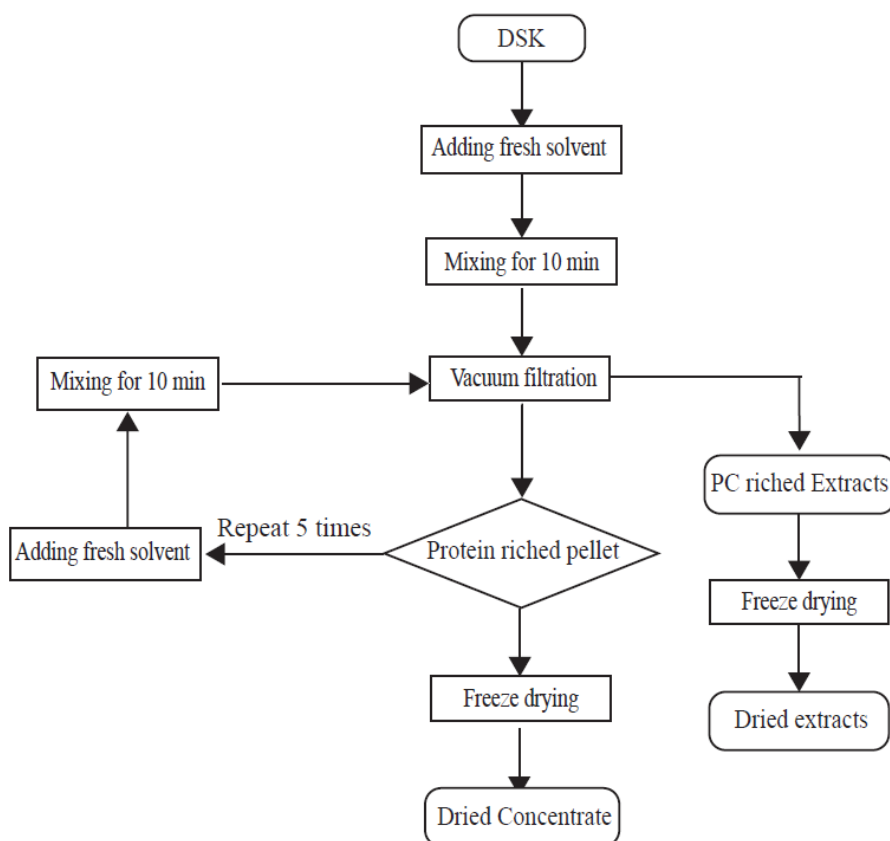
Fig. 4-2 Schematic overview of the aqueous ethanol washing for de-oiled sunflower kernels (DSK).

Quantification of the total phenol content

Fresh extracts (100 µL) obtained from the different conditions of aqueous washing and aqueous ethanol washing process were added to 7.9 mL of water and mixed using a vortex. Subsequently, 500 µL of F-C reagent and 1.5 mL of 20% (w/v) sodium carbonate were added and mixed thoroughly with a vortex. The samples were placed in a water bath (TW8 water bath; Julabo, Boven-Leeuwen, the Netherlands) at 40 °C for 30 min. The absorbance was measured at 750 nm with a spectrophotometer (DR3900 Laboratory VIS Spectrophotometer, Hach, USA). Calibration curves with gallic acid solutions ranging from 0.025 to 4 mg/mL were made for each solvent with a different ethanol content. The total

phenol content (TPC) is expressed as mg gallic acid equivalents (GAE) / g DSK on a dry basis. Each sample was measured in duplicate.

Quantification of CGA

HPLC was used to quantify the content of CGA in the extracts. A Dionex Ultimate 3000 chromatograph (Thermo Fisher, Waltham, MA, USA) was used with a Gemini 3 μm C18 phenol column at 30 °C. The eluent consisted of 0.1% (v/v) trifluoroacetic acid, 23% (v/v) acetonitrile in ultrapure water. A calibration curve for CGA was drawn for concentrations of CGA ranging between 0.0125 and 0.3 mg/mL. The sample was prepared by dissolving 10 mg of freeze-dried extract in 1 mL of ultrapure water. Then dilutions (10 to 20 times) were prepared with ultrapure water based on the TPC results obtained using the F-C method. The dilution was done to achieve a final CGA concentration <0.3 mg/mL. The samples were centrifuged at $15,000 \times g$ for 10 min to remove the insoluble part of the extracts. The injection volume was 10 μL and the flow rate was maintained at 1.0 mL/min. The peak areas of the standard solutions and the extracts were measured at a wavelength of 295 nm using a Chromeleon Chromatography Data system (Thermo Fisher). The results are expressed as mg CGA/g DSK on a dry basis and each sample was measured in duplicate.

Protein analysis

The Dumas method was carried out by combusting a known mass of the freeze-dried extracts at 900 °C in the presence of oxygen. The nitrogen content was determined using a FlashEA 1112 NC Analyzer (Thermo Fisher). The protein content was then derived using a nitrogen conversion factor of 5.6 (Pickardt et al., 2009). Each sample was measured in triplicate.

Yield of PC removal and protein loss

The yield of PC removal (%) and protein loss (%) were calculated as follows:

$$\text{PC yield (\%)} = \frac{\sum_1^n (c_{\text{pc},i,\text{e}} \times m_{i,\text{e}})}{c_{\text{pc,DSK}} \times m_{\text{DSK}}} \times 100\% \tag{1}$$

$$\text{Protein loss (\%)} = \frac{\sum_1^n (c_{\text{pro},i,\text{e}} \times m_{i,\text{e}})}{c_{\text{pro,DSK}} \times m_{\text{DSK}}} \times 100\% \tag{2}$$

93

where $c_{\text{pc,DSK}}$ is the initial PC content in DSK. A value for $c_{\text{pc,DSK}}$ of 39.4 mg GAE/g DSK was obtained from an extensive washing process (10 steps) with 0% and 40% ethanol content. $c_{\text{pc,DSK}}$ was calculated by cumulating the average value of each washing steps. The results are shown as boxplots in Fig. S4-1. The TPC measured was slightly lower than that reported in the literature for defatted sunflower meal (of 42 mg TPC/g dry matter) (Weisz et al., 2009). The variation in the TPC determined from sunflower materials may depend on different factors, such as the variety of the sunflower crops, the de-oiling process, the process conditions for extraction of PCs, and the analytical methods. $c_{\text{pro,DSK}}$ of 510 mg/g DSK was used as the total initial amount of protein present in the DSK, which was obtained from Dumas measurement. $c_{\text{pc},i,\text{e}}$ (mg GAE/g liquid extract) and $c_{\text{pro},i,\text{e}}$ (mg/g liquid extract) are the concentration of PC and protein in the extracts from step i; concentrations were obtained from the F-C and Dumas methods. $m_{i,\text{e}}$ and $m_{i,\text{p}}$ are the mass of the liquid extract and pellet at step i. n is the total number of washing steps.

4.2.2.3 Analysis of the functionality of the concentrates

The functional properties of the concentrates were evaluated with respect to the microstructure, protein nativity, WHC and NSI. These methods were adapted from a previous study (Jia et al., 2021). Protein content was measured using the Dumas method, and the TPC recovery yield (%) in the concentrate was calculated with the amount of PC remained in the concentrate (based on equation (2)) over the amount of TPC in the DSK.

Microstructure

Scanning electron microscopy (SEM) was used to visualize the microstructure of the washed concentrates from aqueous washing and aqueous ethanol washing. The dry samples were placed onto SEM tubes (aluminium pin-type mounts 12.7 mm; JEOL, Nieuw-Vennep, the Netherlands) using double-sided adhesive conductive carbon tabs (12 mm carbon tabs; SPI Supplies Division of Structure Probe, West Chester, PA, USA). The samples were sputter coated with gold. Compressed air was used to distribute the sample evenly on the surface of the carbon tabs. The accelerating voltage was 10 kV. In total, 8 images were taken for each sample analysis, from which one representative image was selected.

Protein nativity

The protein nativity in the original DSK and concentrates from aqueous washing and aqueous ethanol washing was analyzed with differential scanning calorimetry (TA instrument 250; TA Instruments, Newcastle, DE, USA). From each sample, 6 mg was placed in a high-volume pan. Ultrapure water was pipetted to create a dispersion of 15% w/w concentration. The pan was then sealed, and the sample was hydrated for 1 h before measurement. The pan was heated from 25 °C to 130 °C at a heating rate of 5 °C/min. After 1 min, the pan was cooled down to 25 °C at a cooling rate of 20 °C/min. This heating and cooling process was repeated for a second time to make sure the peak indicated protein denaturation. Once the protein was denatured in the first heating step, it was not detected again in the second heating step. Duplicates were measured for each sample of concentrate. The temperature at the onset of protein denaturation (onset T_d), peak temperature of denaturation (peak T_d) and denaturation enthalpy (J/g protein) were collected by Trios data analysis software (TA Instruments).

4

Water holding capacity and nitrogen solubility index

DSK or concentrate from aqueous ethanol washing (1 g) was prepared in a 50-mL Falcon tube into a 2% dispersion by mixing with Milli-Q water, and rotated for 24 h (SB3 rotator; Stuart, Stone, UK) at a speed of 20 rpm for hydration. The dispersion was then centrifuged at 15,000 × g at 25 °C for 10 min. The supernatant was removed with a pipette and the wet pellet was transferred into an aluminium tray and dried in an oven at 105 °C for 24 h. The weight of the wet pellet ($M_{wet\ pellet}$) and after drying ($M_{dry\ pellet}$) was measured. The nitrogen content in the dry pellet ($N_{dry\ pellet}$) and in the original sample ($N_{original}$) was measured using the Dumas method (Section 4.2.2.2). The mass of the original sample and the pellet was measured and expressed as $M_{original}$ and $M_{dry\ pellet}$. Duplicates of WHC and NSI were made for each sample. WHC and NSI was calculated as:

$$\text{WHC} = \frac{M_{\text{wet pellet}} - M_{\text{dry pellet}}}{M_{\text{dry pellet}}} \ [\text{g water /g dry pellet}] \tag{3}$$

$$\text{NSI} = \frac{N_{\text{original}} \times M_{\text{original}} - N_{\text{dry pellet}} \times M_{\text{dry pellet}}}{N_{\text{original}} \times M_{\text{original}}} \ [\%] \tag{4}$$

4.2.3 Equilibrium kinetics and simulation

The equilibrium kinetics of the PCs and protein were calculated using the mass balance of the entire process (Fig. S4-2), and the PC and protein content in the extracts measured by the F-C and Dumas methods. Preliminary research has revealed that a 10-min washing time leads to almost complete removal of PCs. The equilibrium constants $K_{pc,i}$ and $K_{pro,i}$ are defined as the concentration of the component ($c_{pc,i,e}$ or $c_{pro,i,e}$) in the extracts over the concentration of the component remaining in the pellets ($c_{pro,i,p}$ [mg/g dry pellet] or $c_{pc,i,p}$ [mg GAE/g dry pellet]). The concentration of the component in the pellet was not measured and was therefore calculated from the ingredient mass balance (Fig. S4-2):

The ingredient balance: $m_{DSK}c_{DSK} = m_e c_e + m_p c_p$ (5)

Mass of the dry pellet: $m_p = m_{DSK} - m_e$ (6)

The equilibrium constants are given below and rewritten with known parameters using the mass balances described above:

1st step: $K_{pc,1} \equiv \dfrac{c_{pc,1,e}}{c_{pc,1,p}} = \dfrac{c_{pc,1,e} \times (m_{DSK} - m_{1,e})}{c_{pc,DSK} \times m_{DSK} - c_{pc,1,e} \times m_{sol}}$ (7)

2nd step: $K_{pc,2} \equiv \dfrac{c_{pc,2,e}}{c_{pc,2,p}} = \dfrac{c_{pc,2,e} \times (m_{DSK} - \sum_1^2 (m_{i,e}))}{c_{pc,DSK} \times m_{DSK} - \sum_1^2 (c_{pc,i,e} \times m_{sol})}$ (8)

3rd step: $K_{pc,3} \equiv \dfrac{c_{pc,3,e}}{c_{pc,3,p}} = \dfrac{c_{pc,3,e} \times (m_{DSK} - \sum_1^3 (m_{i,e}))}{c_{pc,DSK} \times m_{DSK} - \sum_1^3 (c_{pc,i,e} \times m_{sol})}$ (9)

where $m_{1,e}$, $m_{2,e}$, $m_{3,e}$ stand for the amount of dried extract obtained after freeze drying for each step. m_{sol} stands for the mass of the solvent used for each step and was calculated as the volume of 50 mL multiplied by the density of the water and ethanol mixtures. The amount of PC remaining in the pellet can be calculated by subtracting the amount of PC removed from DSK or the pellet in the previous step. Unfortunately, the loss of part of the pellet happened due to transfer of the material and incomplete removal of the solvent from the pellet, which also included soluble components, could not be avoided. Both effects, which have an opposite effect on the yields in the next steps, were therefore ignored in this calculation. The equilibrium constant K_{pro} at each step was calculated using equations similar to equations 7–9, where $c_{pc,i,e}$ and $c_{pc,DSK}$ are replaced by $c_{pro,i,e}$ and $c_{pro,DSK}$, respectively.

After the equilibrium constant was calculated, $K_{pc,1}$ and $K_{pro,1}$ obtained from the first step of the experiment results were used for the simulation of a multi-step exhaustive washing process to calculate the concentration of the PC and protein in the extract, expressed as $c^s_{pc,i,e}$ (mg GAE/g liquid extract) and $c^s_{pro,i,e}$ (mg/g liquid extract). The following assumptions were made before the simulations: (1) the equilibrium constants K_{pc} and K_{pro} in each step of the multi-steps exhaustive washing process are constants; (2) the amount of protein and PC that will be removed is much lower than the mass of the DSK, therefore the weight of the starting material for each step is assumed to be constant and the same as m_{DSK}. Based on these assumptions, the concentration of PC in the extract of each step was simulated with the follow equations:

1st step: $c^s_{pc,1,e} = \dfrac{K_{pc,1} \times m_{DSK} \times c_{pc,DSK}}{m_{DSK} + K_{pc,1} \times m_{sol}}$ (10)

2nd step: $c^s_{pc,2,e} = \dfrac{(c_{pc,DSK} \times m_{DSK} - c^s_{pc,1} \times m_{sol}) \times K_{pc,1}}{m_{DSK} + K_{pc,1} \times m_{sol}}$ (11)

n step: $c^s_{pc,n,e} = \dfrac{(c_{pc,DSK} \times m_{DSK} - \sum_1^{n-1} c^s_{pc,i} \times m_{sol}) \times K_{pc,1}}{m_{DSK} + K_{pc,1} \times m_{sol}}$ (12)

where $c^s_{pro,i,e}$ was also calculated according to equations 10–12 by replacing the relevant parameters for PC with the protein. The simulated PC removal yield (%) and protein loss (%) were calculated with equations 1 and 2, in which the $c_{pc,i,e}$ and $c_{pro,i,e}$ were replaced by $c^s_{pc,i,e}$ and $c^s_{pro,i,e}$.

4.2.4 Statistics analysis

The statistics in this paper were analyzed using SPSS software, version 25.0 (IBM, Armonk, NY, USA). A univariate general linear model with the least significant difference test was carried out to investigate the significant differences with respect to Table 4-1 and Table 4-2 as well as the total PCs being removed from the DSK in Fig S4-3. Differences were considered significant when $P < 0.05$ and shown as the small upper letters. Correlation between the TPC and CGA content is shown in Fig. S4-1. A Pearson correlation factor was generated, and the significance differences were analyzed at the $P < 0.01$ level.

4.3 Results and discussion

This section presents the results: (1) analysis of the extract regarding removal of PCs and protein loss under different process conditions; (2) PCs removal and protein loss with multi-step washing by simulations; (3) evaluation of the functionality of the washed concentrates with respect to microstructure, protein nativity, WHC and NSI.

4.3.1 Analysis of the extract

The PCs content is often measured using two different methods: the F-C method for the TPC and HPLC (specific CGA). In this study, the HPLC results gave a lower PC content than the F-C method. Zardo et al. (2019) also reported a lower amount of CGA after extraction from sunflower seed cake compared with the TPC results. The difference between the results for the two methods could be explained using CGA as a marker component in the HPLC analysis, whereas in the F-C method, TPC was calculated based on gallic acid equivalents. Nevertheless, the CGA and TPC results were highly correlated (Fig. S4-1); the Pearson correlation factor was 0.962, which was significant at 0.01 level. In the following results, the F-C method was selected for the discussion and simulation, because it accounted for the total PC present in the sunflower material instead of CGA only.

The results of aqueous washing are presented in Fig. 4-3A, with the pH and temperature varied. The TPC removed after 6 steps ranged between 23 and 36 mg GAE/g DSK; pH 7 at 25 °C exhibited the highest value and pH 4 at 25 °C showed the lowest value. Overall, the amount of PC removed at pH 7 at different temperatures was higher than at pH 4. Higher temperature at 75 °C led to higher removal at both pH values. The first step removed most of the PC with all conditions applied, and the effect of additional steps was limited, especially after 3 steps. The protein removed at pH 4 in the first step was low compared with that at pH 7, and hardly any protein was removed in additional steps at pH 4. The low solubility of sunflower protein (mainly globulin) was reported to be pH 4-6 (Albe Slabi et al., 2020; Pickardt et al., 2015a; Subaşı et al., 2020), therefore protein loss at pH 4 is probably mainly due to the loss of the albumin fraction. The effect of temperature on protein extraction was more pronounced at pH 7 than at pH 4. Overall, the highest protein extraction was found at pH 7 and 75 °C.
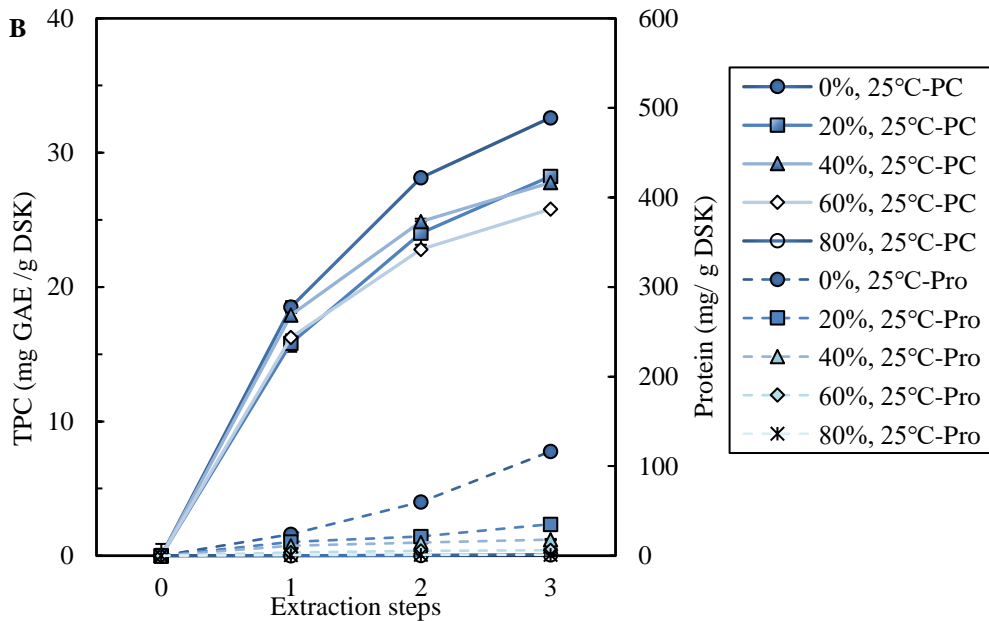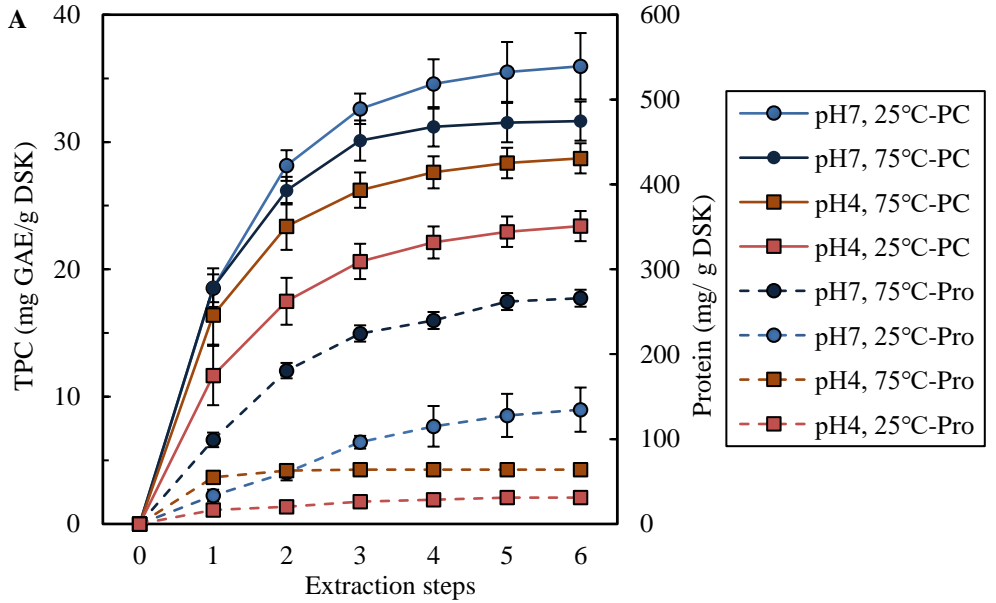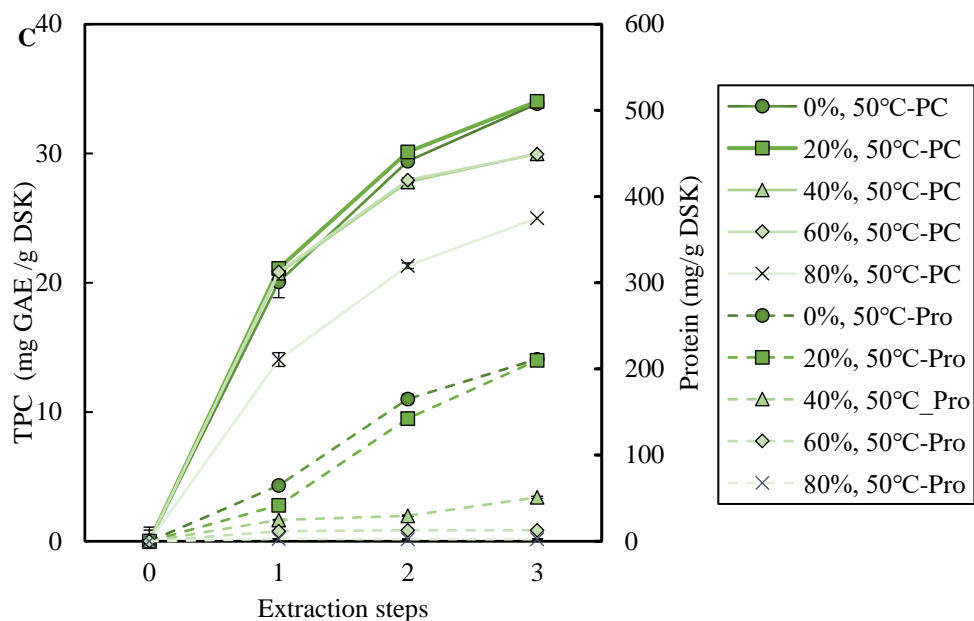
Fig. 4-3 The total amount of phenol content (TPC) and protein in the extracts obtained from aqueous washing (A), at the condition of pH4/25 ℃, pH 4/75 ℃, pH7/25 ℃, pH7/75 ℃; The amount of TPC and protein in the extracts obtained from aqueous ethanol washing at different ethanol contents 0%, 20%, 40%, 60% and 80% at 25 ℃ (B) and 50 ℃ (C). The TPC and protein results are expressed in mg gallic acid equivalent (GAE)/g DSK and mg protein/g DSK.

The amounts of TPC removed by aqueous ethanol washing at 25 and 50 ℃ are shown in Fig. 4-3 (B and C), respectively. The highest TPC value obtained was 34 mg GAE/g DSK from 0% and 20% ethanol content after 3 washing steps at 50℃. This accounts for 86% of the PC removal yield (Weisz et al., 2009). The amounts of TPC removed from the extract by the 1st washing step at 25 ℃ were similar for ethanol content between 0% and 60% and were slightly higher than the value obtained with 80% ethanol content. Hardly any PC was removed with 100% ethanol solvent. These results were in line with a previous study in which it was reported that the use of 50% v/v aqueous ethanol leads to more PC removal (30 mg GAE/g sunflower florets) than the use of 90% v/v aqueous ethanol (23 mg GAE /g sunflower florets) (Ye, Liang, Li, & Zhao, 2015). The 2nd and 3rd steps increased the total extraction of PC, and the amount removed in those steps was much lower than the amount removed in the 1st step. The lower amount removed at high ethanol concentration might be due to the fact that the penetration of the solvent into the sample matrix was hindered at this high ethanol
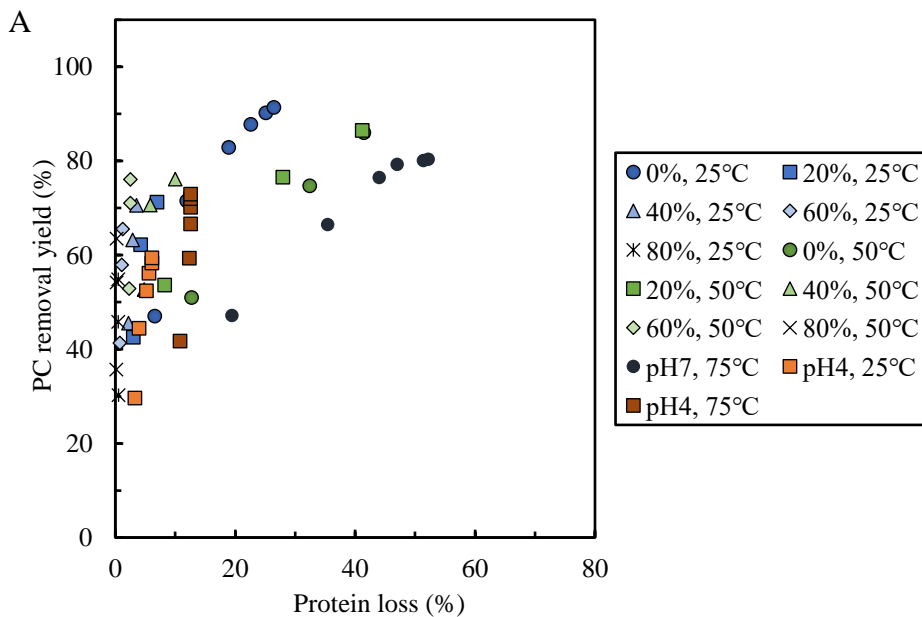
concentration (Zardo et al., 2019). Overall, higher TPC values were measured at temperatures above 50 °C compared with 25 °C at fixed ethanol content, but the TPC values removed were lower with increasing ethanol content. The result of 76% PC yield with 40% ethanol content at 50 °C was found to be the same as the reported CGA yield of 76% with 40% ethanol content at 90 °C after three sequential steps (Scharlack, Aracava, & Rodrigues, 2017). The effect of temperature was also in line with the results presented in previous studies (Sripad et al. 1982; Vázquez-León et al., 2019; Zardo et al., 2019).

The amount of protein in the extracts with different ethanol content and at different temperatures is also shown in Fig. 4-3 (B and C). The total amount of protein extracted by aqueous ethanol was lower when using solvents with higher ethanol content at both 25 °C and 50 °C. The highest amount was 117 mg/g DSK achieved with 0% ethanol content at 25 °C. The amount of protein extracted decreased above 20% ethanol content. This outcome might be a result of the low polarity and denaturation effect of ethanol (Chemat et al., 2012; Wagner, Andreadis, Nikolaidis, Biliaderis, & Moschakis, 2021), which decreased protein solubility and extractability in the solvent (González-Pérez, 2015). A small additional amount of protein was extracted in the 2nd and 3rd steps. This was different from the PC, which were mostly extracted in the first step. Furthermore, similar amounts of protein were found in the extracts obtained with 0% and 20% ethanol content at 50 °C, which were approximately 2 times higher compared with 25 °C with 0% ethanol. At 50 °C, protein extraction was higher when using solvents containing ethanol than the extraction at 25 °C, which might be due to the change of the matrix from which it is extracted as a function of temperature and ethanol content in the solvent (Zhong et al., 2014).

4.3.2 Phenolic compounds removal efficiency versus protein loss

The purpose of the washing process described above is to effectively remove PCs while retaining proteins. The protein extracted is considered as loss of protein. An optimal process is thus to extract all PCs while limiting protein loss. Therefore, the 2 parameters, TPC removal yield (%) and protein loss (%), for different steps were plotted in a cumulative curve (Fig. 4-4A). This allows better understanding of the effect of the washing steps on both parameters and evaluation of the optimal process conditions.

Most of the data points were concentrated in the area ranging from 30% to 75% PC yield and 0% to 15% protein loss. This part of the diagram can be achieved using many different process conditions, such as 3 steps with ethanol content below 60% at 25 °C or 2 steps with water at 25 °C. Increasing the ethanol content to 80% can lead to a PC yield up to 60% with hardly any loss of protein. A further increase in the PC yield of more than 80% can be achieved by increasing the temperature or using pure water. However, those conditions resulted in protein loss of up to 52%. From the results, one can hypothesize that the area with both high PC removal yield and low protein loss can be achieved with high ethanol ratios by applying more steps. The removal of PCs was not complete with 3 washing steps, thus it would be interesting to know the effect of increasing the number of washing steps. For this reason, the equilibrium constants K_{pc} and K_{pro} were calculated, and this is discussed further in the following section.

B

- ● 0%, 25°C
- ■ 20%, 25°C
- △ 40%, 25°C
- ◇ 60%, 25°C
- ✳ 80%, 25°C
- ■ pH4, 25°C
- ■ pH4, 75°C
- ● pH7, 75°C

C

- ● 0%, 50°C
- ■ 20%, 50°C
- △ 40%, 50°C
- ◇ 60%, 50°C
- ✕ 80%, 50°C
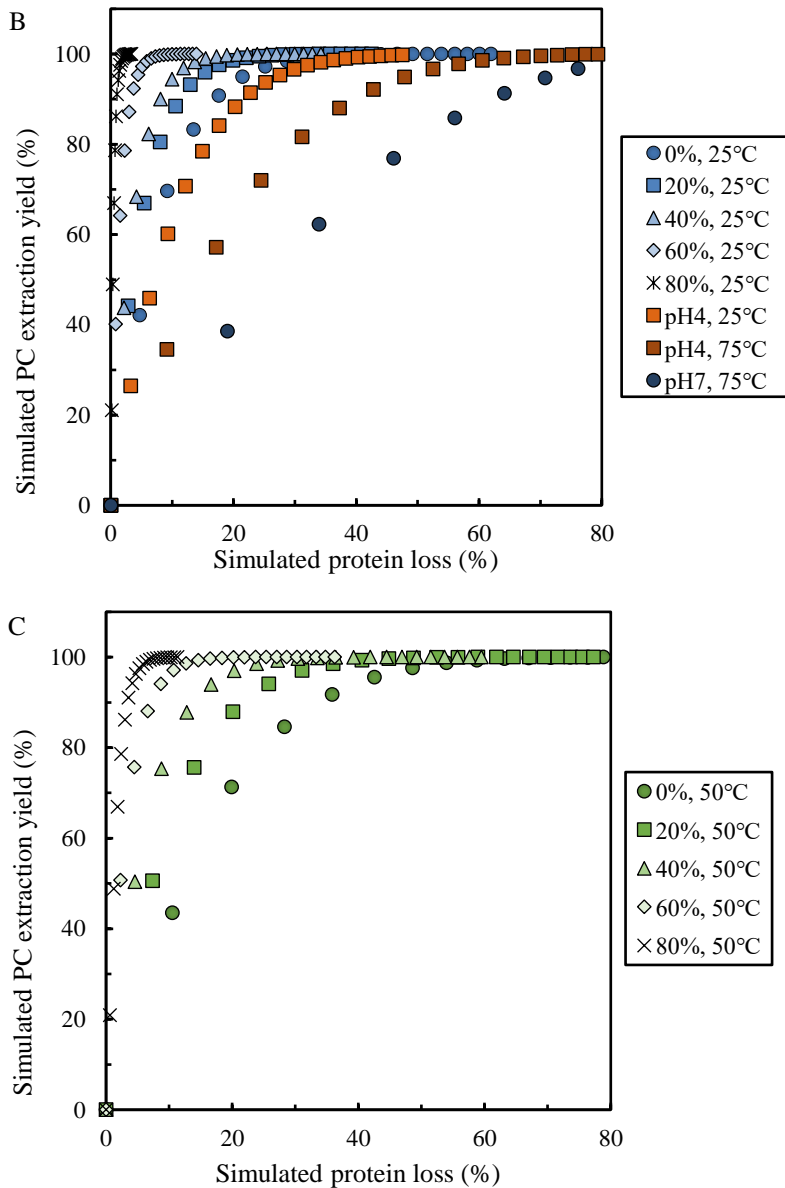
Fig. 4-4 Removal yield (%) of phenolic compounds (PCs) versus protein loss (%) in the extracts from the aqueous washing and aqueous ethanol washing of de-oiled sunflower kernel (DSK) (A). Simulations of multi-step exhaustive washing process for the pH4/25 °C, pH 4/75 °C, pH7/25 °C, pH7/75 °C (B), and different ethanol content 0%, 20%, 40%, 60% and 80% at 25 °C (B) and 50 °C (C); the closed symbols for 25 °C and open symbols for the 50 °C.

4.3.3 Equilibrium kinetics and simulation

The equilibrium constants K_{pc} and K_{pro} were calculated based on the experimental results for the amount of PC removed and protein extracted (Table 4-1). The K_{pc} corresponding to pH 4 was found to be lower than the values at pH 7 or in aqueous ethanol solvents. For the first step of aqueous ethanol washing, K_{pc} was stable between 0.065 and 0.075 at 25 ℃ for different ethanol content, except for the lower value above 80% ethanol content. K_{pc} was higher at 50 ℃ with ethanol content between 20% and 60%, and the value was similar for both temperatures at 0% and 80% ethanol content.

The value for K_{pc} decreased with the additional washing steps and was similar for different ethanol contents and at different temperatures. These results suggested that K_{pc} was independent of the ethanol content and temperature regarding PC removal after the 1st washing step. The decrease in K_{pc} at the 2nd and 3rd steps suggest that the matrix changed by renewing the solvent each time (Zhong et al., 2014). Changes could be caused by extraction of other components or by altering the interaction of PCs with the matrix. The first effect most likely occurred at high water content, whereas the second effect is more likely to occur with an aqueous ethanol solvent. Nonetheless, the value for the K_{pc} was found to be similar as reported in the literature for the PCs extraction from M. oleifera leaves (Vázquez-León et al., 2019).

The K_{pro} value at pH 7 was much larger than the value at pH 4, while a higher temperature enhanced the values. K_{pro} decreased with increasing ethanol content for the first step and K_{pro} at 50 ℃ was larger than at 25 ℃. The equilibrium constants varied at pH 7 for the 2nd and 3rd steps with different ethanol content. Nevertheless, it was found that the impact of solvent, pH and temperature was more pronounced for K_{pro} than for K_{pc}. Thus, a change in the process conditions or solvent quality influenced the loss of protein more than the extraction of PCs. To better understand the consequence of this, we simulated the DSK washing process. In the simulation, K_{pro} and K_{pc} were assumed to be constant for each step and the values were taken from the 1st step. Process conditions of 0%, 20%, 40%, 60% and 80% ethanol and pH 4 of water at 25 ℃ were selected for the simulation, and the simulation outcomes are presented in Fig. 4-4.

Table 4-1. Equilibrium constants calculated from the experimental data for total phenol content by the F-C method and protein content by the Dumas method, indicated as K_{pc} for phenolic compounds and K_{pro} for protein with ethanol ratios of 0%, 20%, 40%, 60% and 80% at 25°C and 50°C taking 3 washing steps into account. The values in the table are compared within the column and different upper case letters indicate a significant difference (P < 0.05).

Aqueous washing	$K_{pc}1$ (* 10^{-3})	$K_{pro}\,1$ (* 10^{-3})	$K_{pc}\,2$ (* 10^{-3})	$K_{pro}\,2$ (* 10^{-3})	$K_{pc}\,3$ (* 10^{-3})	$K_{pro}\,3$ (* 10^{-3})
pH 4, 25°C	36.2 ± 9.0 [a]	3.0 ± 0.1 [a]	14.1 ± 1.6 [a]	6.1 ± 0.1 [a]	6.7 ± 1.7 [a]	1.1 ± 0.004 [a]
pH 4, 75°C	54.1 ± 5.5 [b]	9.2 ± 0.03 [b]	14.9 ± 1.1 [a]	13.5 ± 0.2 [b]	5.2 ± 0.4 [a]	0.2 ± 0.001 [b]
pH 7, 25°C	75.0 ± 5.7 [c]	4.6 ± 0.1 [a]	23.7 ± 0.7 [b]	7.2 ± 0.9 [a]	7.8 ± 3.9 [a,b]	11.9 ± 0.4 [c]
pH 7, 75°C	65.2 ± 11.5 [b,c]	19.6 ± 2.0 [c]	14.5 ± 1.4 [a]	15.9 ± 0.1 [b]	5.8 ±1.2 [a]	8.3 ± 0.1 [d]

| Aqueous ethanol washing	$K_{pc}1$ (* 10^{-3})		$K_{pc}\,2$ (* 10^{-3})		$K_{pc}\,3$ (* 10^{-3})	
Ethanol ratio	25°C	50°C	25°C	50°C	25°C	50°C
0%	75.0 ± 5.7 [a]	82.2 ± 2.5 [a]	23.7 ± 0.7 [a]	17.4 ± 3.0 [a]	7.8 ± 3.9 [a,b]	5.6 ±0.3 [a]
20%	65.5 ± 2.9 [b]	108.7 ±3.0 [b]	19.8 ± 0.6 [b]	19.5 ± 0.3 [a]	7.4 ± 0.5 [a]	5.9 ± 0.7 [a]
40%	76.4 ± 6.0 [a]	106.7 ± 7.0 [b]	18.3 ± 0.9 [b]	18.0 ± 1.0 [a]	6.5 ± 0.5 [a]	4.4 ± 0.1 [b]
60%	69.0 ± 0.7 [b]	105.8 ± 2.0 [b]	18.4 ± 0.2 [b]	19.6 ± 1.8 [a]	7.2 ± 0.2 [a]	4.5 ± 0.4 [b]
80%	46.4 ± 0.3 [c]	59.0 ± 1.2 [c]	18.8 ± 0.1 [b]	22.6 ± 2.0 [a]	9.7 ± 0.1 [b]	9.8 ± 0.6 [c]
	$K_{pro}\,1$ (* 10^{-3})		$K_{pro}\,2$ (* 10^{-3})		$K_{pro}\,3$ (* 10^{-3})	
0%	4.6 ± 0.1 [a]	10.8 ± 0.1 [a]	7.2 ± 0.9 [a]	23.8 ± 1.7 [a]	11.9 ± 0.4 [a]	9.6 ± 0.2 [a]
20%	2.7 ± 0.1 [b]	7.3 ± 0.3 [b]	1.6 ± 0.1 [b]	23.5 ± 1.2 [a]	2.8 ± 1.1 [b]	15.1 ± 2.0 [b]
40%	2.0 ± 0.1 [b]	4.4 ± 0.2 [c]	1.0 ± 0.004 [c]	1.6 ± 0.2 [b]	0.7 ± 0.1 [c]	4.6 ± 0.3 [c]
60%	0.7 ± 0.04 [c]	2.1 ± 0.3 [d]	0.5 ± 0.1 [d]	0.5 ± 0.2 [c]	0.1 ± 0.03 [d]	N.A
80%	0.2 ± 0.03 [d]	0.6 ± 0.01 [e]	0.1 ± 0.03 [e]	N.A*	0.02 ± 0.01 [e]	N.A

Fig. 4-4 (B and C) reveals that all curves can be divided into 2 regions: a region with sharp increase in the amounts of PC removal followed by levelling off. It is interesting to compare the different conditions in which similar amounts of PC are removed. Here, we analyze the protein losses at a PC yield of 95%. For example, a PC yield of 95% can be achieved by a 6-step process with pure water at pH 7, which gives a protein loss of 25%. Alternatively, the washing can be performed using pH 4 and 10 steps, but this leads to a protein loss of 27%. When aqueous ethanol solvents were applied with the ethanol content ranging from 20% to 60%, a PC yield of 95% could also be achieved using 6 steps, but the protein loss decreased from 13% to 3% with increasing ethanol content. More steps were required to reach the 95% yield with 80% ethanol content, but then only 1% of protein was lost. Therefore, the application of a multi-steps process using high ethanol content is preferred when minimal protein loss is required. Overall, it can be concluded that when selecting process conditions, it is more important to focus on limiting protein loss rather than optimizing PC removal.

An efficient industrial translation of a multi-step batch process is a counter-current multi-stage extraction (CME). The CME process is recommended for energy and solvent efficiency compared with exhaustive extraction (Vázquez-León et al., 2019). The simulation of a multi-step exhaustive batch process presented here provides a theoretical basis and potential outlook for the CME process with respect to PC removal and protein loss.

4.3.4 The effect of process conditions on protein functionality

The morphologies of the DSK and the concentrates were visualized with SEM (Fig. 4-5). The original DSK particle consisted of a compact structure, which is known to be a cellular matrix, and spherical particles were present on the surface. Those spherical particles were most likely protein bodies, which have a known particle size of 0.5–10 µm (González-Pérez, 2015; Laguna et al., 2018). The cellular matrices became open laminar structures after washing with 0% ethanol at both 25 and 50 ℃ with all the spherical particles disappeared, leading to pores with a diameter between 10 and 50 µm. The results suggested that the protein present on the surface was fully washed away by the water, which was in line with the high protein loss (Section 4.3.2). When the ethanol content increased above 40% at 25 and 50 ℃, small spherical particles of less than 8 µm became visible on the surface of the structure.

Here, the matrix became dense and compact under these conditions. This observation is in line with results reported for the matrix of okara, which was suggested to be in the glassy state when exposed to a solvent with high ethanol content. As a consequence, the diffusion of the PC to the solvent was hindered (Jankowiak, Kantzas, Boom, & Van der Goot, 2014), which explains why the addition of water to the matrix was needed to facilitate PC removal. At pH 4, the open cell wall matrix was filled with aggregates of 10–30 µm, and the aggregates were found to be more connected when the temperature increased to 75°C. The aggregates found at pH 4 might be associated with the protein aggregation at the isoelectronic point and lowest protein solubility between pH 4 and 6 (Albe Slabi et al., 2020; González-Pérez et al., 2005).
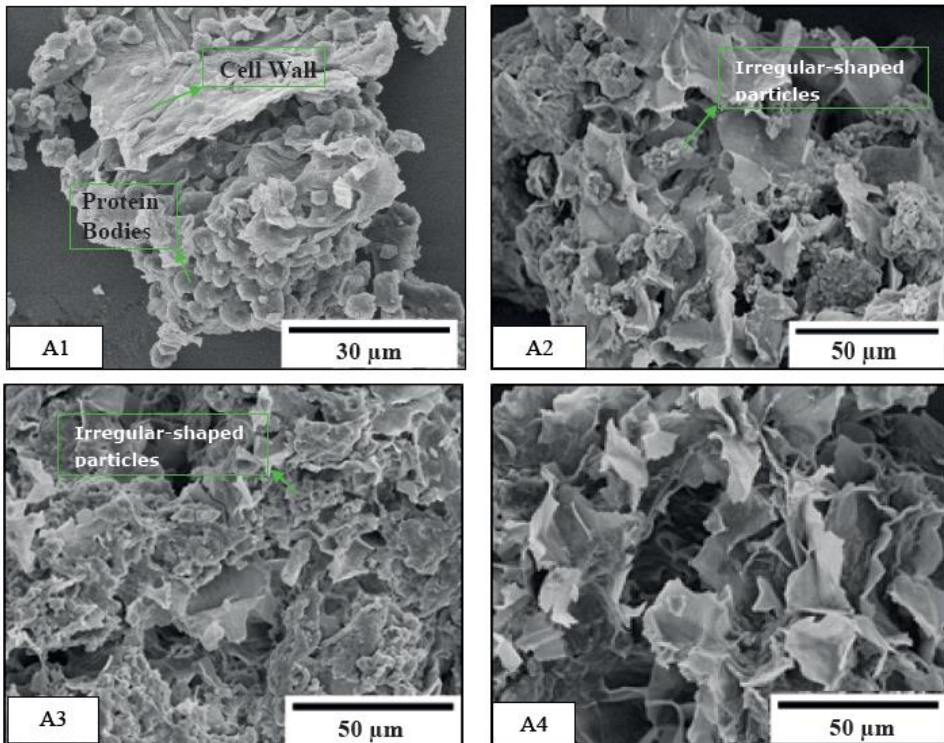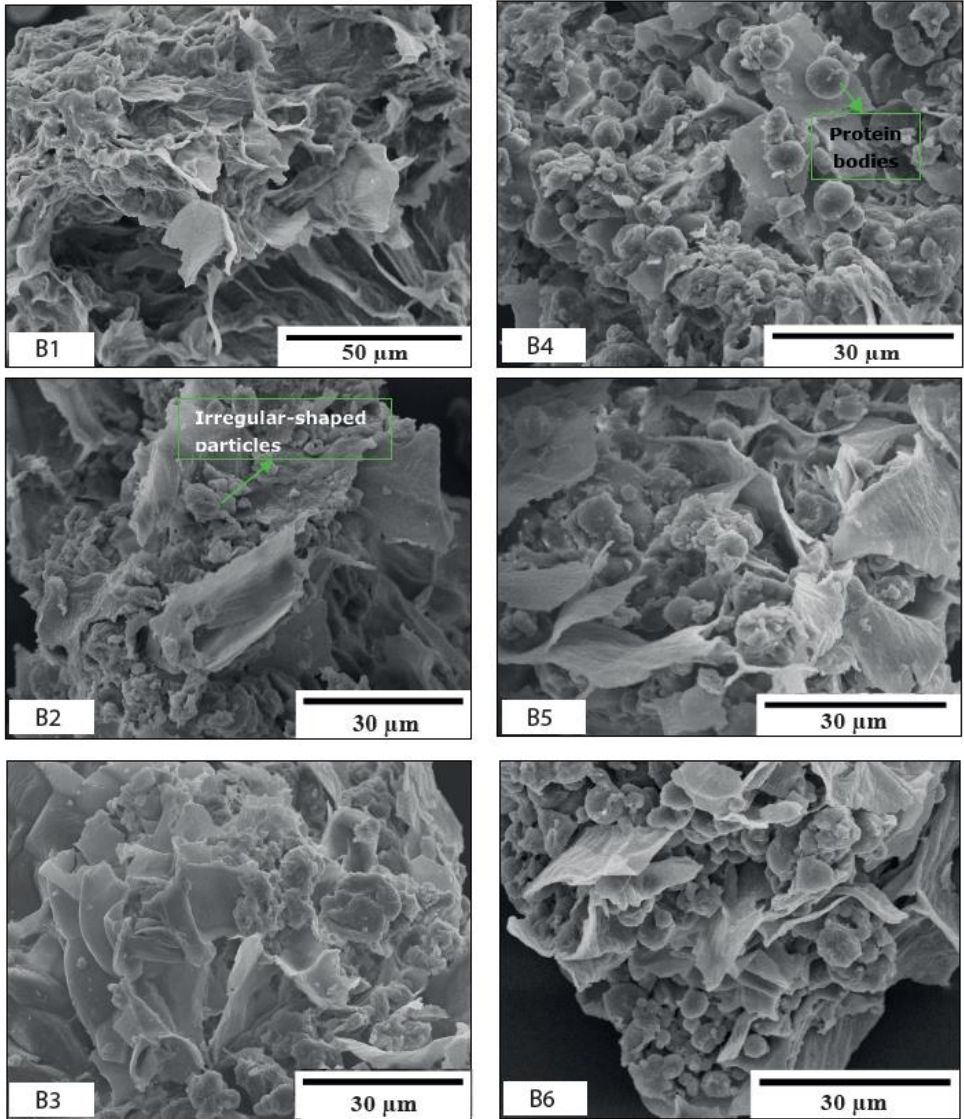
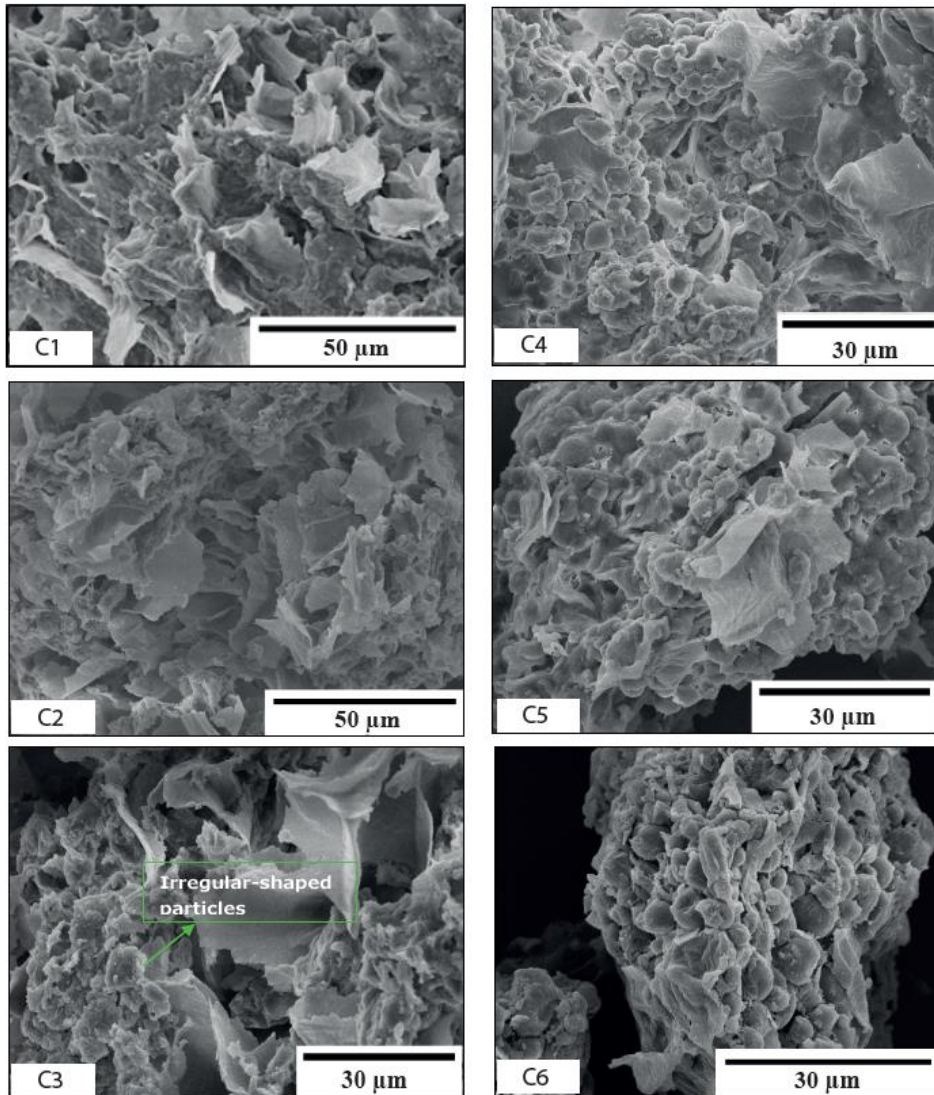**Fig. 4-5** Scanning electron micrographs for the DSK (A1) and aqueous washed concentrates with pH 4 at 25 °C (A2), pH4 at 75 °C (A3), pH 7 at 75 °C (A4); aqueous ethanol washed concentrates with ethanol ratios of 0%, 20%, 40%, 60%, 80% and 100% at 25 °C (B1–B6) and 50 °C (C1–C6). The different scale bars of 30 μm or 50 μm were showed, because the particle size was different. Only one representative image was selected from 8 images.

The functionalities analysis of the concentrate after the process are shown in Table 4-2. Protein content of the material was increased above 20% ethanol content at 25 °C or 40% ethanol at 50 °C, due to the removal of other soluble components. The decreased protein content for concentrates obtained from low ethanol content at both temperatures relates to the high protein loss in the extracts during washing (Fig. 4-3). The TPC recovery yield in the concentrate became higher with increasing ethanol content, which is in line with the TPC removal in the extract (Fig. 4-3). No significant differences between the enthalpy of the denaturation peak of DSK and the concentrates treated with 80% ethanol content at 25 °C and 50 °C were found, which indicates that hardly any denaturation had occurred during extraction. The other conditions resulted in partial denaturation with decreased enthalpy at 25 °C. It is reported that ethanol can induce protein denaturation (Liu, Li, Zhang, & Tang, 2019). Remarkably, the protein was completely denatured with 0% and 20% ethanol at 50 °C although it had not yet reached T_d. Complete denaturation was found with the concentrates obtained by aqueous washing at 0% and 20% ethanol at 50 °C. Besides, complete denaturation was found with pH 7, at 75 °C or at pH 4 at different temperatures (results not shown). The effect of pH on protein nativity was in line with the literature (Molina, et al., 2004). The results indicated that the effect of high temperature on protein nativity was more pronounced at lower ethanol content compared with a high ethanol content. The use of high temperature at low ethanol content and low pH with 0% ethanol content should thus be avoided if protein nativity is important. The DSK washed by aqueous ethanol solvent with ethanol content of 20%–60% at 25 °C and 50 °C showed similar NSI (range, 50%–56%) as the original DSK. The washed concentrates obtained using pure water and 100% ethanol content at 25 °C had slight lower NSI of 34%–41%, which aligns with the results that show partial protein denaturation. Lower NSI values of 16% and 7% were observed with the completely denatured concentrates obtained after extraction with pure water and 20% ethanol content at 50 °C. The results suggested that efficient PC removal with increased ethanol content of 40%–80% can not only limit protein loss but it also preserves protein nativity and solubility. The high protein loss during washing with low ethanol content also showed reduced protein functionalities with complete protein denaturation and low protein solubility.

The concentrates obtained from aqueous ethanol washing showed enhanced WHC under different conditions compared with the original DSK (Table 4-2). The highest WHC

Table 4-2 The functional properties of the original sample DSK and the washed concentrates obtained at different ethanol ratios of 0%, 20%, 40%, 60%, 80% and 100% at 25°C and 50°C. The functional properties including protein content (%), TPC recovery yield (%), protein denaturation at onset denaturation temperature (onset T_d), peak denaturation temperature (peak T_d) and denaturation enthalpy (J/g protein), WHC (g water/ g dry pellet) and NSI (%). The values in the table are compared within the column and different upper-case letters indicate a significant difference ($P < 0.05$).

T (°C)	Ethanol ratio (%)	Protein (g/100g)	TPC recovery yield (%)	DSC Onset T_d [°C]	DSC Peak T_d [°C]	DSC Enthalpy [J/g protein]	WHC (g water/ g dry pellet)	NSI (%)
	DSK	51.0 ± 1.4 [a,b]	N.A	93.3 ± 0.2 [a]	99.8 ± 0.2 [a]	9.4 ± 1.5 [b]	5.7 ± 0.2 [a]	49.2 ± 0.1 [a]
	0%	49.8 ± 0.9 [a]	11.3 ± 1.2 [a]	93.0 ± 0.6 [a]	99.5 ± 0.4 [a]	6.1 ± 1.0 [a]	8.7 ± 0.2 [b]	33.7 ± 5.4 [b]
	20%	56.6 ± 0.3 [c,d]	21.3 ± 2.1 [b]	93.2 ± 0.9 [a]	99.1 ± 0.2 [a]	6.7 ± 1.1 [a]	8.8 ± 0.2 [b]	50.8 ± 0.3 [a]
25	40%	57.9 ± 1.0 [c]	24.1 ± 1.9 [b]	92.9 ± 1.1 [a]	99.0 ± 1.0 [a]	6.5 ± 0.1 [a]	9.2 ± 0.02 [c]	55.6 ± 0.1 [c]
	60%	57.9 ± 0.5 [c]	28.9 ± 0.9 [b]	93.2 ±0.1 [a]	99.6 ± 0.2 [a]	7.4 ± 0.4 [a]	8.8 ± 0.1 [b]	56.5 ± 1.5 [c]
	80%	55.7 ± 0.6 [d]	40.3 ± 0.4 [c]	93.4 ±0.6 [a]	99.5 ± 0.1 [a]	9.1 ± 1.1 [b]	7.6 ± 0.04 [d]	51.5 ± 0.2 [a]
	100%	53.8 ± 1.2 [b]	89.6 ± 0.002 [d]	93.6 ±0.1 [a]	99.5 ± 0.2 [a]	7.1 ± 0.6 [a]	7.0 ± 0.1 [e]	41.5 ± 1.9 [d]
	0%	41.1 ± 1.0 [e]	10.2 ± 1.5 [a]	N.D*	N.D	N.D	10.0 ± 0.1 [d]	6.6 ± 0.9 [e]
	20%	44.5 ± 1.0 [e]	7.6 ± 1.8 [a]	N.D	N.D	N.D	9.4 ± 0.6 [c]	15.9 ± 0.6 [f]
50	40%	55.9 ± 1.1 [d]	18.0 ± 1.4 [b]	93.5 ±0.2 [a]	99.7 ± 0.4 [a]	6.6 ± 1.0 [a]	9.0 ± 0.3 [b,c]	53.3 ± 0.4 [c]
	60%	58.9 ± 1.1 [c]	19.4 ± 1.2 [b]	93.4 ±0.1 [a]	99.6 ± 0.1 [a]	7.3 ± 0.1 [a]	8.0 ± 0.1 [d]	52.9 ± 1.2 [c]
	80%	55.3 ± 1.4 [d]	31.4 ± 1.2 [c]	93.2 ±0.3 [a]	99.6 ± 0.1 [a]	9.8 ± 2.4 [b]	7.8 ± 0.1 [d]	54.0 ± 1.5 [c]
	100%	54.4 ± 0.9 [b,d]	82.2 ± 0.01 [d]	93.2 ±0.1 [a]	99.4 ± 0.1 [a]	8.6 ± 1.3 [a,b]	7.3 ± 0.1 [e]	40.8 ± 2.2 [d]

was found with 40% ethanol at 25 °C and 0% ethanol at 50 °C. A slightly lower value was found with ethanol ratios > 60%. The results suggest that aqueous ethanol washing in general has a positive effect on the WHC of sunflower material, whereas the effect is smaller when using higher ethanol ratios. The WHC is known to be influenced by the composition, such as defatting and protein enrichment, or protein conformational change and hydrophobicity (Jia et al., 2021; Zhang, Yang, Tang, Chen, & You, 2015). The results discussed above suggest that the functionality difference of the concentrates obtained after extraction using solvents with different ethanol content or temperatures were small, except when the pure water was applied. Enhanced WHC after aqueous ethanol washing process might lead to potential structuring properties, such as meat analogue which required a high WHC (Cornet, Edwards, van der Goot, & van der Sman, 2020). Therefore, techno-functional and structuring properties of the washed concentrates by aqueous ethanol washing might be carried out in future study for this application.

4.4 Conclusion

In this study, scientific insight was gained on the effects of the process conditions (pH and temperature) and solvent quality on removal of PCs and protein loss from DSK. The amount of PC removed from DSK was positively affected by neutral pH, a higher temperature of 50 °C and an ethanol content below 60%. However, increasing PC removal also led to higher protein loss in most of those circumstances. In addition, it was found that the effect of altering the process conditions was greater on protein loss than PC removal yield, implying that the optimal process conditions will be mostly governed by the protein loss. Experimental results showed that by fine-tuning the process conditions, the PC removal yield can reach 75% with less than 15% protein loss using only 3 steps. Simulations revealed that PC removal of 95% can be reached in a multi-step exhaustive washing process, with protein loss <3% using an ethanol content >60% at 25°C. If even more steps are allowed or a counter-current process is applied, protein losses can be reduced to <1% using 80% ethanol. In addition to the reduced protein loss, aqueous ethanol washing with high ethanol content is also preferred, because the use of those process conditions preserves the functional properties of native protein best.

4.5 Supporting information
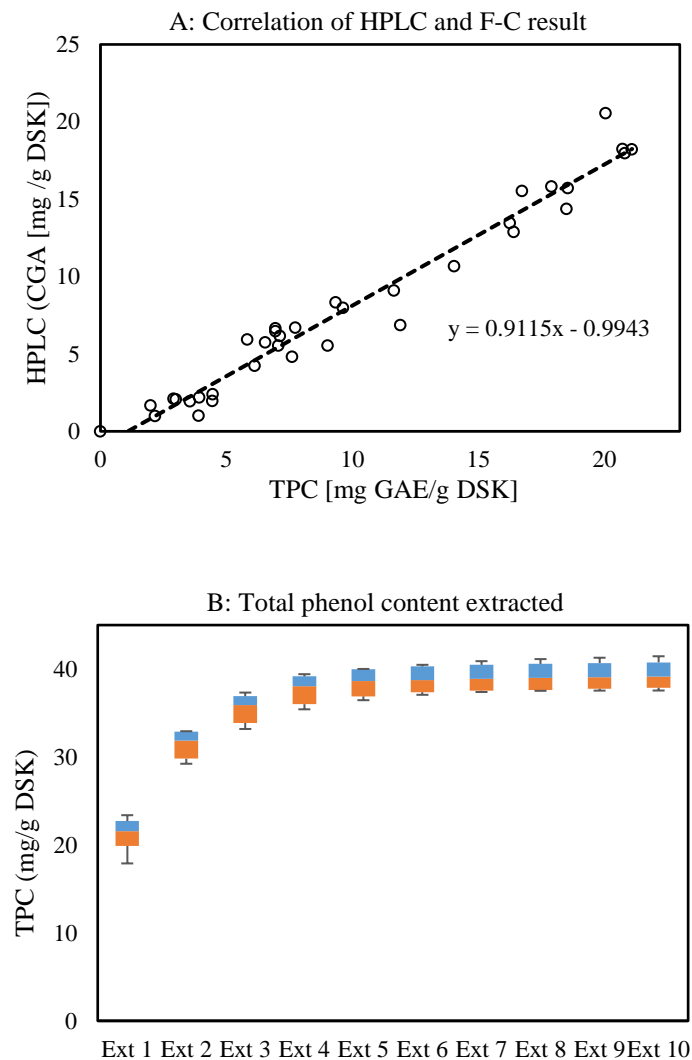
Fig. S4-1 The TPC results determined by Folin-Ciocalteu (F-C) and CGA determined by HPLC are plotted against each other (A); the 1st, 2nd and 3rd step with aqueous ethanol solvents and water at different temperature, and the equation of the trend line is $y = 0.9115x − 0.9943$ and the Pearson correlation efficient factor is 0.9627; The total phenol content from 10 washing steps with 0% ethanol and 40% ethanol are shown as a box plot; the extracts were measured by the F-C method (B).

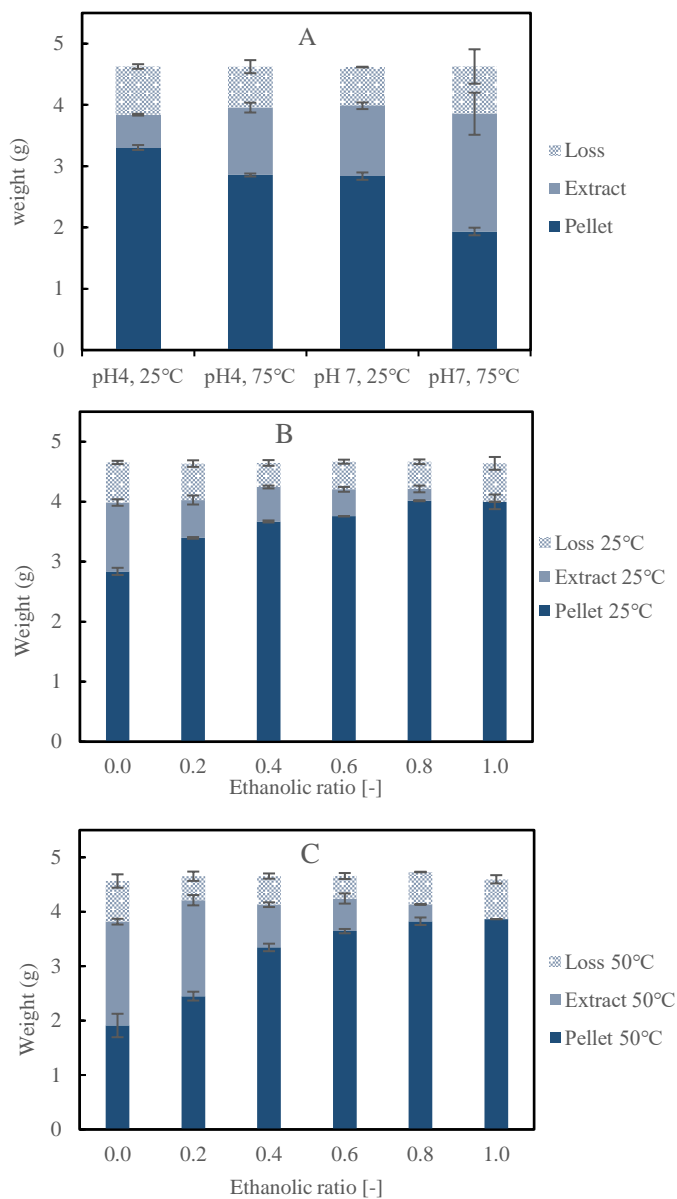**Fig. S4-2**. Mass balance of weight for the pellets, extracts and the loss during the extraction by water at pH 4/7 and 25 °C/75 °C (A); aqueous ethanol extraction at 25 °C (B) and 50 °C (C). The loss was calculated as the difference between the mass of the original DSK and the total mass of the pellets and extracts.
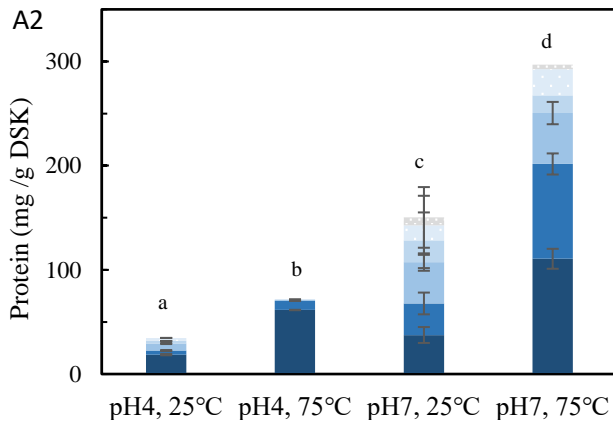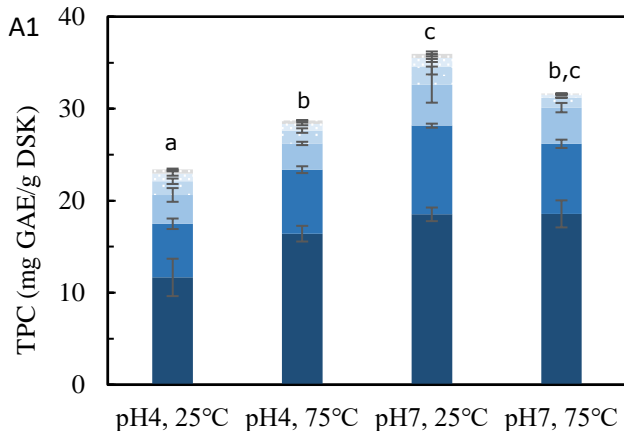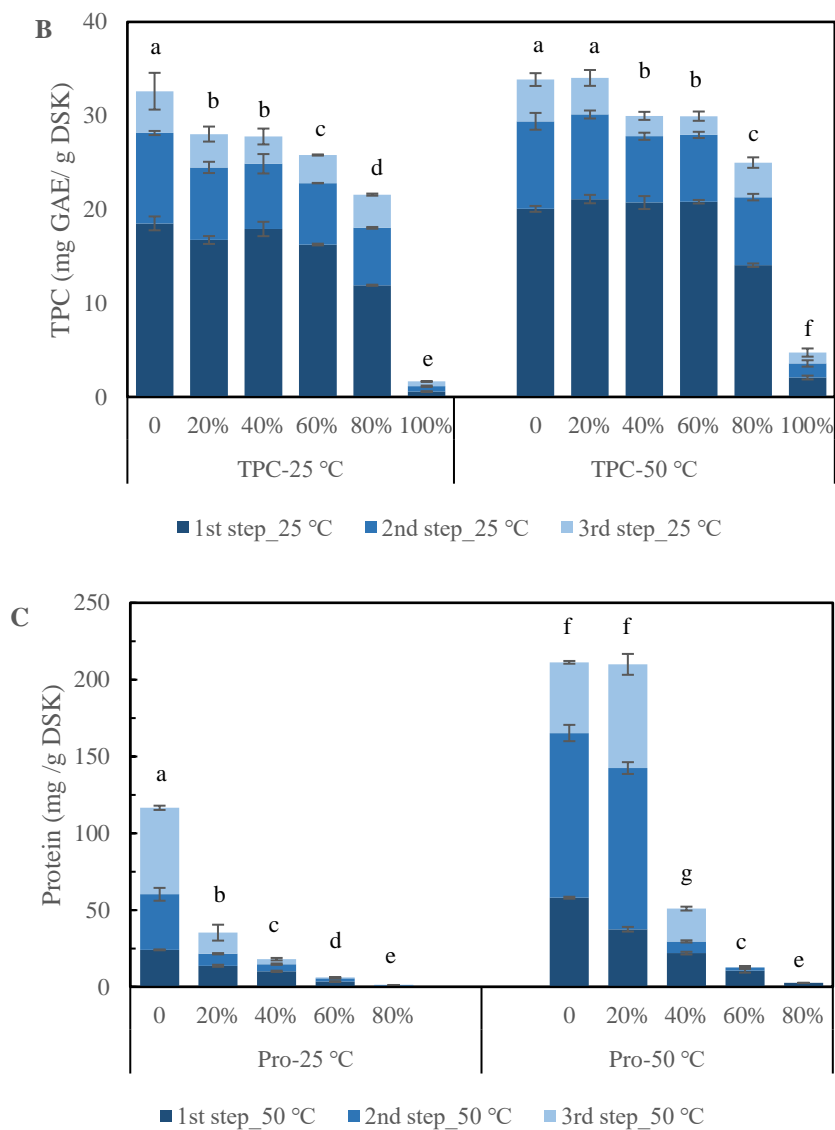
Fig. S4-3 The total amount of phenol content (TPC) and protein in the extracts obtained from aqueous washing (A1 and A2). The amount of TPC and protein in the extracts obtained from aqueous ethanol washing (B and C); the TPC and protein results are expressed in mg gallic acid equivalent (GAE)/g DSK and mg protein/g DSK. Significant differences were analyzed for the TPC with 3 washing steps at 25 °C with lower case letters and at 50 °C with upper case letters.

4.6 References

Albe Slabi, S., Mathe, C., Basselin, M., Framboisier, X., Ndiaye, M., Galet, O., & Kapel, R. (2020). Multi-objective optimization of solid/liquid extraction of total sunflower proteins from cold press meal. *Food Chemistry*, 317(Feb), 126423.

Chemat, F., Vian, M. A., & Cravotto, G. (2012). Green extraction of natural products: Concept and principles. *International Journal of Molecular Sciences*, 13(7), 8615–8627.

Cornet, S. H. V., Edwards, D., van der Goot, A. J., & van der Sman, R. G. M. (2020). Water release kinetics from soy protein gels and meat analogues as studied with confined compression. *Innovative Food Science & Emerging Technologies*, 66, 102528.

Drosou, C., Kyriakopoulou, K., Bimpilas, A., Tsimogiannis, D., & Krokida, M. (2015). A comparative study on different extraction techniques to recover red grape pomace polyphenols from vinification byproducts. *Industrial Crops and Products*, 75, 141–149.

Ghosh, M., & Seijas, J. (2014). Flavonoids and phenolic compounds from *Litsea polyantha Juss*. BARK, (Dec).

González-Pérez, S. (2015). Sunflower: Chemistry, Production, Processing, and Utilization. Sunflower: Chemistry, Production, Processing, and Utilization. *Journal of Agriculture and Food Chemistry*. 50 (6). 1713-1719.

González-Pérez, S., Merck, K. B., Vereijken, J. M., Van Koningsveld, G. A., Gruppen, H., & Voragen, A. G. J. (2002). Isolation and characterization of undenatured chlorogenic acid free sunflower (*Helianthus annuus*) proteins. *Journal of Agricultural and Food Chemistry*, 50(6), 1713–1719.

González-Pérez, S., Vereijken, J.M., Van Koningseld, G. A.., Gruppen, H., & Voragen, A.G.J. (2005). Physicochemical Properties of 2S Albumins and the Corresponding Protein Isolate from Sunflower (*Helianthus annuus*). *Journal of Food Science*, 70(1).

Jankowiak, L., Kantzas, N., Boom, R.M., & Van Der Goot, A. J. (2014). Isoflavone extraction from okara using water as extractant. *Food Chemistry*, 160, 371–378.

Jankowiak, L., Trifunovic, O., Boom, R. M., & Van Der Goot, A. J. (2014). The potential of crude okara for isoflavone production. Journal of Food Engineering, 124, 166–172.

Jia, W., Rodriguez-Alonso, E., Bianeis, M., Keppler, J. K., & van der Goot, A. J. (2021). Assessing functional properties of rapeseed protein concentrate versus isolate for food applications. *Innovative Food Science & Emerging Technologies*, 68(Feb), 102636.

Karefyllakis, D., Altunkaya, S., Berton-Carabin, C. C., Van der Goot, A. J., & Nikiforidis, C. V. (2017). Physical bonding between sunflower proteins and phenols: Impact on interfacial properties. *Food Hydrocolloids*, 73, 326–334.

Karefyllakis, D., Salakou, S., Bitter, J. H., Van der Goot, A. J., & Nikiforidis, C. (2018). Covalent bonding of Chlorogenic Acid induces structural modifications on sunflower proteins. *ChemPhysChem*, 459–468.

Keppler, J. K., Schwarz, K., & Van der Goot, A.J (2020). Covalent modification of food proteins by plant-based ingredients (polyphenols and organosulphur compounds): A commonplace reaction with novel utilization potential. Trends in Food Science & Technology, 101(Oct), 38–49.

Molina, M.I., Petruccelli, S., Añón, M.C (2004). Effect of pH and ionic strength modifications on thermal denaturation of the 11S globulin of sunflower (*Helianthus annuus*), 52, 6023–6029.

Laguna, O., Odinot, E., Bisotto, A., Baréa, B., Villeneuve, P., Sigoillot, J. C., … Lecomte, J. (2019). Release of phenolic acids from sunflower and rapeseed meals using different carboxylic esters hydrolases from Aspergillus niger. *Industrial Crops and Products*, 139(July), 111579.

Laguna, O., Barakat, A., Alhamada, H., Durand, E., Baréa, B., Fine, F., … Lecomte, J. (2018). Production of proteins and phenolic compounds enriched fractions from rapeseed and sunflower meals by dry fractionation processes. *Industrial Crops and Products*, 118(Dec), 160–172.

Liu, L. L., Li, X. T., Zhang, N., & Tang, C. H. (2019). Novel soy β-conglycinin nanoparticles by ethanol-assisted disassembly and reassembly: Outstanding nanocarriers for hydrophobic nutraceuticals. *Food Hydrocolloids*, 91(Oct), 246–255.

Ozdal, T., Capanoglu, E., & Altay, F. (2013). A review on protein–phenolic interactions and associated changes. Food Research International, 51(2), 954–970.

Pedrosa, M. M., Muzquiz, M., García-Vallejo, C., Burbano, C., Cuadrado, C., Ayet, G., & Robredo, L. M. (2000). Determination of caffeic and chlorogenic acids and their derivatives in different sunflower seeds. *Journal of the Science of Food and Agriculture*, 80(4), 459–464.

Pickardt, C., Eisner, P., Kammerer, D. R., & Carle, R. (2015). Pilot plant preparation of light-colored protein isolates from de-oiled sunflower (*Helianthus annuus* L.) press cake by mild-acidic protein extraction and polyphenol adsorption. *Food Hydrocolloids,* 44, 208–219.

4

Pickardt, C., Neidhart, S., Griesbach, C., Dube, M., Knauf, U., Kammerer, D. R., & Carle, R. (2009). Optimisation of mild-acidic protein extraction from defatted sunflower (*Helianthus annuus* L.) meal. *Food Hydrocolloids*, 23(7), 1966–1973.

Prat, D., Wells, A., Hayler, J., Sneddon, H., McElroy, C. R., Abou-Shehada, S., & Dunn, P. J. (2015). CHEM21 selection guide of classical- and less classical-solvents. *Green Chemistry*, 18(1), 288–296.

Rawel, H. M., Meidtner, K., & Kroll, J. (2005). Binding of selected phenolic compounds to proteins. *Journal of Agricultural and Food Chemistry*, 53(10), 4228–4235.

Sathe, S. K., Zaffran, V. D., Gupta, S., & Li, T. (2018). Protein Solubilization. *J Am Oil Chem Soc Protein*, 300.

Scharlack, N. K., Aracava, K. K., & Rodrigues, C. E. C. (2017). Effect of the type and level of hydration of alcoholic solvents on the simultaneous extraction of oil and chlorogenic acids from sunflower seed press cake. *Journal of the Science of Food and Agriculture,* 97(13), 4612–4620.

Sripad, G., & Narasinga Rao, M. S. (1987). Effect of Methods to Remove Polyphenols from Sunflower Meal on the Physicochemical Properties of the Proteins. *Journal of Agricultural and Food Chemistry*, 35(6), 962–967.

Sripad, G., Prakash, V., & Rao, M. S. N. (1982). Extractability of polyphenols of sunflower seed in various solvents. *Journal of Biosciences*, 4(2), 145–152.

Subaşı, B. G., Casanova, F., Capanoglu, E., Ajalloueian, F., Sloth, J. J., & Mohammadifar, M. A. (2020). Protein extracts from de-oiled sunflower cake: Structural, physico-chemical and functional properties after removal of phenolics. *Food Bioscience*, 38(Sep).

Taha, F.S., Mohamed, G.F., Mohamed, S.H., Mohamed, S.S., Kamil, M. M. K. (2011). Optimization of the extraction of total phenolic compounds from sunflower meal and evaluation of the bioactivities of chosen extracts.6(12)1002-1020.

USDA. (2020). Oilseeds: world markets and Trade. Circular Series FOP 06-17. *Global Oilseed Consumption Continues to Grow Despite Slowing Trade and Production*, 1–50.

Vázquez-León, L. A., Olguín-Rojas, J. A., Páramo-Calderón, D. E., Palma, M., Barbero, G. F., Robles-Olvera, V. J., … Rodríguez-Jimenes, G. C. (2019). Modeling of counter-current multistage extraction of Moringa oleifera leaves using a mechanistic model. *Food and Bioproducts Processing*, 115, 165–174.

Wagner, J., Andreadis, M., Nikolaidis, A., Biliaderis, C. G., & Moschakis, T. (2021). Effect of ethanol on the microstructure and rheological properties of whey proteins: Acid-induced cold gelation. *Lwt*, 139(Nov), 110518.

Weisz, G. M., Kammerer, D. R., & Carle, R. (2009). Identification and quantification of phenolic compounds from sunflower (*Helianthus annuus* L.) kernels and shells by HPLC-DAD/ESI-MSn. *Food Chemistry*, 115(2), 758–765.

Ye, F., Liang, Q., Li, H., & Zhao, G. (2015). Solvent effects on phenolic content, composition, and antioxidant activity of extracts from florets of sunflower (*Helianthus annuus* L.). *Industrial Crops and Products*, 76, 574–581.

Zardo, I., de Espíndola Sobczyk, A., Marczak, L. D. F., & Sarkis, J. (2019). Optimization of Ultrasound Assisted Extraction of Phenolic Compounds from Sunflower Seed Cake Using Response Surface Methodology. *Waste and Biomass Valorization*, 10(1), 33–44.

Zhang, Z., Yang, Y., Tang, X., Chen, Y., & You, Y. (2015). Chemical forces and water holding capacity study of heat-induced myofibrillar protein gel as affected by high pressure. *Food Chemistry*, 188, 111–118.

Zhong, C., Zhou, Z., Zhang, Y. M., Jia, S. R., Sun, Z., & Dale, B. E. (2014). Integrating kinetics with thermodynamics to study the alkaline extraction of protein from Caragana korshinskii Kom. *Biotechnology and Bioengineering*, 111(9), 1801–1808.

Chapter 5

Covalent and non-covalent modification of sunflower protein with chlorogenic acid: identifying the critical ratios that affect techno-functionality
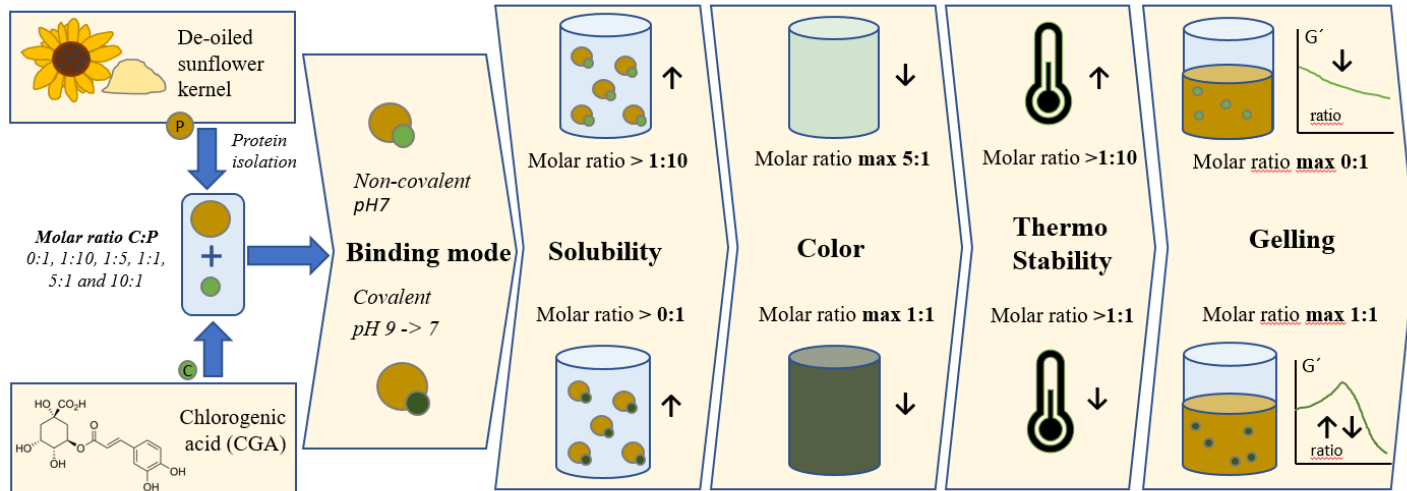
Abstract

Background: Phenolic compounds are removed from plant protein extracts because their interaction with proteins can lead to undesirable sensory and techno-functional changes. The trend toward less refined plant protein fractions requires clarification of the degree to which removal is necessary.

Approach: Chlorogenic acid (CGA) was added to sunflower protein solutions to obtain apparent CGA-protein molar ratios between 1:10 and 10:1. The samples were incubated either at pH 7 to induce non-covalent interactions or at pH 9 to induce covalent interactions. The type and extent of protein modification, physicochemical properties, solubility, and gelling ability were evaluated.

Results: Both binding modes of CGA had a positive effect on protein solubility. Covalently modified samples showed color changes upon a molar ratio of 1:1 and higher. All solutions were able to form gels (protein concentration 10% w/v). Maximum gel strength was obtained at a 1:1 ratio in case of covalent modification. Higher molar ratios led to lower gel strengths and this effect was more pronounced for covalently modified samples than for non-covalent ones.

Conclusion: Depending on the applications, complete removal of CGA is not necessary, since CGA improves the solubility of the sunflower proteins. However, CGA removal to a more favorable ratio between 5:1 and 1:1 is recommended if the material is used for gel formation. Under conditions that promote covalent binding with CGA, ratios above 1:1 lead to significant green coloration. It remains to be tested whether this observation also applies to less refined sunflower ingredients with multiple components.

Graphycal abstract

De-oiled sunflower kernel

Protein isolation

Molar ratio C:P
0:1, 1:10, 1:5, 1:1, 5:1 and 10:1

Chlorogenic acid (CGA)

Binding mode

Non-covalent pH7

Covalent pH 9 -> 7

Solubility

Molar ratio > **1:10**

Molar ratio > **0:1**

Color

Molar ratio **max 5:1**

Molar ratio **max 1:1**

Thermo Stability

Molar ratio >**1:10**

Molar ratio >**1:1**

Gelling

Molar ratio **max 0:1**

Molar ratio **max 1:1**

G´

ratio

5.1 Introduction

Sunflower protein is a promising source of protein for human consumption because of its nutritional value and techno-functional properties. Instead of purification into a protein isolate, modern food design aims at less refined fractions but high techno-functionality (Loveday, 2020; Van der Goot et al., 2016). Sunflower kernels naturally contain phenolic compounds. About 80% of the phenolic compounds is chlorogenic acid (CGA), which is present in a concentration of 2 to 4 g / 100 g in the kernel. CGA can bind reversibly to various proteins by non-covalent interactions (Jiang, Zhang, Zhao, & Liu, 2018; Zhang et al., 2021) through hydrophobic interactions and hydrogen bonds (Prigent et al., 2003). The binding can alter the protein solubility (Ozdal, Capanoglu, & Altay, 2013). Upon oxidation, CGA transforms into *o*-quinones, which can form covalent interactions with proteins, resulting in the formation of green colored adducts (Pierpoint, 1969). In contrast to non-covalent binding, covalent interactions are much stronger. CGA quinones bind covalently to the amino acid residues of lysine and cysteine, for example (Keppler et al., 2020), and this interaction is often perceived negatively because it can reduce protein digestibility, alter protein solubility, and affect organoleptic properties negatively (Karefyllakis, Salakou, Bitter, Van der Goot, & Nikiforidis, 2018; Wildermuth, Young, & Were, 2016). The information above explains why CGA is generally removed when sunflower material is processed into ingredients for food applications.

Despite the negative effects on the proteins, CGA has a high antioxidant activity and possibly beneficial health effects (Lu, Tian, Cui, Liu, & Ma, 2020). Thus, it would not only be a loss in resource efficiency but also in bio-functionality when removing it completely. Furthermore, there are also reports about improved techno-functional properties: covalent interactions of whey protein isolate with caffeic acid in gelatine gels were found to improve the mechanical strength of the gel, as well as induce stable foam formation in protein-colloidal dispersion (Prigent et al., 2007; Strauss & Gibson, 2004). In addition, similar positive effects were found for non-covalent whey protein and CGA interactions (Jiang, Zhang, Zhao, & Liu, 2018). Although the final techno-functionality of these modified proteins depends on the source of the reacting protein and the phenolic compound, a dose-dependent effect on the gelling properties was reported (Cao & Xiong, 2015; Cheng et al.,

2021; Keppler et al., 2020). The results on improved techno-functionality are in contrast to the negative reports. The reason is that little is yet known about the impact of the relative importance of covalent and non-covalent interactions of phenolic compounds and proteins on various techno-functional properties. It is essential to understand up to what extent the CGA can be retained in the material without compromising its potential use in food applications.

The effects of CGA on the overall functionality of sunflower proteins (techno-functional, sensory and biological functionality) cannot be easily summarized. They depend on many factors including the type (covalent, non-covalent), the extent of the interaction (molar ratio of CGA and protein), and the properties of the sunflower proteins (nativity, protein fraction composition). It is possible to study the effect of protein modification using less refined sunflower material instead of protein isolates. However, a sound interpretation of the results is complicated by the fact that this material contains a large number of components (i.e. protein, oil, polysaccharides, phenolic compounds, and small sugars). That is why we will approach here our question using a simplified model mixture comprising CGA and a sunflower protein isolate, which is a common procedure for such studies (Jiang et al., 2018; Qie et al., 2021; Wang et al., 2021). In this work, we will study the following aspects: (1) quantification of the modification degree of covalent and non-covalent binding under different CGA to sunflower protein molar ratios (from 1:10 to 10:1), (2) effect of the binding mode, and the modification degree on the physicochemical and techno-functionality of sunflower proteins, to identify the critical CGA-protein ratios in a model mixture. The outcomes will be used for a discussion on how the results of this study could be translated to design rules for less refined fractions with multiple components. Gelling properties will be the main target functionality here because of their importance for many food applications, such as meat analogues (Kyriakopoulou, Keppler, & Van der Goot, 2021).

5

5.2 Materials and methods

5.2.1 Materials:

De-oiled sunflower kernels (DSK) were provided by Avril Group (Bruz, France). DSK contain 52.7% protein (based on nitrogen content, with conversion factor of 5.6), 7.1% fat, 7.5% ash, 3.9% chlorogenic acid (CGA). The remaining part consists mainly of carbohydrates. The apparent CGA-protein molar ratio of 6.5:1 in DSK was calculated using the assumption of mean molecular weight of 30000 g/mol for sunflower proteins (Geneau-Sbartaï, Leyris, Silvestre, & Rigal, 2008), and 354 g/mol for CGA. Trifluoroacetic acid (purity of 99%), chlorogenic acid (CGA), sodium hydroxide (NaOH), and sodium chloride (NaCl) were purchased from Sigma Aldrich (St.Louis, USA). Acetonitrile ULC-MS (purity > 99%) and hydrochloric acid (HCl) was obtained from Actu-All chemicals (Oss, the Netherlands). Ethanol (purity of 96%) and sodium carbonate (Na_2CO_3) anhydrous were purchased from VWR Chemicals (Leuven, Belgium). For protein extraction, demi-water was used, and for all other experiments, Milli-Q water was used.

5.2.2 Methods

5.2.2.1 Preparation of sunflower protein isolate

Dephenolization

DSK was washed to remove phenolic compounds and other soluble components. The procedure is based on the protocol described in Jia et al., (2021). For this, 100 g DSK was mixed with an aqueous ethanol solution (ethanol content of 40%) in a 1L centrifuge bottle at a solid to liquid weight ratio of 1:5 w/w. The dispersion was stirred with a magnet at 400 rpm for 10 min at room temperature. The mixture was centrifuged at 6000 rpm for 10 min at 20 °C. The wet pellet was redispersed with fresh solvent. The pH of the supernatant was adjusted to 11 with 2M NaOH to detect a possible greenish color, which would indicate the presence of CGA in the dispersion. Up to 9 sequential washing steps were performed until no greenish color could be detected anymore. All supernatants were discarded after the washing process. The final pellet was kept overnight in a vacuum oven (Model VD 23, Binder GmbH) at 30 °C to allow for ethanol evaporation. The pellet was freeze-dried and kept at 4 °C for further fractionation. In total three individual batches were prepared.

Alkaline extraction

Sunflower protein isolate was fractionated using the protocol adapted from González-Pérez et al., (2002). The dephenolized DSK obtained after aqueous ethanol washing were evenly distributed over two centrifuge bottles of 1L. Demi-water was added to the bottle at a solid-to-liquid ratio of 1:10 w/v. The pH value of the dispersion was adjusted to 9 with 2M NaOH, after which it was further mixed with a magnetic stirrer at 400 rpm and continuously adjusted at pH 9 for one hour at room temperature. Afterward, the dispersion was centrifuged for 20 min at 10,000 rpm at 20 °C. The supernatant was freeze-dried and stored at 4 °C for further experiments, these samples are referred to as sunflower protein isolate (SFPI).

The nitrogen content of the SFPI was determined with the Dumas combustion method by using a Nitrogen Analyzer (Flash EA 1112 Series, Thermo scientific, Delft, The Netherlands), with a protein conversion factor of 5.6 (Pickardt, Eisner, Kammerer, & Carle, 2015). Besides, it is assumed that the SFPI was completely dephenolized after the intensive washing and alkaline extraction, based on our previous publication (Jia et al., 2021). The SFPI had a protein purity of 91.6 wt% after freeze-drying based on Dumas analysis. The protein content is slightly lower compared with the reported protein content of 94 wt% and 98 wt% in a purified sunflower isolate (González-Pérez et al., 2002; Karefyllakis, Altunkaya, Berton-Carabin, Van der Goot, & Nikiforidis, 2017), which might be due to different fractionation processes.

Protein modification

A covalent or non-covalent interaction between sunflower protein and CGA was induced by incubating the SFPI protein solution with CGA for 24 h at pH 9 (covalent) or pH 7 (non-covalent) using 2 M of NaOH or 2 M of HCl, respectively. Firstly, a protein stock solution (40 mg/mL) of 16.5 mL and a CGA stock solution (4.6 mg/mL) of 4.5 mL was prepared in falcon tubes. The pH value of both stock solutions was adjusted to either 7 or 9. Afterward, the protein stock solution of 2.5 mL at pH 7, or pH 9, was mixed with CGA stock

5

Table 5-1 Modified protein solutions at different CGA-protein apparent molar ratios in terms of volume, protein and CGA concentrations.

Modified protein solution CGA[*]-protein		Stock protein solution[***]	Stock CGA solution[***]	Milli-Q Water	Protein concentration	CGA concentration
Apparent molar ratios [**]	Mass ratios	mL	mL	mL	mg/ml	mg/ml
Reference	Reference	2.5	0	2.5	20	0
1:10	1:850	2.5	0.025	2.475	20	0.023
1:5	1:450	2.5	0.05	2.45	20	0.046
1:1	1:85	2.5	0.25	2.25	20	0.23
5:1	1:15	2.5	1.25	1.25	20	1.1
10:1	1:10	2.5	2.5	0	20	2.3

[*] *CGA for chlorogenic acid.*

[**]*Assumption of molecular weight of protein (30000 g/mol) and CGA (354g/mol). All values are given as integers*

[***]*Stock protein solution of 40 mg/mL and stock CGA solution 4.6 mg/mL.*

solution at the respective pH using the volumes indicated in Table 5-1. Milli-Q water was added to reach the different mass ratios of 1:850, 1:450, 1:85, 1:15, and 1:10 between CGA and protein in the final mixtures with a protein concentration of 20 mg/mL. These mass ratios correspond to apparent molar ratios of 1:10, 1:5, 1:1, 5:1 and 10:1, based on the assumption of mean molecular weight of dissociated sunflower proteins (30000 g/mol) and CGA (354 g/mol) (Geneau-Sbartaï et al., 2008). For simplicity, we will mainly use the apparent molar ratios in the following sections. All CGA and protein mixtures were vortexed. The pH value of the mixtures was checked and readjusted to either pH 7 or 9. Afterward, the mixtures were rotated (SB3 rotator, Stuart, UK) for 24 h at room temperature at a speed of 20 rpm to allow complete reactions (Karefyllakis et al., 2018). Subsequently, all pH 9 solutions (reference and incubated CGA-protein mixtures) were adjusted to pH 7 for comparison purposes. The same procedure was applied at a higher concentration of 10 % w/v for the thermal measurements (Section 5.2.2.3).

5.2.2.2 Protein analysis

Quantification of CGA and modified proteins

To elucidate if the presence of unbound CGA affects the protein structure, all samples were analyzed with FTIR before and after diafiltration. The CGA diafiltrates of the different mixing ratios were also used as a blank for the respective unfiltered CGA-protein solutions. For the diafiltration, 3 mL of the reference and modified protein solutions were filtered with centrifugal filters (10 kDa, Amicon® Ultra, 4 mL, Merck) at 4000 rpm. The filters were twice refilled with water to remove unbound CGA and other small molecules. The original sample, as well as the diafiltrated samples, were used for FTIR analysis as well as for RP-HPLC.

The amount of bound and unbound CGA in the reference, the covalently or non-covalently modified protein solution was determined based on the methods reported previously (Ali, Keppler, Coenye, & Schwarz, 2018). A reversed-phase high performance liquid chromatography (RP-HPLC) was used for the measurement with a PLRP-S column (300˚A, 8 m, 150×4.6 mm). The eluents were 0.1% trifluoroacetic acid (v/v) in water (A) and acetonitrile (B). The gradient was applied under the following conditions: 10% to 18% B, 22

min; 18% to 80% B, 8 min; 80% B, 3 min; 80% to 10% B, 2 min; 10% B, 7 min. The run time was 42 min. 50 µL of eluent was injected with a flow rate of 0.6 mL/min. All reference and modified protein solutions were filtered using syringe filters (Whatman®, Merck, 0.45 µL for RP-HPLC). The filtered samples of 10 µL were injected into the system and the flow rate was maintained at 0.6 mL/min. A calibration of CGA standard between 0.05-0.35 mg/mL was conducted (Fig.S5-1). The Diode array detector (Chromeleon Chromatography Data system, Thermo Fisher, the Netherlands) was set to the wavelengths of 280 and 330 nm for protein and CGA analysis, respectively.

RP-HPLC can also be used to semi-quantify the non-covalent modification degree (Ferraro et al., 2015). Three assumptions were made: (1) the unbound CGA was completely removed by the diafiltration (see 5.2.2.2), (2) at 330 nm, the absorption of CGA in the diafiltrated samples corresponds to non-covalently bound CGA, (3) the absorption of the CGA in the non-diafiltrated samples includes both unbound and non-covalently bound CGA. Thus, the percentage of the non-covalently bound CGA can be calculated by the amount of CGA in the diafiltrated solution divided by the total CGA detected with the non-diafiltrated solution in equation (1). Also, the apparent modification degree can be calculated with equation (2).

$$\text{Non-covalently bound CGA} = \frac{C_{\text{CGA,diafiltrated}} \times V_{\text{dilfiltrated}}}{C_{\text{CGA,total}} \times V_{\text{total}}} \times 100\% \qquad (1)$$

$$\text{Apparent modification degree} = \frac{C_{\text{CGA,diafiltrated}} \times V_{\text{dilfiltrated}} \times MW_{\text{protein}}}{C_{\text{protein,total}} \times V_{\text{total}} \times MW_{\text{CGA}}} \qquad (2)$$

where the $C_{CGA,diafiltrated}$ and $V_{dilfiltrated}$ indicates the concentration of CGA and the volume of the diafiltrated solution, and the $C_{CGA,total}$ and V_{total} indicates the concentration of CGA and the volume of the non-diafiltrated solution.

Protein molecular profile

The protein molecular weight distribution of the reference and modified protein solutions were determined using sodium dodecyl sulfate-polyacrylamide gel electrophoresis (SDS-PAGE) as previously described (Jia, Rodriguez-Alonso, Bianeis, Keppler, & van der Goot, 2021). For this, a protein solution (2 mg/mL) was prepared in a falcon tube using Milli-

Q water. The reference and modified protein solutions were prepared with Tris-buffer containing 2% w/w SDS, 10% glycerol, 0.5% w/v bromophenol blue, and 5% β-mercaptoethanol. The solutions were vortexed and heated at 95 °C for 10 min, after which the sample was centrifuged at 10.000 rpm for 1 min. The electrophoresis was performed at 200 V for approximately 40 min in a Mini-Protean II electrophoresis cell (Bio-rad, Veenendaal, Netherlands).

Protein secondary structure

The protein secondary structure of the reference and the filtered and unfiltered modified protein solutions was measured using an ATR-Fourier Transform Infrared (FTIR) spectrometer with a thermally controlled Bio ATR2 unit at 25 °C and MCT detector (Confocheck™ system, Bruker Optics, Ettingen, Germany). The Confocheck™ is optimized for protein analytics in aqueous solutions (Keppler, Heyn, Meissner, Schrader, & Schwarz, 2019). Interferograms were accumulated over the spectral range 4000-500 cm^{-1}, with a resolution of 4 cm^{-1}. Measurements were conducted at 25 °C against the respective solvent mixtures (e.g. obtained by the filtration described above) without protein as background and averaged over 60 scans at a resolution of 0.7 cm^{-1}. The solutions were loaded in triplicates and two measurements were performed per load, an average value was calculated out of the total 6 measurements. For each measurement, 20 µL of the sample was injected into the cell. For evaluation, the measured spectra in the frequency range of the amide band I (1580-1700 cm^{-1}) and were then vector-normalised. The second derivative was calculated using 9 smoothing points.

5.2.2.3 Functionalities analysis

Color measurement

The UV-vis absorbance of the reference and modified protein solutions were measured by a spectrophotometer (DR6000 UV/VIS, Hach, the Netherlands) using a multi wavelength scan between 400-800 nm. The solutions were first centrifuged at 12, 000 x g for 10 min and the supernatant was further diluted 20 times to fit the absorbance range below 2 AU.

Water holding capacity and Nitrogen solubility index

The water holding capacities (WHC) and nitrogen solubility index (NSI) of the protein solutions were measured using a method based on a protocol described previously (Jia et al., 2021). A 2% w/v protein solution of reference or the modified protein samples was made in a falcon tube. Protein modifications upon CGA-addition was prepared with the same method as described in section 5.2.2.1. The samples were vortexed and rotated overnight with a rotator (SB3 rotator, Stuart, UK) at a speed of 20 rpm. Afterward, the samples were centrifuged at $15,000 \times g$ at 25 °C for 20 min. The supernatant was removed with a pipette and the wet pellet was transferred into an aluminium tray and dried in an oven at 105 °C (Model E28, Binder, Germany) for 24 h. The weight of the wet pellet ($M_{wet\,pellet}$) and afterward dried pellet ($M_{dry\,pellet}$) was measured. The dry masses of the original sample and the pellet were measured and expressed as $M_{original}$ and $M_{dry\,pellet}$. The WHC of the dry pellet was calculated with equation (3). The protein content $Pro_{original}$ in the initial sample can be calculated from the Dumas result described in section 2.2.1. Thus, the remaining pellet indicates the insoluble protein $Pro_{dry\,pellet}$, and the NSI can be calculated in equation (4).

$$\text{WHC} = \frac{M_{\text{wet pellet}} - M_{\text{dry pellet}}}{M_{\text{dry pellet}}} \text{ [g water /g dry pellet]} \tag{3}$$

$$\text{Solubility} = \frac{Pro_{original} - Pro_{\text{dry pellet}}}{Pro_{original}} * 100\% \text{ [\%]} \tag{4}$$

Protein thermal stability and nativity

The protein thermal stability and nativity of reference and modified protein samples with 10% w/v protein concentration (see 5.2.2.1) were analyzed with differential scanning calorimetry (DSC) (TA instrument 250; TA Instruments, Newcastle, DE, USA). The samples of 40 µL were weighed and added to a high-volume pan and sealed. The pan was heated from 25 to 130 °C using a heating rate of 5 °C/min. After 1 min, the pan was cooled down to 25 °C using a cooling rate of 20 °C/min. This heating and cooling process was repeated for a second time to make sure the peak indicated protein denaturation. Duplicates were measured for each sample. The onset protein denaturation temperature (onset T_d), the peak temperature of

denaturation (onset T_d) and the denaturation enthalpy (J/g protein) were collected by Trios data analysis software (TA Instruments).

Rheological properties

To identify the necessary protein concentration for gelling experiments, various concentrations of unmodified SFPI solutions of 5 mL were prepared in test tubes (4%, 6%, 8%, 10%, 16%, and 20% w/v at pH 7). All samples were subsequently heated at 95 °C for 30 min using a water bath. Afterward, the solutions were cooled to 4 °C overnight. The concentration above which the sample did not fall or slip when the tube was inverted was noted as the least gelation concentration (LGC). The gelling behavior of the modified protein solutions was then measured at 10% w/v, also for a comparison with other publications which often use 10% for the sunflower protein gels (González-Pérez & Vereijken, 2007a; Malik, Sharma, & Saini, 2016).

The rheological properties of the reference and modified protein solutions were studied by monitoring the storage (*G'*) modulus and loss modulus (*G''*) during thermal treatment. An Anton Paar MCR 502 rheometer (Graz, Austria), equipped with concentric cylinder CC17 geometry, was used for the measurement. The method was previously applied to other plant protein fractions as well (Kornet et al., 2021; Peng et al., 2021). First, the linear viscoelastic properties of the reference sample were evaluated. Subsequently, a temperature sweep was applied to the reference and the solutions with protein and CGA. The samples were heated from 20 to 95 °C using a heating rate of 3°C/min, then held at 95 °C for 5 min and cooled to 20 °C using a cooling rate of 3 °C/min. Silicon oil was added on top of the solution inside the cylinder to avoid water evaporation during thermal treatment. The storage (*G'*) and loss modulus (*G''*) dependency on temperature and frequency was recorded. After cooling, a frequency sweep was performed in the range of 0.1 to 10 Hz at a constant strain of 1%, and *G'* and *G''* were recorded as a function of frequency. Strain sweep was performed to the gels in the range of 0.1 to 1000% at a constant frequency of 1Hz at 20 °C. *G'* and *G''* were recorded as a function of strain for 10 min to collect 100 data points. The analysis was done for all solutions, but in the SFPI solution with CGA at 1:5 molar ratio, triplicates analysis was done to ensure the obtained result. Subsequently, the gels were subjected to a frequency sweep from 0.01 to 10 Hz (at a strain of 1%).

Additional experiments were performed with the dephenolized sunflower protein concentrate (protein content of 60 % in dry base), which was prepared by an aqueous ethanol washing process (section 2.2.1 of dephenolization). The covalent modification was induced here in a solution of 10% w/v with CGA-protein molar ratios of 1:10, 1:5, 1:1, 5:1, and 10:1. It is noteworthy that protein concentration in the solution is only 6% w/v.

5.2.2.4 Statistic analysis

The data derived from the DSC, water holding capacity, and protein solubility measurement was analyzed using SPSS software (IBM statistical analysis Version 25.0). Univariate general linear model with LSD test was performed to investigate significant differences in between the different apparent CGA-protein molar ratios of 1:10, 1:5, 1:1, 5:1, and 10:1 and reference samples of pure protein but similar pH-treatments. Differences were considered significant if $P < 0.05$.

5.3 Results & discussion

5.3.1 Sunflower protein modification analysis

The modified covalent and non-covalent sunflower protein by chlorogenic acid (CGA) was analyzed by RP-HPLC. The sunflower protein isolate (SFPI) free of CGA was used as a reference benchmark.

Reference sample

The chromatogram of the CGA standard (Fig. 5-1 A and C) showed the absorbance of CGA after ~10 min retention time (RT) at 330 nm and 280 nm (Prigent et al., 2003; Salgado, Molina Ortiz, Petruccelli, & Mauri, 2011). No CGA was detected in the reference sample at 330 nm (Fig. 5-1 B), which indicated effective removal of CGA by the intensive aqueous ethanol washing and alkaline extraction. However, a small peak was evident at ~28 min for the SFPI reference sample at 330 nm. A similar chromatogram was obtained at 280 nm (Fig. 5-1 D), here the peak at 28 min corresponded to sunflower proteins. Thus, the peak at 28 min detected at 330 nm wavelength (Fig. 5-1 B) might be the absorbance of covalently bound CGA, which was probably created during the protein fractionation process.

Non-covalent modification

The chromatograms of the non-covalently modified samples with CGA-protein molar ratios at 1:10 and 10:1 is shown in Fig. 5-2. The chromatograms of all the modified samples are shown in Fig.S5-2,5-3 (supplementary data). As expected, the peak height of free CGA at a RT of 10 min increased with increasing CGA-protein molar ratio (Fig. 5-2A). Covalent interactions with proteins can be excluded for the most part. Only at higher molar ratios of 5:1 and 10:1 is a slight peak area increase observed at 28 min RT (detected at 330 nm), from 10 to 18 mAU*min between reference and 10:1 modification. Non-covalent interaction cannot be directly seen in RP-HPLC as the interaction is reversible and those interactions might get lost due to the conditions and eluent used in the RP-HPLC measurement. However, diafiltration can be used to remove unbound CGA prior to RP-HPLC analysis.
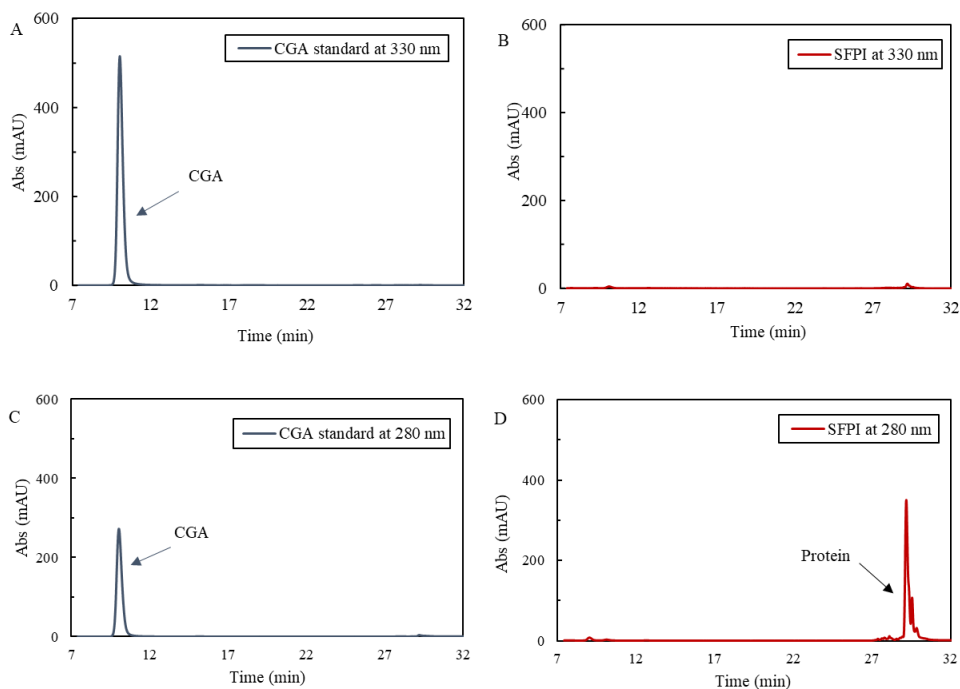
Fig. 5-1 RP-HPLC chromatogram at the wavelength of 330 nm of standard CGA sample (A) and the reference SFPI sample (B) at pH 7, as well as at 280 nm of standard CGA (C) and modified SFPI samples (D).

This CGA removal is shown in Fig. 5-2B as a lower CGA peak at 10 min RT of the diafiltrated sample compared with the non-diafiltrated modified protein samples. The peak area was converted into the CGA concentration with the CGA standard calibration curve (Fig.S5-1). Thus, the concentration difference between the remaining CGA in the diafiltrated samples and the non-diafiltrated protein samples roughly gives the percentage of non-covalently bound CGA (Carson et al., 2019) (Fig. 5-2C). Approximately 25% and 20% of the added CGA was non-covalently bound to the protein between the molar ratios of 1:10 and 1:1. This corresponds to an apparent modification degree of less than 0.2 mol of CGA per mol of protein. At higher mixing ratios of 5:1 and 10:1, about 16 % of the added CGA was non-covalently bound. The degree of modification corresponds to 1-1.5 mol CGA per mol protein. However, the calculated modification degree is an underestimation of the actual modification level, since the non-covalent interaction is reversible and the binding equilibrium is likely to be affected by the diafiltration (Ozdal et al., 2013).
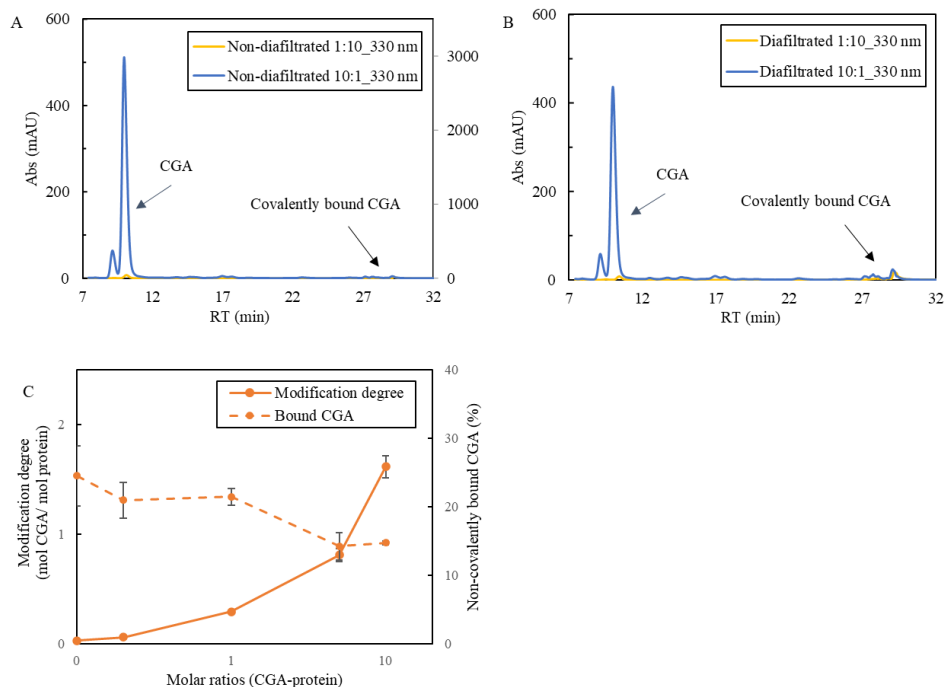
Fig. 5-2 RP-HPLC chromatogram of non-covalently modified protein samples at the apparent CGA-protein molar ratios of 1:10 and 10:1 (A), and the accordingly dialyzed samples at 330 nm (B). The modification degree (mol CGA/ mol protein) and the percentage of the non-covalently bound CGA of the modified samples at different molar ratios (X-axis in log) is shown in C.

Covalent modification

The chromatograms of covalently modified protein samples with a CGA-protein ratio of 1:10 and 10:1 is shown in Fig. 5-3. The chromatograms of all the modified samples are shown in Fig. S5-4, 5-5 (supplementary data). The covalent protein modification can be detected using the same RP-HPLC method as used for the non-covalent interactions, because both unbound CGA and irreversibly protein-bound CGA absorb at the 330 nm but elute at different retention times (Ali et al., 2018). While unbound CGA elutes after 10 min RT, its various oxidized quinone derivatives are evident between 7 and 27 min, and protein bound CGA elutes with the protein after 28 min. The second peak after 29 min could indicate that multiple CGA are covalently bound per protein (affecting the protein hydrophobicity and thus prolonging the retention time) (Keppler et al. 2014). The areas of both peaks at the RT

of 28 and 29 min became larger with higher CGA-protein ratios (Fig. 5-3C, Fig. S5-4), which suggests the degree of covalently modified proteins significantly increased above an apparent molar ratio of 1:1. A plateau was nearly reached at the CGA-protein molar ratio of 10:1 and the result suggested that most of the proteins (or available binding sites) were conjugated with the CGA (Liang & Were, 2020).
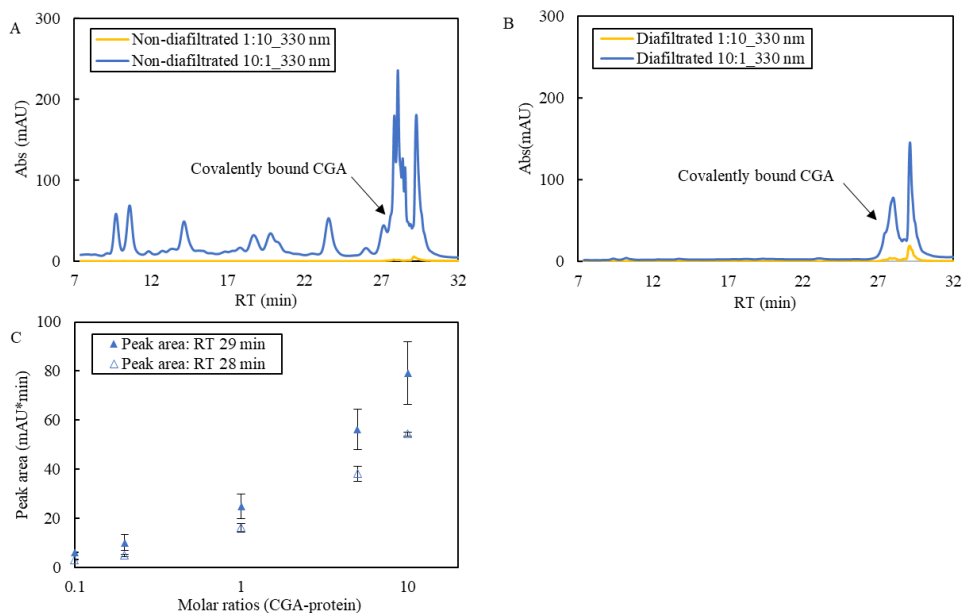

Fig. 5-3 RP-HPLC chromatograms of covalently modified protein samples at the apparent molar ratios of 1:10 and 10:1 (A), and the accordingly dialyzed samples at 330 nm (B). The peak area of the dialyzed modified SFPI samples with different molar ratios (X-axis in log) at the retention time of ~ 29 min (closed symbol) and ~ 28 min (open symbol) (C).

5.3.2 Effect of CGA modification on Protein chemical properties

Protein profile

The SDS-PAGE profiles of unmodified and modified SFPI are shown in Fig. 5-4. The molecular weights of the proteins after adding a reducing agent were mainly in the range between 10 to 50 kDa. Sunflower proteins are known to consist of water soluble 2S albumins with the molecular weight (MW) between 10 and 20 kDa and 11S globulins named helianthinin with the MW between 19 and 50 kDa under reducing conditions (González-Pérez et al., 2002; Karefyllakis et al., 2017). In total three dissociated polypeptide groups of helianthinin in the presence of β-mercaptoethanol were reported: two acidic ones with the

MW of 36.8-42.9 kDa and 31-35.3 kDa respectively, and the neutral polypeptide group had a MW of 21.0-29.6 kDa (Geneau-Sbartaï et al., 2008; González-Pérez et al., 2005). These polypeptides were also detected here, as shown in Fig. 5-3. Another band with 50 kDa was probably related to the helianthinin (Karefyllakis et al., 2018). Besides, the band found at 10 and 20 kDa can be related to the 2S albumins and the rest of the bands are clustered as globulins (González-Pérez & Vereijken, 2007b). The protein profile of all the modified samples remained similar to the reference, except for the covalently modified samples with CGA-protein ratios above 1:1. In those samples, the 50 kDa band disappeared and the bands between 25-37 kDa became less intense, whereas unclear bands between 50-250 kDa became visible. Thus, it is most likely that covalent CGA-protein complexes were formed with large MW at higher molar ratios between 1:1 and 10:1. This aggregation is in line with previous research (Karefyllakis et al., 2018). Overall, the SDS-page results confirm the formation of covalent CGA-protein complexes as described above in the results of RP-HPLC, especially for higher ratios of 5:1 and 10:1.
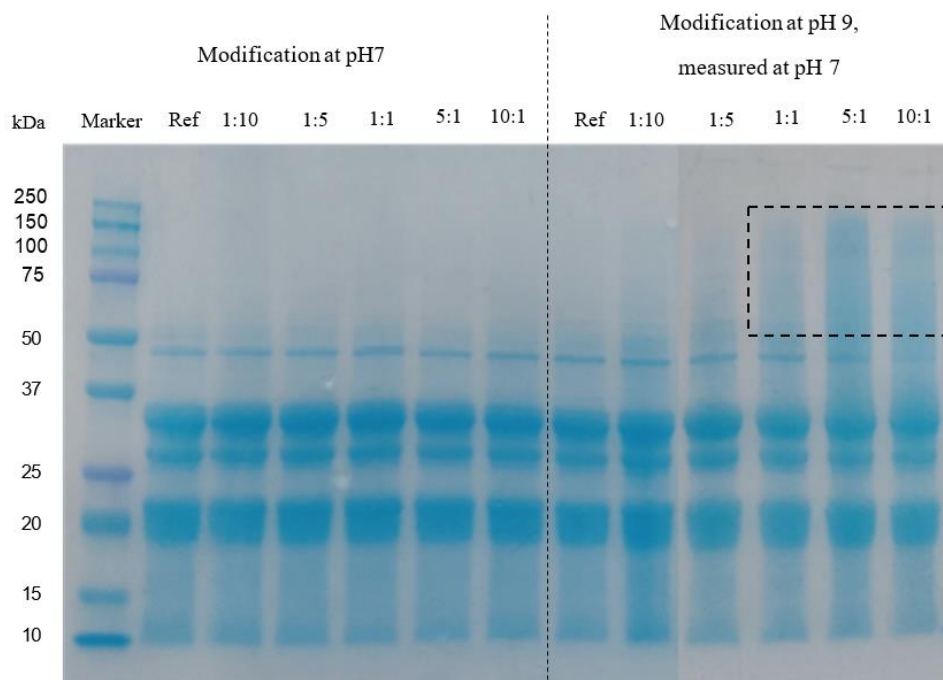

Fig. 5-4 Protein molecular profiles measured by SDS-PAGE, with respect to the reference and modified protein samples at pH7 and pH9.

Protein secondary structure

The protein secondary structures of the reference and modified proteins before and after diafiltration were measured with ATR-FTIR (Fig. 5-5). For all the samples, the 2nd derivative intensity of β-sheets (1635 cm^{-1}) (Subaşı et al., 2020) was highest among all the other structures. This observation aligns with previous research (Malik, Sharma, & Saini, 2016). For the pH 9 reference sample (Fig.5-5A, B), the pH-shift (24 h incubation at pH 9, then back to pH 7) affected the secondary structure: more intramolecular β-sheets (1635 cm^{-1}) and fewer intermolecular aggregates (1621 cm^{-1}) (Kayser et al., 2020) were evident compared with the reference sample incubated at pH 7 for 24 h. The secondary structure of the reference protein was not changed by the removal of salt by diafiltration (Fig. 5-5B). Thus, the pH-dependent change could be caused by the pH shift, which is a known type of structural protein modification in which the numerous multiple subunits of globulins are broken down into their individual subunits and thus into soluble protein aggregates (Jiang et al., 2017).

In the non-covalently modified samples, the concentration of intramolecular β-sheets (1635 cm^{-1}) increased as a function of added CGA (Fig. 5-5C). CGA addition resulted in a higher 2nd derivative intensity for the samples with a CGA-protein molar ratio of 5:1 and 10:1 (-0.00064 AU) than the lower CGA content (above -0.0005AU). Further, the α-helix structure (1657 cm^{-1}) and the random coil structures (1645 cm^{-1}) (Keppler et al., 2019) decreased for the CGA-protein ratios of 5:1 and 10:1. The 2nd derivative intensity at 1621 cm^{-1} was lower for these two molar ratios as well, suggesting increasing intermolecular interactions that typically occur in solutions with phenolic compounds and proteins. Diafiltration led to a smaller difference between the samples with molar ratio above 5:1 (Fig. 5-5D). This suggested that diafiltration affected the binding equilibrium between CGA and protein. In general, less structural changes were found for the covalently modified protein samples than for the non-covalent ones (Fig. 5-5E). The most pronounced change was the α-helix structure at 1657 cm^{-1}, and the amount decreased with higher molar ratios of 5:1 and 10:1. A similar effect was observed previously for covalently modified sunflower protein isolate (Karefyllakis et al., 2018). The limited effect of the CGA addition on protein structure is probably a result of the fact that the covalently modified protein samples have underlying

additional structural modifications caused by the pH-shift. The diafiltration showed only a small effect on the 2nd derivative Amide I intensity bands in these samples (Fig. 5-5F). Since covalent interactions are mostly irreversible, they are expected to be unchanged by the diafiltration step.
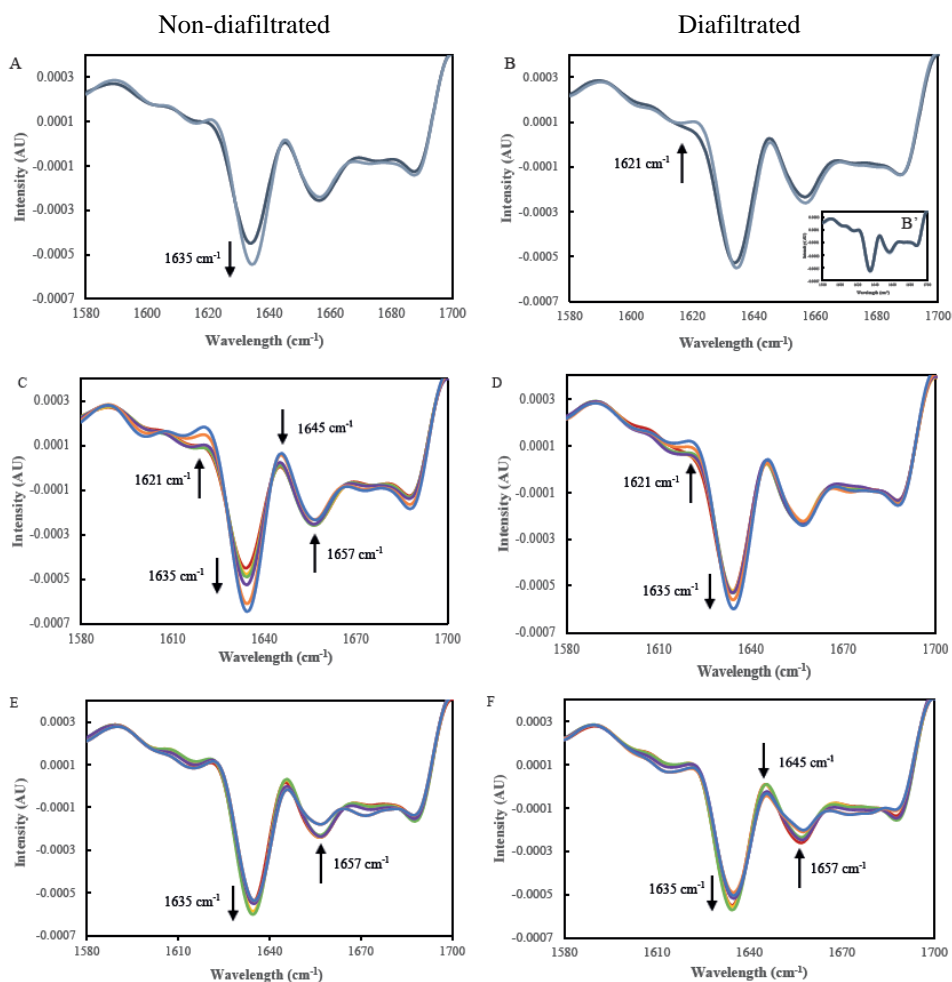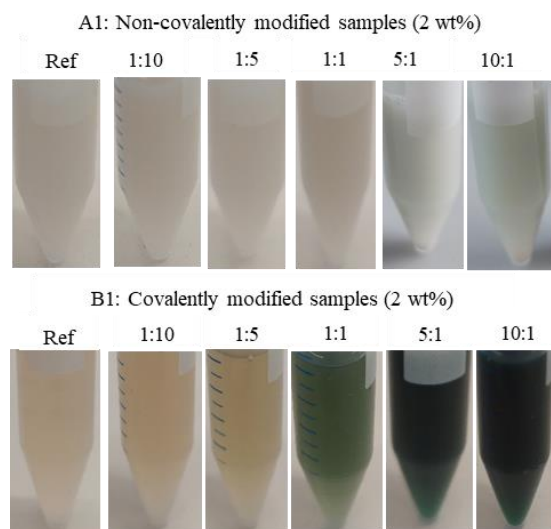

Fig. 5-5 Secondary derivative FTIR spectra in the Amide I region of reference samples incubated at **pH 7 or pH 9** (A), and the diafiltrated reference samples (B). Besides, the covalently modified samples with both non-diafiltrated and diafiltrated are compared in B' inside Fig B. The non-covalently modified samples with CGA (C) and the diafiltrated samples (D), as well as the covalently modified samples (E) and the diafiltrated samples (F). Different molar ratios between the protein and CGA are shown as reference, 1:10, 1:5, 1:1, 5:1, 10:1. All the samples were measured at pH7.

5.3.3 Functional properties

In the previous experiments all samples were measured before and after diafiltration to better characterize their binding behavior and elucidate how the pH-shift, and the presence of unbound CGA, affects the analysis and protein structure. The evaluation of the functional properties of the covalently and non-covalently modified SFPI was carried out without diafiltration step.

Color measurement

The non-covalently modified samples were colorless at low apparent CGA-protein molar ratios, but some light green color was observed in solutions with a CGA-protein molar ratio of 5:1 and 10:1 (Fig. 5-6). The absorption peak found at the wavelength of 700 nm for these two samples also confirmed the absorption of red color (thus green transmission). This green color suggests a covalent interaction (Wildermuth et al., 2016), which was also observed in the RP-HPLC-chromatograms, in which a small peak at ~28 min became visible at higher modification levels (Fig. 5-2B). In contrast, the solutions containing the covalently modified proteins with CGA-protein molar ratios of 1:10 and 1:5 and the reference solution had a light-yellow color. A green color was observed for the solution with higher molar ratios between 1:1 and 10:1. This observation was also confirmed with a peak absorption in the range of 0.04 and 0.4 AU at 700 nm. This consecutive stronger occurrence of the green color formation is most likely associated with the increased rate of covalent modification observed in RP-HPLC (Fig. 5-3C), as well as the changes in protein secondary structure as observed with FTIR. The green color was also observed for covalently modified sunflower protein with CGA-protein molar ratio of 1:1 and onwards, or the amino acid/CGA molar ratio of 1:1 (Iacomino et al., 2017; Karefyllakis et al., 2018).
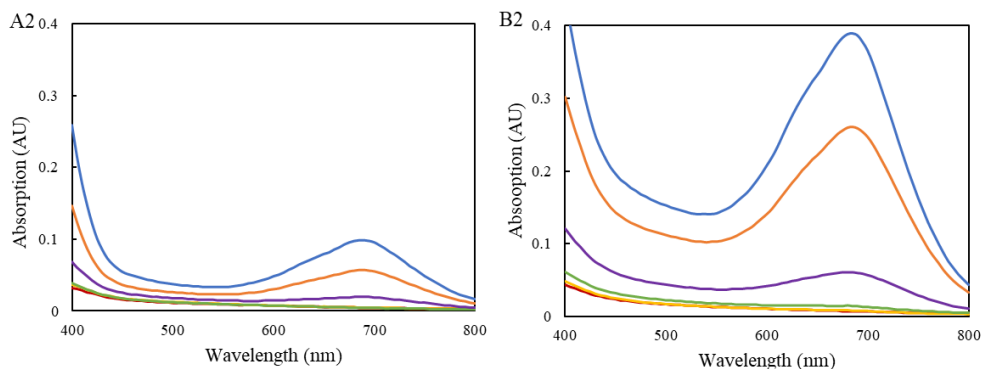

A1: Non-covalently modified samples (2 wt%)
Ref   1:10   1:5   1:1   5:1   10:1

B1: Covalently modified samples (2 wt%)
Ref   1:10   1:5   1:1   5:1   10:1

Fig. 5-6 Non-covalently modified sunflower protein solutions at 2 wt% (A1), UV-Vis spectra between the wavelength 400-800 nm for the non-covalently modified samples (A2) and covalently modified sunflower protein solutions at 2 wt% (B1) and the corresponding UV-Vis spectra (B2). Different molar ratios between the reference and CGA are shown as following: reference, 1:10, 1:5, 1:1, 5:1, 10:1.

Protein solubility and water holding capacity

The protein solubility of the reference solution was about 67%. After applying a pH-shift the protein become almost completely soluble, which might be linked to the observed change in protein secondary structure (FTIR, **Fig. 5-5**). The addition of CGA at pH 9 did not reduce the high solubility of the solution. As a result, the WHC and NSI of this solution at pH 9 could not be measured.
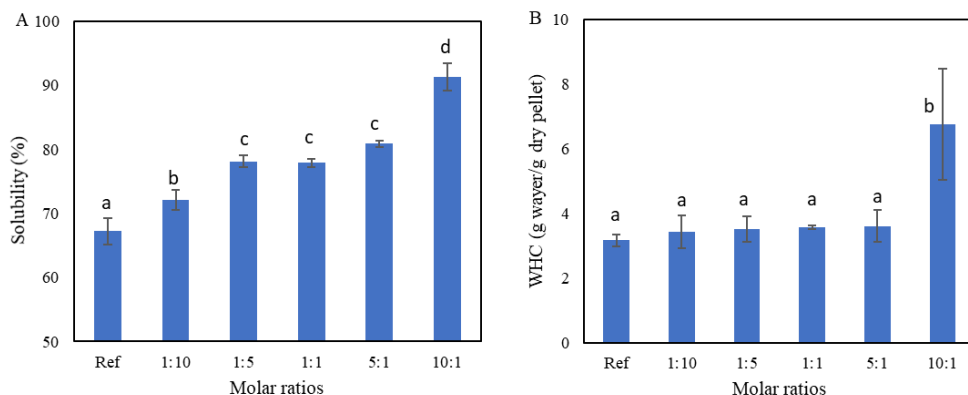

Fig. 5-7 Apparent protein solubility (%) (A) and apparent water holding capacity (WHC) (g water/g dry pellet) (B) of the non-covalently modified samples at different molar ratios.

Thus, only the effect of non-covalently bound CGA on protein solubility and WHC could be determined. The solubility of the protein was already largely increased above a molar ratio of 1:1 (Fig. 5-7), where 20 % of the added CGA was protein bound (which corresponds to more than 0.5 mol CGA per mol protein) (Fig. 5-2). An explanation for the increase of the solubility could be the polar nature of CGA, which makes the protein more hydrophilic when bound to protein. Similar findings were reported previously that the CGA can positively affect the solubility of globulin from white bean both at pH 7 or pH 9 (Sęczyk, Swieca, Kapusta, & Gawlik-Dziki, 2019). The WHC for all the non-covalently modified protein samples was approximately 3 g /g dry pellet except for a significantly higher value of 7 g water/g dry pellet obtained for the CGA-protein molar ratio of 10:1. The result was found to be in line with the reported 3 ml water /g sunflower protein isolate by previous studies (Khalil, Ragab, & Hassanien, 1985). The large increase of WHC with the ratio of 10:1 might be explained by the large increase of β-sheets (Fig. 5-5C), which have a large surface area and could contribute to the intermolecular hydrogen bonding and is most likely to hold more water (Malik & Saini, 2017).

Protein thermal stability and nativity

The onset and peak denaturation temperature (T_d) was rather similar for the reference and all the modified protein samples (93-94 °C and 99-100 °C, respectively) in Table 5-2. The results indicated that the protein modification by CGA hardly affected the onset and peak T_d of the protein. The denaturation enthalpy (E_d) of the reference sample was found to be 9.5 J/g protein when incubated at pH 7, and 11.8 J/g protein after the pH-shift. This difference in the E_d-value might be associated with the differences observed in the protein secondary structure by FTIR in Fig. 5-5 (A and B). The energy value found here was slightly lower than the value of 14.9 J/g sunflower protein reported by González-Pérez et al., (2003), which might be due to a different fractionation process, experimental condition and protein composition. The E_d-value was found to increase slightly for the non-covalently modified proteins with lower molar ratios of 1:10 and 1:5, indicating a minor structural stabilization caused by the non-covalent modification. This was in line with the previous findings that some proteins became more thermal stable by non-covalently protein-phenol interactions (Rawel, Czajka, Rohn, & Kroll, 2002). Though a slightly lower E_d-value was

observed for the samples with higher CGA-protein ratios, the E_d-value was still higher compared with the reference sample. Prigent et al., (2003) also reported that at high CGA-bovine serum albumin ratios, the non-covalent modification increased the energy needed for the protein denaturation. For the covalently modified protein samples, the highest E_d-value (13.3 J/g protein) was found at a low CGA-protein molar ratio of 1:10. The increase in the E_d-value was also reported for soy glycinin modified with CGA at pH 9 (Rawel et al., 2002). A decrease in E_d was found with further increasing of CGA-protein ratios from 1:5 till 10:1, while at the same time the onset T_d was slightly higher. These changes are in line with the more intense changes of the protein secondary structure observed in FTIR in Fig. 5-5 (E and F), and the evidence of multiple binding sites in RP-HPLC (Fig. 5-3B), as well as the large aggregate formation in SDS-PAGE (Fig. 5-4).

Table 5-2: The onset denaturation temperature (onset T_d), peak T_d) and enthalpy of denaturation (E_d J/g protein) for the reference and modified protein solutions at pH 7 and pH 9 at varied apparent CGA-protein molar ratios of 1:10, 1:5, 1:1 5:1 and 10:1.

Non-covalent modification	Onset T_d (°C)	Peak T_d (°C)	Enthalpy E_d (J/g protein)
Ref	93.8 ± 0.3 [a]	100.0 ± 0.3 [b]	9.5 ± 1.6 [a]
1:10	93.0 ± 1.1 [a]	100.2 ± 0.3 [ab]	12.2 ± 0.4 [ab]
1:5	93.5 ± 0.2 [a]	100.1 ± 0.2 [b]	13.0 ± 1.5 [b]
1:1	93.8 ± 0.5 [a]	100.2 ± 0.3 [ab]	12.6 ± 0.7 [ab]
5:1	93.9 ± 0.5 [a]	100.8 ± 0.3 [a]	11.8 ± 0.8 [ab]
10:1	93.4 ± 0.5 [a]	99.9 ± 0.3 [b]	10.7 ± 1.4 [ab]
Covalent modification	Onset T_d (°C)	Peak T_d (°C)	Enthalpy E_d (J/g protein)
Ref	92.6 ± 0.5 [a]	99.3 ± 0.6 [ab]	11.8 ± 1.0 [b]
1:10	92.4 ± 0.5 [a]	98.7 ± 0.7 [b]	13.2 ± 1.3 [b]
1:5	92.2 ± 0.2 [a]	98.5 ± 0.3 [b]	10.2 ± 1.2 [b]
1:1	93.7 ± 0.3 [b]	98.7 ± 0.2 [b]	5.7 ± 1.2 [a]
5:1	94.6 ± 0.9 [b]	100.4 ± 0.5 [a]	6.4 ± 1.4 [a]
10:1	93.8 ± 0.7 [b]	99.6 ± 0.3 [ab]	5.1 ± 1.5 [a]

To sum up, the use of low CGA-protein ratios slightly improved the protein thermostability in case of non-covalent modifications at pH 7 while the thermostability of covalently modified protein largely decreased above the molar ratios of 1:1.

Rheological properties

The least gelling concentration (LGC) of the reference sample incubated at pH 7 was tested by heating, and subsequent cooling of the solutions with concentrations ranging from 4% to 20% w/v (Fig. 5-8). The LGC was 5% w/v, which is lower compared to the 8 to 10% w/v reported for the sunflower kernel protein isolate free of polyphenols in literature (González-Pérez & Vereijken, 2007; Malik & Saini, 2017). Fig. 5-8 shows that all the modified protein solutions of 10% w/v gelled, except for the covalently modified sample with the ratio of 10:1. The rheological properties (*G'* and *G''*) of the references and covalently/non-covalently modified samples were further analyzed by temperature sweep (20-95-20 ℃) in Anton Paar in Fig. 5-9 (complete data from rheological measurements are shown in Fig. S5-7 and Fig. S5-8). For the reference sample, the *G'* and *G''* value can be divided into three regions: a stable region from 20 to 90 ℃ (approximately 0.5 Pa for *G'* and 0.1 Pa for *G''*); a steep increase from 90 till 95 ℃ (0.5-22 Pa for *G'* and 0.1-2 Pa for *G''*) and a further increase region during cooling from 95 to 20 ℃ (22-411Pa for *G'* and 2-80 Pa for *G''*). The steep increase of *G'* indicated gel formation at 90 ℃, and this temperature is close to the onset T_d of approximately 93 ℃ (Table 5-2). For the reference sample after the pH-shift, the steep increase region of *G'* and *G''* was found to start at a higher temperature, as expected from Table 5-1. Thus, the pH-shift of the reference sample influenced the gelling temperature. The *G'* value increased further upon cooling since the gel was known to become more firm upon cooling (Kornet et al., 2021). The *G'* value for both of the reference samples were similar (~400 Pa) after cooling (Fig.5-9A4 and B4), which were slightly lower than the 500 Pa reported for the sunflower protein isolate (10% w/v) in a previous study (González-Pérez & Vereijken, 2007).

For the non-covalently modified samples at the two extreme molar ratios of 1:10 and 10:1, similar trends for the *G'* and *G''* values were found for the reference sample. The *G'* values were lower (200-300 Pa) after cooling for the non-covalent modified samples compared to the reference sample (400 Pa), suggesting a decreased gel strength. The protein gel network might be disrupted due to the CGA binding (Malik & Saini, 2017). Samples with covalently modified proteins required a longer holding time at 95 ℃ to show a steep increase region at 10:1 ratio. It is noteworthy that the steep increase of the *G'* value with the 10:1 ratio

upon heating indicated gel formation, although no gel was observed in Fig. 5-6C. A possible explanation is a weak gel formation at the 10:1 ratio, which might be broken when inverting the tube (Fig. 5-8).
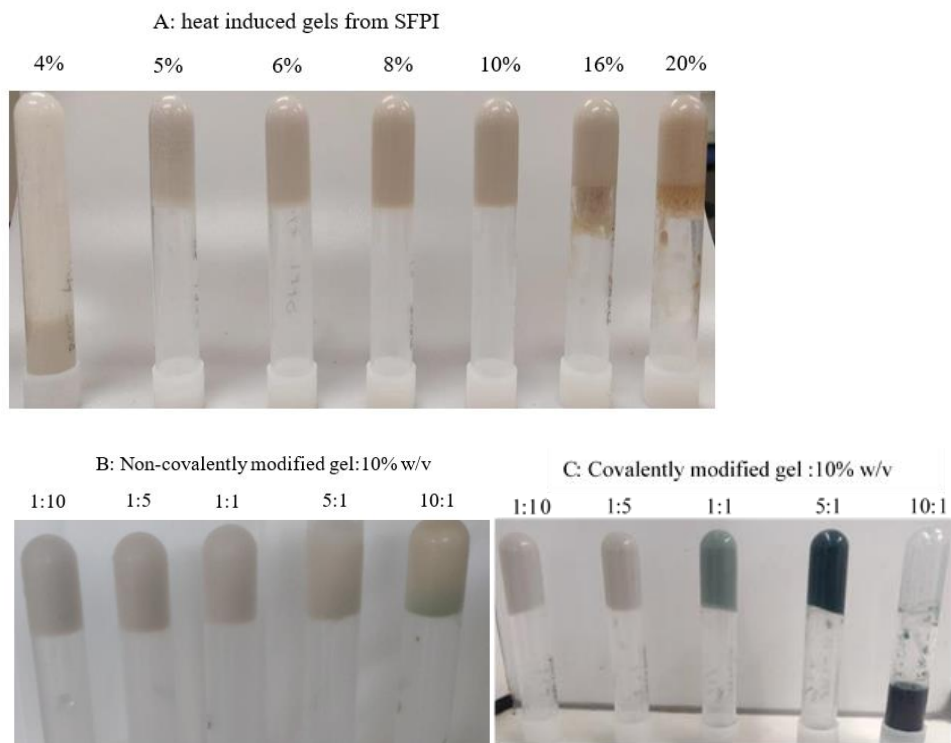

Fig.5-8 Thermal induced gel from the SFPI solutions between 4-20% w/v (A). Non-covalently modified sunflower protein gels at 10% w/v (B), covalently modified protein gels at 10% w/v (C).

For covalently modified protein gels, the G' value at the end of cooling was increased with increasing CGA-protein ratios up to 1:1 (Fig. 5-9B4) indicating that CGA could have favored protein aggregation (as observed in SDS-PAGE, Fig.5-4). A further increase of the CGA content resulted in a large decrease of the G' value and the lowest value was found to be 104 Pa for the gel with a CGA-protein molar ratio of 10:1. Such a dose-dependent reaction was also reported in a study on myofibrillar protein: the G' value of the CGA modified protein was enhanced at low CGA concentrations of 6 and 30 µM (approximate CGA-protein ratios of 1:10 and 1:2) (Cao & Xiong, 2015), while they found a large decrease of G' at a CGA

concentration of 150 µM (approximate CGA-protein ratio of 2:1). It was explained that excessive covalent binding of CGA to proteins hinders the formation of a protein gel network (Ali, Homann, Khalil, Kruse, & Rawel, 2013; Malik et al., 2016). The *G'* and *G"* dependencies on frequency and strain for the non-covalently and covalently modified protein gels after cooling were determined through a frequency and strain sweep (Fig. S5-7 and Fig. S5-8). For all the samples, the *G'* and *G"* values slightly increased with frequency. The length of the linear viscoelastic (LVE) regime was determined by using a strain sweep at a constant frequency. The critical strain (γ_c) was taken as the end LVE regime. The γ_c values measured for the sunflower proteins were found to be even higher compared to the soy and pea protein gels (Kornet et al., 2021; Peng et al., 2022), suggesting stronger gels compared to soy and pea proteins. Overall, the functional properties assessed here showed a clear dose-dependent effect for covalent modifications, whereas the effect was less pronounced for the non-covalent modifications.
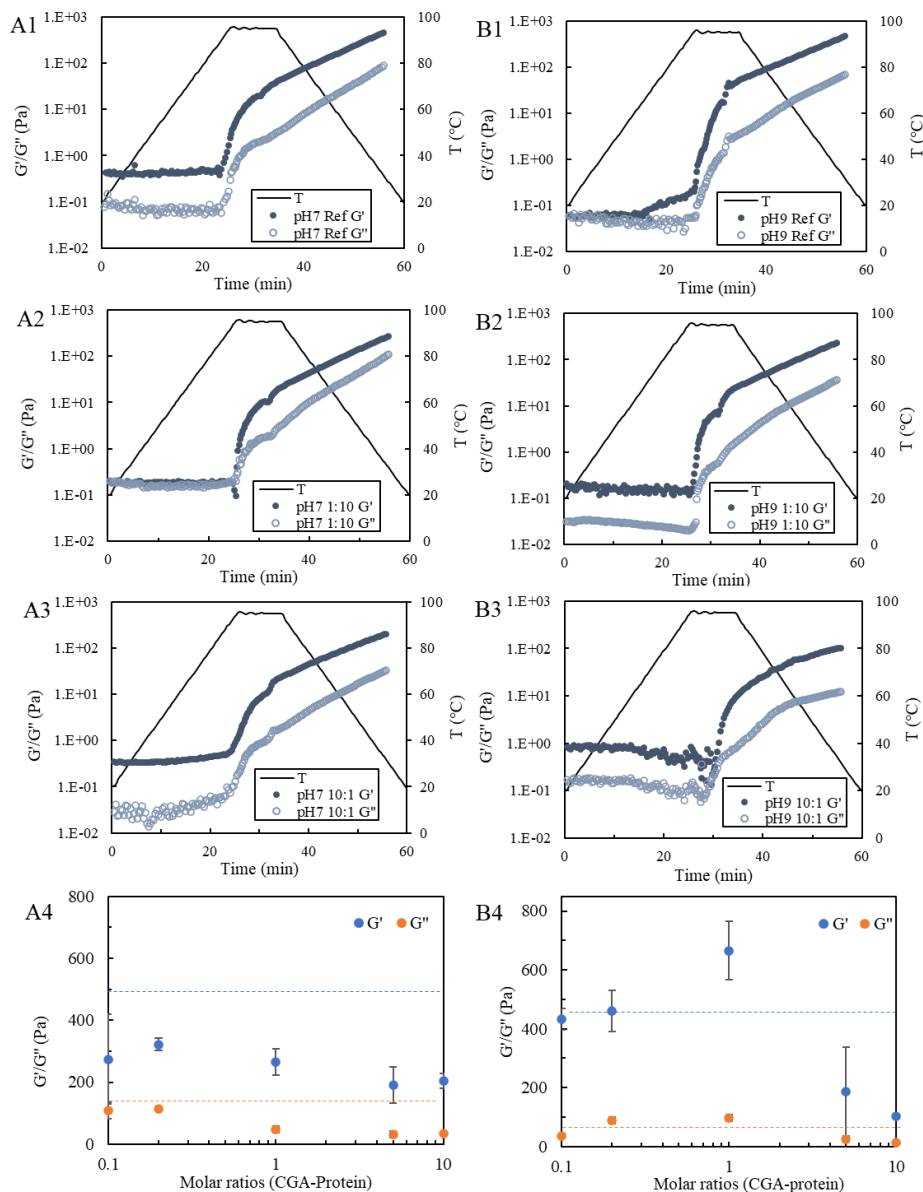
Fig. 5-9 The rheological properties of G' and G'' for the non-covalently modified samples (10% (w/v)): (A1-A3); and the covalently modified samples (10% (w/v)): reference (B1-B3) by temperature sweep (20-95-20 °C) at 1% strain and 1 Hz. The G' and G'' value at the end of cooling for the reference sample and the non-covalently modified protein samples (A4) or covalently modified protein samples (B4) (dotted blue and orange line are for the G' and G'' value for the reference sample.

5.3.4 Outlook: CGA removal towards less refined protein concentrates

The results presented above showed that CGA affected the functional properties of sunflower protein. In general, the effects were limited and often in a positive direction. Only a large dose of CGA that is capable of binding covalently to the protein influences the functional properties negatively (i.e. the solutions turned green and the gels become much weaker).

Based on the above discussions, it becomes clear that a certain amount of CGA can be accepted in a protein isolate derived from sunflower. In case process conditions are applied that lead to covalent interactions (mainly high pH, high temperature), a CGA-protein molar ratio up to 1:1 is still acceptable when aiming at preserving high techno-functionality (i.e., solubility, gelling ability) without negative visual consequences (i.e., green color). In contrast, non-covalent CGA modifications have no clear negative effect on the sunflower proteins at the tested molar ratios (1:10-10:1) except slight decrease for the G' and G''. These outcomes align with previous studies in which Karefyllakis et al., (2017) even improved the emulsifying properties of sunflower proteins by non-covalent modification with CGA at 1:1 or higher mixing ratios. The conclusion that a certain amount of CGA can be accepted in a protein isolate is relevant when considering the current discussion about the necessity for highly refined food ingredients. In modern food applications, the use of less refined protein fractions of plants is suggested. Thus, a future study should investigate whether a certain amount of CGA can also be permitted in less refined de-oiled sunflower kernels. These kernels contain a CGA-protein molar ratio of roughly 4.5:1-8:1 (Geneau-Sbartaï et al., 2008; Saeed & Cheryan, 1988). As a first step, we also evaluated an acceptable CGA-protein molar ratio (tested ratio between 1:10-10:1, results not shown) with dephenolized sunflower protein concentrate instead of isolate, where 28% carbohydrates were still present. The outcome was similar to the presented results with the isolate and a critical ratio of 1:1 was also concluded with covalent modification conducted at pH 9. The results indicated that the carbohydrate impurities in the concentrate do not affect the protein modification rate by CGA.

However, the question is now whether the added free CGA into the dephenolized protein isolate or concentrate represents the behavior of the original CGA in de-oiled sunflower kernels. Additional factors can play a role as well. First, the structure of the raw

material can be relevant as CGA is mainly located in inside the cell wall structure of the protein bodies (Sastry & Rao, 1990). Thus, an intact cell wall structure might limit the exposure of CGA to the proteins for reaction. Second, the process conditions for dephenolization can be relevant: the DSK was dephenolized in this study by an aqueous ethanol washing process, and the process conditions applied (solvent quality, temperature, and pH value) were already found to induce some protein-CGA interactions, thereby affecting the functional properties (Jia et al., 2021). Finally, the presented study focused only on techno-functionality of modified sunflower protein, while the sensory and biological properties were not taken into consideration. Clearly, a future study should focus on whether the critical ratio found in the simplified model blends also holds for less refined sunflower materials, and also for other than techno-functional properties.

5.4 Conclusion

The dose-dependent effects on functional properties of covalently and non-covalently modified sunflower protein isolate by chlorogenic acid (CGA) were studied using different molar ratios. It was found that CGA can bind both covalently and non-covalently, depending on the process conditions applied to induce the interactions. Non-covalent interactions induced structural changes of the protein, which also increased the denaturation temperature and solubility. The effects on the color formation and gelling properties were limited. The effect of covalent interactions on protein structure was less clear, mainly because the process conditions used to induce interactions (the pH-shift) had a much larger effect. Nevertheless, covalent interactions led to changes in functional properties: a dose-dependent effect was observed for the gelling capacity, with a maximum at 1:1 ratio. At higher CGA dosages, gelling properties were negatively influenced, and green color was observed.

Overall, the presented results can be used for tailoring the techno-functionality of the sunflower protein fractions by identifying the critical CGA protein ratios, which retain or even improve techno-functional properties in less refined fractions irrespective of the mode of interaction that might later be induced by applications. This study was performed with a well-defined mixture of pure sunflower protein isolate and CGA. Experiments with a multi-component material such as de-oiled sunflower kernel are yet to be done to understand the effect of CGA on sunflower proteins in less refined ingredients.
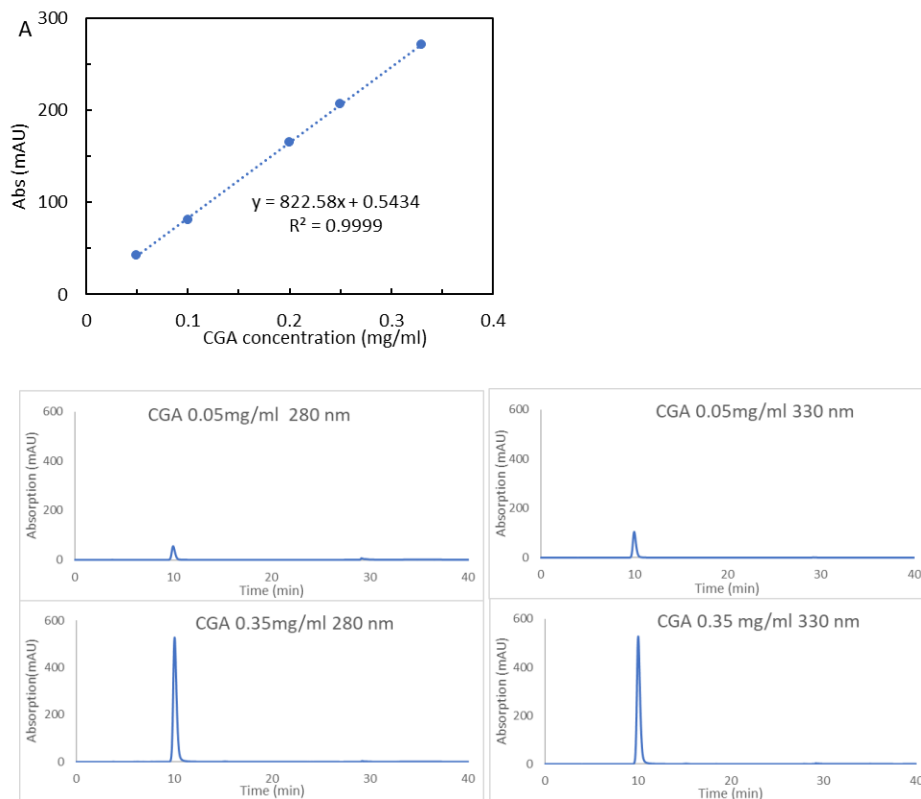
5

5.5 Supporting information

Fig. S5-1 The calibration curve of CGA standard between the concentration of 0.05-0.35mg/ml in RP-HPLC at the retention time of ~10 min. Chromatography of the CGA standard at the wavelength of 280 and 330nm.
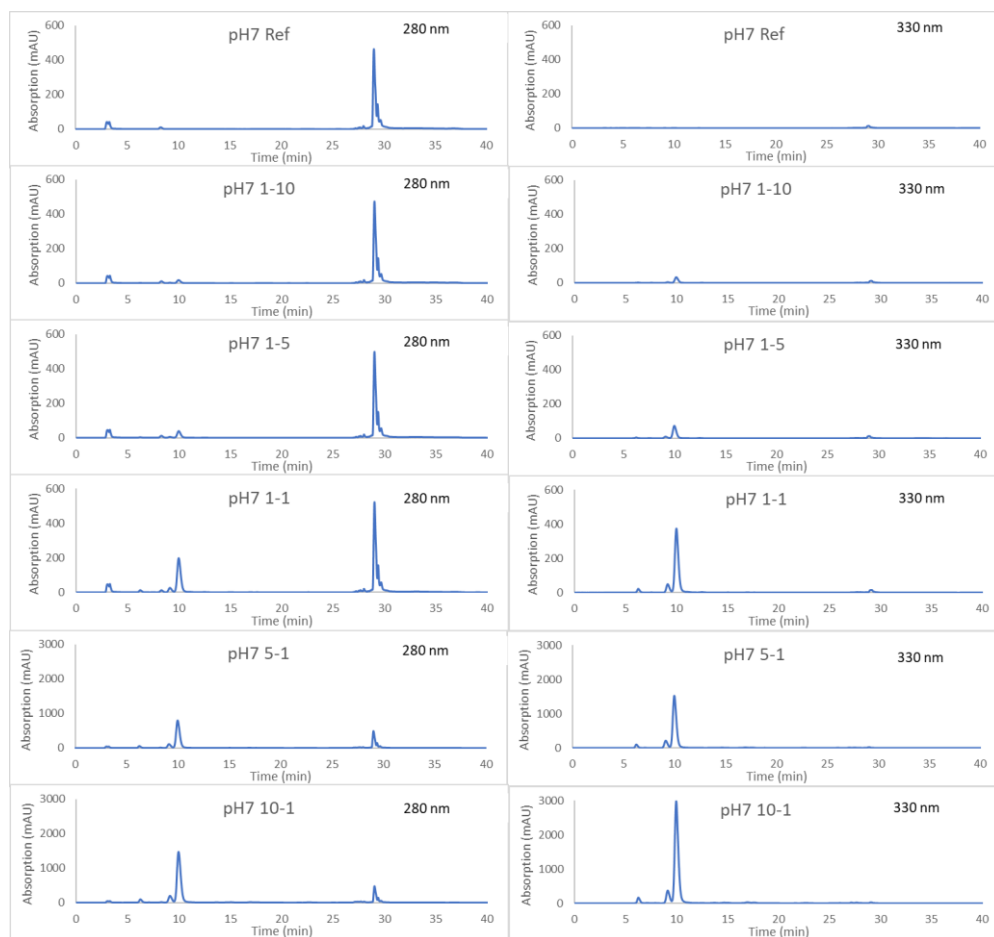
Fig. S5-2 The chromatography for the non-covalently modified SFPI samples with CGA at pH 7 for incubation of 24 h, measured at the wavelength of 280nm and 330nm.

Fig. S5-3. The chromatography for the non-covalently modified SFPI samples with CGA at pH 7 for incubation of 24 h, measured at the wavelength of 280nm and 330nm, the samples were treated with diafiltration.
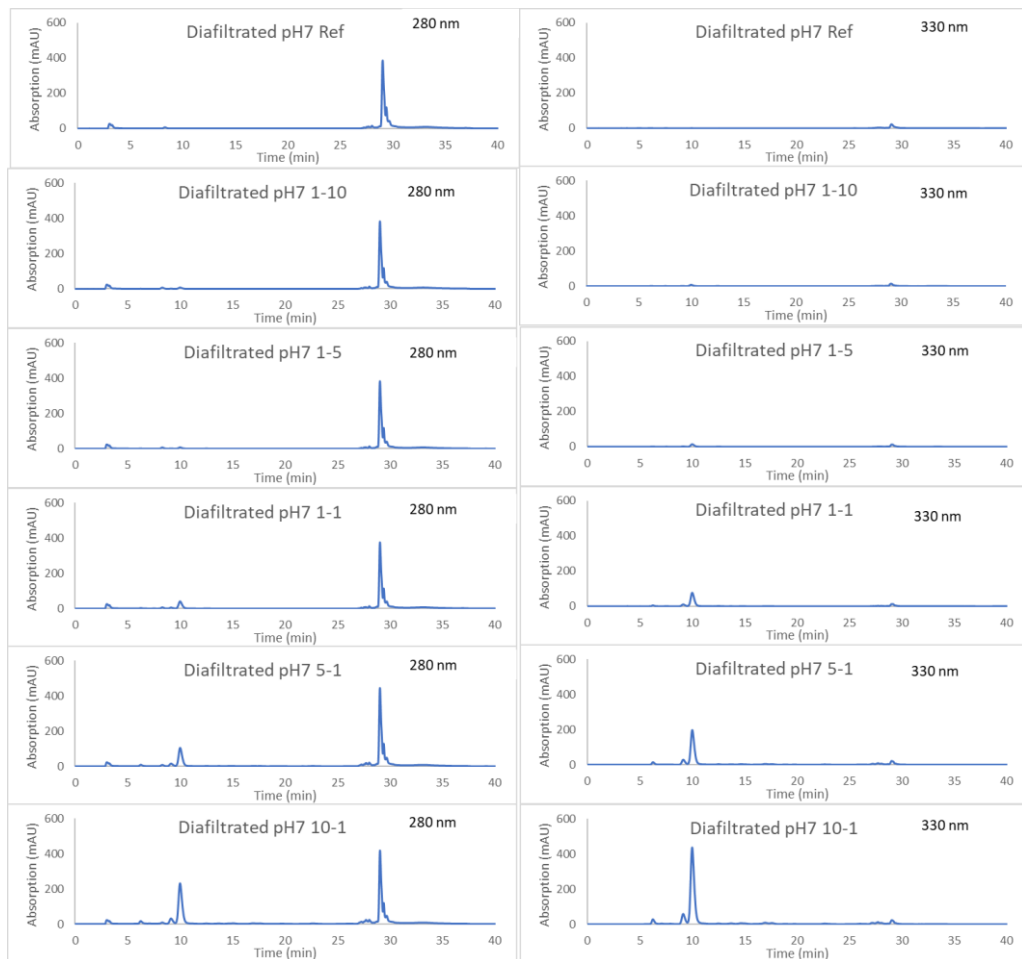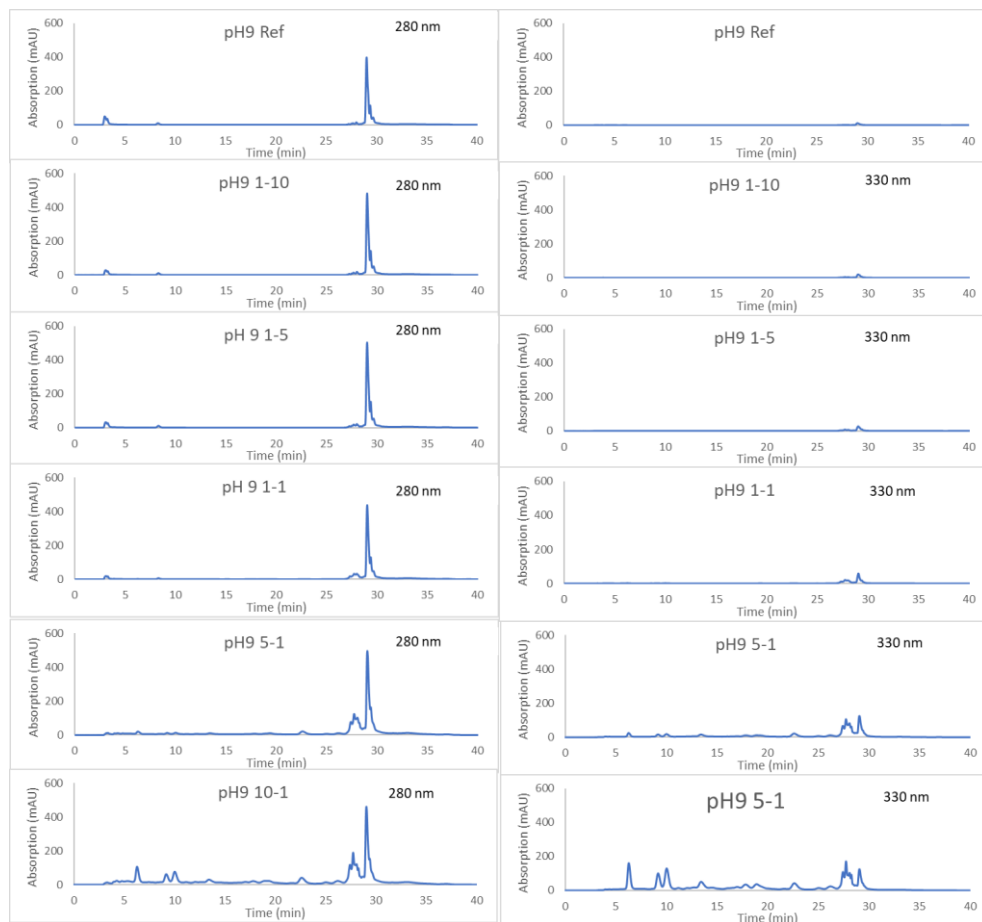
Fig. S5-4. The chromatography for the covalently modified SFPI samples with CGA when incubated at pH 9 for 24 h, and measured at pH 7 at the wavelength of 280nm and 330nm.

Fig. S5-5 The chromatography for the covalently modified SFPI samples with CGA when incubated at pH 9 for 24 h, and measured at pH 7 at the wavelength of 280nm and 330nm, and the sample were treated with diafiltration.
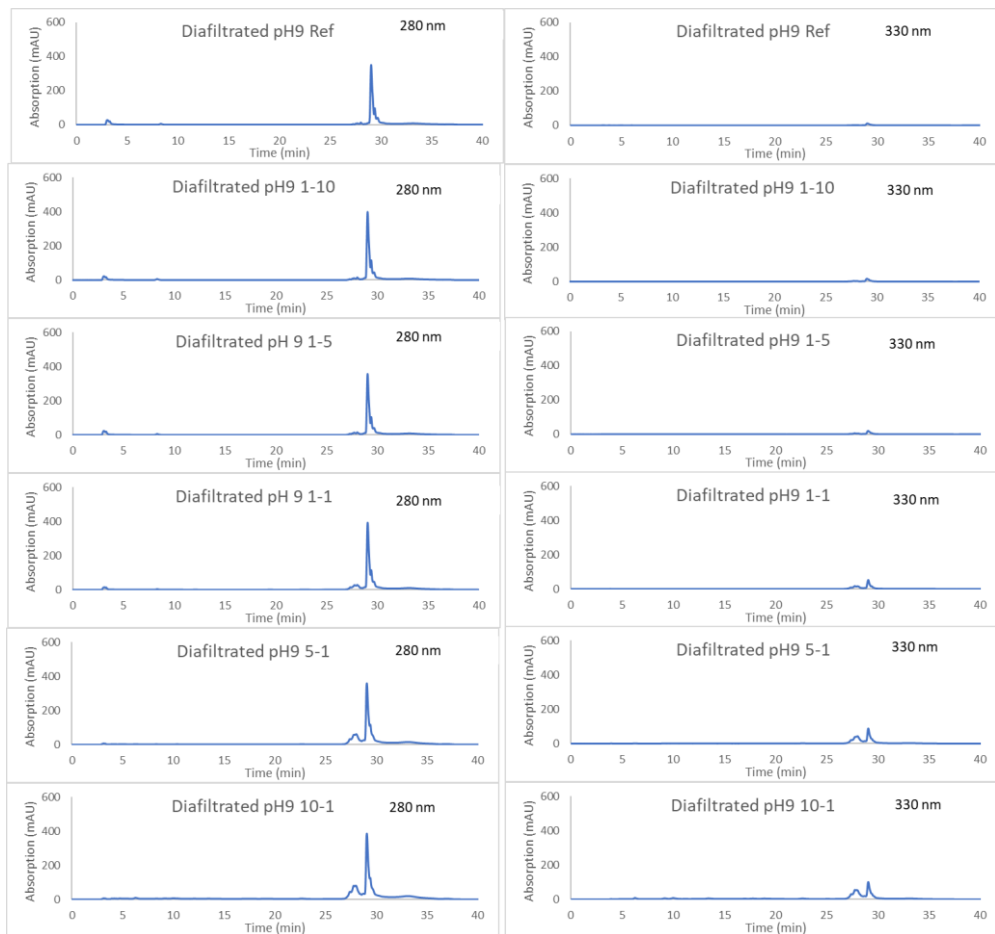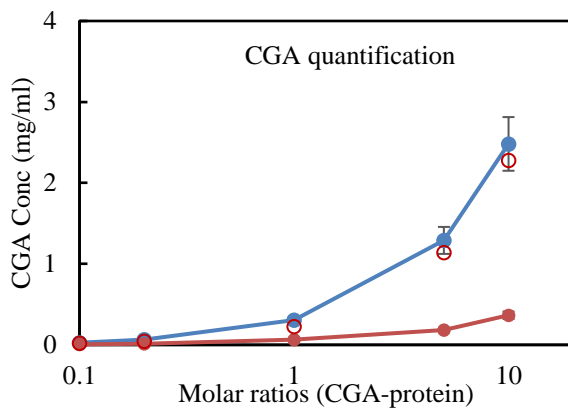
Fig. S5-6 The quantification of the CGA in the modified samples is shown at 330 nm (blue line), as well as the dialyzed samples (red line). The theoretical amount of CGA added is shown as red open circle symbol.

Fig. S5-7 The rheological properties of *G'* and *G''* with for the covalently modified samples (10% (w/v)) under different molar ratios: reference, 1:10, 1:5, 1:1, 5:1 and 10:1 by the temperature sweep (A1-A6) at 1% strain and1 Hz; frequency sweep at 1% strain and the frequency in between 0.1-10Hz (B1-B6); strain sweep at 1Hz and the strain in between 0.1-1000% (C1-C6). All the samples were measured at pH 7.

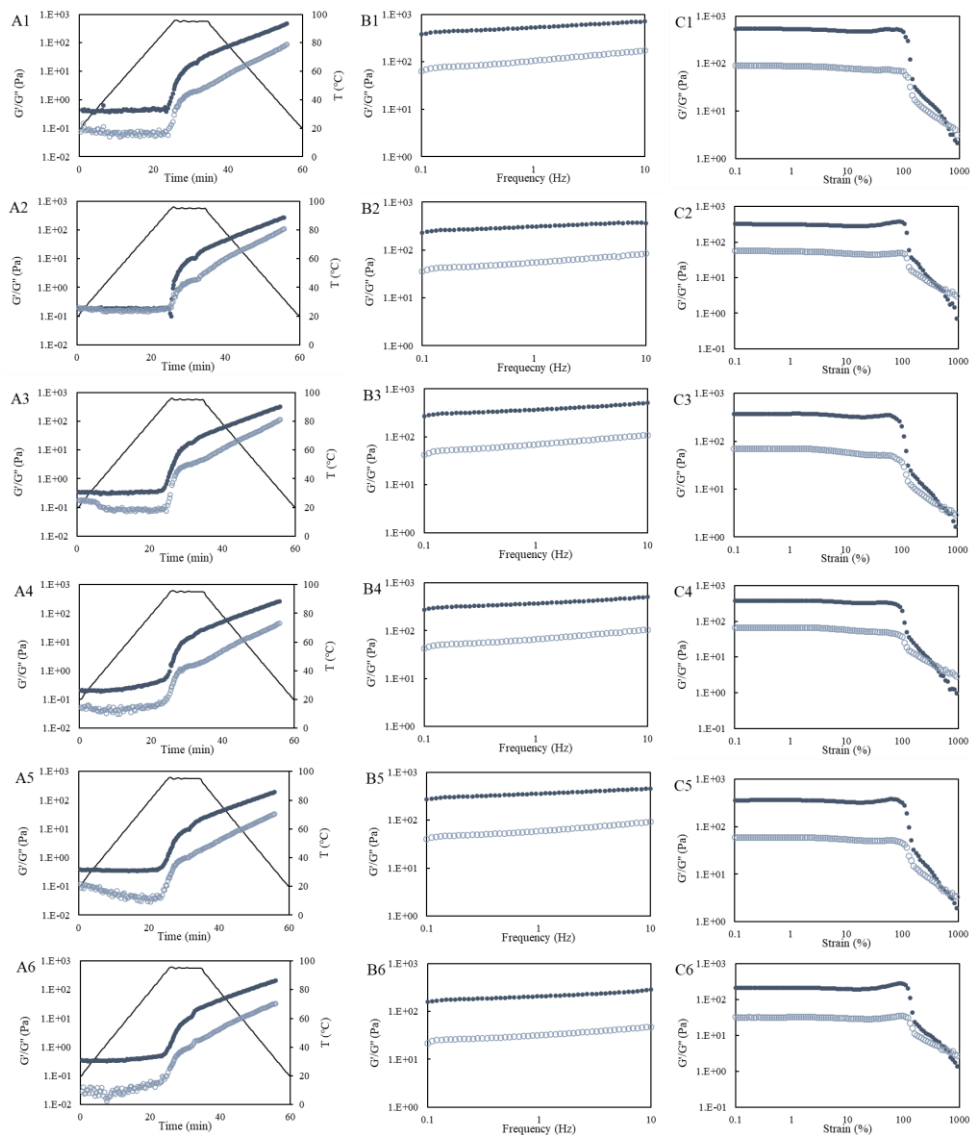**Fig. S5-8** The rheological properties of *G'* and *G''* with the for the covalently modified samples (10% (w/v)) under different molar ratios: reference, 1:10, 1:5, 1:1, 5:1 and 10:1 by the temperature sweep (A1-A6) at 1% strain and1 Hz; frequency sweep at 1% strain and the frequency in between 0.1-10Hz (B1-B6); strain sweep at 1Hz and the strain in between 0.1-1000% (C1-C6). All the samples were measured at pH 7.
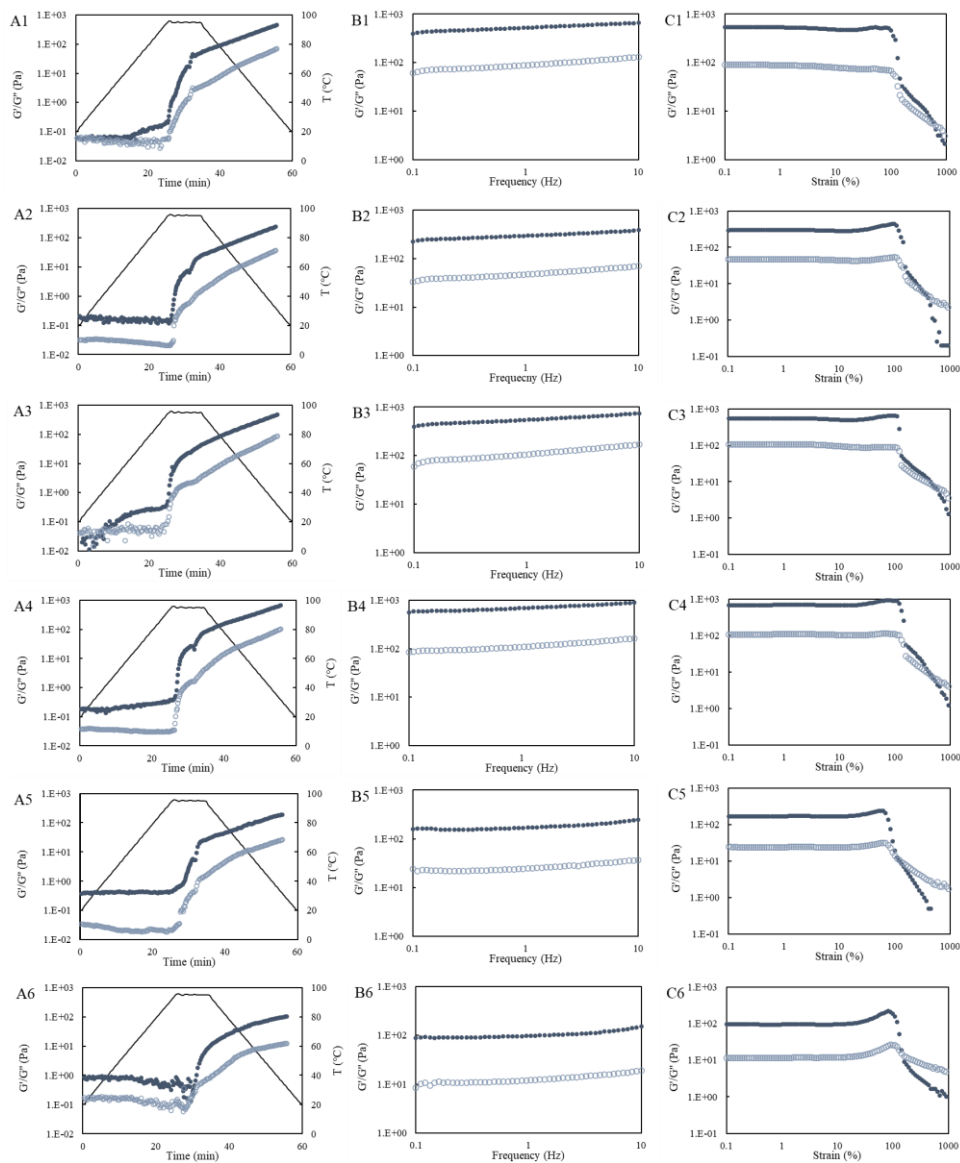
5.6 References

Ali, M., Homann, T., Khalil, M., Kruse, H. P., & Rawel, H. (2013). Milk whey protein modification by coffee-specific phenolics: Effect on structural and functional properties. *Journal of Agricultural and Food Chemistry*, *61*(28).

Ali, M., Keppler, J. K., Coenye, T., & Schwarz, K. (2018). Covalent whey protein–rosmarinic acid interactions: a comparison of alkaline and enzymatic modifications on physicoc. *Journal of Food Science*, *83*(8), 2092–2100.

Cao, Y., & Xiong, Y. L. (2015). Chlorogenic acid-mediated gel formation of oxidatively stressed myofibrillar protein. *Food Chemistry*, *180*, 235–243.

Carson, M., Keppler, J. K., Brackman, G., Dawood, D., Vandrovcova, M., Fawzy El-Sayed, Coenye, T., Schwarz, K., Clarke, S.A., Skirtach, A.G., Douglas, T.E.L.(2019). Whey protein Ccmplexes with green tea polyphenols: antimicrobial, osteoblast-stimulatory, and antioxidant activities. *Cells Tissues Organs*, *206* (1–2), 106–117.

Cheng, J., Tang, D., Yang, H., Wang, X., Zhu, M., & Liu, X. (2021). The dose-dependent effects of polyphenols and malondialdehyde on the emulsifying and gel properties of myofibrillar protein-mulberry polyphenol complex. *Food Chemistry*, *360* (2020), 130005.

Ferraro, V., Madureira, A. R., Fonte, P., Sarmento, B., Gomes, A. M., & Pintado, M. E. (2015). Evaluation of the interactions between rosmarinic acid and bovine milk casein. *RSC Advances*, *5*(107), 88529–88538.

Geneau-Sbartaï, Ć., Leyris, J., Silvestre, F., & Rigal, L. (2008). Sunflower cake as a natural composite: Composition and plastic properties. *Journal of Agricultural and Food Chemistry*.

González-Pérez, S., Merck, K. B., Vereijken, J. M., Van Koningsveld, G. A., Gruppen, H., & Voragen, A. G. J. (2002). Isolation and characterization of undenatured chlorogenic acid free sunflower (*Helianthus annuus*) proteins. *Journal of Agricultural and Food Chemistry*, *50* (6), 1713–1719.

González-Pérez, S., Van Koningsveld, G. A., Vereijken, J. M., Merck, K. B., Gruppen, H., & Voragen, A. G. J. (2005). Emulsion properties of sunflower (*Helianthus annuus*) proteins. *Journal of Agricultural and Food Chemistry*, *53* (6), 2261–2267.

González-Pérez, S., & Vereijken, J. M. (2007). Sunflower proteins: overview of their physicochemical, structural and functional properties. *Journal of the Science of Food and Agriculture*, *87*(12), 2173–2191.

González-Pérez,S. (2003). *Physico-chemical and functional properties of sunflower proteins*. Wageningen University and research center. PhD thesis.

Iacomino, M., Weber, F., Gleichenhagen, M., Pistorio, V., Panzella, L., Pizzo, E., … Napolitano, A. (2017). Stable Benzacridine Pigments by Oxidative Coupling of Chlorogenic Acid with Amino Acids and Proteins: Toward Natural Product-Based Green Food Coloring. *Journal of Agricultural and Food Chemistry*, *65*(31), 6519–6528. https://doi.org/10.1021/acs.jafc.7b00999

Jia, W., Rodriguez-Alonso, E., Bianeis, M., Keppler, J. K., & van der Goot, A.J. (2021). Assessing functional properties of rapeseed protein concentrate versus isolate for food applications. *Innovative Food Science & Emerging Technologies*, *68*, 102636.

Jia, W, Kyriakopoulou, K., Roelofs, B., Ndiaye, M., Vincken, J.-P., Keppler, J.K., & van der Goot, A.J. (2021). Removal of phenolic compounds from de-oiled sunflower kernels by aqueous ethanol washing. *Food Chemistry*, *362 (May),* 130204.

Jiang, J., Zhang, Z., Zhao, J., & Liu, Y. (2018). The effect of non-covalent interaction of chlorogenic acid with whey protein and casein on physicochemical and radical-scavenging activity of in vitro protein digests. *Food Chemistry*, *268 (May)*, 334–341.

Jiang, S., Ding, J., Andrade, J., Rababah, T. M., Almajwal, A., Abulmeaty, M.M., & Feng, H. (2017). Modifying the physicochemical properties of pea protein by pH-shifting and ultrasound combined treatments. *Ultrasonics Sonochemistry*, *38*(Jan), 835–842.

Karefyllakis, D., Altunkaya, S., Berton-Carabin, C.C., van der Goot, A.J., & Nikiforidis, C.V. (2017). Physical bonding between sunflower proteins and phenols: Impact on interfacial properties. *Food Hydrocolloids*, *73*, 326–334.

Karefyllakis, D., Salakou, S., Bitter, J.H., Van der Goot, A.J., & Nikiforidis, C. (2018). Covalent bonding of chlorogenic acid induces structural modifications on sunflower proteins. *ChemPhysChem*, 459–468.

Kayser, J. J., Arnold, P., Steffen-Heins, A., Schwarz, K., & Keppler, J. K. (2020). Functional ethanol-induced fibrils: Influence of solvents and temperature on amyloid-like aggregation of beta-lactoglobulin. *Journal of Food Engineering*, *270* (Oct), 109764.

Keppler, J.K., Schwarz, K., & van der Goot, A.J. (2020). Covalent modification of food proteins by plant-based ingredients (polyphenols and organosulphur compounds): A commonplace reaction with novel utilization potential. *Trends in Food Science & Technology*, *101* (Oct), 38–49.

Keppler, J.K., Heyn, T. R., Meissner, P. M., Schrader, K., & Schwarz, K. (2019). Protein oxidation during

temperature-induced amyloid aggregation of beta-lactoglobulin. *Food Chemistry*, *289* (March), 223–231.

Khalil, M., Ragab, M., & Hassanien, F. R. (1985). Some functional properties of oilseed proteins. *Molecular Nutrition and Food Research*, *29* (3), 275–282.

Kornet, R., Veenemans, J., Venema, P., van der Goot, A.J., Meinders, M., Sagis, L., & van der Linden, E. (2021). Less is more: limited fractionation yields stronger gels for pea proteins. *Food Hydrocolloids*, *112*, 106285.

Kyriakopoulou, Keppler, & Van Der Goot (2021). Functionality of Ingredients and Additives in Plant-Based Meat Analogues. *Foods*, 10(3), 600.

Liang, Y., & Were, L. (2020). Cysteine's effects on chlorogenic acid quinone induced greening and browning: Mechanism and effect on antioxidant reducing capacity. *Food Chemistry*, *309* (July).

Loveday, S. M. (2020). Plant protein ingredients with food functionality potential. *Nutrition Bulletin*, *45*(3), 321–327.

Lu, H., Tian, Z., Cui, Y., Liu, Z., & Ma, X. (2020). Chlorogenic acid: A comprehensive review of the dietary sources, processing effects, bioavailability, beneficial properties, mechanisms of action, and future directions. *Comprehensive Reviews in Food Science and Food Safety*. 1-29

Malik, M.A., Sharma, H. K., & Saini, C.S. (2016). Effect of removal of phenolic compounds on structural and thermal properties of sunflower protein isolate. *Journal of Food Science and Technology*, *53*(9), 3455–3464.

Malik, M.A., & Saini, C.S. (2017). Polyphenol removal from sunflower seed and kernel: Effect on functional and rheological properties of protein isolates. *Food Hydrocolloids*, *63*, 705–715.

McManus, J. P., Davis, K. G., Beart, J. E., Gaffney, S. H., Lilley, T. H., & Haslam, E. (1985). Polyphenol interactions. Part 1. Introduction; some observations on the reversible complexation of polyphenols with proteins and polysaccharides. *Journal of the Chemical Society, Perkin Transactions 2*, *28* (9), 1429–1438.

Ozdal, T., Capanoglu, E., & Altay, F. (2013). A review on protein–phenolic interactions and associated changes. *Food Research International*, *51*(2), 954–970.

Peng, Y., Kyriakopoulou, K., Keppler, J. K., Venema, P., & van der Goot, A.J. (2022). Effect of calcium enrichment on the composition, conformation, and functional properties of soy protein. *Food Hydrocolloids*, *123* (Sep), 107191.

Peng, Y., Kyriakopoulou, K., Ndiaye, M., Bianeis, M., Keppler, J. K., & Van der Goot, A.J. (2021). Characteristics of soy protein prepared using an aqueous ethanol washing process. *Foods 2021, 10* (9), 2222.

Pickardt, C., Eisner, P., Kammerer, D.R., & Carle, R. (2015). Pilot plant preparation of light-colored protein isolates from de-oiled sunflower (*Helianthus annuus L.*) press cake by mild-acidic protein extraction and polyphenol adsorption. *Food Hydrocolloids*, *44*, 208–219.

Pierpoint, W.S. (1969). *o*-Quinones formed in plant extracts. Their reactions with amino acids and peptides. *Biochemical Journal*, *112* (5).

Prigent, S.V.E., Voragen, A. G., Visser, A. J., Van Koningsveld, G.A., & Gruppen, H. (2007). Covalent interactions between proteins and oxidation products of caffeoylquinic acid (chlorogenic acid). *Journal of the Science of Food and Agriculture*, *87* (April), 2502-2510

Prigent, S.V.E., Gruppen, H., Visser, A.J.W.G., Van Koningsveld, G.A., De Jong, G.A.H., & Voragen, A.G.J. (2003). Effects of non-covalent interactions with 5-O-caffeoylquinic acid (chlorogenic acid) on the heat denaturation and solubility of globular proteins. *Journal of Agricultural and Food Chemistry*, *51*(17), 5088–5095.

Qie, X., Chen, W., Zeng, M., Wang, Z., Chen, J., Goff, H. D., & He, Z. (2021). Interaction between β-lactoglobulin and chlorogenic acid and its effect on antioxidant activity and thermal stability. *Food Hydrocolloids*, *121*(July), 107059. https://doi.org/10.1016/j.foodhyd.2021.107059

Rawel, H.M., Czajka, D., Rohn, S., & Kroll, J. (2002). Interactions of different phenolic acids and flavonoids with soy proteins. *International Journal of Biological Macromolecules*, *30* (3–4), 137–150.

Saeed, M., & Cheryan, M. (1988). Sunflower protein concentrates and isolates low in polyphenols and phytate. *Journal of Food Science*. 53 (4), 1127-1131.

Salgado, P.R., Molina Ortiz, S.E., Petruccelli, S., & Mauri, A.N. (2011). Sunflower protein concentrates and isolates prepared from oil cakes have high water solubility and antioxidant capacity. *JAOCS, Journal of the American Oil Chemists' Society*, *88* (3), 351–360.

Sastry, M.C.S., & Rao, M.S.N. (1990). Binding of chlorogenic acid by the isolated polyphenol-free 11S protein of sunflower (*Helianthus annuus*) Seed. *Journal of Agricultural and Food Chemistry*, *38* (12), 2103–2110.

Strauss, G., & Gibson, S. M. (2004). Plant phenolics as cross-linkers of gelatin gels and gelatin-based coacervates for use as food ingredients. *Food Hydrocolloids*, *18*(1), 81–89.

Subaşı, B. G., Casanova, F., Capanoglu, E., Ajalloueian, F., Sloth, J.J., & Mohammadifar, M.A. (2020). Protein extracts from de-oiled sunflower cake: Structural, physico-chemical and functional properties after removal of phenolics. *Food Bioscience*, *38* (Sep).

Van Der Goot, A.J., Pelgrom, P.J.M., Berghout, J.A.M., Geerts, M.E.J., Jankowiak, L., Hardt, N. A., Keijer, J., Schutyser, M., Nikiforidis, C.V., Boom, R. M. (2016). Concepts for further sustainable production of foods.

Wang, T., Chen, X., Wang, W., Wang, L., Jiang, L., Yu, D., & Xie, F. (2021). Effect of ultrasound on the properties

5

of rice bran protein and its chlorogenic acid complex. *Ultrasonics Sonochemistry*, *79*, 105758.

Wildermuth, S.R., Young, E.E., & Were, L. M. (2016). Chlorogenic acid oxidation and its reaction with sunflower proteins to form green-colored complexes. *Comprehensive Reviews in Food Science and Food Safety*, *15*(5), 829–843.

Zhang, Y., Lu, Y., Yang, Y., Li, S., Wang, C., Wang, C., & Zhang, T. (2021). Comparison of non-covalent binding interactions between three whey proteins and chlorogenic acid: Spectroscopic analysis and molecular docking. *Food Bioscience*, *41*(Feb), 101035.

Chapter 6

Effect of aqueous ethanol washing on functional properties of sunflower materials for meat analogue application

Abstract

Background: The use of less refined ingredients is a trend in the design of modern food products, such as meat analogues. Sunflower kernel is rich in protein and considered as an alternative plant protein source. The effect of process conditions used to make ingredients from sunflower needs to be investigated on the functional and structuring properties of the sunflower materials prepared with different de-oiling techniques.

Approaches: Pre-pressing and de-oiling with 96% ethanol was applied to obtain de-oiled sunflower kernel (DSK). The other product, pressed sunflower kernel (PSK), was obtained by more intensive pressing only. DSK and PSK were further treated with aqueous ethanol washing, and their washed concentrates were obtained to study the effect of oil and phenol removal.

Key findings: DSK and DSKC formed a fibrous product at 40 wt% by shearing and heating at 140 °C in a shear cell. The washed DSK led to stronger products upon shearing and heating. However, PSK, before and after washing only formed a crumble gel under the same conditions. On other functional properties, such as water holding capacity, NSI, and rheological properties, the differences were remarkably small between DSK and PSK, and the washed materials.

Conclusions: The remaining oil in the sunflower material is crucial for the structuring potential, while the phenol content does not seem to have a relevant influence. The primary de-oiling process turned out to be a determining factor for further oil removal with aqueous ethanol washing.

6.1 Introduction

The need for protein products for human consumption is expected to increase significantly, with the world population reaching 10 billion by 2050 (Arrutia, Binner, Williams, & Waldron, 2020). Most animal-based protein products such as meat and dairy have a large impact on the environment regarding land use and carbon footprint (Nijdam, Rood, & Westhoek, 2012). A transition towards enhanced use of plant proteins can mitigate environmental effects. Plant-based meat analogues are gaining importance to address consumer desire for meat-like products and to facilitate future food supply. Sunflower seeds (Helianthus annus) are considered a promising plant protein source for this purpose. It is the third-largest oilseed produced worldwide after soybean and rapeseed (Pilorgé, 2020). Two methods are often used to extract the oil, being mechanical pressing and solvent extraction. Pressed cake refers to the co-product obtained directly after pressing. An additional de-oiling step with organic solvent can be applied to the pressed cake to give a meal with an even lower oil content (Arrutia et al., 2020). However, the oil extraction methods can affect the suitability of the sunflower material for food application, since the protein might become denatured (González-Pérez & Vereijken, 2007). After full oil extraction, the obtained cake or meal mainly consists of protein and polysaccharides. Based on this composition, it is possible that sunflower cake/meal can be used as an important ingredient for the plant-based meat analogue (Grabowska et al., 2016; Jia, Curubeto, Rodríguez-Alonso, Keppler, & Van der Goot, 2021).

The use of sunflower cakes and meals for human consumption is often thought to be limited due to the presence of a high amount of indigestible hulls, and phenolic compounds, of which chlorogenic acid (CGA) is the most prevalent one (González-Pérez & Vereijken, 2007). The suspected limitation is because CGA can bind covalently and non-covalently to protein, leading to the structural changes of proteins, color formation, and decreased digestibility (Ozdal, Capanoglu, & Altay, 2013). Thus, it is often suggested that CGA removal is essential to make sunflower cake/meal suitable for food application, even despite the potential health benefits of CGA (Karefyllakis, Salakou, Bitter, van der Goot, & Nikiforidis, 2018). Aqueous ethanol washing is a well-known method in the food industry to remove the phenolic compounds from oilseeds and to obtain a protein-rich concentrate.

6

Besides the removal of phenolic compounds, aqueous ethanol washing is also considered an effective method for oil removal (Citeau, Regis, Carré, & Fine, 2018). In terms of functionalities, aqueous ethanol washing treatment can increase the water holding capacity of the legume protein fractions (pea, lentil, fababean, and navy bean) obtained via air classification (Peter, 2018; Wang, Guldiken, Tulbek, House, & Nickerson, 2020). However, the complete removal of CGA from the de-oiled sunflower kernel requires intensive washing with many steps, which is often associated with protein loss (Jia et al., 2021). Thus, a research question is now whether complete removal of phenolic compounds is necessary or that a certain amount of CGA can be permitted.

This study aims to understand the effect of the primary de-oiling process and subsequent aqueous ethanol washing process on the functional and structuring properties of sunflower materials and relate those to the extent of oil and CGA removal. Two primary de-oiling processes are studied: (1) de-oiled sunflower kernel (DSK) obtained by pre-pressing and de-oiling with 96% ethanol from sunflower kernel and (2) pressed sunflower kernel (PSK) obtained by full pressing of the sunflower kernel without further processing. The compositions of all the tested samples were analyzed. Then, the functional properties were quantified on protein molecule profile, protein thermal stability, particle morphology, water holding capacity, and nitrogen solubility index. Further, the rheological properties of the tested samples were measured with a closed cavity rheometer. The structuring potential for fiber formation of the tested samples was tested using the shear cell, and the fibrous products were measured using a tensile test with a texture analyzer.

6.2 Materials & methods

6.2.1 Materials

De-oiled sunflower kernel (DSK) and pressed sunflower kernel (PSK) were provided by Avril Group (Bruz, France). Both materials were originated from the same variant of de-hulled sunflower kernel (protein, oil, fibers, and carbohydrates content in dry base: 23%, 59%, 7%, 11%, respectively). DSK was obtained by pre-pressing followed by further de-oiling by using 96% ethanol. PSK was full pressed. The dry matter content of DSK and PSK (95.3% and 91.4%) were considered for all the analyses when describing concentrations. Chlorogenic acid (CGA) and sodium chloride (NaCl) were purchased from Sigma Aldrich (St.Louis, USA). Ethanol (96%) was purchased from VWR Chemicals (Leuven, Belgium). For all experiments, Milli-Q water was used unless stated otherwise.

6.2.2 Methods

6.2.2.1 Aqueous ethanol washing

Aqueous ethanol washing was applied to remove the phenolic compounds (PCs), oil and other small components, such as sugars from DSK and PSK, as described by Jia et al., (2021). An aqueous-ethanol solvent with 40% ethanol was selected because it was found that this solvent gave effective PCs removal while preserving the functional properties of the washed concentrate under this condition and protein losses were limited. The use of aqueous ethanol solvent also resulted in the partial oil removal (Citeau et al., 2018). Protein concentrates were obtained by washing DSK and PSK with an aqueous ethanol solvent (40% ethanol) in a solid-to-liquid ratio of 1:5. Firstly, DSK and PSK were mixed with the aqueous ethanol solvent and then stirred with a magnetic stirrer using a rotational speed of 700 rpm at room temperature for 10 min. After that, the mixture was centrifuged (Sorvall Lynx 4000 centrifuge, Thermo Fisher, USA) at $10,000 \times g$ for 10 min. The wet pellet was collected after the centrifugation and the extract was discarded. The wet pellet was either freeze-dried into a dry concentrate or further washed with a fresh batch of aqueous ethanol solvent. The same process was repeated until the pellet was washed to the desired number of washing steps being 1, 4 or 10 times. The washed pellets DSKCs (DSKC1/DSKC4/DSKC10) and PSKCs (PSKC1/PSKC4/PSKC10, with the digits indicating the number of washing steps) were all

6

165

freeze-dried (Epsilon 2-6D LSCplus, Christ, Germany) and milled with a Blade Miller (Model A11B, IKA, Germany) into a fine powder. The samples were then stored in a plastic bag at – 20 °C. In total 2 batches of all samples were prepared. The process scheme was showed in Fig. 6-1.
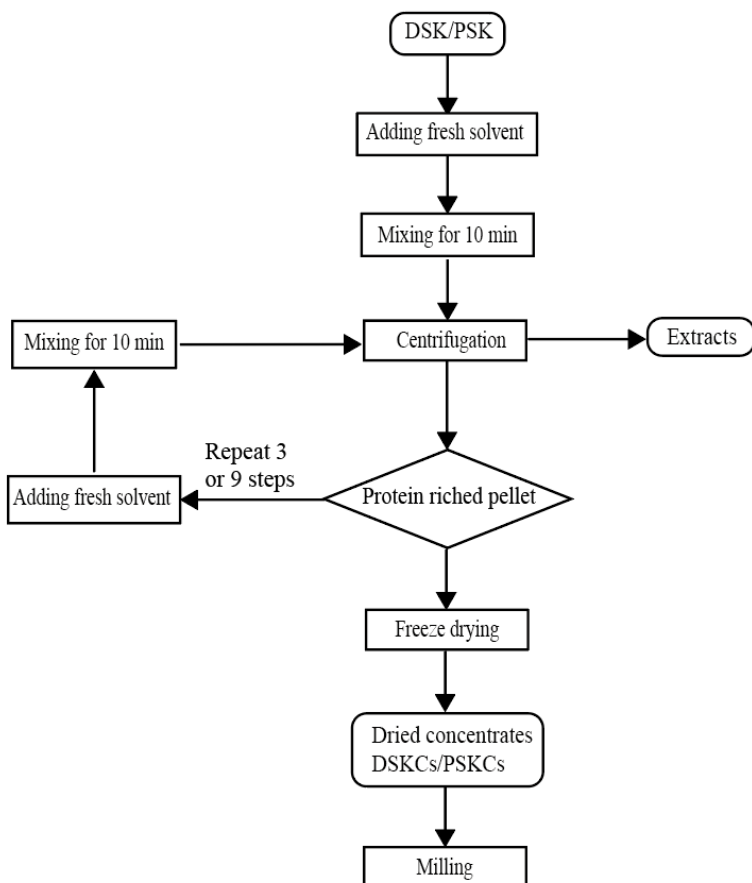
Fig. 6-1 Schematic overview of the for aqueous ethanol washing of de-oiled sunflower kernels (DSK) and pressed sunflower kernels (PSK) for 1, 4 or 10 steps.

The composition of the DSK, PSK, DSKCs, and PSKCs were analyzed in terms of protein, ash, moisture, oil, chlorogenic acid (CGA) and carbohydrate content. The nitrogen content was determined with the Dumas combustion method using a Nitrogen Analyzer (Flash EA 1112 Series, Thermo scientific, Netherlands). A nitrogen conversion factor of 5.6

was used to calculate the protein content for sunflower materials (Pickardt et al., 2009). Each sample was measured in triplicate. Ash, moisture, and oil content was determined with the method: AACC 08-01, AACC 44-15.02, and AACC 30-25.01, receptively. The CGA content in the extract was determined using the high-performance liquid chromatography (HPLC) method (Jia et al., 2021). A Dionex Ultimate 3000 chromatography (Thermo Fisher, Waltham, MA, USA) was used with a Gemini 3 μm C18 column at 30 °C. The extract was centrifuged at $15,000 \times g$ for 10 min to remove any insoluble components and was further diluted to achieve a final CGA concentration < 0.3 mg/mL. The CGA content was calibrated in a range of 0.05-0.3 mg/mL in HPLC. The peak areas of the samples were measured at a wavelength of 295 nm. All samples were determined in duplicate. The total amount of CGA ($m_{CGA,total}$) in DSK was calculated as the sum of the CGA obtained in all the extracts obtained from 10 washing steps (equation 1). The CGA contents (%) in DSKC1 ($m_{CGA,1}$) and DSKC4 ($m_{CGA,4}$) after the washing process were calculated as the total CGA content (%) remained in the subsequent extracts (equation 2 and 3). The CGA content for the PSK and the washed PSCKs were calculated in the same way:

Total CGA in DSK: $\quad m_{CGA,total} = \frac{\sum_{i=1}^{10} C_{i,CGA} \times V_{i,ext}}{m_{DSK}} \times 100\%\ [\%]$ (1)

CGA in DSKC1: $m_{CGA,1} = \frac{\sum_{i=2}^{10} C_{i,CGA} \times V_{i,ext}}{m_{DSKC1}} \times 100\%\ [\%]$ (2)

CGA in DSKC4: $m_{CGA,4} = \frac{\sum_{i=5}^{10} C_{i,CGA} \times V_{i,ext}}{m_{DSKC4}} \times 100\%\ [\%]$ (3)

where the concentration of the CGA in the extracts was expressed as $C_{i,CGA}$ (g /mL) and the volume of the extract is expressed as $V_{i,ext}$ (mL).

The total carbohydrates were calculated as the difference in DM and the known contents of components (protein, oil, CGA, ash).

6.2.2.2 Functionality analysis

Soluble protein molecule profile

SDS-PAGE was used to characterize the molecular size distribution of proteins present in DSK, PSK, DSKCs, and PSKCs samples. A dispersion was prepared in a falcon

tube using Milli-Q water to obtain a soluble protein concentration of 2 mg/mL for each sample. The dispersions were allowed to hydrate overnight and were prepared with Tris buffer containing 2% w/w SDS, 10% glycerol, 0.5% w/v bromophenol blue and 5% β-mercaptoethanol. Then, the samples were heated at 95 °C for 10 min and centrifuged at 12,000 × g for 1 min. The electrophoresis was performed at 200 V for approximately 40 min in a Mini-Protean II electrophoresis cell (Bio-rad, Veenendaal, Netherlands). An SDS-PAGE marker of 5 μL and the samples of 15 μL were loaded onto the gel wheels. The gels obtained after electrophoresis were stained using Bio-safe Coomassie Blue (Bio-rad, Netherlands). After 1 h, the gels were washed with Millipore water and scanned using a Gel scanner (Biorad - GS900, Netherlands). Duplicates were performed for each sample and one single lane was selected to present the result.

Protein thermal properties with DSC

The thermal properties of DSK, PSK, DSKCs, and PSKCs samples were analyzed using DSC (TA instrument 250, USA). A slurry of 15% (w/v) was prepared by mixing a sample of 6 mg with Milli-Q water in a high-volume pan of 60 μL. The pan was hermetically sealed and placed into the DSC cell. The pan was heated from 25 to 140 °C with a heating rate of 5 °C/min. Both the onset and peak denaturation temperature (T_d) and the integrated enthalpy (E_d) of the endothermic peaks were collected by the Trios data analysis software. The enthalpy was expressed per gram of protein in the dispersion to allow for the different protein contents in the samples. The measurements were performed in triplicates.

Morphology with SEM

Scanning electron microscopy (SEM) was used to visualize the microstructure of the DSK, PSK, DSKCs, PSKCs samples. The dry samples were placed onto SEM tubes (aluminum pin-type mounts 12.7 mm; JEOL, Nieuw-Vennep, the Netherlands) using double-sided adhesive conductive carbon tabs (12 mm carbon tabs; SPI Supplies Division of Structure Probe, West Chester, PA, USA). The samples were sputter-coated with gold. Compressed air was used to distribute the sample evenly over the surface of the carbon tabs. The accelerating voltage was 5 kV. In total, 8 pictures were taken for each sample analysis, from which two representative picture was selected at the scale of 20 and 100 μm.

Water holding capacity (WHC) and nitrogen solubility index (NSI)

The WHC of the DSK, PSK, DSKCs, and PSKCs samples were measured with a 2% w/w dispersion. A sample of 1 g was placed into falcon tubes after which 49 mL Milli-Q water was added. Then this dispersion was vortexed for a duration of 10 s. The sample dispersion was rotated overnight (24 hours) with a rotator (SB3 rotator, Stuart, UK) at a speed of 20 rpm to allow full hydration. The samples were then centrifuged (Sorvall Lynx 400 centrifuge, Thermo Fisher, USA) at 15,000 × g at 20 ℃ for 10 min. The supernatants were discarded, and the wet pellets were transferred into an aluminum pan. The wet pellets were weighed as $M_{wet\ pellet}$ and dried in an oven overnight at 105 ℃. The dried pellet was weighted as $M_{dry\ pellet}$. The original sample was weighed as $M_{original}$. The nitrogen content in the dry pellet ($N_{dry\ pellet}$) and in the original sample ($N_{original}$) was measured using the Dumas method (Section 6.2.2.2). All measurements were performed in duplicates. The WHC and NSI-values were calculated as follows:

$$WHC = \frac{M_{wet\ pellet} - M_{dry\ pellet}}{M_{dry\ pellet}} \text{ [g water /g dry pellet]} \tag{4}$$

$$NSI = \frac{N_{original} \times M_{original} - N_{dry\ pellet} \times M_{dry\ pellet}}{N_{original} \times M_{original}} \text{ [\%]} \tag{5}$$

6.2.2.4 Structuring properties

Rheological properties

The rheological properties of DSK, PSK, DSKCs, and PSKCs were measured using a Closed Cavity Rheometer (CCR) (RPA elite, TA instruments, USA) (Dekkers, Emin, Boom, & van der Goot, 2018; Emin, Quevedo, Wilhelm, & Karbstein, 2017a). Approximately 5 g of sample with a DM of 40% was made and vacuum-sealed in a plastic bag. After 30 min of hydration, the sample was taken and placed in-between two plastic foils in the CCR. A pressure of 4 bars was applied to prevent water evaporation. Temperature sweeps were performed by heating the samples from 40 to 150 ℃ with a heating rate of 10 ℃/min at 1 Hz frequency and 1% strain. Afterward, the samples were cooled down to 50 ℃ by blowing dry air over the disk. Besides, an isothermal measurement was performed by keeping the samples

at set temperatures of 90, 120, and 140 ℃ with 1 Hz frequency and 1% strain for 15 min. All measurements were performed in duplicates and the mean value was taken for comparison.

Shear cell processing

The in-house designed high-temperature conical shear cell (HTSC) (Wageningen University, Wageningen, the Netherlands) was used for the structuring of the PSK, DSK, PSKCs, and DSKCs samples. The protein materials can be structured with a defined simple shear flow produced from rotating the bottom cone and the stationary upper cone at preheated temperatures using an external oil bath (Grabowska et al., 2016b). The samples were prepared at 40 wt% with an approximate weight of 90 g. A 1% NaCl solution was made using demineralized water, and then the sunflower concentrates were added to this solution. The protein mixtures were hydrated for 30 min, which was then transferred to the preheated HTSC for shearing and heating at 140 ℃, 30 rpm for 15 minutes. The samples were stored in plastic bags. All tests were done in duplicate. The macrostructures of the sheared and heated products were inspected visually by bending of the samples and the photos were taken using the camera (Samsung A52 phone, the Netherlands).

Texture analysis

The mechanical properties of the sheared and heated DSK/DSKCs samples were measured using a texture analyzer (Stable Micro System, Godalming, UK), based on the method reported previously (Manski, van der Goot, & Boom, 2007). Tensile stress, tensile strain, and Young's modulus (YM) were measured via uniaxial tensile tests. Three tensile bars were cut from the samples using a dog-bone-shaped cutter. Bars were taken in parallel and perpendicular directions along the shearing direction. The width and thickness of the tensile bars were measured using a digital caliper (Mitutoyo, Kawasaki, Japan) to calculate the initial cross-sectional area. The initial length of the tensile bar was 15.5 mm (L_0). The force needed to break the sample was recorded by the Exponent software (Stable Micro System). The true stress $\sigma(t)$ and true strain $\varepsilon(t)$ were calculated based on the assumption that the volume of the tensile bar did not change during elongation (Choung & Cho, 2008; Raheem, 2014).

$$\sigma(t) \ = \ \frac{F(t)}{A_0} \times \frac{L(t)}{L_0} \ [\text{Pa}] \tag{6}$$

$$\varepsilon(t) = \ln \frac{L(t)}{L_0} \ [\text{mm/mm}] \tag{7}$$

where L_0 is the initial length of the sample and $L(t)$ is the length of the sample at fracture time t. A_0 is the initial cross-sectional area. YM was calculated from the slope of the tensile stress-strain curve with the tensile strain between 0.5 and 1.5. The anisotropic index (*AI*) was calculated as the quotient of the parallel value and the perpendicular value:

$$AI_\sigma \ = \ \frac{\sigma_\text{par}}{\sigma_\text{per}} \ [\text{-}] \tag{8}$$

$$AI_\varepsilon \ = \ \frac{\varepsilon_\text{par}}{\varepsilon_\text{per}} \ [\text{-}] \tag{9}$$

$$AI_{YM} \ = \ \frac{YM_\text{par}}{YM_\text{per}} \ [\text{-}] \tag{10}$$

6.2.5 Statistics analysis

The statistics in this paper were analyzed using SPSS software, version 25.0 (IBM, Armonk, NY, USA). A univariate general linear model with the least significant difference (LSD) test was carried out to investigate the significant differences (Table 6-1, Table 6-2, and Fig.6-7). Differences were considered significant when $P < 0.05$.

6

6.3 Results & discussion

6.3.1. Composition and morphology

The composition analysis showed similar protein content in DSK (55%) and PSK (54%) (Table 6-1). PSK contained more oil, ash, and CGA than the DSK implying that the concentration of carbohydrates should be lower in PSK than in DSK. The differences in the composition are most likely due to the differences in the de-oiling process when producing DSK and PSK. The compositional values are in line with previous studies that reported protein content of around 50% after pressing and additional de-oiling (Anjum, Nadeem, Khan, & Hussain, 2012; Salgado, Molina Ortiz, Petruccelli, & Mauri, 2011). Besides, a similar total carbohydrate content of ~ 20% was reported for the de-hulled sunflower cake (Anjum et al., 2012). Aqueous ethanol washing led to a protein enrichment up to 4 washing steps whereas protein content was hardly changed by additional washing. The oil was partially removed in the case of DSKC, and this oil removal continued when more washing steps were applied. However, hardly any oil was removed in PSKC up to 4 washing steps and 8% of the oil even remained in PSKC10. Aqueous ethanol washing was effective for CGA removal. Most of CGA was removed for DSKC4, DSKC10, PSKC4, and PSKC10. Ash content hardly changed upon washing and the concentration of carbohydrates in the washed DSKC samples increased slightly. The powder morphologies of all samples were visualized by SEM (Fig. 6-2). The particles were shown as a cellular matrix, which is in line with the sunflower materials in previous research (Düsterhöft, Bonte, Venekamp, & Voragen, 1993). The cellular matrix of DSK particles was found to have an open structure on the surface. However, the PSK particle had a more closed and compact surface structure. The differences in the morphologies between PSK and DSK might explain the difference in further oil removal by the aqueous ethanol washing process. The closed and compact surface structure of PKS probably limited the extraction of oil during the washing process. Thus, the results show that PSK material contains higher oil content with a more compact and closed surface morphology compared with DSK. Aqueous ethanol washing was more effective for oil removal in DSK than PSK, and the differences in the composition and morphology became less obvious by the washing process. CGA removal was similar for both materials upon aqueous ethanol washing.

Table 6-1 Composition (%) in dry base of the DSK, PSK and DSKC1/4/10 and PSKC1/4/10 in terms of protein, oil, ash, phenolic compounds (CGA), moisture and carbohydrates.

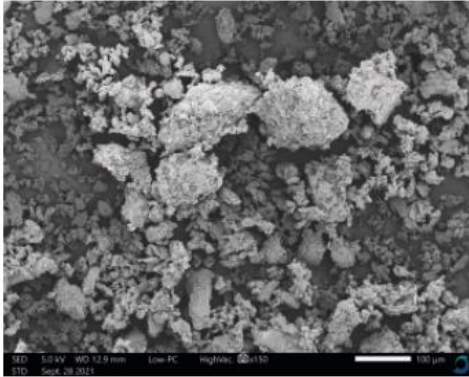| Composition Dry base	Protein %	Oil %	Ash %	PC (CGA) %	Carbohydrate %
DSK	55.3 ± 0.4^a	7.4 ± 0.2^a	7.8 ± 0.01^a	3.9 ± 0.1^a	25.6
DSKC1	57.0 ± 0.3^b	5.9 ± 0.2^b	7.5 ± 0.04^a	2.4 ± 0.1^b	27.2
DSKC4	59.6 ± 0.5^{ce}	4.5 ± 0.1^c	8.2 ± 0.6^{ab}	0.6 ± 0.01^c	27.2
DSKC10	60.8 ± 0.2^c	3.3 ± 0.9^d	7.7 ± 0.1^{ac}	N.A	28.3
PSK	54.0 ± 0.3^d	10.1 ± 0.3^e	9.3 ± 0.1^d	5.3 ± 0.1^d	21.3
PSKC1	57.5 ± 0.1^e	10.2 ± 0.9^e	9.9 ± 0.3^e	1.2 ± 0.003^e	20.5
PSKC4	57.4 ± 0.3^f	10.0 ± 0.8^e	9.9 ± 0.3^e	0.1 ± 0.02^f	18.5
PSKC10	59.7 ± 0.1^e	8.2 ± 0.2^f	9.8 ± 0.1^{de}	N.A	22.3

Significant differences were compared for the protein, oil, ash and CGA content between the samples of DSK, DSKC1/4/10, PSK, PSKC1/4/10 and indicated as small upper letters.

Table 6-2 Functional properties of the DSK, PSK, DSKC1/4/10 and PSKC1/4/10 with respect to the onset denaturation temperature (T_d), peak denaturation temperature (peak T_d) and denaturation enthalpy E_d (J/g protein), WHC (g water/ g dry pellet) and NSI (%).
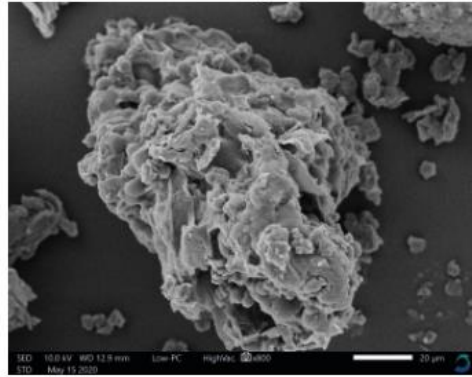
Functional properties	Onset T_d (°C)	Peak T_d (°C)	Enthalpy E_d (J/g protein)	WHC (g water/g dry pellet)	NSI (%)
DSK	93.3 ± 0.2^{ac}	99.8 ± 0.2^a	9.4 ± 1.5^a	5.7 ± 0.2^a	49.1 ± 0.1^a
DSKC1	93.2 ± 0.2^{ac}	99.1 ± 0.1^a	7.8 ± 0.2^{ac}	5.9 ± 0.6^a	52.3 ± 2.4^b
DSKC4	92.9 ± 0.3^a	99.0 ± 0.2^a	8.0 ± 0.7^{ac}	9.3 ± 0.6^{ce}	71.2 ± 1.8^c
DSKC10	92.6 ± 0.1^a	98.7 ± 0.1^a	7.9 ± 0.2^{ac}	10.5 ± 0.9^{be}	69.8 ± 2.3^c
PSK	94.9 ± 1.0^d	97.9 ± 3.2^a	12.2 ± 0.8^b	6.4 ± 0.8^a	31.9 ± 1.0^d
PSKC1	93.8 ± 0.5^c	99.8 ± 0.1^a	10.0 ± 1.8^{ad}	8.7 ± 0.5^c	61.1 ± 2.6^e
PSKC4	93.5 ± 0.01^{ac}	99.8 ± 0.02^a	8.3 ± 0.5^{ac}	9.8 ± 0.1^e	64.1 ± 1.2^e
PSKC10	92.6 ± 0.2^{ab}	99.2 ± 0.1^a	8.5 ± 0.7^a	7.7 ± 0.1^d	41.3 ± 1.4^f

Significant differences were compared for Onset T_d, peak T_d, E_d, WHC and NSI between the samples of DSK, DSKC1/4/10, PSK, PSKC1/4/10 and indicated as small upper letters.
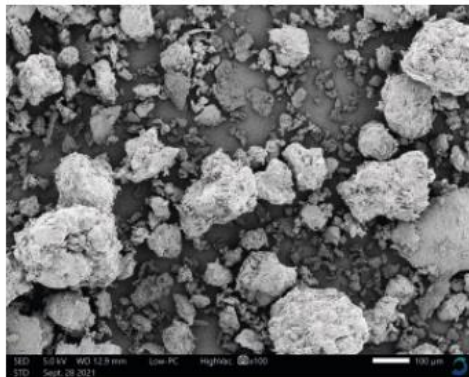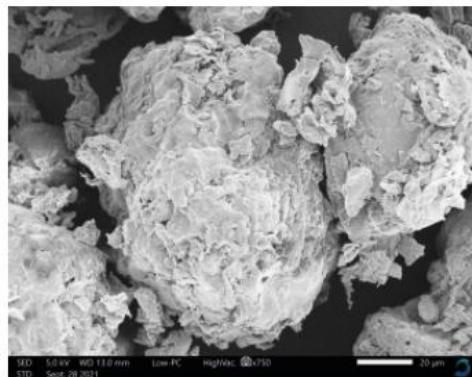
A1-1: DSK_100 µm

A1-2:DSK_20 µm
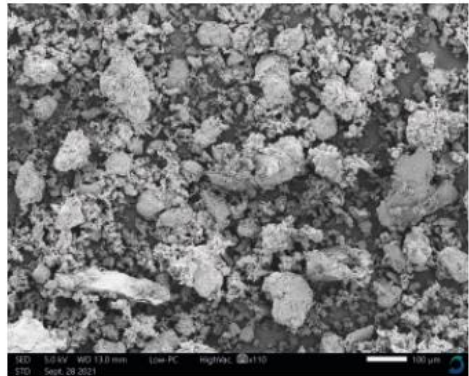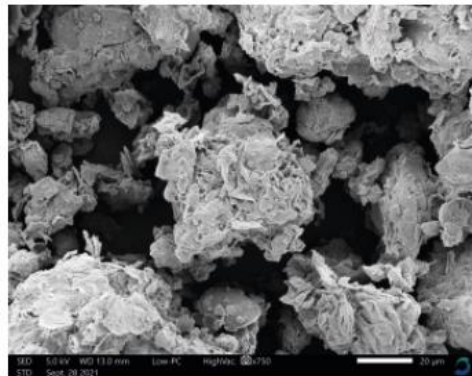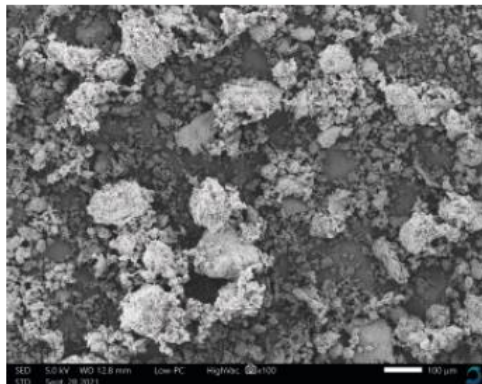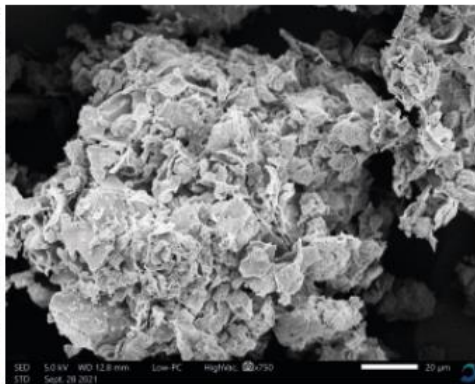

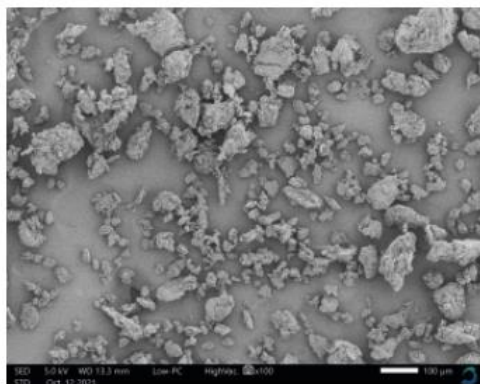A2-1: DSKC1_100 µm

A2-2: DSKC1_20 µm

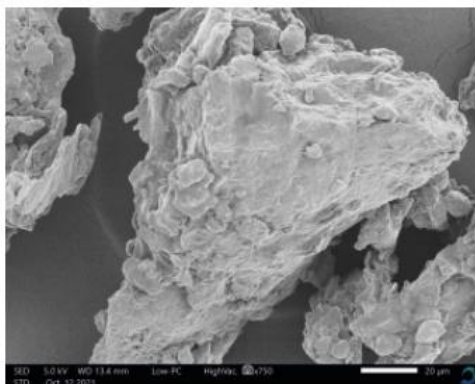

A3-1: DSKC4_100 µm

A3-2: DSKC4_20 µm

A4-1: DSKC10_100 μm

A4-2: DSKC10_20 μm

B1-1: PSK_100 μm

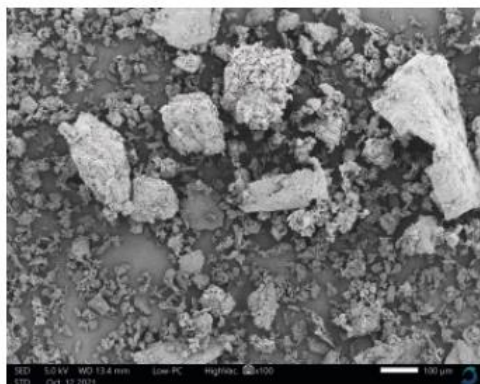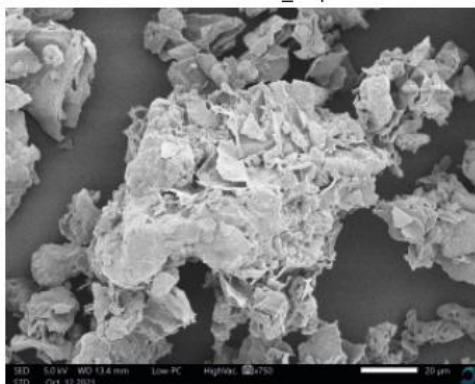**B1-2: PSK_20 μm**

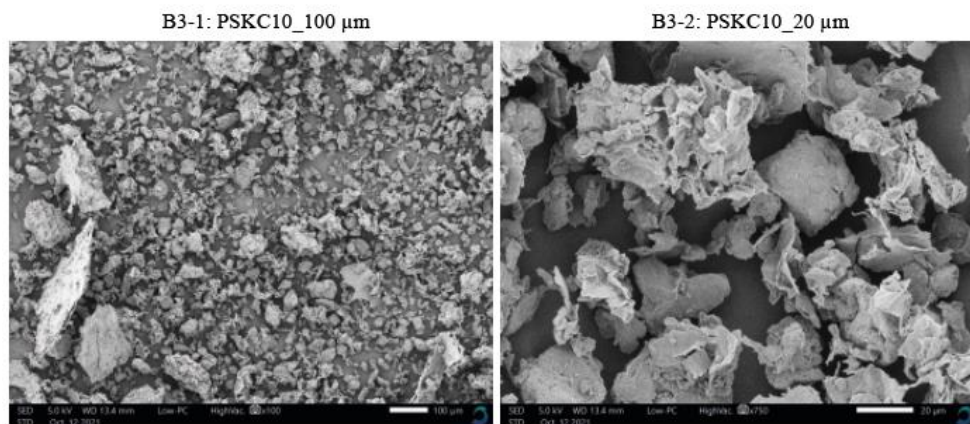**B2-1: PSKC4_100 μm**

B2-2: PSKC4_20 μm

Fig. 6-2 Scanning electron micrographs of DSK(A1), DSKC1/4/10 (A2-A4), PSK (B1) and PSKC4/10 (B2/B3) samples. The different scale bars of 100 µm and 20 µm were showed.

6.3.2 Functional properties

Fig. 6-3 showed the profiles of the soluble protein fraction from DSK and PSK in the presence of β-mercaptoethanol. The bands in the molecular weight of 21 to 27 kDa and 32 to 44 kDa probably correspond to 11S globulin subunits, which are composed of basic and acidic polypeptides, respectively. The small band corresponding to a molecular weight of 10 kDa was assigned to the 2S albumins (Dalgalarrondo, Raymond, & Azanza, 1984). An additional band at 50 kDa appeared in the DSKCs after the washing process, while this band was less visible in the case of PSKCs. The band at 50 kDa was previously observed with the sunflower protein isolate under reducing conditions (Karefyllakis, Salakou, Bitter, Van der Goot, & Nikiforidis, 2018). Table 6-2 showed the onset denaturation temperatures (Onset T_d), peak denaturation temperatures (peak T_d), and enthalpies (E_d) of the protein in all the samples. The onset T_d of DSK and PSK became lower when applying more washing steps. However, no significant differences were found with the peak T_d of both DSK and PSK samples between the different washing steps. The results show that the denaturation behavior of the protein in the DSKCs and PSKCs was not changed by the washing process and the number of steps applied. The highest E_d-value was observed for PSK (12 J/g protein), followed by a similar result of PSKC1 and DSK (10 J/g protein). These results suggest that the protein in DSK was already partially denatured compared with PSK. A further decrease in protein nativity was found with the PSKCs and DSKCs (approximately 8 J/g protein) after aqueous

ethanol washing. The result was expected as aqueous ethanol washing is known to have an effect on the protein nativity of sunflower materials (González-Pérez & Vereijken, 2007; Tranchino, Costantino, & Sodini, 1983), evidenced by the report of similar results with the de-oiled sunflower meal previously (Molina et al., 2004; Jia et al., 2021b).
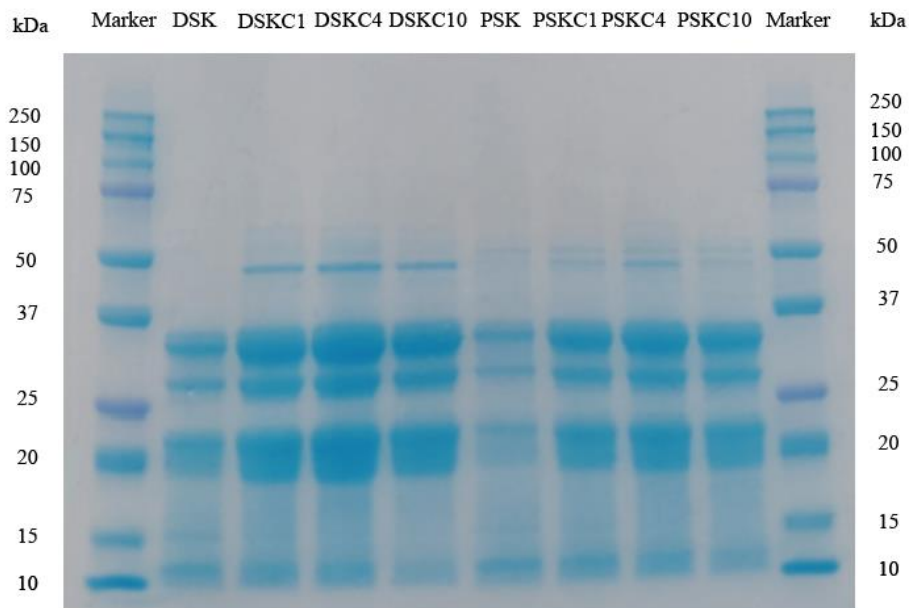
Fig. 6-3 SDS-PAGE for the soluble protein fractions of DSK, DSKC1/4/10, PSK and PSKC1/4/10 samples by adding the 2-mercaptoethanol.

Table 6-2 also showed the water holding capacity (WHC) and nitrogen solubility index (NSI) of all the samples. Similar results of WHC were found with DSK, DSKC1, and PSK (~ 6 g water/g dry pellet). A large increase was found when more washing steps were applied. DSKC10 had a WHC of ~10g water/g dry pellet even. The pellet from PSKC1 held more water than the pellet from PSK, and this value was even higher for PSKC4 (8.7 to 9.7 g water/g dry pellet). The nitrogen solubility index measurement showed that the protein in PSK was less soluble than the protein in DSK (32% versus 49%) (Table 6-2). This might be due to the less opened surface morphology of the PSK particles, which can limit the access of the water during hydration. A large increase in NSI was already observed for PSKC1 and PSKC4 (61% and 64%) after washing process but the solubility was lower for the PSKC10 (41%). The NSI values for DSKC4/10 samples were increased to approximately 70%. The

protein nativity with the washed DSKCs and PSKCs was only slightly affected by the washing process (Table 6-2), thus not likely to reduce the solubility. A reason for the increased solubility by aqueous ethanol washing might be found in the altered protein profile. The additional band at 50 kDa appeared for the washed sample (Fig. 6-3) might indicate the formation of protein-phenol complex, which can be more soluble than the original proteins, due to the hydrophilic nature of CGA (Jia, Kyriakopoulou, et al., 2021). This 50 kDa and is less visible in PSK, which could be a reason for the lower protein solubility. Nonetheless, results suggest a positive effect of aqueous ethanol washing on WHC and NSI for both washed DSKC and PSKC samples, and the effect was more pronounced for the DSKC than the PSKC samples.

Changes in WHC and protein solubility as a result of aqueous ethanol washing have been reported for other crops as well. Just like in the results presented here, the effect of the washing is not consistent for all crops or fractions of crops (Wang et al., 2020). Factors like removal of certain protein and non-protein components including oil and phenols, denaturation and aggregations are crop dependent and therefore explain why a consistent effect of washing is lacking in overall protein solubility and WHC.

6.3.3 Structuring properties

Rheological properties in CCR

The elastic and loss moduli (G' and G'') of the DSK, PSK, and washed DSKCs and PSKCs (40 wt%) are shown in Fig. 6-4. The G' value was always higher than the G'' value in the temperature sweep measurement. In total three regions were found for the G' during heating of DSK. From 40 to 90 ℃, the G' value decreased, followed by an increase of G' when heated from 90 to 125 ℃. A decrease of G' value was detected by further heating from 125 to 150 ℃. This effect of temperature on G' and G'' shows certain similarities to the behavior of wheat gluten and rapeseed meal during heating. Emin et al., (2017) and Pietsch et al., (2017) reported that the increase in moduli values above 90 ℃ is due to the polymerization/aggregation reactions of the exposed hydrophobic group from protein, which resulted in the formation of a crosslinked network. The decrease in moduli above 130 ℃ was explained by the depolymerization of the structure, which was caused by the breakdown of

the disulfide bonds. Sunflower protein is known to have gel-forming properties upon heating (González-Pérez & Vereijken, 2007), which explains the increase of the *G'* value above 90 ℃.

Though the PSK and DSK samples showed a similar trend for *G'* and *G''* values during heating, the values were higher for DSK than PSK. This higher value for the DSK sample might be related to its lower oil and higher carbohydrate content than the PSK sample (Table 6-1). The *G'* values were higher upon aqueous ethanol washing up to 4 washing steps. DSKC samples showed a higher *G'* value than the PSKC samples by heating. These differences became smaller after aqueous ethanol washing, which were hardly noticed after 4 washing steps. Cooling increased both of the *G'* and *G''* values, which was an expected effect due to the rearrangement of the disulphide bond, which can make the structure more firm (Schofield, Bottomley, Timms, & Booth, 1983). A similar strengthening was also reported in the case of high moisture extrusion. The cooling die also solidified the product formed in the extrusion process (Osen & Schweiggert-Weisz, 2016; Schofield et al., 1983). Time sweeps measured at a constant temperature of 90, 120 and 140 ℃ for the DSK, PSK, DSKCs, and PSKCs are shown in Fig. 6-5**.** In general, the G' and *G''* values at 90 and 120 ℃ were nearly constant during the time sweep. Both values were found to decrease when heated at 140 ℃ for 15 minutes. Aqueous ethanol washing resulted in an increase in the *G'* and *G''* values at 90 and 120 ℃ for DSKC and PSKC up to 4 washing steps. Further, increasing the washing steps or temperature hardly affect the *G'* and *G''* values with the washed samples. A similar trend was reported for the aqueous ethanol washed soy protein concentrate, rapeseed protein concentrate during time sweep at 120 and 140 ℃ (Jia et al., 2021). Without washing, DSK showed higher *G'* and *G''* values compared with PSK. However, just as found in the case of the temperature sweep, the differences between DSK and PSK largely disappeared after washing at all temperatures measured.

From all the rheological measurements, it can be concluded that DSK and PSK have different rheological properties before washing. However, upon washing the differences mainly disappear, suggesting that aqueous ethanol washing affected on the rheological properties. Remarkable, the differences in oil and CGA content did not affect in those measurements.

179
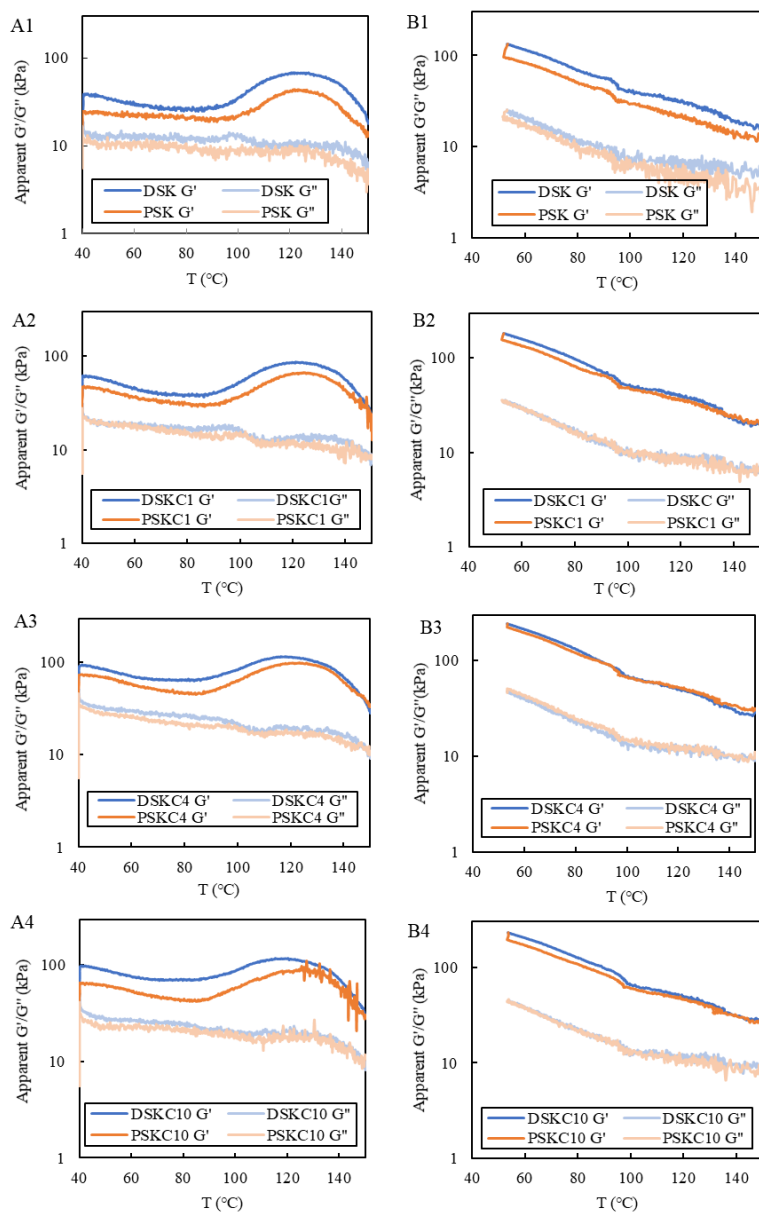
Fig. 6-4 Viscoelastic modulus G'/G'' for temperature sweep from 40 to150 °C with respect to DSK/PSK (A1), DSKC1/PSKC1 (A2), DSKC4/PSKC4 (A3) and DSKC10/PSKC10 (A4). The cooling profile from 150 to 50 °C for DSK, DSKCs, PSK, and PSKCs samples from B1 to B4. All DSK and DSKC results are in blue and PSK and PSKC results are in orange, and dark blue or orange are for the G' value and light blue or light orange line are for the G'' value.

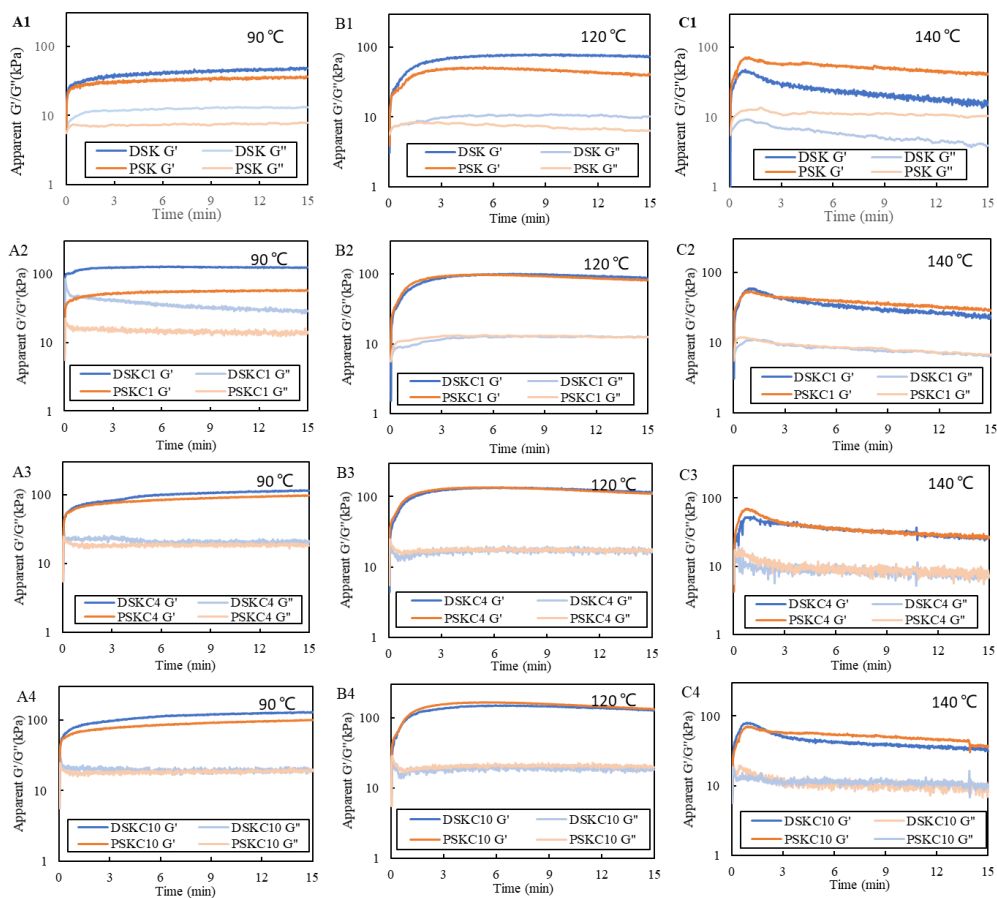**Fig. 6-5** Viscoelastic modulus *G'/G''* for time sweep of DSK/PSK (A1-C1), DSKC/PSKC1(A2-C2), DSKC/PSKC4 (A3-C3), and DSKC/PSKC10 (A4-C4) at 90, 120 and 140°C, in which all DSK and DSKC results are in blue and PSK and PSKC results are in orange, and dark blue or orange are for the *G'* value and light blue or light orange line are for the *G''* value.

Structuring properties in shear cell

Fig. 6-6 showed the macrostructure of the sheared and heated sunflower materials (40 wt% DM) by shear cell. DSK alone can already form a fibrous structure in the shear cell and similar fibrous structures were formed for DSKCs samples. However, the macrostructure of PSK showed a crumbly gel-like structure, which was brittle and easily broken. Also, the washed PSKCs did not form fibrous products. The mechanical properties of the sheared and heated DSK and DSKCs samples were measured using a texture analyzer (Fig. 6-7). The DSK sample of 40 wt% was found to have the lowest tensile stress and Young's modulus (YM) at the parallel direction. It was not possible to measure the tensile stress and strain for for the DSK sample at perpendicular direction since the tensile bar sample for this sample broke prior to the analysis due to the brittleness. The tensile stress and YM values of the washed DSKC samples were larger at parallel/perpendicular direction after aqueous ethanol washing up to 4 steps, whereas the difference was small between the DSKC4 and DSKC10. The increase in tensile stress and YM upon more the washing steps indicated the increase of the mechanical strength and stiffness of the sample. The AI-value decreased by more steps of the aqueous ethanol washing process, though this decrease was not accompanied by a less fibrous appearance of the sample. In terms of tensile strain, the differences between the DSK and washed samples were small. The difference between AI-value of the tensile strain and YM was small between the different washing steps. Thus, aqueous ethanol washing process had a stronger effect on the AI-value of the tensile stress than the tensile strain and the YM.
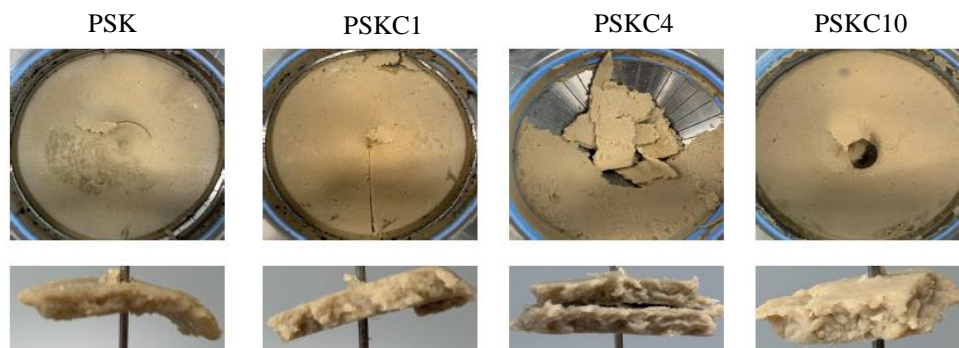
DSK	DSKC1	DSKC4	DSKC10

PSK	PSKC1	PSKC4	PSKC10
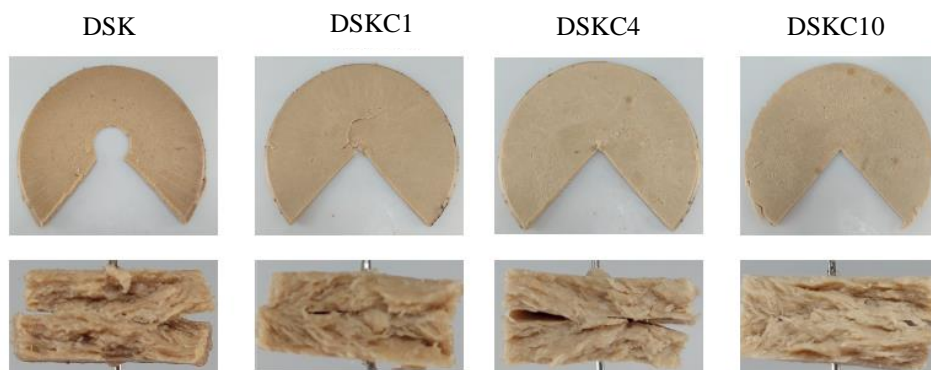
Fig. 6-6 Macro structure of the sheared and heated products of DSK, PSK, DSKC1/4/10 and PSKC1/4/10 with 40 wt% DM, processed at 140 ℃, 30 rpm and 15 min.

The difference in the structuring properties of DSK and PSK might be related to the large difference in the oil content. The DSK and DSKCs samples contain a lower amount of oil (3.3%‐7.4%) compared to the PSK and PSKCs sample (8.2%‐10.1%). The tensile stress was plotted as a function of oil content in Fig. 6-7A'. The tensile stress of the DSK and DSKCs products decreased with higher oil content. The extrapolation of the trendline suggests that an oil content higher than 8% prevents the formation of a coherent fibrous product. All PSK samples contained more than 8% oil indeed, which could be an explanation for the observation that only crumbly products were obtained. The presence of oil was also reported to cause material lubrication and to influence the structuring properties of the ingredients in high moisture extrusion (Cheftel, Kitagawa, & Queguiner, 1992; Kyriakopoulou, Keppler, & Van Der Goot, 2021). As a result, the plant protein ingredients are often de-oiled for their usage in meat analogue applications (Kyriakopoulou et al., 2019). From the shear cell experiments, it seems that oil was released during the shearing and heating at a high temperature of 140 °C. As a result, it hindered the formation of a full protein network throughout the whole product. This effect is similar to the role of oil in wheat doughs, where it acts as a shortening agent through preventing the formation of a gluten network to make puff pastry products (Huschka, Challacombe, Marangoni, & Seetharaman, 2011; Inoue, Sapirstein, & Bushuk, 1995). Though this effect might be beneficial for certain dough application, it is clearly an undesired effect in the case of making fibrous products. It is also interesting to note that the differences in the structuring properties were not observed when using the CCR to measure the rheological properties (Fig. 6-3 and Fig. 6-4). In CCR

measurements, only the heating effect was examined by temperature and time sweep within the linear viscoelastic region. It is possible that limited deformation does not lead to release of oil from the PSK matrix or that the effect of oil is only visible at large deformation (Manski et al., 2008).
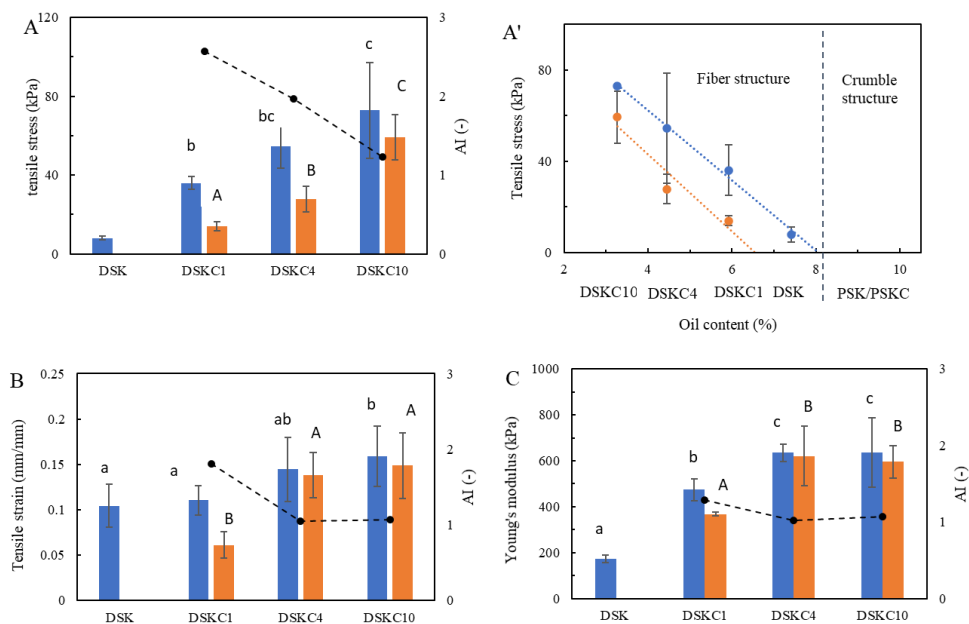
Fig. 6-7 Tensile stress (kPa), strain (mm/mm) and Young's modulus (kPa) of the sheared and heated products of DSK, PSK, DSKC1/4/10 and PSKC1/4/10 washing steps at parallel (blue bar) and perpendicular (orange bar) (A-C). The anisotropic index (AI) are shown as grey dotted line with grey sphere symbol. Significant differences between the products of DSK, DSKC1, DSKC4 and DSKC 10 are shown in terms of the tensile stress, strain and YM at parallel direction (small letter) or perpendicular direction (capital letter). The tensile stress at parallel (blue dot) and perpendicular (orange dot) direction of DSK and DSKCs products were plotted as a function of oil content (A').

Part of the aim of this study was to better understand the effect of the presence of phenolic compounds on the functional and structural properties of sunflower materials. The results though suggest that the presence of phenolic compounds does not affect the fibrous structure formation of the de-oiled sunflower kernel in the shear cell. It is known that the covalent interaction between protein and CGA can negatively affect the gelling properties at high CGA content and can give rise to off-colors. However, the sheared and heated DSK, PSK, or DSKCs and PSKCs products showed no green color formation. The green color is

an indication of covalent interaction between sunflower protein and chlorogenic acid (Prigent, Voragen, Visser, Koningsveld, & Gruppen, 2007). These covalent interactions between the CGA and protein are favored at alkaline pH and are therefore less likely to occur in the shear cell experiment where the pH of the sunflower product is close to neutral (results not shown). The occurrence of covalent interactions at a lower extent or the non-covalent interactions cannot be ruled out, but based on the results presented here, the effect of CGA on the structuring properties was not noticeable regarding the tested sunflower materials. It is also interesting to note that the differences in the structuring properties were not observed when using the CCR to measure the rheological properties (Fig. 6-3 and 6-4). In CCR measurements, only the heating effect was examined by temperature and time sweep within the linear viscoelastic region. It is possible that limited deformation does not lead to a release of oil from the PSK matrix or that the effect of oil is only visible at large deformation (Manski, Van der Zalm, Van der Goot, & Boom, 2008).

Thus, the shear cell experiment result presented that the DSK and DSKCs (40 wt%) formed fiber structure when sheared and heated at 140 °C, while PSK and PSKCs only formed crumble structure under the same conditions. The difference in oil content of the samples was suggested as the main reason for the different structuring properties, whereas the effect of CGA was less noticeable.

6.4 Conclusion

The effect of aqueous ethanol washing on composition, functional, and structuring properties was assessed using two starting materials DSK and PSK. After 10 times washing process, compositions of DSK and PSK were similar, except for the oil content. Phenolic compounds were effectively removed by the aqueous ethanol washing. Partial oil removal was obtained in DSK, while oil could not be removed in the case of PSK. Thus, primary de-oiling process could influence further oil removal by aqueous ethanol washing. The differences in functional properties between DSK and PSK before the washing process were largely disappeared upon washing.

Despite high similarities in functional properties, we still observed differences in structuring properties. DSK and DSKCs formed a fibrous structure at 140 °C, while PSK and PSKCs could not be used to make fibrous products. The removal of the phenolic compounds

is not required for structuring properties of DSK/DSKCs, whereas the differences in oil content are crucial for the fibrous structure formation of DSK and PSK samples. Too much oil can prevent the formation of a coherent network throughout the full product, thereby only creating a crumbly product. Based on all structuring experiments of DSK and PSK, it is suggested that the oil content should not exceed the oil content present in DSK, which is about 8%.

6.5. References

Anjum, F.M., Nadeem, M., Khan, M.I., & Hussain, S. (2012). Nutritional and therapeutic potential of sunflower seeds: A review. *British Food Journal*, *114* (4), 544–552.

Arrutia, F., Binner, E., Williams, P., & Waldron, K. W. (2020). Oilseeds beyond oil: Press cakes and meals supplying global protein requirements. *Trends in Food Science and Technology*, *100* (Jan), 88–102.

Cheftel, J. C., Kitagawa, M., & Queguiner, C. (1992). New protein texturization processes by extrusion cooking at high moisture levels. *Food Reviews International*. 8 (2) 235-375.

Citeau, M., Regis, J., Carré, P., & Fine, F. (2018). Value of hydroalcoholic treatment of rapeseed for oil extraction and protein enrichment. *Ocl*, *26*, 1.

Dalgalarrondo, M., Raymond, J., & Azanza, J.L. (1984). Sunflower seed proteins: Characterization and subunit composition of the globulin fraction. *Journal of Experimental Botany*, *35*(11), 1618–1628.

Dekkers, B.L., Emin, M.A., Boom, R.M., & van der Goot, A.J. (2018). The phase properties of soy protein and wheat gluten in a blend for fibrous structure formation. *Food Hydrocolloids*, *79*, 273–281.

Düsterhöft, E.M., Bonte, A.W., Venekamp, J.C., & Voragen, A.G.J. (1993). The role of fungal polysaccharidases in the hydrolysis of cell wall materials from sunflower and palm-kernel meals. *World Journal of Microbiology & Biotechnology*, *9* (5), 544–554.

Emin, M.A, Quevedo, M., Wilhelm, M., & Karbstein, H.P. (2017). Analysis of the reaction behavior of highly concentrated plant proteins in extrusion-like conditions. *Innovative Food Science & Emerging Technologies*, 44 (September), 15-20

González-Pérez, S., & Vereijken, J. M. (2007). Sunflower proteins: overview of their physicochemical, structural and functional properties. *Journal of the Science of Food and Agriculture*, *87*(12), 2173–2191

Grabowska, K.J., Zhu, S., Dekkers, B.L., De Ruijter, N.C.A., Gieteling, J., & Van Der Goot, A.J. (2016). Shear-induced structuring as a tool to make anisotropic materials using soy protein concentrate. *Journal of Food Engineering*. 188 (77-86).

Huschka, B., Challacombe, C., Marangoni, A. G., & Seetharaman, K. (2011). Comparison of oil, shortening, and a structured shortening on wheat dough rheology and starch pasting properties. *Cereal Chemistry*, *88* (3), 253–259.

Inoue, Y., Sapirstein, H.D., & Bushuk, W. (1995). Studies on frozen doughs. IV. Effect of shortening systems on baking and rheological properties. *Cereal Chemistry*, *72* (2), 221–226.

Molina, M.I., Petruccelli, S., Añón, M.C (2004). Effect of pH and ionic strength modifications on thermal denaturation of the 11S globulin of sunflower (*Helianthus annuus*), 52, 6023–6029.

Jia, W., Rodriguez-Alonso, E., Bianeis, M., Keppler, J.K., & Van der Goot, A.J. (2021). Assessing functional properties of rapeseed protein concentrate versus isolate for food applications. *Innovative Food Science & Emerging Technologies*, *68* (Feb), 102636.

Jia, W, Curubeto, N., Rodríguez-Alonso, E., Keppler, J.K., & Van der Goot, A.J. (2021). Rapeseed protein concentrate as a potential ingredient for meat analogues. *Innovative Food Science and Emerging Technologies*, *72* (July), 102758.

Jia, W, Kyriakopoulou, K., Roelofs, B., Ndiaye, M., Vincken, J.-P., Keppler, J. K., & van der Goot, A. J. (2021). Removal of phenolic compounds from de-oiled sunflower kernels by aqueous ethanol washing. *Food Chemistry*, *362* (May), 130204.

Karefyllakis, D., Salakou, S., Bitter, J. H., Van der Goot, A. J., & Nikiforidis, C. (2018). Covalent bonding of chlorogenic acid induces structural modifications on sunflower proteins. *ChemPhysChem*, 19, 459–468.

Kyriakopoulou, K., Dekkers, B., & van der Goot, A. J. (2019). Plant-based meat analogues: Sustainable Meat Production and Processing. (C.M.galanakis, Ed.), *Academic Press*. 103-126.

Kyriakopoulou, K., Keppler, J.K., & Van Der Goot, A.J. (2021). Functionality of ingredients and additives in plant-based meat analogues konstantina. *Foods*, 10, 600.

Manski, J.M., Van der Goot, A.J., & Boom, R.M. (2007). Formation of fibrous materials from dense calcium caseinate dispersions. *Biomacromolecules*, *8* (4), 1271–1279.

Manski, J.M., van der Zalm, E.E.J., Van der Goot, A.J., & Boom, R.M. (2008). Influence of process parameters on formation of fibrous materials from dense calcium caseinate dispersions and fat. *Food Hydrocolloids*, *22* (4), 587–600.

Nijdam, D., Rood, T., & Westhoek, H. (2012). The price of protein: Review of land use and carbon footprints from life cycle assessments of animal food products and their substitutes. *Food Policy*, *37* (6), 760–770.

Osen, R., & Schweiggert-Weisz, U. (2016). High-Moisture Extrusion: Meat Analogues. In *Reference Module in Food Science*. https://doi.org/10.1016/B978-0-08-100596-5.03099-7

Ozdal, T., Capanoglu, E., & Altay, F. (2013). A review on protein-phenolic interactions and associated changes. *Food Research International*, *51*(2), 954–970.

Peter, R. (2018). Properties of aqueous-alcohol-washed protein concentrates prepared from air-classified pea protein and other air-classified pulse protein fractions. PhD thesis.

Pickardt, C., Neidhart, S., Griesbach, C., Dube, M., Knauf, U., Kammerer, D. R., & Carle, R. (2009). Optimisation of mild-acidic protein extraction from defatted sunflower (*Helianthus annuus L.*) meal. *Food Hydrocolloids*, *23* (7), 1966–1973.

Pietsch, V.L., Emin, M.A., & Schuchmann, H.P.(2017). Process conditions influencing wheat gluten polymerization during high moisture extrusion of meat analog products. *Journal of Food Engineering*. 198, 28-35

Prigent, S.V., Voragen, A. G., Visser, A.J., Van Koningsveld, G.A., & Gruppen, H. (2007). Covalent interactions between proteins and oxidation products of caffeoylquinic acid (chlorogenic acid). *Journal of the Science of Food and Agriculture*, *87* (13), 2502–2510.

Salgado, P.R., Molina Ortiz, S.E., Petruccelli, S., & Mauri, A.N. (2011). Sunflower protein concentrates and isolates prepared from oil cakes have high water solubility and antioxidant capacity. *JAOCS, Journal of the American Oil Chemists' Society*, *88*(3), 351–360.

Schofield, J.D., Bottomley, R.C., Timms, M.F., & Booth, M.R. (1983). The effect of heat on wheat gluten and the involvement of sulphydryl-disulfide interchange reactions. *Journal of Cereal Science*, *1* (4), 241–253.

Tranchino, L., Costantino, R., & Sodini, G. (1983). Food grade oilseed protein processing: sunflower and rapeseed. *Qualitas Plantarum Plant Foods for Human Nutrition*, *32*(3–4), 305–334.

Wang, Y., Guldiken, B., Tulbek, M., House, J.D., & Nickerson, M. (2020). Impact of alcohol washing on the flavour profiles, functionality and protein quality of air classified pea protein enriched flour. *Food Research International*, *132*(Jan), 109085

Chapter 7

General discussion
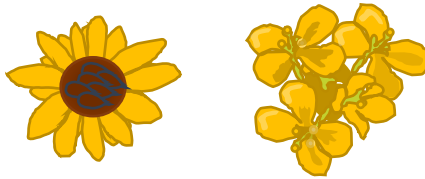
7.1 Outline

The aim of this thesis was to create the scientific insight to allow the use of the co-products rapeseed meal and de-oiled sunflower kernel for meat analogue applications. To reach this aim, the following questions were answered: (1) how to remove phenolic compounds and what is the effect on the overall composition of both materials (Chapters 2 & 4); (2) what are the key functionalities that determine the structuring properties of both materials by shear cell technology (Chapters 3 & 6); (3) is the removal of phenolic compounds necessary from a functional and structuring point of view (Chapters 5 & 6).

7.2 Main findings and conclusions

Chapter 2 compares the techno-functional properties of rapeseed protein concentrate (RPC) and rapeseed protein isolate (RPI). RPC was obtained through aqueous ethanol washing of rapeseed meal, and RPI was produced from rapeseed meal by alkaline extraction, ultrafiltration, and dialysis. It was found that the protein in RPI was still in its native state and had high solubility, but considerable amount of phenolic compounds were still present. An RPI dispersion (40% dry matter [DM]) showed poor gelling properties demonstrated by a low complex modulus (G^*) measured using a closed cavity rheometer. RPC consisted mainly of proteins and polysaccharides and washing removed almost all the phenolic compounds. The protein in RPC was completely denatured, leading to reduced protein solubility and sand-like behavior of the RPC particles when dispersed in water. However, the high G^* of an RPC dispersion with 40 wt% DM suggested its potential use in meat analogues. Thus, the RPC obtained by aqueous ethanol washing was further investigated for its structuring properties.

Chapter 3 describes the structuring properties of RPC for meat analogue application using shear cell technology. Two recipes of RPC-only and RPC-wheat gluten (WG) mixtures were investigated at 40 wt% DM. Shear cell experiments showed that both RPC-only and RPC-WG mixtures could be transformed into fibrous products. The fibrous structure formed above a process temperature of 140 °C for RPC-only, which was higher than the temperature of 130 °C needed for RPC-WG (1:1) mixture. The RPC-WG mixtures at 140 °C showed a more pronounced anisotropic structure than the RPC-only product. The sheared and heated RPC-WG product was lighter in color than the RPC-only product.

Nevertheless, the RPC-only product contained more pronounced fibers compared with soy protein concentrate under the same conditions. Overall, it was concluded that RPC is a promising protein source for meat analogue application.

Chapter 4 describes the effect of the process temperature, pH, and solvent quality on the removal of phenolic compounds from de-oiled sunflower kernel using an aqueous ethanol washing process. The amount of phenolic compounds removed from de-oiled sunflower kernel was found to be most effective at pH 7, an extraction temperature of 50 °C, and a solvent with an ethanol content below 60%. However, removal of phenolic compounds was accompanied by protein loss for most of those process conditions, and a change in process conditions had a greater effect on protein loss than on the yield of removal of phenolic compounds. More washing steps (up to 3) also led to thremoval of more phenolic compounds under all conditions than when using just a single washing step. A simulation of the process is described in the final part of the chapter. The simulation results revealed that the theoretical protein losses could be reduced to <1% with 95% of phenolic compounds removed using 80% ethanol at 25 °C provided more washing steps are allowed or a counter-current process is applied.

Chapter 5 describes to what extent chlorogenic acid (CGA) should be removed from de-oiled sunflower kernel to prevent a negative influence on the functional properties of sunflower protein. A simple model blend consisting of CGA and sunflower protein was investigated under apparent CGA-protein molar ratios of 1:10, 1:5, 1:1, 5:1, and 10:1 (which is equal to mass ratios of 1:850, 1:450, 1:85, 1:15, and 1:10, respectively). The pH of the blend was altered in such a way that covalent interactions (pH-shift: 24 h incubated at pH 9 and back to pH 7) and non-covalent interactions (24 h incubated at pH 7) were induced selectively. The results showed that non-covalent interactions induced structural changes in the protein, whereas the effect of covalent interactions on the protein structure was less clear, mainly because the process conditions used to induce interactions (pH-shift) had a much larger effect on the proteins molecular structure than the interactions with CGA had. Covalent interactions led to changes in functional properties at higher CGA-protein molar ratios. Green color was observed, and gelling properties were negatively influenced above a critical CGA-

7

protein molar ratio of 1:1. In the case of non-covalent interactions, the effects on the color formation and gelling properties were limited.

In **Chapter 6,** two sunflower materials were investigated for their potential use in structuring processes: pressed sunflower kernel obtained by full pressing, and de-oiled sunflower kernel, obtained by pre-pressing and 96% ethanol de-oiling. Additional aqueous ethanol washing was applied to both de-oiled sunflower kernels and pressed sunflower kernels to remove phenolic compounds. Despite similarities in the composition and functional properties of these fractions, we still observed differences in their structuring properties. All the de-oiled sunflower kernel and its washed concentrate (40 wt% DM) formed a fibrous structure by shearing and heating at 140 °C in the shear cell. However, pressed sunflower kernel and its washed concentrate formed a crumble gel under the same conditions, which was most likely due to the high oil content (8%–10%). The pre-treatment was found to influence further oil removal by aqueous ethanol washing. Less than 8% of the oil was recommended to allow the formation of a fibrous structure. The presence of phenolic compounds did not affect the structuring properties, which further confirmed the findings of the simple model blend in **Chapter 5**.

7.3 Fractionation for meat analogue application

7.3.1 Process control: compositional effect

Rapeseed and sunflower seeds consist of many components, including protein, oil, polysaccharides, phenolic compounds, and other minor components. The aim of conventional fractionation processes is to make highly refined ingredients, such as protein isolate, which requires considerable amounts of water, chemicals, and energy to produce (Geerts, 2018; Loveday, 2020). These high purity ingredients are mostly mixed again in the manufacture of foods. Therefore, mild fractionation is now often suggested, which has the potential to better use the natural components present in the plant material. This approach is based on the fact that a process should focus on the desired functionality of the ingredients rather than purity (Van der Goot et al., 2016). Thus, fractionation routes to obtain less refined rapeseed and sunflower protein concentrates were discussed in terms of compositional change, functional properties and structuring properties.

The main fractionation process to obtain the protein concentrates from rapeseed and sunflower seeds consists of de-hulling, oil extraction, and aqueous ethanol washing to remove the hulls, oil, and phenolic compounds. Unlike sunflower seeds, complete de-hulling was difficult to achieve for rapeseed ((Carré, Citeau, Robin, & Estorges, 2016) and **Chapter 2**). Thus, more steps, e.g., sieving or milling of the rapeseed protein concentrate, were necessary to either remove macroscopic hulls or decrease the size of the hull. In case of aqueous ethanol washing, 70% ethanol and 75 °C is the standard procedure to obtain rapeseed protein concentrate from rapeseed meal. Washing process has already been applied in rapeseed meal in industry for oil extraction, protein enrichment and the glucosinolates removal (Citeau, Regis, Carré, & Fine, 2019). For sunflower materials, there is no standard procedure for pilot-scale production yet. Therefore, the process conditions of aqueous ethanol washing were assessed in a lab-scale experiment for de-oiled or pressed sunflower kernel (**Chapter 6**). It was found that 4 washing steps using an aqueous ethanol mixture with 40% ethanol at 25 °C effectively removed the phenolic compounds (CGA). Multi-step washing or counter-current multistage extraction with high ethanol content was recommended to effectively remove the phenolic compounds (CGA) while retaining as much protein as possible from de-oiled sunflower kernel (**Chapter 4**). The compositions of rapeseed meal, de-oiled or pressed sunflower kernel are compared before and after the aqueous ethanol washing process (Fig. 7-1A). Although the washing process leads to protein loss (**Chapter 4**), the protein content of the rapeseed protein concentrate was similar to the de-oiled/pressed sunflower kernel concentrate, which were enriched after the washing process. The washing process was effective for the removal of phenolic compounds for all three materials. The oil in rapeseed meal was completely removed, whereas some oil remained in the washed de-oiled or pressed sunflower kernel. The difference was mainly caused by the process conditions of aqueous ethanol washing. An aqueous ethanol mixture (40% ethanol) at 25 °C applied to de-oiled or pressed sunflower kernel was less effective for the oil removal than 70% ethanol at 75 °C applied to rapeseed meal. This is because ethanol is a better solvent for oil than water, and high temperature favors the dissolving oil (Rao & Arnold, 1956).
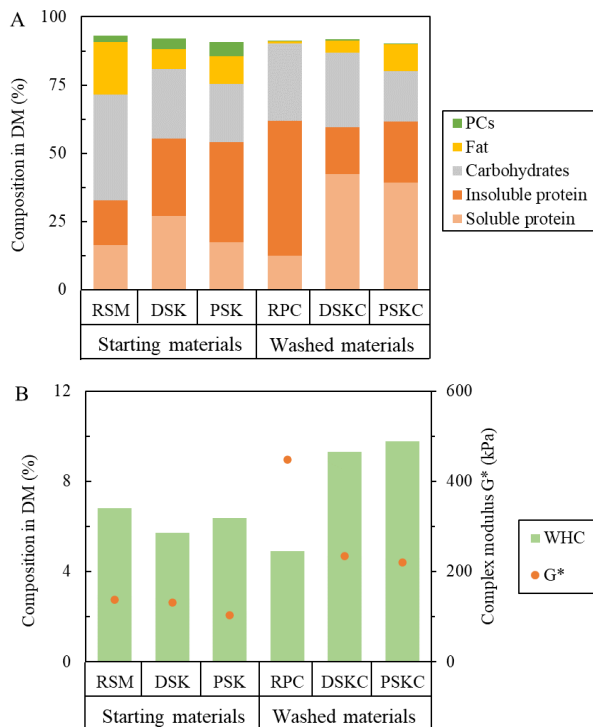
Fig. 7-1 Composition (mean value %) of rapeseed meal (RSM), de-oiled sunflower kernel (DSK), pressed sunflower kernel (PSK), and aqueous ethanol washed rapeseed concentrate (RPC), de-oiled sunflower kernel concentrate (DSKC), and pressed sunflower kernel concentrate (PSKC) after 4 washing steps. The mean water holding capacity (WHC, g water/g insoluble pellet) of the samples in 2 wt% dispersion is shown. All the data were extracted from this thesis.

7.3.2 Process control: functional properites

As described in the previous section, the protein content in all materials was similar after washing though different washing conditions were applied. However, the protein in washed rapeseed concentrate became insoluble due to complete protein denaturation at the high temperature applied in aqueous ethanol washing. For de-oiled/pressed sunflower kernel concentrates, the protein was still native and showed slightly increased solubility after the washing process since the process temperature applied to sunflower materials was much lower compared to that of rapeseed meal. Thus, the different process conditions not only change the composition of the rapeseed and sunflower materials but also affect their functional properties, such as protein solubility. The water holding capacity and rheological properties were discussed here as well. The water holding capacity (WHC) of rapeseed and sunflower materials was comparable before the washing process, but the effect of washing was different on WHC for the different materials (Fig. 7-1B). The washing process largely

increased the WHC of the de-oiled or pressed sunflower kernel concentrate, but the WHC of rapeseed protein concentrate was slightly reduced. When mixed with water, rapeseed protein concentrate formed sand-like particles upon hydration that did not dissolve or swell. The sand-like particles formed a loose pellet upon centrifugation (**Chapter 2**). The de-oiled/pressed sunflower protein concentrates also formed a loose pellet. The loose pellet is a challenge for accurate measurement of the water holding capacity because the falcon tube cannot be turned upside down to drain the excess water from the pellet. The loose pellet was composed of the sand-like particles with the water mainly filling the spaces between the particles, which was different from the consistent pellet with the water held inside the semi-continuous protein network as found by Peters (2016) for soy and wheat gluten. The rheological properties of rapeseed and sunflower materials are shown in Fig. 7-1B. The complex modulus, G^*, measured at the end of cooling using an Anton Paar MCR 502 rheometer is taken as a measure of material strength (Data from **Chapters 2 & 6**). An increase in G^* for the rapeseed and sunflower materials was observed after aqueous ethanol washing, and the effect was more pronounced for the rapeseed protein concentrate. The increase was most likely due to the removal of oil and enrichment of protein by the aqueous ethanol washing process.

7.3.3 Process control: structuring properties

Structuring properties of rapeseed and sunflower protein materials were discussed here for meat analogue applications using shear cell technology. The structuring properties were investigated in this thesis under different process temperatures or blending with wheat gluten (**Chapter 3**). Rapeseed protein concentrate (40 wt% DM) formed a fibrous structure when sheared and heated at 140 °C or higher. This high temperature was mainly due to the need for the melting of the sand-like particles described above (**Chapter 3**). At a lower temperature of 120 °C, the particles remained intact and only a crumbly product was formed. A wheat gluten and rapeseed protein concentrate mixture (1:1) did not require a high temperature to form a fiber structure; 130 °C was sufficient for this mixture.

Confocal laser scanning microscopy images suggested a continuous protein phase and a dispersed phase of carbohydrates of the fibrous products. In the continuous phase, the protein from wheat gluten was not distinguishable from the protein in rapeseed protein

concentrate (**Chapter 3**). However, previous studies reported that protein from wheat gluten forms a separate phase when mixed with soy protein isolate or pea protein isolate at 120 °C (Dekkers, Emin, Boom, & Van der Goot, 2018; Schreuders et al., 2019). One can hypothesize that the protein from wheat gluten also formed a separate phase in blends with rapeseed protein concentrate as well, but CLSM images suggested intensive mixing. Phases could not always be clearly distinguished. Whether the mixing of protein from wheat gluten and other plant protein occurred at a molecular level even is still unclear and requires further investigation.

For sunflower materials, de-oiled sunflower kernel (40 wt% DM) formed a fibrous structure when sheared and heated at 140 °C. The pressed sunflower kernel showed no fiber formation in the shear cell under the same conditions. The high oil content in the pressed sunflower kernel was suggested as the main reason because the presence of oil was reported to hinder extrusion processes as well through the lubrication effect of the oil (Bohrer, 2019; Kyriakopoulou et al., 2019) (**Chapter 6**). When striving for a process that does not involve a solvent, oil pressing needs further investigation. **Chapter 6** also demonstrated that the presence of CGA did not have a clear effect on the structuring properties. Thus, CGA content is not a dominant factor in the ability of sunflower materials to form a fibrous product.

7.4 Characteristics of fibrous structure

The tensile stress and strain are plotted in a texture map with the data from the tensile test for all the fibrous products from rapeseed and sunflower materials (40 wt% DM) at 140 °C (Fig. 7-2). The tensile properties of wheat gluten, soy protein concentrate, and the blend of rapeseed or soy protein concentrate and wheat gluten (1:1) are also included for comparison (all data from **Chapter 3**). Tensile stress and strain indicates the material's mechanical strength and deformability, respectively (Mezger, 2010). Texture maps were proposed to describe the textures of the products into 4 different categories: mushy, rubbery, brittle, and tough (Schreuders et al., 2021; Truong & Daubert, 2001). The toughness of all products was increased in the order of de-oiled sunflower kernel, de-oiled sunflower kernel concentrate, rapeseed protein concentrate, and soy protein concentrate. However, although soy protein concentrate was found to be highest for toughness, the product was not as fibrous as the other products (**Chapter 3**). Thus, the fibrous structure does not relate directly to anisotropy in the

tensile properties. The wheat gluten product was in the rubbery region, implying the highest elasticity. It explains why the addition of wheat gluten increases the elasticity of the materials described above toward rubbery, as shown in Fig. 7-2.

The results for the tensile properties presented here were not in line with the complex modulus measured in Fig. 7-1. Although the rheological measurements showed that rapeseed protein concentrate had the highest G^* by heating, its toughness was lower than the fibrous product of soy protein concentrate in Fig. 7-2. The small deformation of the temperature sweep was applied within the linear viscoelastic region, which cannot demonstrate both the heating and shearing effect applied in the shear cell. Thus, combining a small deformation and a large deformation as a rheological tool is recommended to understand the influence of heating and shearing in a shear cell (Schreuders et al., 2021).

Overall, we did not find the crucial functional properties that can fully explain the structuring potential of the material. However, the importance of phase separation is confirmed, but the role of temperature is not completely clear. The presence of remaining oil is also a point for further research. It seems to behave similarly to dough materials, where it acts as a shortening agent and prevents protein network formation (Huschka et al., 2011; Inoue et al., 1995).
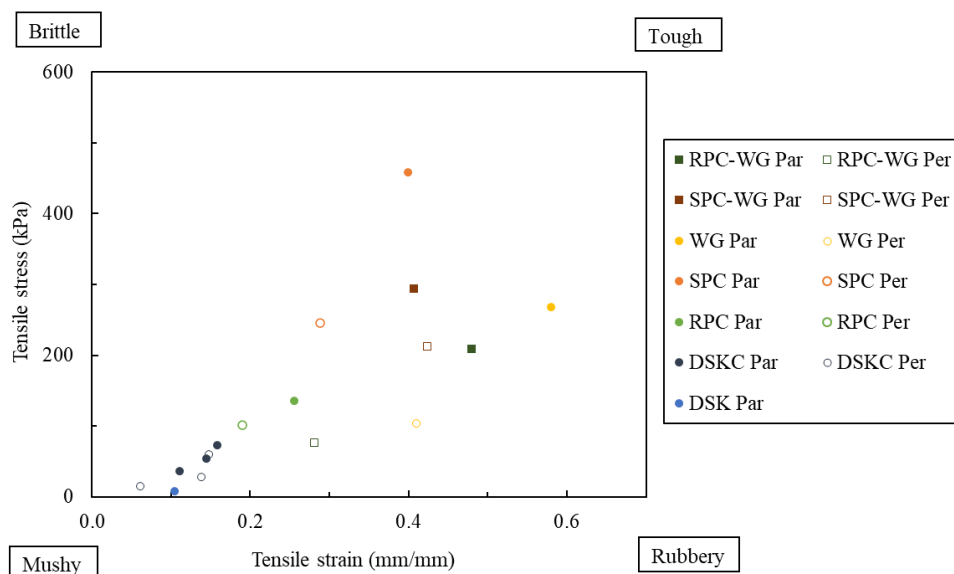
7

Fig. 7-2 Texture map of the mean value of tensile strain (mm/mm) and tensile stress (kPa) of DSK, DSKC, RPC, SPC, WG, mixtures of RPC-WG (1:1) and SPC-WG (1:1) product at 40 wt% DM by shearing and heating at 140 °C, 30 rpm for 15 min. The closed symbols are for the parallel direction (Par) and the open symbols are for the perpendicular direction (Per).

7.5 Reflection on the necessity of removal of phenolic compounds

One of the main challenges for using rapeseed and sunflower ingredients in food applications is the presence of phenolic compounds. Interaction between chlorogenic acid (CGA) and proteins can lead to the formation of green color and altered functional properties of the protein (Keppler et al., 2020; Prigent et al., 2007). Thus, the complete removal of CGA is often considered as a prerequisite for the use of sunflower material in food applications, which would necessitate extensive washing with aqueous ethanol mixtures (**Chapter 4**). Therefore, the possibility of retaining CGA in sunflower protein was studied using different simple model blends consisting of (1) dephenolized sunflower protein isolate and CGA and (2) dephenolized sunflower protein concentrate and CGA (**Chapter 5**). The color and behavior of the gel of the covalently modified protein samples from concentrate or isolates are compared in Fig. 7-3. Similarities were observed for the modified concentrates and isolates; both groups of modified samples gelled except the samples with high CGA

concentration. In addition, the gelled samples turned green at an apparent CGA-protein molar ratio of 1:1, and color became darker green when more CGA was added. Differences in gelling properties between the modified concentrates and isolates were observed by the temperature sweep using an Anton Paar MCR 502 rheometer. The modified concentrate samples formed a stronger gel with higher G' and G'' values compared with the modified isolate samples. In addition, the G' and G'' values were increased for the modified concentrate samples when heated from 20 °C to 95 °C which was not observed for the modified isolate samples. Sunflower protein denatured at an onset temperature of 93 °C (**Chapter 5**), meaning that gelation can be expected when using isolates; this effect is less relevant for sunflower protein concentrate in which other components were present besides protein. In terms of non-covalent modification, the functional properties and color were preserved when the blend of dephenolized sunflower protein isolate and CGA were treated at pH 7 for 24 h regardless of the CGA-protein ratio (1:10 to 10:1) (**Chapter 5**).

The results from this study suggest that the negative effect of the color and gelling properties from covalent modification can be prevented by controlling the CGA-protein interactions in a simple model blend with either isolate or concentrate. However, further investigation is needed to reveal whether the de-oiled or pressed sunflower kernel with CGA present in its natural form, behaves similarly to the blend. Thus, the effect of different levels of CGA content in de-oiled or pressed sunflower kernel (apparent molar ratio of 6.5:1 or 9:1) was tested for meat analogue application (**Chapter 6**). The results suggest that the amount of phenolic compounds present in the concentrate has almost no effect on the structuring properties. Therefore, it seems that the conditions applied in the shear cell did not lead to covalent interactions.

Thus, prevention of covalent interactions is more important than removal of phenolic compounds for food application. A route to prevention of covalent interactions between CGA and proteins in foods is to carefully choose the ingredients and the pH. For example, the use of sweeteners with low pH and a lot of reducing sugars, such as agave syrup and honey, will prevent covalent interactions between proteins and CGA better than maple syrup, which has higher pH and low reducing sugars (Liang & Were, 2018; Wildermuth et al., 2016). Of course, the study presented here only investigated the effect on structuring

7

properties only; the effect of phenolic compounds should be also studied for sensory effects and digestibility for food application. The effect of phenolic compounds on the structuring properties of rapeseed materials was not included in this study but may be an interesting topic for future study.

7.6 Suggestions for future research

From this study, we concluded that the functional and structuring properties of rapeseed and sunflower materials are largely dependent on the process routes. The de-oiling technique and aqueous ethanol washing process not only change the composition of the material but also affect the morphology of the particles (**Chapters 2 & 3**). Further, washing can alter the hydrophobicity of the concentrate and isolate. As a next step, we suggest investigating the effect of aqueous ethanol washing on the thermally induced melting behavior of rapeseed concentrate particles and their morphology. Better understanding might lead to routes that allow melting of the particles from rapeseed protein concentrate at a lower temperature. The first step is to study the glass transition temperature by thermal analysis using differential scanning calorimetry (Alves, Mano, Balaguer, Meseguer Dueñas, & Gómez Ribelles, 2002) or oscillatory shear rheometry (Rui et al., 2017). Another possibility is to apply a pre-treatment to the rapeseed protein concentrate before processing it in the shear cell, such as intensive milling to break the particles. Microwave technologies combined with ultrasonication have also been reported as a method to break down lignocellulosic biomass. A similar effect may apply to dense rapeseed particles (Hoang et al., 2021).

A1: dephenolized sunflower protein **concentrate** (10 wt%)

| 1:10 | 1:5 | 1:1 | 5:1 | 10:1 |

B1: dephenolized sunflower protein **isolate** (10 wt%)

| 1:1 | 1:5 | 1:1 | 5:1 | 10:1 |
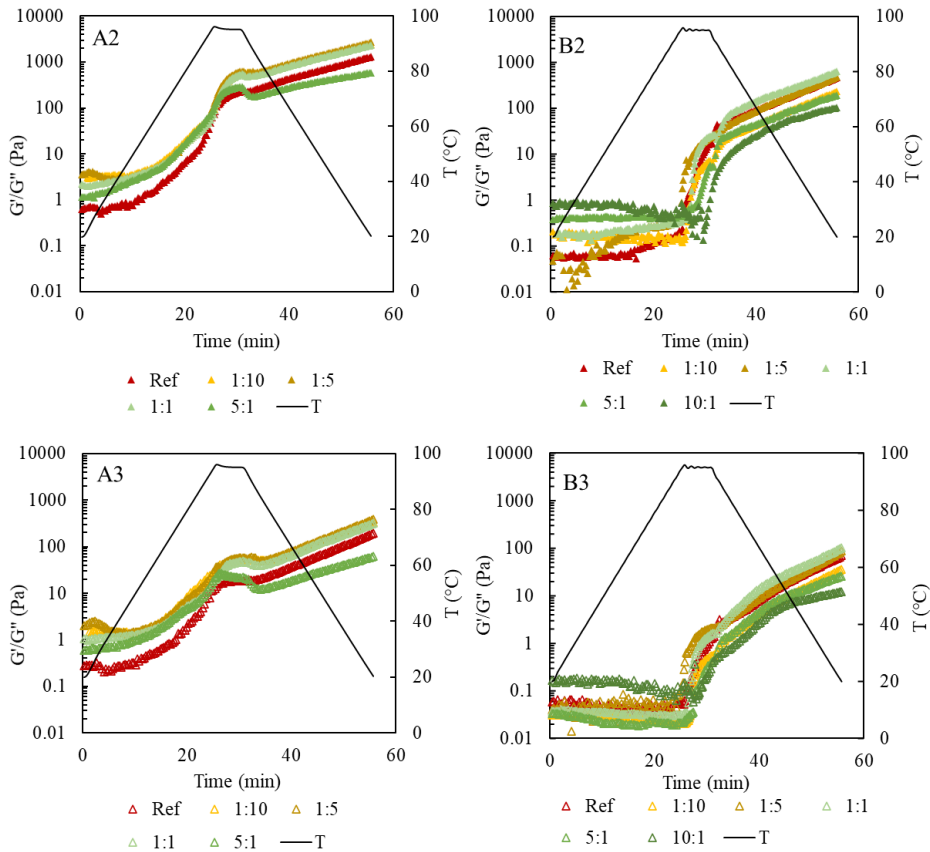
Fig. 7-3 Heat-induced gel from covalently modified SFPC (A1) and SFPI (B1) dispersions by CGA at 10 wt% DM at apparent CGA/protein molar ratios of 1:10, 1:5, 1:1, 5:1 and 10:1. The rheological properties of G' (Pa) by temperature ramp (20 °C–95 °C–20 °C) were measured with covalently modified SFPC (A2) and SFPI (B2) (closed symbols) and the G'' (Pa) value of SFPC (A3) and SFPI (B3) samples (open symbols). Rheological measurements were performed in an Anton Paar rheometer.

From the model blend study on the effect of phenolic compounds (mainly CGA) on sunflower protein, we observed that the presence of phenolic compounds does not affect the structuring properties in a shear cell (**Chapters 5 & 6**). Thus, from this perspective, aqueous ethanol washing is not necessary for the removal of phenolic compounds. A aqueous ethanol washing is, however, more important for rapeseed meal than for sunflower meal, because it is also necessary to remove other anti-nutrients, such as glucosinolates (Citeau et al., 2019).

Thus, it is necessary to understand to what extent it is necessary to remove these undesired components.

The research described in this thesis reveals the potential of using de-oiled sunflower kernel for structuring properties in the shear cell for meat analogue application (**Chapter 6**). The oil content was found to be an important factor for the structuring properties. A fibrous structure could only be formed below an oil content of 8%, and the mechanical strength of the product was increased by decreasing the oil content. However, it remains to be investigated: how to incorporate the oil in the plant material for sensory purposes; the effect of temperature, dry matter content of the de-oiled sunflower kernel in the shear cell; the microstructure of the fibrous product by confocal laser scanning microscopy.

Another point observed from this study is the effect of adding wheat gluten to rapeseed protein concentrate. The addition of wheat gluten increased the elasticity of the fibrous product, and the fibrous structure was more pronounced (**Chapters 3 & 7**). Here, mixing wheat gluten with de-oiled or pressed sunflower kernel was tested in a shear cell at a 1:1 ratio of 40 wt% at 140 °C (Fig. 7-4), and fibrous products were formed in both cases. Although the pressed sunflower kernel did not show a fibrous structure due to a high oil content (10 wt%), mixing with wheat gluten allows a fibrous structure to form by lowering the oil content in the mixture. Another test was performed by mixing rapeseed protein concentrate with de-oiled sunflower kernel or soy protein concentrate at a 1:1 ratio of 40 wt% in a shear cell at 140 °C. Although no fibrous structure was formed, the structure was different from that of the single protein material reported in this study. This knowledge is useful for the creation of desired structures using different protein blends.
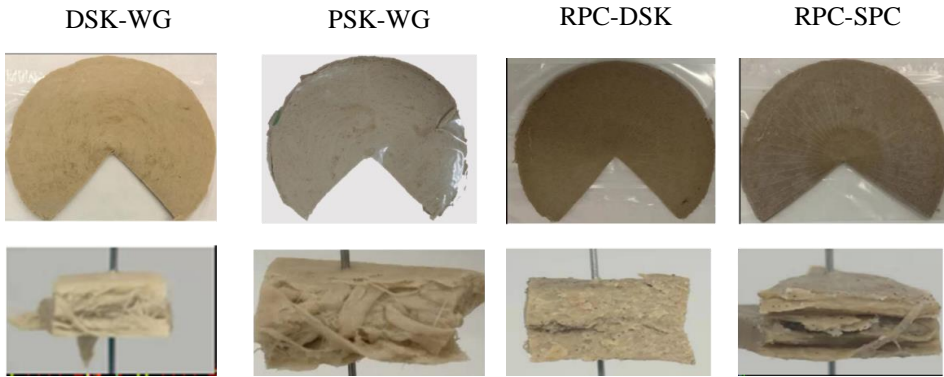
Fig. 7-4 Heated and sheared product of de-oiled sunflower kernel and wheat gluten (DSK-WG), pressed sunflower kernel and wheat gluten (PSK-WG), rapeseed protein concentrate and de-oiled sunflower kernel (RPC-DSK), and rapeseed protein concentrate and soy protein concentrate (RPC-SPC) in a 1:1 ratio with 40 wt% DM at 140 °C for 30 rpm for 15 min.

This thesis covers research on the functional and structuring properties of rapeseed and sunflower material for meat analogue application. However, also other aspects have to be considered for the development of a successful meat analogue product: (1) sensory properties (taste, color, flavor, juiciness): the sensory properties are important for consumer acceptance of plant-based meat analogues; (2) allergy risk: it is important to consider the allergy risk when labeling novel foods containing rapeseed protein, because allergic reactions from rapeseed protein (2S napins) are considerably more prevalent than those caused by sunflower albumin (Wanasundara, 2011); (3) digestibility and food safety: the removal of anti-nutrients is important for less refined rapeseed and sunflower ingredients, as well as the analysis of the protein quality based on the protein digestibility-corrected amino acid score (PDCAAS); (4) scale-up production: the study described in this thesis on rapeseed and sunflower materials is limited to lab scale. The next step toward commercialization that requires pilot plant trials is to better understand the fractionation process and the resulting structuring properties. Structuring can also be extended to extrusion in addition to shear cell experiments.

203

7.7 Concluding remarks

Rapeseed and sunflower meals are considered as a by-product stream, with the main application as animal feed. Challenges exist in their use as food ingredients due to the presence of phenolic compounds, which was the starting point for this research. This thesis provides scientific insight on the fractionation of rapeseed and sunflower protein concentrate by aqueous ethanol washing to remove the phenolic compounds. It is concluded that rapeseed protein concentrate and de-oiled sunflower kernel are promising protein sources for developing future meat analogue products.

7.8. References

Alves, N.M., Mano, J.F., Balaguer, E., Meseguer Dueñas, J.M., & Gómez Ribelles, J.L. (2002). Glass transition and structural relaxation in semi-crystalline poly (ethylene terephthalate): A DSC study. *Polymer*, 43 (15), 4111–4122.

Bohrer, B.M. (2019). An investigation of the formulation and nutritional composition of modern meat analogue products. *Food Science and Human Wellness*, 8 (4), 320–329.

Carré, P., Citeau, M., Robin, G., & Estorges, M. (2016). Hull content and chemical composition of whole seeds, hulls and germs in cultivars of rapeseed (Brassica napus) . *Ocl*, 23(3), A302.

Citeau, M., Regis, J., Carré, P., & Fine, F. (2019). Value of hydroalcoholic treatment of rapeseed for oil extraction and protein enrichment. *OCL*, 26 (1).

Dekkers, B.L., Emin, M.A., Boom, R.M., & van der Goot, A.J. (2018). The phase properties of soy protein and wheat gluten in a blend for fibrous structure formation. *Food Hydrocolloids*, 79, 273–281.

Geerts, M.E.J. (2018). Functionality-driven fractionation the need for mild food processing. PhD thesis.

Hoang, A.T., Nižetić, S., Ong, H.C., Mofijur, M., Ahmed, S.F., Ashok, B., … Chau, M. Q. (2021). Insight into the recent advances of microwave pretreatment technologies for the conversion of lignocellulosic biomass into sustainable biofuel. *Chemosphere*, 281(May).

Huschka, B., Challacombe, C., Marangoni, A. G., & Seetharaman, K. (2011). Comparison of oil, shortening, and a structured shortening on wheat dough rheology and starch pasting properties. *Cereal Chemistry*, 88(3), 253–259.

Inoue, Y., Sapirstein, H.D., & Bushuk, W. (1995). Studies on frozen doughs .IV. Effect of shortening systems on baking and rheological properties. *Cereal Chemistry*, 72 (2), 221–226.

Keppler, J.K., Schwarz, K., & van der Goot, A.J. (2020). Covalent modification of food proteins by plant-based ingredients (polyphenols and organosulphur compounds): A commonplace reaction with novel utilization potential. *Trends in Food Science & Technology*, 101(Oct), 38–49.

Kyriakopoulou, K., Dekkers, B., & van der Goot, A. J. (2019). *Plant-based meat analogues: Sustainable Meat Production and Processing*. (C. M.galanakis,Ed.), *Academic Press*. Elsevier Inc.

Liang, S., & Were, L.M. (2018). Chlorogenic acid induced colored reactions and their effect on carbonyls, phenolic content, and antioxidant capacity in sunflower butter cookies. *LWT*, 87, 16–22.

Loveday, S.M. (2020). Plant protein ingredients with food functionality potential. *Nutrition Bulletin*, 45 (3), 321–327.

Mezger, T. G. (2010). The rheology handbook: For users of rotational and oscillatory rheometers. Vincentz Network GmbH & Co KG. 114-120.

Peters, J. (2016). Water-binding of protein particles. PhD thesis. PhD thesis.

Prigent, S.V.E., Voragen, A. G., Visser, A. J., Van Koningsveld, G.A., & Gruppen, H. (2007). Covalent interactions between proteins and oxidation products of caffeoylquinic acid (chlorogenic acid). *Journal of the Science of Food and Agriculture*, *87* (April), 2502-2510

Rao, R.K., & Arnold, L.K. (1956). Alcoholic extraction of vegetable oils. III. Solubilities of babassu, coconut, olive, palm, rapeseed, and sunflower seed oils in aqueous ethanol. *Journal of the American Oil Chemists Society*, 33(9), 389–391.

Rui, L., Xie, M., Hu, B., Zhou, L., Saeeduddin, M., & Zeng, X. (2017). Enhanced solubility and antioxidant activity of chlorogenic acid-chitosan conjugates due to the conjugation of chitosan with chlorogenic acid. *Carbohydrate Polymers*, 170, 206–216.

Schreuders, F.K.G., Sagis, L.M.C., Bodnár, I., Erni, P., Boom, R.M., & van der Goot, A.J. (2021). Small and large oscillatory shear properties of concentrated proteins. *Food Hydrocolloids*, 110 (July).

Schreuders, F.K.G., Dekkers, B.L., Bodnár, I., Erni, P., Boom, R.M., & van der Goot, A.J. (2019). Comparing structuring potential of pea and soy protein with gluten for meat analogue preparation. *Journal of Food Engineering*, 261(May), 32–39.

Schreuders, F.K.G., Sagis, L.M.C., Bodnár, I., Erni, P., Boom, R.M., & van der Goot, A.J. (2021). Mapping the texture of plant protein blends for meat analogues. *Food Hydrocolloids*, 118, 106753.

Truong, V.D., & Daubert, C.R. (2001). Textural characterization of cheeses using vane rheometry and torsion analysis. *Journal of Food Science*, 66(5), 716–721.

Van Der Goot, A.J., Pelgrom, P.J.M., Berghout, J.A.M., Geerts, M.E.J., Jankowiak, L., Hardt, N. A., … Boom, R. M. (2016). Concepts for further sustainable production of foods. *Journal of Food Engineering*.

Wanasundara, J.P.D. (2011). Proteins of brassicaceae oilseeds and their potential as a plant protein source. *Critical Reviews in Food Science and Nutrition*. 51 (7), 635-677.

Wildermuth, S.R., Young, E.E., & Were, L.M. (2016). Chlorogenic acid oxidation and its reaction with sunflower Proteins to Form Green-Colored Complexes. *Comprehensive Reviews in Food Science and Food Safety*, 15 (5), 829–843.

7

Summary

English summary

Summary

A current trend in food industry is towards more plant protein-based products and less meat. It includes broader availablity of appealing meat analogues that help consumers adapting towards less meat. The plant protein sources used for meat analogues are mostly based on commercial soy or pea protein concentrates or isolates currently. To reduce dependency on soy and pea, alternative plant protein sources should be explored to fulfill the future protein supply and consumer demands. Rapeseed and sunflower seeds are broadly used for oil production, while the co-products of rapeseed and sunflower meal after the oil extraction are mainly applies as animal feed. With high protein content and rich nutritional given the amino acid composition, rapeseed and sunflower cake/meal are considered as a potential plant protein source for foods as well. Therefore, the aim of this work was to enable the use of the co-product of rapeseed meal and de-oiled sunflower meal kernel for meat analogue application throug creatng new scientific insights in the fractionation process of those seed and thestructuring potential of resulting ingredients. This thesis addressed a research question whether complete removal of phenolic compounds from de-oiled sunflower kernel is necessary

In **chapter 2**, rapeseed protein concentrate and isolate (RPC and RPI) were fractionated from rapeseed meal, and their functional properties were compared. The RPC was obtained by aqueous ethanol washing and consisted of 62% protein (DM) and 28% polysaccharides (DM). The washing process removed almost all the phenolic compounds and oil. The RPI was fractionated with alkaline extraction, ultrafiltration and dialysis. It contained 94% protein (DM), but still contained a considerable amount of phenolic compounds (3.6% DM) after fractionation. The protein in RPC was completely denatured and had a low protein solubility, whereas the protein in RPI was still native and highly soluble. RPC particles were found to be sand-like when dispersed in water. Nevertheless, a concentrated RPC dispersion (40 wt% DM) lead to a much higher complex modulus (G^*) by the temperature sweep using closed cavity rheometer compared to the RPI dispersion of 40 wt% DM.

The high complex modulus (G^*) of the RPC dispersion suggested its potential for use as ingredient in meat analogues (**Chapter 3**). The structuring properties of RPC were studied with two recepies: RPC-only and RPC-wheat gluten (WG) mixture of 40 wt% DM

in the shear cell. It was found that RPC-only formed fibrous structure when the temperature was above 140 °C, while RPC-WG (1:1) mixture of 40 wt% formed fibrous structure at lower temperature of 130 °C. Further, a more pronounced anisotropic structure with increased anisotropic index (AI) on tensile stress was found in all ratios of RPC-WG compared with RPC-only. Moreover, sheared RPC-WG product had a remarkably lighter color than the RPC-only product. It was concluded that RPC is a promising alternative protein source for meat analogue applications.

Chapter 4 presents research on the aqueous ethanol washing of the de-oiled sunflower kernel to remove the phenolic compounds (PCs). The parameters of PCs removal yield and the protein loss were assessed under varied process conditions (temperature, pH and solvent quality). Results showed that the PCs removal was accompanied by protein loss in most of studied conditions, and the effect of process conditions were greater on protein loss than PC removal yield. More washing steps always led to higher removal yield of PCs. A simulation of multi-steps washing process was performed using the equilibrium constant derived from the experimental data. It was concluded that an intensive washing with multi-steps (using aqueous ethanol mixtures with 80% ethanol) were necessary to remove 95% of PCs, which also recovered most of the protein after the process. However, this extensive process conditions raised a research question whether complete removal of phenolic compounds is necessary from the de-oiled sunflower kernel for the meat analogue application.

Chapter 5 describes up to what extent the PCs should be removed from the de-oiled sunflower kernel to prevent a negative influence on the functional properties of the sunflower protein. To do so, a simple model blend was studied, in which chlorogenic acid (CGA) and sunflower protein was mixed at apparent CGA-protein molar ratios of 1:10, 1:5, 1:1, 5:1 and 10:1 (which corresponds to mass ratio's of 1:850, 1:450, 1:85, 1:15 and 1:10). The outcome of this simple model blend showed the possibility to keep the CGA in the sunflower protein even when non-covalent interaction (incubated for 24 h at pH 7) occurred between CGA and sunflower protein. However, partial removal of CGA was necessary in case the covalent interaction (pH-shift: 24 h incubation at pH 9, then shift back to pH 7) could not be avoided. Covalent interactions above an apparent CGA-protein ratio of 1:1 led to green color formation and the gelling properties were negatively influenced. Besides, the result showed

that non-covalent interactions induced structural changes of the protein. The effect of covalent modification on gelling properties was also validated in a model blend of CGA and dephenolized sunflower protein concentrate. Also in this blend, the CGA-protein molar ratio should not exceed 1:1.

The study in **Chapter 5** was limited to a model blend, where CGA was added into the de-phenalized sunflower materials. This blend might not represent the sunflower materials where the CGA was still naturally present. Therefore, In **Chapter 6,** the amount of CGA allowed in pressed sunflower kernel (PSK) and de-oiled sunflower kernel (DSK) for structuring properties was further investigated. The PSK and DSK were obtained by the different oil extraction methods. PSK was obtained after intensive pressing, without additional de-oiling steps, whil DSK was obtained after mild pressing followed by ethanol washing. In this study, additional aqueous ethanol washing was applied to both DSK and PSK to generate the concentrates with different CGA content. CGA could be extracted from both materials, but the differences were on oil removel, which was possible for DSK, but not for PSK. Upon shear cell processing, it was found that both DSK and DSK-washed concentrates (40 wt% DM) formed fibers. However, only crumble products were formed when processing PSK or the PSK-washed concentrates (40 wt% DM). Results suggested that the amount of CGA presented in the sunflower materials did not affect their structuring properties in shear cell because CGA was effectively removed in both washed concentrates and both DSK with and without CGA gave fibrous products. The main reason for the different structuring property was found to be the oil content (10% versus 7.4% in PSK and DSK), which was suggested to be the determining factor to prevent fiber formation in case of PSK.

In **Chapter 7**, the main findings and conclusion of this thesis were reviewed. The fractionation processes were discussed regarding their effects on the functional and structuring properties of the rapeseed and sunflower materials. Aqueous ethanol washing can effectively remove the phenolic compounds and oil from rapeseed meal but also lead to the formation of sand-like particles, which only melt at high temperature. The melting of these particles was found to be prerequisite for the fibrous structure formation. It was suggested to further study the different process conditions from aqueous ethanol washing and its impact on the particle melting behavior to lower the required temperature for the fibrous structure

formation using shear cell. High oil content (above 8%) in a less refined sunflower ingredient was found to negatively affect the fibrous structure formation, whereas the presence of phenolic compounds was not a problem for the structuring purpose in shear cell. Although the phenolic compounds removal was not considered to be necessary for the fiber formation, its impact on the sensory properties still requires further investigation for meat analogue application. Overall, it can be concluded that rapeseed protein concentrate and de-oiled sunflower kernel ingredients have good potential for meat analogue applications.

S

List of abbreviations

AI	Anisotropic Index
ATR-FTIR	Attenuated total reflectance-Fourier transform infrared spectroscopy
CCR	Closed cavity rheometer
CGA	Chlorogenic acid
CLSM	Confocal laser scanning microscope
CME	Counter-current multi-stage extraction
DM	Dry matter content
dRSM	Defatted rapeseed meal
DSC	Differential Scanning Calorimetry
DSK	De-oiled sunflower kernel
DSKC1	De-oiled sunflower kernel concentrate of 1 washing step
DSKC4	De-oiled sunflower kernel concentrate of 4 washing steps
DSKC10	De-oiled sunflower kernel concentrate of 10 washing steps
F-C	Folin-Ciocalteu
GAE	Gallic acid equivalent
HPLC	High-performance liquid chromatography
HTSC	High-temperature conical shear cell
K_{pc}	Equilibrium constant for phenolic compounds
K_{pro}	Equilibrium constant for protein
LGC	Least gelling concentration
mRPC	Milled rapeseed protein concentrate
NSI	Nitrogen solubility index
PC	Phenolic compounds
PSK	Pressed sunflower kernel
PSKC1	De-oiled sunflower kernel concentrate of 1 washing step
PSKC4	De-oiled sunflower kernel concentrate of 4 washing steps
PSKC10	De-oiled sunflower kernel concentrate of 10 washing steps
RPC	Rapeseed protein concentrate
RP-HPLC	Reversed-phase high-performance liquid chromatography

RPI	Rapeseed protein isolate
RSM	Rapeseed meal
SDS-PAGE	Sodium dodecyl sulphate polyacrylamide gel electrophoresis
SEM	Scanning electron microscope
SFPI	Sunflower protein isolate
SPC	Soy protein concentrate
SPI	Soy protein isolate
sRPC	Sieved rapeseed protein concentrate
T_d	Denaturation temperature
TPC	Total phenol content
UV-vis	Ultraviolet-visible spectroscopy
WG	Wheat gluten
WHC	Water holding capacity
XRT	X-ray microtomography
YM	Young's modulus

A

Acknowledgements

I would like to acknowledge all those who had contributed and participated in this thesis. It has been a long journey to finally achieve this step. Somehow, it is hard to realize that the journey is coming to an end. I really glad to see myself developed in a good way with joy during these 4 years and become more knowledgeable and confident. Looking back on this journey, I am grateful for all your help and accompany.

Firstly, I would like to thank my supervisors Atze Jan, Julia, and Elvira. **Atze Jan (promotor)**, thank you for giving me this great opportunity to perform this PhD study and guide me through the entire study. You had taught me to be more critical in thinking and writing, to challenge myself with higher standards in academic research. Also, you helped me to build up self-confidence when presenting. **Julia (co-promotor)**, I am really glad to have your guidance and supervision for the second half of my PhD study. I enjoyed all the discussions we had together with Atze Jan. You always came up with valuable suggestions and feedback which brought the research to a high level. Also thank you for painting the rapeseed flower and meal for the cover design. **Elvira (supervisor)**, I appreciate all your support and help in the first half of my PhD study. We had been through a tough beginning to explore the different materials. After some failed experiments, finally, we figured out the potential ingredient for the meat analogue. I would like to appreciate the great support from **Konstantina**, you encouraged me whenever I had difficulties in the research and always happy for my achievements, and I was always inspired during our chatting. I am very happy to have you as my co-author in the paper as well.

Further, I am happy to join the Plant Meat Matters project, a big thanks to all the project partners, and special thanks to the Avril group, **Marine, Mbalo, and Oliver**. Thank you for your continued support, and your passion in turning this research work into a patent that could bring value also to the industry. This makes me feel like I really achieved something. **Ariette**, thank you for your support during the PMM meetings and the patent filing work. Thanks to all the project fellow PhDs and researchers: **Yu, Jan, Steven, Nynke, Ariane, Birgit, Jacqueline, and Nam-Phuong**. I learned a lot from you with the project meetings, journal club, and discussions and enjoyed all the times we have been together.

To the students: **Jesse, Shan, Uyen, Dieuwertje, Leila, Nicolas, Bente, Roos, Divjyot, Ignatia and Sofia**. It was a great pleasure to work together with you, thanks a lot for your contribution to this research work. **Marjan, Ilona, and Evelyn**, thank you for all your great support with the administration work. **Jarno,** I want to express my great thanks to you for

your patient when I forgot how the shear cell works for N times or whenever there is an issue with it. Also, I want to thank you for letting me join the FPE gardening, I will not forget the nice time I had in the Dolderstraaat with you, Lu, Fiona and Julia. I want to thank you for helping me when there is any issue in the corridor I lived and helping with moving the house. **Maurice, Wouter and Jos**, thank you so much for helping me with the lab work, instructions with the lab facilities as well as problem-solving. **Martin**, thank you for helping me out with the expense declaration and the My-HR system.

Polly and Yafei, thank you for being my Paranymphs. **Polly,** your cake had never disappointed me, and thank you for helping with the thesis cover design. I still would like to play more badminton with you, it feels so great to be with you on the same side of the court. **Yafei and Rimmer,** thanks for showing me how to make the mojito, it was a really nice experience. I enjoyed a lot of the chatting with you about the project and life. I am happy that my experience of the PhD can be useful for you. **Yu**, I am so happy to study and work together with you on the same project, we shared the knowledge, inspired and supported each other during the research and in personal life. I really enjoyed our trips during the PMM meeting to France, Switzerland, etc. and I would not forget those long walks we had during the trips. Thank you for telling me all the tips about finalizing the PhD thesis. **Sicong**, thank you for bringing me outside Wageningen with your car during the Covid times, this released and comforted me so much from the little room in Wageningen. Also thank **Sicong**, **Qinhui, and Martin** for the trip to Canada Niagara waterfalls on my birthday, which was an unforgettable experience for me, also made my little dream come true. **Lu**, it was nice to study the Netherlands together with you. The roasted duck dinner you prepared was so delicious, and I believe it was a good start for the year 2022. **Floor,** I am lucky to have you as my colleague, that you are always generous in sharing the experience with me either on the device (CCR) or with the research. **Ruoxuan, Isabel, Sirinan, Joanna, Erik, Jilu, Boxin, Katharina, Murat, Ivanna, Luc, Iris, Julia V., Hilda, Kubra,** I enjoyed all the chattings we had, and the time spent together in FPE. **Anna, Miek, Andrea, Anouk, Yizhou, Herahau, Nynke and Silvia**, I am happy to join the trip to the EFFoST in Lausanne together with you. **Lina,** thank you for bringing me stuff from China during the Covid times. **Fiona, Dimitris, Patricia, and Juliana**, thank you for your guidance and suggestions at the beginning of my PhD study.

Thanks to my office mates in FPE, **Anja, Evelien, Jun, Sten, Polly, Yifeng, and Raquel.** It was great to be office mates with you., thank you for all the chattings we had, the Netherlands practicing during the coffee break time, also for your support and understanding during the

final stressful thesis writing times. You made the office an amazing place to work. Thanks **Sten** for encouraging me with the sporting: running. **Anja,** thank you for helping me to check some parts of the thesis even during your maternity leave.

Yingzi & Xiufeng, I feel really happy to meet you here during my PhD, I enjoyed all the time that we had spent together. Thank you for you accompany during all these four years, that you supported and listened to me, which really means a lot to me. **Jinfeng,** my old classmate, it was nice to meet you again here, and I want to appreciate all your support for my PhD study. **Junnan, Xiaofei, Lei, Zhihong, Wenjie, Xiaoning,** it was nice to know you during the PhD study, here we shared the struggling of this journey and cheered up each other.

感谢在国内的家人和朋友，谢谢你们持续的支持和鼓励。致我最最亲爱的爸妈，谢谢你们对我出国留学的大力支持。 虽然这些年在荷兰读博士，我们交流沟通有时差，但你们总是为我腾出时间，甚至牺牲自己晚上睡觉的宝贵时间开解我。谢谢你们在我成长的道路上陪伴着我，见证我每一点一滴的进步和变化，希望这本小小的论文能让你们感到欣慰，没有辜负你们的期望。

Author

About the author

About the author

Wanqing Jia was born on 14th June 1988, in Fujian Province, China. She started her bachelor's study in Fujian Agriculture and Forestry University in Food Science and Engineering in 2005. After graduation in 2009, she continued one year of MSc study in the same university, then she applied for the MSc study in 2010 at Wageningen University (WUR), the Netherlands, with a specialization in Dairy technology under Food technology, and graduated in 2012.

Contact: wanqing001@live.cn

After graduation, she started her career first in Royal FrieslandCampina in Beilen, the Netherlands, and worked as a product developer for infant nutrition. Afterward, she moved back to Shanghai, China, in 2013 and worked for Hero group as Regulatory and Nutrition Manager for Infant Nutrition. After 2 years working in Shanghai, she relocated to Hohhot, China, and worked for the Yili Group as Nutrition R&D Manager for two years. In 2017, after 5 years working in the food industry, she decided to go back to the academic and continued her study as a PhD candidate in the Food Process Engineering group in WUR, the Netherlands. The results of the PhD work were presented in this thesis.

List of publications

This thesis:

Jia, W., Rodriguez-Alonso, E., Bianeis, M., Keppler, J.K., Van der Goot, A.J. Assessing functional properties of rapeseed protein concentrate versus isolate for food applications. *Innovative Food Science & Emerging Technologies* (**2021**). 68, 102636.

Jia,.W., Curubeto, N., Rodriguez-Alonso, E., Keppler, J.K., and Van der Goot, A.J. Rapeseed protein concentrate as a potential ingredient for meat analogues. *Innovative Food Science and Emerging Technologies* (**2021**). 72. 102758.

Jia, W., Kyriakopoulou, K., Roelofs, B, K., Ndiaye, M., Vincken, JP, Keppler, J.K., and Van der Goot, A.J. Removal of phenolic compounds from de-oiled sunflower kernels by aqueous ethanol washing. *Food chemistry* (**2021**). 362, 130204.

Jia, W., Singh Sethi, D., Van der Goot, A.J., and Keppler, J.K. Covalent and non-covalent modification of sunflower protein with chlorogenic acid: identifying the critical ratios that affect techno-functionality. *Submitted.*

Jia, W., Ignatia Regina Sutanto., Keppler, J.K., and Van der Goot, A.J. Effect of aqueous ethanol washing on functional properties of sunflower materials for meat analogue application. *Submitted.*

Other publications:

Warmerdam.A., Paudel,E., **Jia, W**., Boom, R.M., Janssen, A.E.M. Characterization of β-galactosidase isoforms from *Bacillus circulans* and their contribution to GOS production. *Applied Biochemistry and Biotechnology* (**2013**). 170 (2).340-358.

A

Overview of completed training activities

Discipline specific activities	
Courses	
Han-Sur-Lesse winterschool (Wageningen, TU delft, BE)	2018
Food proteins: functionality, modifications and analysis (Vlag, Wageningen, NL)	2018
Rheology workshop (WUR, Wageningen, NL)	2018
17th European school on rheology (KU Leuven, BE)	2019
Microscopy and spectroscopy in food and plant science (VLAG, Wageningen, NL)	2019
Conferences	
Science and Technology for Meat Analogues (Wageningen, NL)	2018
2nd innovations in food science & technology (Amsterdam, NL)	2019
33rd EffoST International Conference (Rotterdam, NL)	2019
Food Science Symposium (Wagenignen, NL)	2020
15th Plant-Based Foods & Proteins Summit North America (Virtual online)	2020
NIZO plant protein functionality conference (Virtual online) [b]	2020
Research Conference Plant-Based Foods & Proteins Europe (Virtual online)	2021
Science and Technology for Meat Analogues (Wageningen, NL) [a]	2021
35th EFFoST International Conference (Lausanne, CH) [a]	2021
4th Food structure & Functionality Symposium (Virtual online) [b]	2021
General courses	
PhD week (VLAG)	2018
Project and time management (WGS)	2018
Applied statistics (VLAG)	2018
Brain training (WGS)	2018
Chemometrics (VLAG)	2019
Scientific Writing (WGS)	2019
Scientific Publishing (WGS)	2019
Scientific artwork – Vector graphics and images (WGS)	2020
Optional courses and activities	
Preparing PhD research proposal	2018
FPE weekly meetings & Group days[a,b]	2017-2021
PhD study tour Canada[a,b]	2018

Food structure journal club[a]	2018-2021

[a] *Oral presentation;* [b] *Poster presentation.*

VLAG: Advanced Studies in Food Technology, Agrobiotechnology, Nutrition and Health Sciences; WGS: Wageningen Graduate Schools.

NL: the Netherlands; BE: Belgium; CH: Switzerland.

A